

# **AIR QUALITY IN CHRISTCHURCH**

## **AN ASSESSMENT OF FACTORS CONTRIBUTING TO VISIBILITY DEGRADATION**

---

**A thesis**

**Submitted in fulfilment of the requirements for the Degree of  
PhD in Environmental Science**

**At the University of Canterbury**

**by  
Emily Wilton**

---

**Canterbury University 2003**

TD  
883.7  
.N52  
.C5  
.W755  
2003<sup>a</sup>

---

## ABSTRACT

---

The cause of visibility degradation in Christchurch has been a concern for those responsible for management of the air quality for many years. In the late 1990s, Environment Canterbury, the local air quality regulator, become concerned that the regulatory measures proposed to reduce the 24-hour average mass  $PM_{10}$  concentrations, targeting emissions from domestic fires, would have little impact on reduced daytime visibility. The lack of improvement in visibility may then have advanced the perception that the air plan measures were unsuccessful in reducing  $PM_{10}$  mass.

A research programme was designed to determine the causes of reduced visibility in Christchurch, and to examine variations in the composition of summer versus winter haze and implications for the management of reduced visibility in Christchurch. The study also examined the relationship between visibility perception and light extinction.

The causes of reduced daytime visibility in Christchurch were assessed based on the results of an air quality monitoring programme. This included the measurement of light scattering by particles ( $B_{sp}$ ), light absorption by particles ( $B_{ap}$ ) and light absorption by gases ( $B_{ag}$ ), which were summed with the Rayleigh scattering constant to give an estimate of total light extinction. The composition of particulate was measured using a combination of techniques including proton induced x-ray emission, ion chromatography and a series 5400 carbon analyser. Hourly average  $PM_{2.5}$  concentrations were also measured using a TEOM sampler.

Results indicated maximum daytime light extinction values of around  $1000 \text{ Mm}^{-1}$  during the winter compared to around  $400 \text{ Mm}^{-1}$  during the summer months. The main contributor to light extinction was light scattering by particles which accounted for about 64% on average, compared to 15%  $B_{ap}$ , 17%  $B_{sg}$  and 3%  $B_{ag}$ . The contribution of  $B_{sp}$  and  $B_{ap}$  increased during the haze episodes to 71% and 25% respectively for the top 10% of light extinction data. The main sources contributing to poor visibility during both summer and winter were found to be motor vehicle emissions (30% winter, 40% summer) and secondary particles (50% winter, 40% summer). Domestic fires contributed less than 10% on average during the winter. Other minor sources included soil,  $NO_2$  ( $B_{ag}$ ), and light scattering by gases ( $B_{sg}$ ).

The study indicates that measures proposed by Environment Canterbury to reduce emissions from domestic fires will not result in significant improvements in daytime visibility in Christchurch.

---

## Acknowledgements

---

There are so many inspirational people that have made this task much easier.

My supervisors, Andy Sturman and Rachel Spronken Smith were excellent and I am most appreciative of their guidance, enthusiasm and wisdom.

The staff at Environment Canterbury are fantastic. Of the many wonderful people there I would like to particularly thank Ken Taylor, my manager of many years, for being a constant source of wisdom, motivation and sound advice, Bob Ayrey, for his expertise, encouragement, and the lunchtime bike rides that helped keep us both sane and Teresa Aberkane for her skills and dedication, and for putting up with sharing an office with me for so many years. Ken, Bob and Teresa you are just the best and I am extremely grateful for all your encouragement, knowledge and most of all your friendship.

I am also very appreciative of the contribution of other members, past and present, of the air quality team at Environment Canterbury, in particular, Mayurie Gunatilaka, Mark Harvey and Tracy Beck for their help with instrumentation and sampling as well as Paul Woods and other laboratory staff.

Thank you so much also to Kim Knight for her generosity and patience in reading the report, providing much appreciated advice on style and grammar and for her positivity (yes, yes.....not a real word) and encouragement.

Further afield, in the less hazy Wellington region, Bill Trompetter at Geological and Nuclear Sciences conducted the PIXE analysis on the filters and was awesome at sharing his knowledge on factor analysis.

One thing that is always very difficult when conducting air quality research is getting access to suitable monitoring sites. The Christchurch Polytechnic was extremely decent in allowing us to use its rooftop and to install our instruments in its 6<sup>th</sup> floor science laboratory. Thank you so much to David Hawke and the Christchurch Polytechnic for being so interested and willing to assist.

Finally I am grateful to my friends and family for their encouragement and to my husband, Hedley for his patience, for being such an inspiration and for the many hours spent keeping the computer up to spec so it could handle all the data files.

---

# Contents

---

<b>Chapter 1</b>	<b>Introduction .....</b>	<b>1</b>
1.1	Visibility in Christchurch .....	4
1.2	Objectives and hypothesis .....	8
1.3	Overview of thesis.....	8
1.4	Summary.....	9
<b>Chapter 2</b>	<b>Processes, perception, monitoring and causes of visibility degradation.....</b>	<b>10</b>
2.1	Introduction.....	10
2.2	Factors influencing visibility .....	10
2.2.1	Light extinction .....	11
2.2.2	Light absorption and scattering by particles.....	16
2.2.3	Summary .....	21
2.3	Visibility and Human Perception .....	21
2.3.1	Pollution and other impacts on perception of visibility .....	22
2.3.2	Perception, visual range and light extinction .....	23
2.3.3	Community perception and visibility management .....	25
2.3.4	Guidelines/ standards and legislation .....	26
2.3.5	Summary .....	28
2.4	Monitoring Methods.....	28
2.4.1	Visual Range .....	28
2.4.2	Digital Camera .....	29
2.4.3	Apparent contrast.....	30
2.4.4	Optical measurements.....	30
2.4.5	Visibility Surveys .....	33
2.4.6	Summary .....	33
2.5	Sources of visibility degradation.....	34
2.5.1	Methods for assessing sources of reduced visibility .....	34
2.5.2	Analysis of particle composition .....	35
2.5.3	Extinction budget analysis case studies .....	35
2.5.4	Summary .....	41
2.6	Haze investigations in New Zealand .....	42
2.7	Summary.....	44
<b>Chapter 3</b>	<b>Air Quality in Christchurch .....</b>	<b>45</b>
3.1	Introduction.....	45



3.2	Meteorology .....	45
3.3	Air quality monitoring .....	48
3.3.1	Monitoring network .....	48
3.3.2	Trends .....	49
3.3.3	Seasonal variations .....	52
3.3.4	Daily variations .....	53
3.4	Legislative Background .....	54
3.4	Sources of PM <sub>10</sub> in Christchurch .....	55
3.5	Air quality management in Christchurch .....	57
3.6	Summary .....	58
<b>Chapter 4</b>	<b>Site, Equipment and Methodology .....</b>	<b>59</b>
4.1	Introduction .....	59
4.2	Methodology .....	59
4.3	Monitoring site .....	61
4.4	Equipment .....	62
4.4.1	Conversions of instrument outputs .....	65
4.5	Data analysis .....	67
4.5.1	Factor analysis – PCA .....	67
4.5.2	Multiple regression analysis .....	69
4.6	Visibility survey .....	69
4.6.1	Selection of images .....	70
4.6.2	Survey design .....	70
4.7	Summary .....	70
<b>Chapter 5</b>	<b>Measurements of visibility and air quality .....</b>	<b>72</b>
5.1	Light extinction and air quality data .....	72
5.2	Daily variations in light extinction and air quality .....	76
5.3	Meteorology .....	81
5.3.1	Impact on light extinction .....	83
5.4	Particulate measurements .....	88
5.4.1	PM <sub>2.5</sub> concentrations .....	89
5.4.2	Elemental carbon measurements .....	91
5.4.3	Elemental and organic carbon .....	92
5.4.4	Carbon proportion of PM <sub>2.5</sub> .....	93
5.5	Summary .....	93
<b>Chapter 6</b>	<b>Sources of PM<sub>2.5</sub> mass .....</b>	<b>95</b>
6.1	Concentrations of elements .....	95
6.1.1	Seasonal variations .....	97

6.2	Correlations between elements .....	99
6.3	Factor analysis .....	102
6.3.1	Source profiles.....	102
6.3.2	Source contributions to PM <sub>2.5</sub> mass.....	109
6.4	Summary.....	113
<b>Chapter 7</b>	<b>Source contributions to light extinction .....</b>	<b>115</b>
7.1	Sources of particulate mass on high extinction days.....	115
7.2	Source strength and light extinction on all days .....	116
7.3	Source contributions to light scattering .....	119
7.4	Source contributions to light absorption.....	121
7.5	Overall contributions to light extinction.....	122
7.5.1	Contributions on high light extinction days .....	122
7.5.2	Seasonal variations in contributions to light extinction .....	124
7.6	Comparison to reconstructed light extinction .....	125
7.7	Summary.....	126
<b>Chapter 8</b>	<b>Case Studies .....</b>	<b>128</b>
8.1	Winter Haze .....	128
8.1.1	18 May 2000 .....	128
8.1.2	20 June 2000 .....	133
8.2	Summer Haze.....	137
8.2.1	22 February 2001.....	137
8.2.2	28 February 2001.....	141
8.3	Comparison of case study days .....	144
8.4	Summary.....	145
<b>Chapter 9</b>	<b>Visibility perception – fog, smog or haze .....</b>	<b>146</b>
9.1	Visibility perception survey .....	146
9.1.1	Survey results .....	146
9.1.2	Development of a visibility standard for Christchurch .....	149
9.1.3	Implications for further studies .....	150
9.2	Factors influencing perception.....	151
9.2.1	Inconsistencies in the visibility study .....	151
9.2.2	Moisture .....	155
9.3	Summary.....	158
<b>Chapter 10</b>	<b>Discussion and conclusion .....</b>	<b>159</b>
10.1	Major research findings .....	159
10.2	Limitations of the research .....	160
10.3	Implications for visibility management.....	161

10.4 Future research .....	163
<b>REFERENCES .....</b>	<b>164</b>
<b>APPENDICES .....</b>	<b>171</b>
<b>Appendix A: - Visibility Survey .....</b>	<b>172</b>
<b>Appendix B: Filter sampling periods .....</b>	<b>173</b>
<b>Appendix C: Monthly summary statistic for concentrations of elements .....</b>	<b>175</b>
<b>Appendix D: Pearsons correlation matrices for Teflon and polycarbonate filters .....</b>	<b>178</b>
<b>Appendix E: Comparison of St Albans and Polytechnic wind data .....</b>	<b>180</b>
<b>GLOSSARY OF TERMS .....</b>	<b>183</b>
<b>GLOSSARY OF ELEMENTS (used in PIXE analysis) .....</b>	<b>193</b>

---

## Tables

---

Table 2.1: Proposed visibility indicators for New Zealand (MfE, 1999a).....	27
Table 3.1: Daily PM <sub>10</sub> emissions (kg) by time of day (Wilton, 2001).....	56
Table 4.1: Visibility monitoring programme. ....	59
Table 4.2: Limits of detection (LOD) for PIXE and IC analyses. ....	68
Table 5.1: Seasonal variations in poor visibility. ....	74
Table 6.1: Summary statistics for particulate collected on daytime filters from 06:00 to 13:00 from February 2000 to April 2001. ....	96
Table 6.2: Pearson correlation matrix for concentrations of elements on filters. ....	100
Table 6.3: Source profiles – PCA rotated loading matrix.....	104
Table 6.4: Element contributions to source profiles. ....	105
Table 6.5: Burning profiles for wood burning from this study. ....	107
Table 6.6: Composition of Mt Victoria tunnel “motor vehicle” fingerprints (from Markwitz <i>et al.</i> , 2001). ....	108
Table 9.1: Summary of initial visibility survey results for photo list one, organised in order of increasing light extinction. ....	147
Table 9.2: Summary of initial visibility survey for photo list two organised in order of increasing light extinction.....	148
Table 9.3: Summary of visibility survey (photo list one) – all respondents.....	149
Table 9.4: Survey and light extinction data for images with anomalous survey results. ....	152
Table 9.5: Comparison of visibility data at 09:00 and 10:00 on the 4 May 2000. ....	156
Table 9.6: Summary data for high light extinction days. ....	157
Table A1: Filter sample numbers, dates and times.....	173
Table A2: Monthly summary statistics for concentrations of elements by month of year.....	175
Table A3: Pearsons correlation matrix for concentrations of elements on Teflon filters. ....	178
Table A4: Pearsons correlation matrix for concentrations of elements on polycarbonate filters. ....	179

## Chapter 1 Introduction

The term visibility can mean different things to different people. For example, to an air traffic controller, visibility is described in terms of visual range, that is, how far they can see. A less simplistic definition is that provided by the USEPA (1998a): “The appearance of scenic features when viewed from a distance”. This definition encompasses qualities of the image, such as colour, texture and contrast, not captured by historical descriptions of visibility, and includes factors that influence the visual impact of an object in the distance.

These factors include characteristics of the observer, optical illumination, optical characteristics of the object and the intervening atmosphere (Figure 1.1). Characteristics of the observer that impact on what is seen include their detection threshold and psychological response. For example, a person with impaired vision will see less clearly than a person with good eyesight.

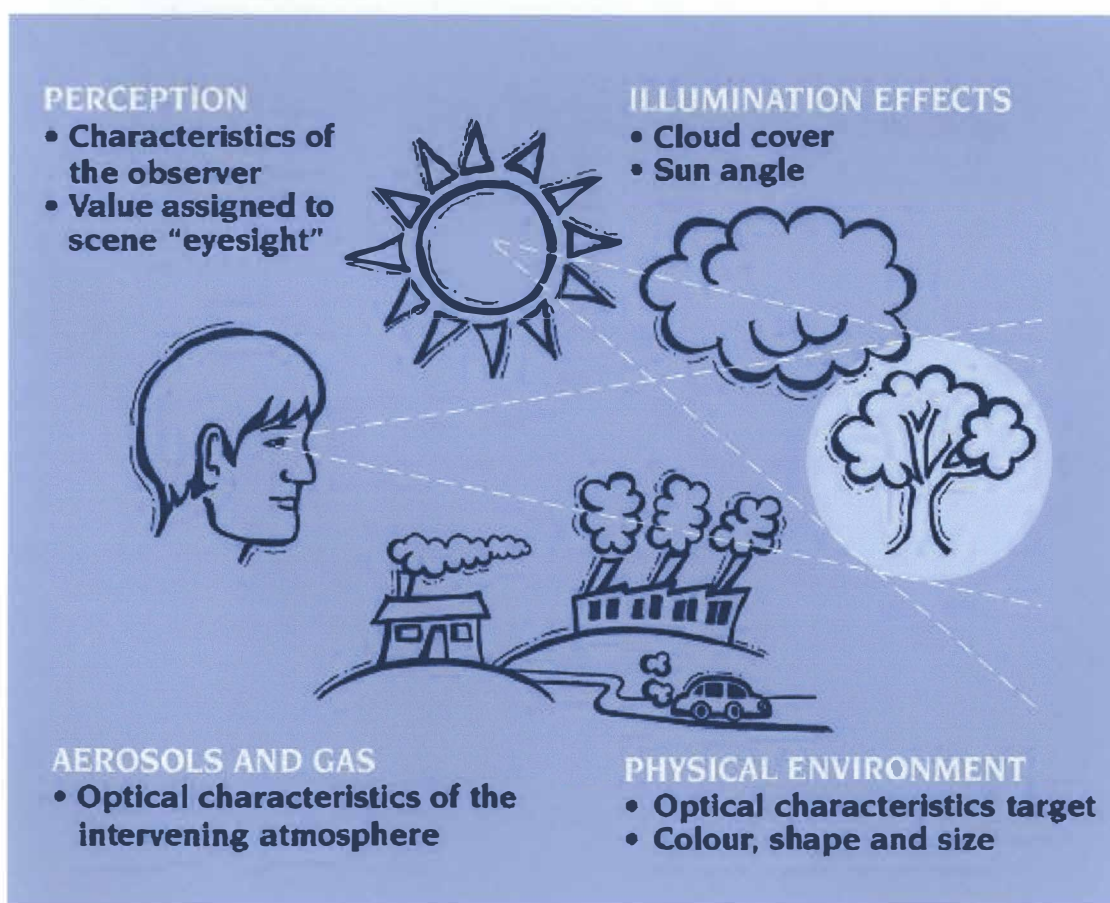


Figure 1.1: Factors influencing visibility (adapted from USEPA (1998a))



In Christchurch, the visibility of the Southern Alps, approximately 60 kilometres to the north-west of the city, is much better on mornings when the prevailing airflow is from the north-west. Under these conditions there is often cloud covering the city and much of the area towards the Alps, but a clear sky above the mountains (as shown in Figure 1.2). This illustrates the effect of sun angle and cloud cover on visibility.



Figure 1.2: Illustration of the impact of illumination on the Southern Alps under north-westerly airflow, viewed from Christchurch.

The optical characteristics of the object being viewed also impact on its visibility. This is also illustrated in Figure 1.2 by the limited contrast between the whiteness of the mountains in the distance and the sky. Texture and brightness are also properties of the target that impact on its clarity (USEPA, 1998a).

Particles and gases contained in the air between the observer and the object reduce visibility by scattering and absorbing light. These processes are described in detail in Chapter 2. Visibility is also a function of path-length as the greater the distance to the object the more scattering and absorption that occurs. The optical characteristics of the atmosphere are the aspects of visibility that can be managed to preserve or enhance visibility.

Particles and gases that scatter and absorb light can originate from a number of sources and can be of primary or secondary origin. Primary particles are those that are emitted directly to the atmosphere and include sources such as combustion, abrasion and natural emissions. Secondary particles are formed as a result of chemical reactions in the atmosphere. In some

cities photochemical pollution is the main contributor to degraded visibility. Photochemical pollution occurs as a result of chemical reactions involving nitrogen oxides and sunlight. The secondary particles formed during these reactions create haze, such as that observed in Los Angeles. Natural emissions, such as chloride from sea salt or terpenes from trees, can result in visibility reduction in otherwise pristine locations. Wind blown dust can also have a major impact on visibility, as frequently observed in Australia.

Visibility has been identified as a major air quality issue in a number of countries and is particularly important in areas where views are considered an important tourist attraction. Extensive visibility studies have been carried out in such areas as the Grand Canyon because of the importance of visibility to the visitors' experience. Visibility can also be a major issue for residents, particularly if they perceive their location as being a desirable and clean place to live. Over the last two decades, studies relating to visibility have become increasingly popular in the United States and Canada. This reflects the high value placed on amenity effects of air pollution in these locations.

Across the whole of New Zealand, visibility is generally considered to be excellent. However, brown haze is noticeable in a number of urban areas, including Christchurch and Auckland, and localised sources of degraded visibility occur in most areas (Figure 1.3). This study focuses on Christchurch and considers the issue of visibility degradation in that city. In this Chapter, an overview of visibility degradation and visibility issues in Christchurch is presented and the research objectives and hypothesis and the structure of the thesis are described.



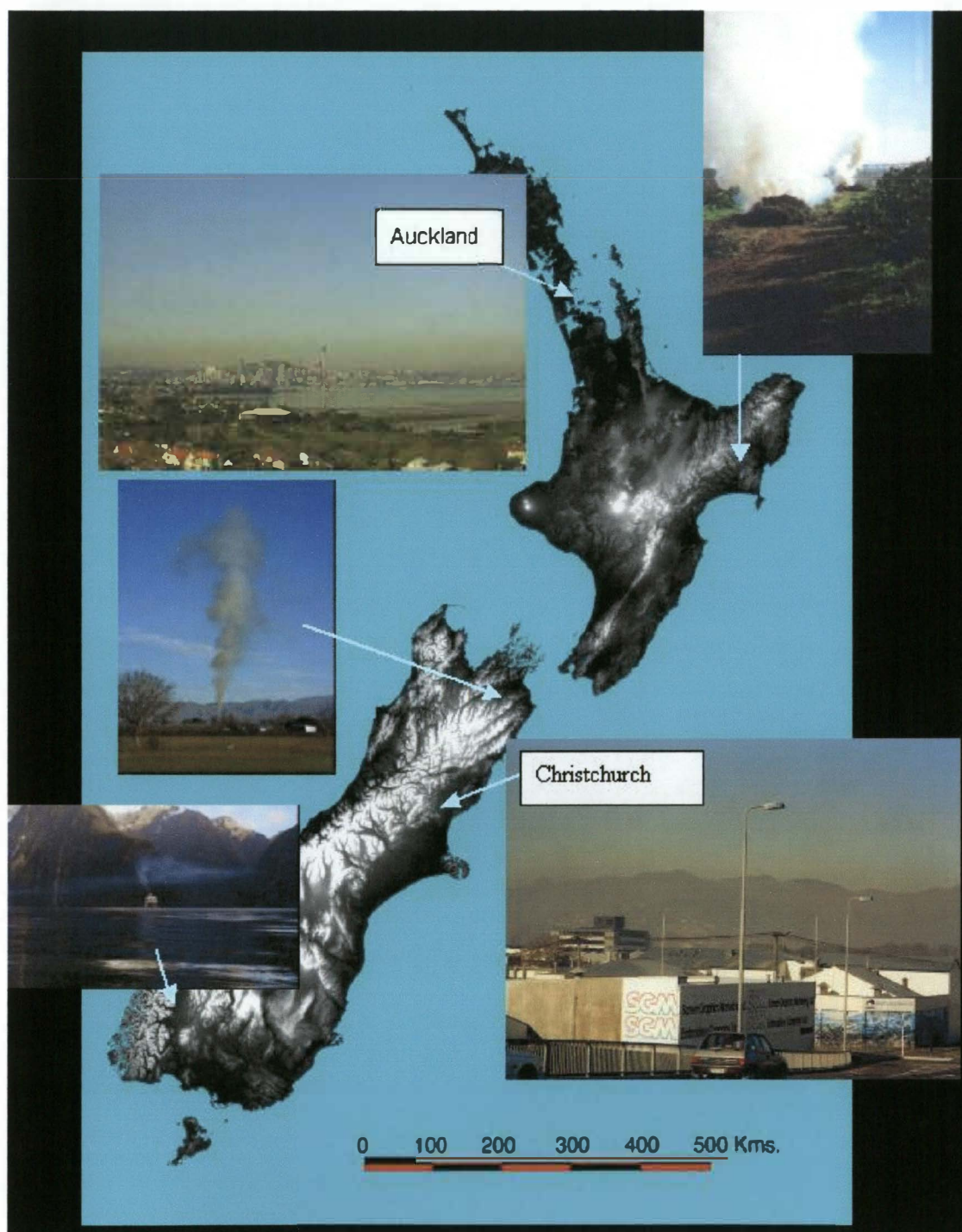


Figure 1.3: Illustration of brown haze in Christchurch and Auckland (Auckland photograph courtesy of Jayne Metcalfe, Auckland Regional Council).

## 1.1 Visibility in Christchurch

Christchurch is located in the South Island of New Zealand and has a population of more than 300,000. Located on the Canterbury Plains, the topography of the city is largely flat, although some elevation is provided by the Port Hills to the south. The Southern Alps, located approximately 60 kilometres to the west, the gradual slope of the Canterbury Plains, and the

Pacific Ocean bordering the city to the east, impact on the meteorology of Christchurch. Temperatures in the city average around 17 °C during the summer and decrease to an average of around 8 °C during the winter months<sup>1</sup>.

In Christchurch, brown haze is a common daytime occurrence during the winter months (Figure 1.3). This haze is typically observed on calm frosty days and coincides with periods of stable air and low wind speeds. Haze is also visible, although less common, during the summer months, particularly when viewing the city from the Port Hills. While it is possible that photochemical reactions could contribute to summer haze in Christchurch, air quality monitoring during these months has found low concentrations of ozone, a component of photochemical pollution (Aberkane, 2001).

While there is some indication that visibility is a major concern for Christchurch residents, (Lamb, 2001), there is confusion over air quality issues in the city. In particular, submissions on a proposed coal ban indicated that many people did not differentiate between the management of PM<sub>10</sub> to reduce 24-hour average concentrations to protect health, and the management of visibility. Consequently, there appears to be an expectation that measures proposed to reduce PM<sub>10</sub> concentrations to acceptable health guidelines will also address visibility problems. This is also illustrated in public responses to visibility issues presented in the local newspaper, The Press (Figure 1.4).

---

<sup>1</sup> Data from the St Albans monitoring site in Christchurch for temperature at 1 metre.

Sir—Christchurch's ongoing smog problem has recently caused Environment Canterbury to recommend even tougher regulations against open fires and solid-fuel burners than three years ago.

The Auckland Regional Council, however, is blaming the Auckland smog problem, said to be worse than London, on traffic. It makes one wonder whose experts are correct.

We are informed that the PM<sub>10</sub> particulates from fires and solid-fuel burners are the cause of Christchurch's air pollution, yet the smog haze is still evident in summer (with no fires burning) when Christchurch is viewed from the Port Hills.

Surely if we, as a community, are serious about solving the Christchurch clean air issue we should not just be targeting one factor, but be looking at all areas for solutions, including reducing electricity prices instead of increasing them, as has just occurred.

FREDAVISSE  
August 18, 2000

### Air quality

Sir—Once again the issue of Christchurch's "winter smog" hits the front page (May 19), and councillors pinpoint wood burners as the culprits. Why is it they have a perpetual blind spot for vehicle emission?

As a regular commuter across the Port Hills, I witness regularly, throughout all four seasons, the same murky blanket of filth over Christchurch. Can I suggest that a Press photographer go back to the Sign of the Takahe several times during January or February to bring this point home? Readers and councillors will be amazed to discover that, invariably, on cloudless midsummer days, the alps are blotted from view by a contaminated atmosphere not always visible from street level.

How many home fires are burning at that time of year? None whatsoever.

CHRIS WATKINS  
May 20, 2000

Figure 1.4: Letters to the Editor, published in Christchurch newspaper, The Press.

A small number of studies have considered reduced visibility in Christchurch (e.g., Thompson, 1996; NIWA, 1998; Wilson, 1999). The most extensive of these (Wilson, 1999) suggested that light scattering and light absorption by particles each contribute about 40% of light extinction. However, little is known about the sources of visibility degradation in Christchurch and the extent to which measures proposed to reduce 24-hour average PM<sub>10</sub> concentrations for health reasons will improve daytime visibility.

Figure 1.5 provides details of an approach to visibility management in Christchurch. It is assumed, based on the results of a survey by Lamb (2001) that current levels of visibility are unacceptable. As a result, research identifying the causes of reduced visibility, their interaction with natural phenomena, and the management options required to achieve acceptable levels of visibility, are required. This thesis attempts to address these research needs and has a particular emphasis on identifying the key contributors to reduced visibility in Christchurch.



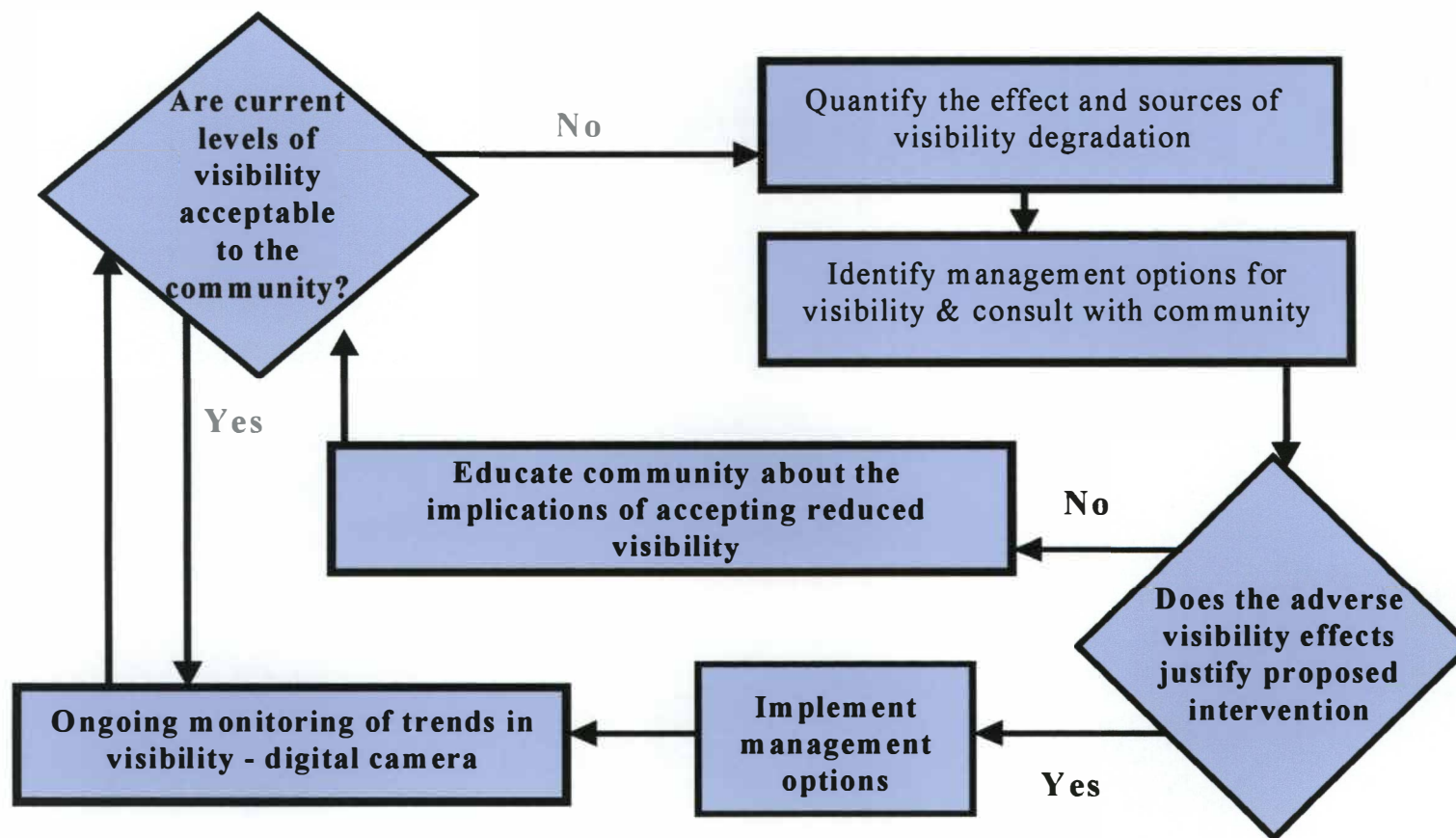


Figure 1.5: Schematic diagram of process for managing visibility in Christchurch.

## 1.2 Objectives and hypothesis

The objective of the research is to:

- Determine the contribution of different factors to reduced visibility in Christchurch.
- To examine temporal variations in causes of reduced visibility.
- To assess the relationship between perceived air quality and the physical and chemical properties contributing to visibility degradation.

### Hypothesis

*The physical and chemical factors contributing to reduced daytime visibility in Christchurch are complex, vary with season and have a significant impact on perceived air quality.*

The research proposes to answer the following key questions:

- What causes reduced visibility and brown haze in Christchurch? That is, to what extent do different contaminants and physical properties contribute to light extinction in Christchurch?
- What variations exist, if any, in the composition of summer versus winter haze in Christchurch?
- What are the implications of this knowledge to the management of reduced visibility in Christchurch?
- What is the relationship between perceived air quality and light extinction in Christchurch?

## 1.3 Overview of thesis

The purpose of this thesis is to contribute to the understanding and management of visibility in Christchurch. Sources of reduced visibility will be identified and temporal variations in visibility and contributing species and their interaction with meteorological parameters will be assessed. Results are considered in the context of:

- Visibility degradation and the objectives of the thesis (Chapter 1).
- Current understanding of visibility principles and overseas studies (Chapter 2).
- Air quality and air quality management in Christchurch (Chapter 3).

The purpose of Chapter 1 is to introduce the research topic, provide an overview of visibility issues in Christchurch and outline the research objectives and hypothesis. The theory of light extinction and relevant visibility research carried out overseas and in New Zealand is discussed in Chapter 2. Chapter 2 also details the physical processes by which particles and gases reduce visibility and the influence of particle size and composition. Methods used to determine sources of visibility degradation are discussed, as is research relating to human perception of visibility.

Chapter 3 provides the research context and includes the topographical and meteorological characteristics of the Christchurch environment, local air quality issues, the legislative framework, and air quality management in Christchurch. The need for further research into causes of reduced visibility in Christchurch is established in the context of future visibility management.

The methodology and instrumentation used for assessing factors contributing to visibility degradation in Christchurch are detailed in Chapter 4. This includes the monitoring periods and the methods use to analyse data to meet the research objectives. Results of the monitoring presented in Chapter 5 include details of seasonal variations in light extinction in Christchurch as well as comparison of the results of different monitoring methods for particles and carbon measurements.

The contribution of different particulate sources to the measured particle mass are presented in Chapter 6 based on the results of statistical analyses of the composition of the particulate collected on filters. Chapter 7 then considers the contributions of these sources to light scattering and absorption by particles and the overall contributions of different sources to light extinction. A selection of summer and winter high extinction days are examined in Chapter 8 to provide further detail on variations in contributing factors, as well as seasonal differences.

In addition to examining the physical properties of visibility degradation, a study of the relationship between light extinction and visibility perception is included in Chapter 9. This presents the results of a survey in which participants were required to rate the visibility in a selection of Christchurch images and indicate whether or not they considered the amount of visibility degradation to be unacceptable. Chapter 10 considers the results detailed in Chapters 6-9 in the context of the research objectives and thesis hypothesis detailed in Section 1.4. The thesis concludes with a glossary of terms and elements referred to throughout the thesis.

## **1.4 Summary**

Visibility, the extent to which objects can be seen from a distance, is a major air quality issue for many people. Visibility is influenced by a number of factors. In particular, particles and gases in the atmosphere influence visibility by scattering and absorbing light. While visibility in New Zealand is generally regarded as being excellent, in Christchurch visibility is impaired at times during both the summer and winter months. It is likely that current visibility in Christchurch is unacceptable to the Christchurch community. This Chapter identifies the need for further research into sources of visibility degradation before measures to manage visibility in Christchurch can be proposed. The theory underlying the assessment of visibility degradation, relevant visibility research and factors influencing visibility perception and its relationship to light extinction is considered in Chapter 2.

## **Chapter 2 Processes, perception, monitoring and causes of visibility degradation**

### **2.1 Introduction**

Visibility research relevant to this thesis generally falls into one of four broad areas: factors influencing visibility, perception of visibility, monitoring methods, and assessment of causes of reduced visibility. This Chapter discusses each of these aspects of visibility in turn. The first category, factors influencing visibility, focuses on light extinction and the processes by which visibility is reduced because of air quality. This is outlined in Section 2.2 and includes the influence of particle size and composition on visibility, and the impact of relative humidity.

Studies relating to visibility perception (Section 2.3) include assessing acceptable levels of visibility (e.g., Pryor, 1996; Ely *et al.*, 1991), the impact of increases in contaminant concentrations on visibility (USEPA, 1998a) and establishing guidelines or policy for visibility (e.g., the United States Clean Air Act amendments 1977).

Monitoring methods for visibility include the use of optical instruments, as well as the assessment of images. Several studies have examined the potential for using images to quantify the effects of degraded visibility and methodologies for relating images to concentrations of contaminants (e.g., Richards, 1988). Section 2.4 discusses these studies and the current use of different methods in visibility assessments.

Major research into the causes of reduced visibility has been carried out in a number of locations in the United States (e.g., as detailed in Schichtel *et al.*, 2001) and in Canada (Pryor, *et al.*, 1997). Section 2.5 examines the methods used to identify the relative contributions of different factors to reduced visibility and presents three major investigations as case studies.

Visibility research in New Zealand has primarily focused on monitoring methods and visibility/perception surveys although some attempts at assessing causes have been made. Section 2.6 gives an overview of visibility research previously carried out in New Zealand.

### **2.2 Factors influencing visibility**

The way that different factors can influence visibility is fundamental to any research into the causes or sources of visibility degradation. Chapter 1 identifies a number of factors that impact on the



visual impact of an object in the distance, including characteristics of the observer, optical illumination, optical characteristics of the object and the intervening atmosphere. The focus of this Section is how the intervening atmosphere impacts on visibility degradation.

The impact of the intervening atmosphere in reducing visibility occurs because of particles and gases in the air between the observer and the object. These particles and gases reduce the intensity of the light beam, a process that is referred to as light extinction. Visibility studies involving assessment of light extinction generally relate to the impact of anthropogenic causes of visibility degradation, that is, particles and gases from anthropogenic sources. In addition to light extinction, measures used to describe visibility include visual range (Koschmieder, 1924) and contrast (Horvath, 1994). These methods are outlined in Section 2.4.

### 2.2.1 Light extinction

The extinction coefficient ( $B_{\text{ext}}$ ) determines the extent to which visibility is reduced per unit of distance because of air quality. The units typically used for light extinction are inverse megametres ( $\text{Mm}^{-1}$ ) (the reciprocal of 1 million metres) or inverse kilometres ( $\text{km}^{-1}$ ) (USEPA 1998b). Thus light extinction refers to the amount of light lost as it travels more than one million metres and is given by:

$$B_{\text{ext}} (\text{Mm}^{-1}) = B_{\text{sp}} + B_{\text{sg}} + B_{\text{ap}} + B_{\text{ag}} \quad \text{Equation 2.1}$$

where

- $B_{\text{sp}}$  is light scattering due to particles
- $B_{\text{sg}}$  is light scattering due to gases
- $B_{\text{ap}}$  is light absorption due to particles
- $B_{\text{ag}}$  is light absorption due to gases

Each of these components is now considered in turn.

#### Light scattering by particles ( $B_{\text{sp}}$ )

Light scattering occurs when the radiant energy of light is retained by the particles or gases, causing a brief polarisation of the molecules, ions or atoms present. This polarisation is followed by re-emission of the radiation in all directions as the particles or gases return to their original state (Skoog, 1985).

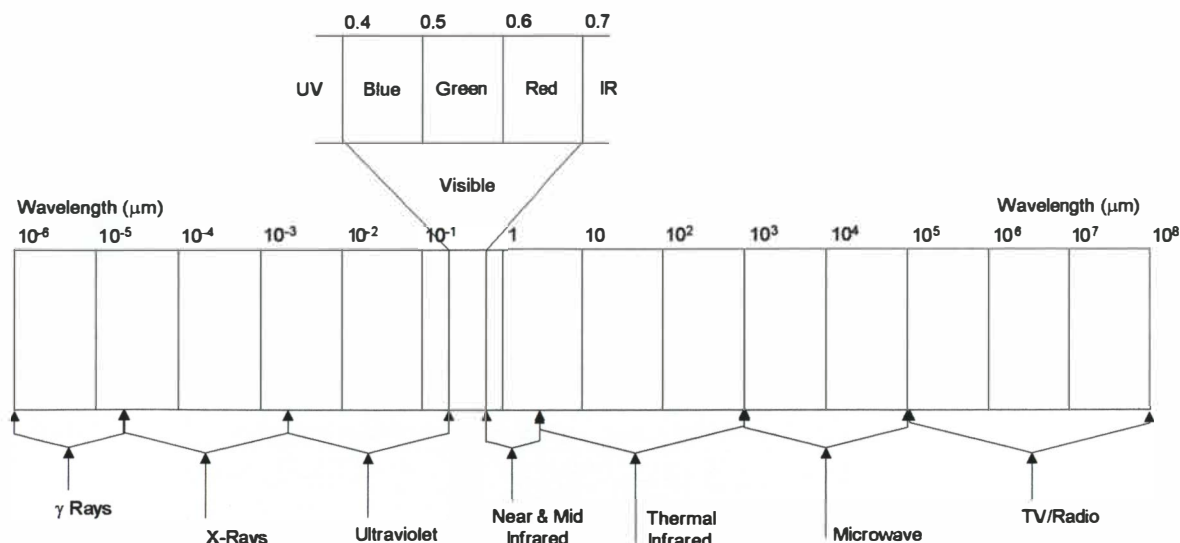


Figure 2.1 The electromagnetic spectrum, highlighting the visibility section of the spectrum (adapted from Skoog, 1985).

Light scattering by particles in the visible part of the spectrum (Figure 2.1) is primarily described by Mie theory (Carroll, 1996), although extremely fine particles ( $< \sim 0.005 \mu\text{m}$ ) could exhibit Rayleigh scattering (Figure 2.2). Particles of a size that is within a factor of 10 of the wavelength of radiation will scatter light according to Mie theory (Carroll, 1996). Consequently, scattering by Mie theory is dominated by the  $0.2 - 2 \mu\text{m}$  size fraction. These fine particles scatter light more effectively, per unit mass, than gases or larger particles, because of their size relative to the wavelength of visible light. For Mie scattering, a size parameter ( $\alpha$ ) is usually defined in terms of the ratio of the scattering particle radius ( $r$ ) to a given wavelength ( $\lambda$ ):

$$\alpha = \frac{2\pi r}{\lambda} \quad \text{Equation 2.2}$$

The amount of scattering that occurs depends on the index of refraction of the material, the size of the particle and the shape of the particle.

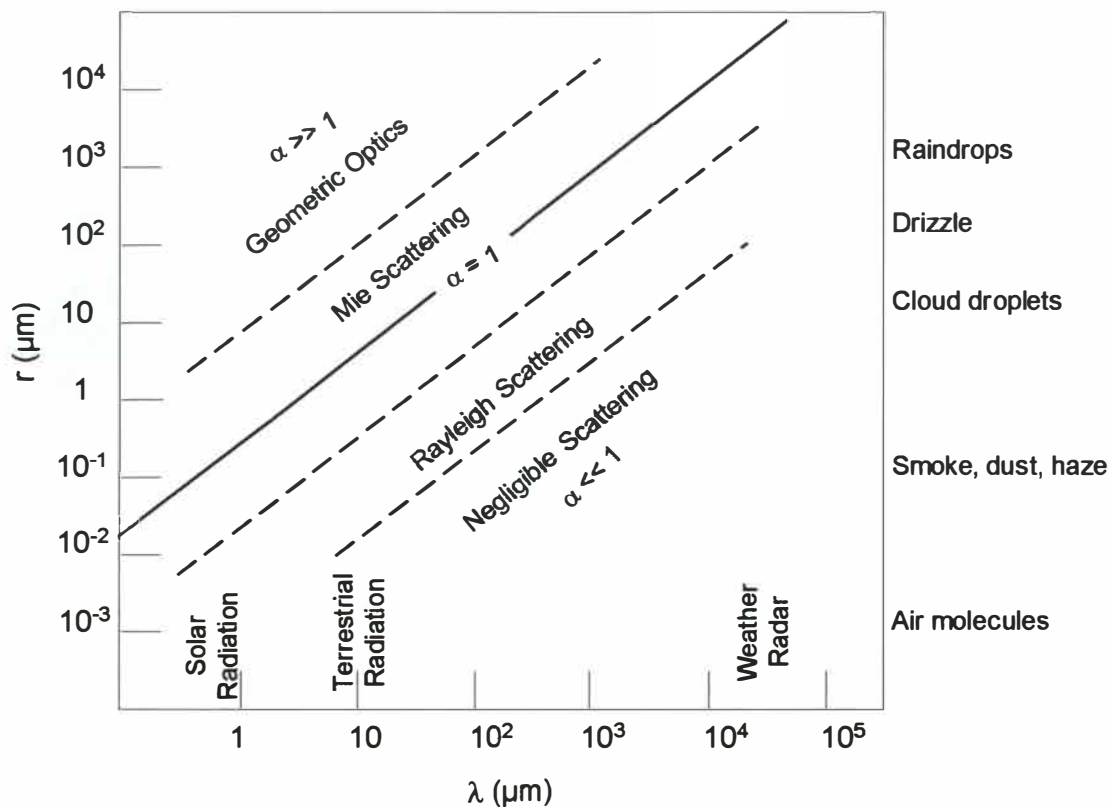


Figure 2.2: Radiation wavelength regimes of radiative phenomena for ranges of particle sizes and wavelengths (from Carroll, 1996)

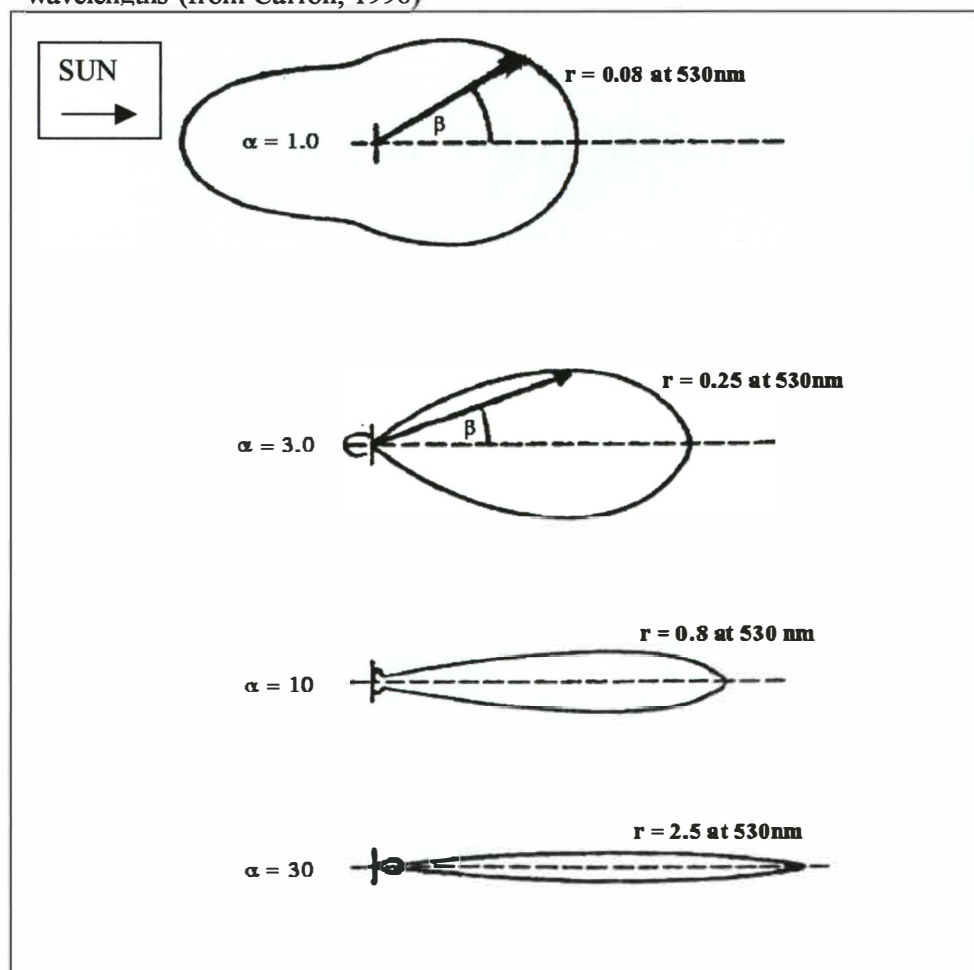


Figure 2.3: Mie scattering patterns for increasing particle sizes (adapted from Carroll, 1996).

The angular distribution of scattered light ( $\beta$  in figure 2.3) refers to the angle between the original direction of light propagation and the new direction of propagation and is a function of particle size. The amount of radiation scattered in the direction of  $\beta$  is given by Equation 2.3 (from Carroll, 1996).

$$S_{\lambda}(\beta) = (E_{\lambda} k(\alpha) A(z) \sec Z dz) P(\beta) \quad \text{Equation 2.3}$$

where  $\beta$  is the scattering angle,  $P(\beta)$  is the phase function describing the probability distribution of scattering directions,  $E_{\lambda}$  = monochromatic irradiance (flux/unit area),  $k(\alpha)$  = scattering efficiency per unit cross sectional area of scatter,  $A(z)$  = total cross sectional area presented to the radiation in an incremental layer;  $dz$  is the thickness of a horizontal layer of air,  $Z$  is the zenith angle and  $\sec Z$  represents the path length correction for situations in which the beam is not perpendicular to the layer.

Figure 2.3 illustrates the effect of  $\alpha$  on the pattern of light scattering and scattering angle ( $\beta$ ) with greater scattering in the forward direction and an increase in forward scatter with increasing particle size. As a result, haze looks worse when viewed in the direction of the sun. Scattering angles between forward and backscatter also impact on the brightness of the haze. Light scattering by larger, coarser particles occurs primarily in the original direction of light (see  $\alpha=30$ , Figure 2.3) where it mostly contributes much less to air light under most viewing angles (White *et al.*, 1994). Thus larger particles result in a smaller  $\beta$  angle and a narrower set of viewing angles than finer particles.

### **Light scattering by gases ( $B_{sg}$ )**

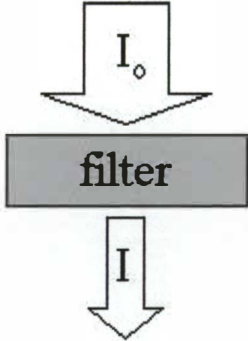
Gaseous pollutants have little effect on visibility and scatter light in much the same way as it is scattered by gases in clean air. Light scattering by gases in the atmosphere ( $B_{sg}$ ) is described by Rayleigh scattering theory. Rayleigh scattering by gases is constant for any given wavelength and does not vary with increasing concentration. Shorter wavelength radiation (blue) is scattered more efficiently than longer wave radiation (red), resulting in the blue colour of the sky during the daytime. During sunrise and sunset there is a greater path length through the atmosphere between the viewer and the sun, so that nearly all the blue light is scattered out of the light beam and the longer wavelengths (red) are dominant.

Rayleigh scattering by gases in the visibility wavelengths typically ranges from  $9 \text{ Mm}^{-1}$  in high altitudes to about  $12 \text{ Mm}^{-1}$  at low altitude (Sisler & Malm, 1997). Wilson (1999) calculated Rayleigh scattering owing to gases of  $13.7 \text{ Mm}^{-1}$  for Christchurch at 530 nm, for standard pressure and a temperature range of 0-15°C.

## Light absorption by particles ( $B_{ap}$ )

Particle absorption occurs when electromagnetic energy from the radiation (light) is transferred to the particles. For example, a photon may be destroyed and its energy transformed in some way. If a light wave of a given frequency strikes a material with electrons having the same vibrational frequencies, then those electrons will absorb the energy of the light wave and transform it into vibrational motion. The chemical composition of the particle plays a major role in its ability to absorb light. The absorption of light by a particular material occurs because the frequency of the light matches the frequency at which electrons in the atoms of that material vibrate. Different atoms and molecules have different natural frequencies of vibration, so they will selectively absorb different frequencies of visible light.

Light absorption by particles and gases in the air is described by the Bouger-Lambert (Beer's) Law. For particles collected on a filter Beer's Law is given by Equations 2.4 (Twomey, 1977).



The diagram illustrates the setup for Beer's Law. It shows a downward-pointing arrow labeled  $I_0$  representing incident light intensity. This arrow points to a gray rectangular box labeled "filter". Below the filter, another downward-pointing arrow labeled  $I$  represents the transmitted light intensity.

$$A = \ln(I_0/I)$$

Equation 2.4

where

- $A$  is the absorbance - how much light was absorbed while passing through the filter
- $I$  is the intensity of light transmitted
- $I_0$  is the original intensity of light before passing through the filter.

Calculation of absorption coefficient is based on the change in filter transmission ( $I/I_0$ ) for a given volume of sample air. The absorption coefficient without correcting for filter type and loading, is shown in Equation 2.5 (Twomey, 1977).

$$b_{ap} = (\text{area/volume}) \ln(I_0/I)$$

Equation 2.5

where

- $b_{ap}$  is the absorption coefficient [ $m^{-1}$ ]
- area is the area of the sample spot [ $m^2$ ] - different for each instrument
- volume is the volume of air sampled in averaging period [ $m^3$ ]

## Light absorption by gases ( $B_{ag}$ )

With the exception of nitrogen dioxide, gaseous pollutants play little part in reduced visibility due to light absorption ( $B_{ag}$ ). This is because  $NO_2$  is the main gaseous ambient air pollutant that occurs in sufficient concentrations to absorb light in the visible spectrum. Other gases that absorb light include bromine, which is not found in sufficient concentrations in ambient air and ozone, which absorbs light only weakly and is therefore not generally included in visibility studies.

The main ambient air gas that absorbs light is  $NO_2$  and as concentrations increase so does light absorption by gases ( $B_{ag}$ ). Nitrogen dioxide absorbs shorter wavelength radiation (blue), and in ambient air results from emissions of nitrogen oxides, which get converted to  $NO_2$  through chemical reactions in the lower atmosphere. Motor vehicles are the main source of nitrogen oxides in most locations.

### 2.2.2 Light absorption and scattering by particles

Particle size is clearly an important factor impacting on light scattering and is described by Mie theory (Section 2.2.1). Consequently, the formation of particles and the distribution of different sized particles will impact on visibility degradation. Similarly, the chemical composition of the particles can impact on visibility degradation, particularly in terms of light absorption. Background information on particle size distribution, classification and formation are presented in this Section, as well as information on the chemical composition of particles in terms of their effect on both scattering and absorption. These factors are also considered in the context of the chemical phase and relative humidity, and the effect of their interaction on visibility.

#### Particle size

Particulate matter can be classified according to fine and coarse modes, which largely separate particles on the basis of the source of the material (figure 2.4). Primary fine-mode particles result from the condensation of molecules, typically from combustion processes, while secondary fine mode particles result through the reaction of gases, such as  $SO_2$  with  $NH_3$ , in the atmosphere (QUARG, 1996). These fine-mode particles are formed through the nucleation<sup>2</sup> of such species and grow by coagulation<sup>3</sup> and the condensation of other gases on the nuclei. Fine mode particles can be classified as either nucleation mode (i.e., new particles in ultra-fine or nuclei mode), or accumulation mode (i.e., particles grown through coagulation and condensation) (Chow, 1995; USEPA, 1996; QUARG, 1996).

---

<sup>2</sup> Molecules of complementary substances combine to form a condensation nucleus.

<sup>3</sup> The combination of existing particles.



Nucleation mode particles are extremely small, with a particle size range of approximately 1 nm to 0.1  $\mu\text{m}$ . While the greatest numbers of particles of total suspended particulate are typically present in the nucleation mode, the small size of these particles means only a small contribution to the total mass concentration (Chow, 1995). Particles in the accumulation mode are roughly in the size range 0.05  $\mu\text{m}$  to 2  $\mu\text{m}$  and can constitute a significant portion of particulate mass concentration (QUARG, 1996). These particles are long-lived in the atmosphere, as removal mechanisms are least efficient in this size range (USEPA, 1996)

Coarse-mode particles are formed by mechanical processes such as crushing, grinding and abrasion of surfaces, during which larger pieces of material are broken down to smaller pieces. Fungal spores, pollen, and plant and insect fragments are examples of natural bio-aerosol, which may form part of suspended coarse-mode particles (USEPA, 1996). Coarse particles also include wind blown soils and sea-spray. The latter is a marine aerosol derived from the surface of the sea in conjunction with wind. The size distribution of marine aerosol is generally between 0.1 and 20  $\mu\text{m}$ , peaking at 6-8  $\mu\text{m}$ .

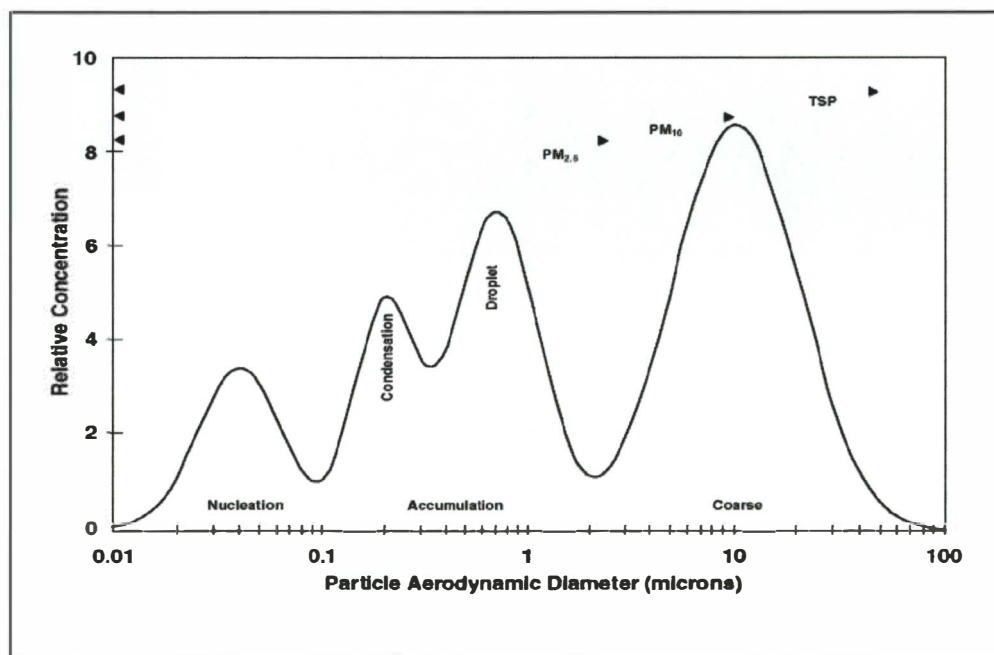


Figure 2.4: Relative concentrations of particles by aerodynamic diameter (microns), (from Chow, 1995).

Mie theory indicates that it is the fine ( $<PM_{2.5}$ ) size fraction that most effectively scatters light. Similarly light absorption is most effective for particles around 1  $\mu\text{m}$  (QUARG, 1996). Particles of this size fraction are generally the greatest contributor to reduced visibility. As indicated above, the greatest number of particles occurs within this size fraction. However, particle mass is dominated by larger particles. The thesis herein focuses largely on particle mass.



Coarse particles can also reduce visibility, but are typically one-half to one-third as effective as fine particles (Canadian Environmental Protection Act (CEPA), 1998). Groblicki *et al.*, (1981) found that in Denver most of the visibility reduction was due to particles smaller than 2.5 microns ( $\mu\text{m}$ ) in diameter, although a minor contribution came from elemental carbon larger than 2.5  $\mu\text{m}$ . In the eastern United States, light scattering by coarse particles is assumed to be negligible owing to vegetation effects and high relative humidity (White *et al.*, 1994). However, in the south-western United States, where vegetation is sparse and humidity low, coarse particles were found to contribute 25-33% of total light scattering (White *et al.*, 1994). The contribution was also found to be significant in the Grand Canyon area where Malm & Day (1999) found the mass-scattering efficiency of coarse particles to be greater than 0.4 to 0.6  $\text{m}^2 \text{g}^{-1}$ , with values of up to 1.0  $\text{m}^2 \text{g}^{-1}$  at times. These scattering and absorption efficiencies are expressed as square metres of light scattered per gram of contaminant and are multiplied by the concentration of contaminant in mass per cubic metre to give light extinction in inverse metres. That is,  $\text{m}^2 \text{g}^{-1} \cdot \text{gm}^{-3} = \text{m}^{-1}$ .

Particle size relative to the wavelength of light also influences the observed colour of haze. Particles smaller than the wavelength of light will give a bluish tinge to the haze (Carroll, 1996). However, as haze often consists of particles of a range of sizes, the observed colour can be a mix of the visible spectrum, giving a brown appearance. When the particles are much larger than the wavelength of light (e.g. >2.5  $\mu\text{m}$ ), the scattered light is white. While particle light absorption is a function of wavelength, the dependence is less marked than it is for light scattering by particles.

### **Particle composition**

The analysis of particles in terms of chemical composition is referred to as speciation. Most of the  $\text{PM}_{2.5}$  mass in urban and non-urban areas can be defined by a combination of elemental carbon, organic carbon, ammonium, nitrate, sulphate, sodium chloride, water and geological material (Chow, 1999). These different types of particles can have varying impacts on visibility. For example, sulphate particles degrade visibility primarily through their contribution to fine particle scattering (White, 1990), while elemental carbon contributes to both light absorption and light scattering. Nitrates contribute to light scattering, but are not as effective as sulphates per unit mass, while organic particles are less effective at light scattering (CEPA, 1998). Overseas studies have indicated that the main visibility reducing species are nitrate, sulphate, elemental carbon and nitrogen dioxide.

Elemental carbon is a chemically inert substance and is emitted from all processes involving the combustion of carbonaceous fuels. Elemental carbon, often referred to as black carbon or soot, is usually saturated with other combustion by-products that may be toxic or carcinogenic. Elemental

carbon has a 6-member carbon graphitic ring. Because of its microcrystalline structure, elemental carbon absorbs light very effectively (about  $10 \text{ m}^2\text{g}^{-1}$ , in the visual spectrum). This is the largest absorption of any common contaminant (Magee Scientific Company, 1992). As there is no standard method for discriminating particulate in terms of organic or elemental carbon, the relative quantity of each depends on the analytical method used (Chow, 1999).

Organic carbon, present as particulate, typically consists of thousands of separate compounds. Particulate organic carbon can originate from combustion, geological processes, road dusts and photochemistry (Chow, 1999). Semi volatile organic carbon species (a subset of organic carbon) exist in the atmosphere in equilibrium between particle and gas phases. Evaporative losses of semi-volatile organic compounds can occur. In western areas of the United States, organic carbon contributes approximately equally with sulphates and dust in the extinction budget (Laulainen & Trexler, 1997).

Particulate nitrate and sulphate are typically formed as a result of secondary reactions detailed in the following Section, although some primary emissions of these substances do occur. Sampling for particulate nitrate is subject to both positive and negative artefacts due to the reversible gas-to-particle phase equilibrium. Because the equilibrium is reversible, ammonium nitrate particles can evaporate into the atmosphere after collection on a filter, due to changes in temperature and relative humidity (Chow, 1999). In recent years, sampling systems have been designed to take account of the aerosol to gaseous interface, to minimise positive and negative artefacts in measured nitrate, sulphate and ammonium concentrations. However, some negative artefacts may still occur with the use of denuder systems because of reductions in the partial pressure of ammonia over the sample. Pressure drop in the instrument may also result in negative artefacts due to volatilisation. Both nitrates and sulphates are water-soluble and reside in the  $\text{PM}_{2.5}$  size fraction.

The chemical composition of nitrates or sulphates generally has little effect on light scattering for any given particle size (Tang, 1996). The exceptions are sulphuric acid and sodium chloride, which scatter light more efficiently than other inorganic salt aerosols such as  $\text{NH}_4\text{HSO}_4$ ,  $(\text{NH}_4)_2\text{SO}_4$ ,  $(\text{NH}_4)_3\text{H}(\text{SO}_4)$ ,  $\text{NaHSO}_4$ ,  $\text{Na}_2\text{SO}_4$ ,  $\text{NH}_4\text{NO}_3$  and  $\text{NaNO}_3$ ,  $\text{H}_2\text{SO}_4$  and  $\text{NaCl}$ . (Tang, 1996). Horvath (1992) also indicates that  $\text{NH}_4\text{NO}_3$  is more effective at light scattering than  $(\text{NH}_4)_2\text{SO}_4$ .

### **Sources of visibility reducing particles**

Particles can come from a wide variety of sources. Combustion processes are likely to be a significant source of particles in urban areas. The relative significance of different combustion types, such as domestic heating, transport or industrial combustion, will depend on location specific factors. Wind blown dust is another source of particles that can result in degraded visibility. This

can be a significant source overseas where sand and dust storms occur (QUARG, 1996). More locally, wind blown dusts can be observed from the Port Hills on windy days in the more rural areas towards the mountains. Breaking of waves on the sea causes the ejection of many tiny droplets of seawater into the atmosphere. These droplets dry by evaporation, leaving sea salt particles suspended in the air, and resulting in a localised haze. The majority of particles from this source are coarse in size, but some are small enough to have an appreciable atmospheric lifetime (QUARG, 1996). These natural sodium chloride particles (NaCl) can also react with anthropogenic sulphuric acid ( $\text{H}_2\text{SO}_4$ ) to form sodium sulphate ( $\text{Na}_2\text{SO}_4$ ) particles. Nitric acid ( $\text{HNO}_3$ ) also reacts with sea salt particles to form sodium nitrate ( $\text{NaNO}_3$ ) and contributes to coastal nitrogen loading (Pryor & Sorenson, 2000)

Particles can also result from secondary reactions in the lower atmosphere (USEPA, 1996). Where these reactions occur, sources of oxides of nitrogen ( $\text{NO}_x$ ), and oxides of sulphur ( $\text{SO}_x$ ) will also contribute to visibility reduction. Concentrations of  $\text{NO}_x$  influence particulate both indirectly, by enhancing the concentrations of the most common atmospheric oxidants, and directly, through reactions which result in the formation of particulate nitrate. Some reactions by which  $\text{NO}_x$  and  $\text{SO}_x$  contribute to ambient  $\text{PM}_{10}$  are as follows:

1.  $\text{NO}$  reacts with ozone to produce  $\text{NO}_2$  under certain conditions. Sulphur dioxide ( $\text{SO}_2$ ) and nitrogen dioxide ( $\text{NO}_2$ ) react with hydroxyl radical ( $\text{OH}$ ) during the daytime to form sulphuric and nitric acid ( $\text{HNO}_3$ ). Particulate may be formed if these acids react with ammonia or sodium to produce ammonium or sodium sulphates and nitrates (USEPA, 1996);
2. During the night time,  $\text{NO}_2$  reacts with ozone ( $\text{O}_3$ ) and forms nitric acid. Particulate may be formed if the nitric acid reacts with ammonia to produce ammonium nitrate (USEPA, 1996);
3.  $\text{NO}_2$  reacts with  $\text{NO}_3$  to form the  $\text{N}_2\text{O}_5$  radical and nitric acid which can then form nitrates e.g.,  $(\text{NH}_4)\text{NO}_3$  (USEPA, 1996);
4.  $\text{SO}_2$  also dissolves in cloud and fog droplets, where it may react with dissolved  $\text{O}_3$ , hydrogen peroxide ( $\text{H}_2\text{O}_2$ ), organic peroxides such as methylperoxide ( $\text{CH}_3\text{OOH}$ ) or if catalysed by certain metals, with oxygen ( $\text{O}_2$ ), yielding sulphuric acid or sulphates that form an aerosol when the droplet evaporates (Brimblecombe, 1986).

Gas-phase sulphuric acid has a moderate vapour pressure, but interacts with water to produce much lower vapour pressure combinations of the water and  $\text{H}_2\text{SO}_4$  molecules. Low temperatures and high relative humidities tend to enhance particle sulphate nucleation.

## Impact of relative humidity

High relative humidity occurs when the dew point temperature<sup>4</sup> and the air temperature are nearly equal. Secondary particles have additional implications for reduced visibility under conditions of high relative humidity. This is because the hygroscopic properties of these sulphates and nitrates result in increases in the size of the particles, in the presence of water, to a size range that most effectively scatters light. Similarly, water vapour can also attach to some organic particles resulting in an additional impact on light scattering by increasing particle size. Light scattering by particles can increase by an order of magnitude as the relative humidity increases from 20-30% to 90-95% (Laulainen & Trexler, 1997). High relative humidity can also increase the quantities of sulphate, as SO<sub>2</sub> dissolves in the aerosol droplets and is oxidised more rapidly in solution producing sulphate, as described in bullet point three above.

The process by which particles acquire water is complex and in many cases particles can gain and lose water at different rates (Middleton & Laulainen, 2000). If all other factors remain the same, an increase in relative humidity will result in poorer visibility.

### 2.2.3 Summary

The physical processes leading to visibility degradation by air pollution are scattering and absorption by particles and gases. With the exception of NO<sub>2</sub>, which absorbs blue light, the impact of gases is minor and does not vary with increasing concentration. Particle size and composition strongly impact on visibility with smaller particles (0.3-0.7 µm) having greater effectiveness at scattering light. Nitrate, sulphate, elemental carbon and NO<sub>2</sub> generally play a significant role in causing degraded visibility. Sources of air pollutants impacting on visibility include combustion, wind blown dust, sea salt and secondary reactions involving nitrogen and sulphur oxides with ozone.

## 2.3 Visibility and Human Perception

Human perception of visibility plays a key role in both the assessment and the management of visibility. This is because visibility degradation is an amenity effect that depends entirely on perception of the problem. As discussed previously, the perception of visibility will depend on factors that cannot be regulated, such as sun angle and cloud cover. The management of visibility focuses on the effects of air pollution, and therefore an understanding of the relationship between

---

<sup>4</sup> The dew point is the temperature to which the air would have to be cooled at constant pressure to become saturated with respect to a plane surface of pure liquid water (Carroll, 1996).

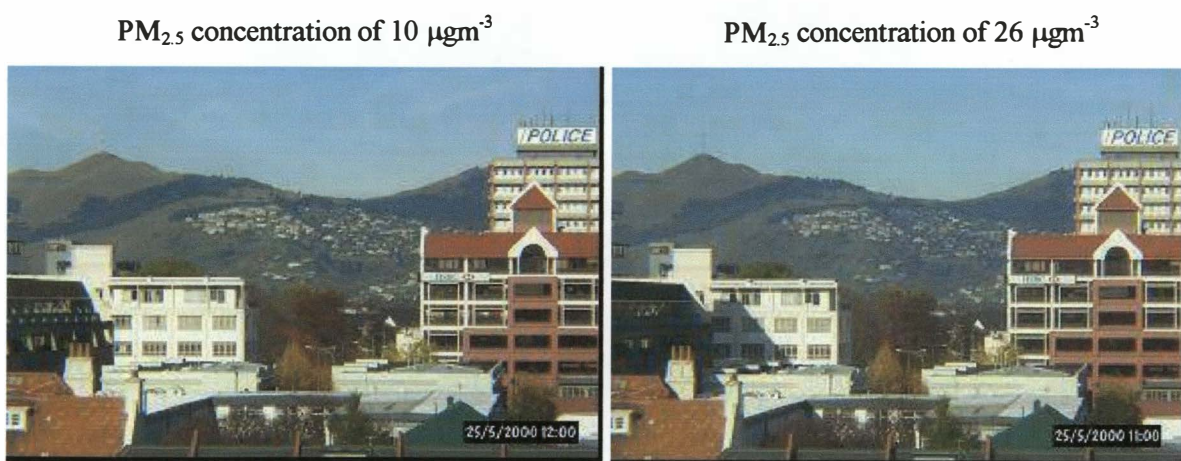


air pollution and perception is required. This Section investigates this relationship and considers the influence of perception on the management of visibility.

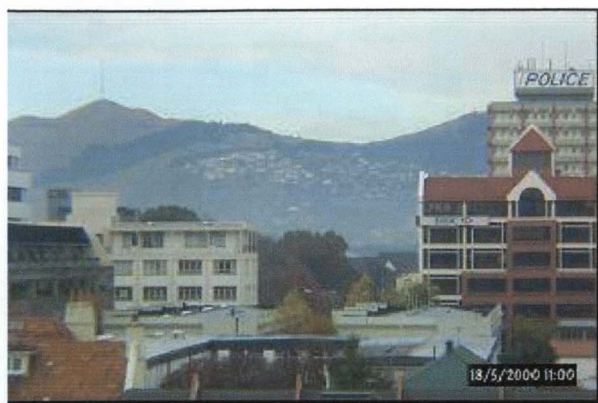
### 2.3.1 Pollution and other impacts on perception of visibility

While there are a number of factors that influence visibility, the role of pollution in the perception of visibility is particularly important. Visibility is more sensitive to changing pollution levels than any other pollution effect. In addition, overseas studies have found that the same amount of pollution can have dramatically different effects on visibility depending on existing conditions. For example, if background levels of visibility are good, the impact of a  $10 \mu\text{gm}^{-3}$  increase in  $\text{PM}_{10}$  has a significant impact on visibility perception. If background visibility is poor, the effect of a  $10 \mu\text{gm}^{-3}$  increase in  $\text{PM}_{10}$  is less noticeable. This suggests that in more polluted areas a larger reduction in fine particle concentrations is needed to achieve a given level of perceived visibility improvement.

Visibility theory, however, tells us that in any location, the impact on visibility of a  $10 \mu\text{gm}^{-3}$  increase in particles will depend on the size distribution and the composition of the particles. Figure 2.5 shows an example of the effect of a  $10 \mu\text{gm}^{-3}$  increase in  $\text{PM}_{2.5}$  concentrations for a clear day and for a dirty day in Christchurch. Unlike the examples given for overseas studies, this illustration does not suggest that increases against a clear background have more visual impact in Christchurch.



PM<sub>2.5</sub> concentration of 58 µgm<sup>-3</sup>



PM<sub>2.5</sub> concentration of 67 µgm<sup>-3</sup>



Figure 2.5. Air quality in Christchurch on clear and hazy days and the effect of adding 10 µgm<sup>-3</sup> of PM<sub>2.5</sub>.

The effect of cloud cover and illumination on the perception of visibility can also be a major factor in the appearance of haze. While the focus of this research is on aspects of visibility that can be managed, it is important to note the impact of illumination effects particularly when considering the role of perception. Figure 2.6 illustrates the effect of illumination on days with relatively similar pollution levels and meteorological conditions. In these images, the appearance of haze is greater in the first image than in the second image, where sunlight is penetrating the cloud and giving brightness to the hill in the distance.



Figure 2.6: Impact of illumination for days with similar light extinction values and meteorological conditions.

### 2.3.2 Perception, visual range and light extinction

The relationship between visibility perception and the scientific assessment of visibility in terms of light extinction is clearly complex. Light extinction, expressed in previous Sections as inverse Mega-metres (Mm<sup>-1</sup>), is useful in relating visibility directly to concentrations of contaminants. However, the correlation between light extinction and human perception of haze is not linear (USEPA, 1998a). In an attempt to relate perception to extinction Pitchford and Malm (1994),

developed the deciview index. This deciview index describes the relationship between perception and extinction and is given as:

$$dv = 10\ln(bext/10) \quad \text{Equation 2.6}$$

It was proposed that a change of one deciview is approximately a 10% change in extinction coefficient, which represents a change in scenic quality that would be noticed by most people regardless of the initial visibility conditions. This concept has been recently challenged by Richard (1999) who claimed that, a change of one deciview would be imperceptible to most people. An alternative methodology was proposed by Richards (1999) that incorporated distance from the observer to the object. While scientifically superior (Watson, 2002) this approach was considered more difficult to implement.

Notwithstanding these criticisms, the deciview scale has been used to report visibility in the United States, often in conjunction with a visual range distance, which is the greatest distance at which a small black object is visible along a horizontal path (see Section 2.4.1). For example, in the eastern United States, the currently accepted estimate for natural visibility is around 8-11 deciviews, which is 100-130 km, whereas in the western United States it is about 4.5-5 deciviews or 175-185 km (The National Park Service, 1999). Figure 2.7 shows trends in deciviews for the Grand Canyon National Park. It can be seen that the best visibility range is represented by deciview values less than about 8. Because of human activities, visibility in the west is often as low as ~ 30 deciviews or 20-30 km (The National Park Service, 1999). The use of the deciview scale for reporting visibility appears to be limited to the United States at this stage. European visibility seems to be more commonly reported in visual range distance, with good visibility away from towns and cities being around 40-50 km, but up to 100-150 km on rare occasions (Horvath, 1995 as reported in QUARG, 1996).

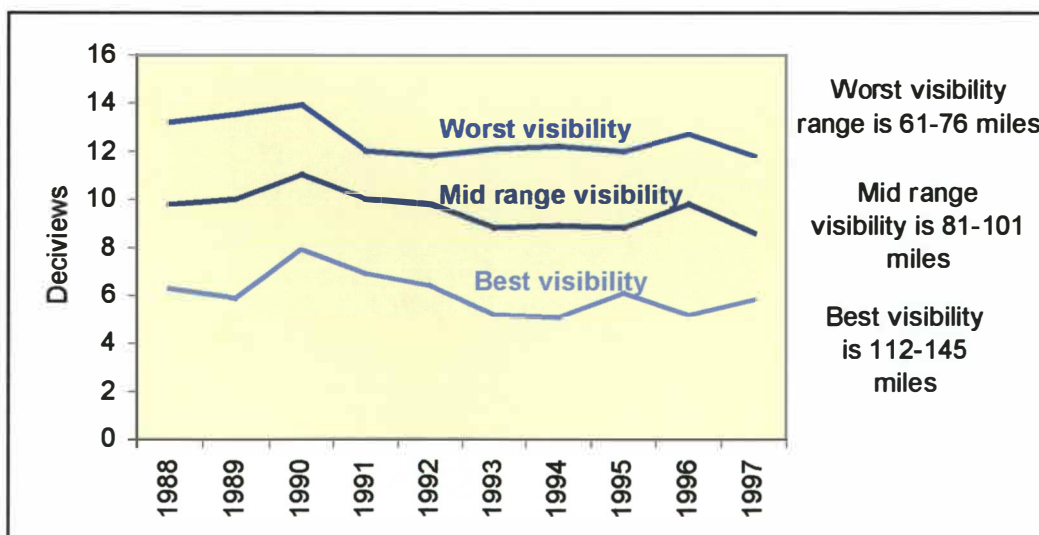


Figure 2.7: Trends in deciviews in the Grand Canyon National Park from 1988 to 1997.



An alternative to using an expression of visibility based on visual range, light extinction or the more perception related deciviews, is an expression based solely on the concentration of particles. This method is used in Canada where a 10% increase in  $PM_{2.5}$  from background levels defines the level above which effects on visual range are noticeable. While this method may be appropriate for a location where the composition and size distribution of particles is relatively consistent, data could not be extrapolated to other areas where these factors differed. For example, in Canada a noticeable change in visibility would be expected to occur for a  $1-2 \mu g m^{-3}$  increase in  $PM_{10}$  levels at rural Canadian sites and a  $2-5 \mu g m^{-3}$  increase in  $PM_{10}$  at urban Canadian sites (CEPA, 1998). In contrast, examination of the photographs and corresponding  $PM_{10}$  concentrations in Christchurch for this study suggests that under many situations, a  $10 \mu g m^{-3}$  is unlikely to produce a noticeable change in visibility. This difference is most likely to be attributable to a greater proportion of sulphate in the particulate measured in Canada.

### 2.3.3 Community perception and visibility management

The acceptability or otherwise of existing levels of visibility to a community can play a key role in the management of the visual quality of the air. In New Zealand, the Resource Management Act (1991) requires community consultation and cost benefit analysis before regulation is imposed. Because visibility is an amenity effect, the concept of acceptability has additional significance. The acceptability of reduced visibility could be described as a combination of processes:

1. The perception of the visual quality of the air (i.e., is it bad or good?).
2. The perception of the implications of poor visibility.
3. A willingness, or lack of it, to meet the costs associated with improving visibility.

Because visibility is the principal atmospheric characteristic through which humans perceive air pollution, they may assume that other adverse effects associated with air pollution, such as health effects, are present when the visual air quality is poor (e.g., CRC, 1999). This may or may not be the case, depending on the sources and characteristics of the visibility degradation. On the other hand, the community might perceive the visibility to be particularly poor because of the amenity effect. However, it may become acceptable to the community if it were to learn that the cost of having good visibility involved heavy regulations on the use of motor vehicles, for example.

Contrary to this view and the model presented in Chapter 1 (Figure 1.5) for visibility management in New Zealand, in the United States cost has no role in the setting of standards, irrespective of whether the standard is based on adverse effects or amenity effects (Ely *et al.*, 1991). The setting of standards or guidelines for visibility management, including United States examples, is discussed in detail in the following Section.

### 2.3.4 Guidelines/ standards and legislation

The assessment of the acceptability of visibility by a community (as discussed in Section 2.3.3) depends on the legislation and the presence or absence of guidelines or standards for visibility. If there is a standard or legislative requirement relating to visibility, the community is likely to have little involvement in the ongoing management of the problem. In the United States, the 1977 amendments to the Clean Air Act required the prevention of any future impairment and the remedying of any existing impairment in visibility resulting from anthropogenic air pollution in Class 1 national parks and wilderness areas. The regulations require states to review how emissions within their area affect visibility in Class 1 areas, and to make “reasonable progress” in reducing this effect and in preventing future impairment (The National Park Service, 1999). More specifically, a proposed rule requires that haze in Class 1 areas be monitored and that the average haze level during the 20% of the days that have the highest  $PM_{2.5}$  concentrations decrease by one deciview every 10-15 years. It also requires that the average haze during the best  $PM_{2.5}$  concentrations not increase by more than 0.1 deciviews (Richards, 1999). Thus, in designated areas of the United States, community assessment of visibility plays little role in its management.

The process of setting an appropriate standard for visibility in Denver is discussed in Ely *et al.*, (1991). In the Denver study, the public<sup>5</sup> was surveyed regarding the degree of acceptability of visibility as viewed from photographic slides. The response was then converted to a light extinction index by the coincidental measurement of the optical characteristics at the time the images were taken. The concept of acceptability was based exclusively on the perception of the vista. Light extinction and the visual assessment were well correlated ( $r = 0.87$ ). However, in general these correlations are not expected to be high because of the many non-extinction factors that impact on perception (Ely *et al.*, 1991). A standard for visibility of  $0.076 \text{ km}^{-1}$  ( $76 \text{ Mm}^{-1}$ ) was selected based on a value above which 50% of the participants found the levels of visibility to be unacceptable. A similar methodology used by Pryor (1996) found a range of acceptable visibility from  $0.09 \text{ km}^{-1}$  to  $0.105 \text{ km}^{-1}$ .

The introduction of legislation relating to visibility has also been considered in other countries. In Canada, consideration was given to the introduction of a reference level for  $PM_{2.5}$  because of the effect of particles on visibility. The Canadian Environmental Protection Act (CEPA) concluded that concentrations of  $PM_{2.5}$  from  $6\text{--}14 \mu\text{gm}^{-3}$  have demonstrated effects on visual range in Canada. Although they identified that degradation in visual range occurred at  $PM_{2.5}$  concentrations 10% higher than average background concentrations, they were unable to identify a single background

---

<sup>5</sup> Because of resource constraints a random selection of the public was not possible.

concentration for all of Canada. Consequently, they recommended that no reference level for PM<sub>2.5</sub> based on visibility be identified at that stage (CEPA, 1998).

In New Zealand, the Ministry for the Environment has signalled an interest in establishing a criterion to protect visibility. A 1997 report (MfE, 1997) indicates that further investigations and identification of a suitable measurement method are required before visibility can be included on its list of air quality indicators requiring monitoring. A series of subsequent reports were prepared (MfE 1999a, 1999b, 1999c) that provide guidance on visibility measurement methods, amenity values and management, and a risk assessment of visibility in New Zealand. Actions required to protect and enhance visibility in New Zealand were recommended as follows:

- Develop and implement guidelines and indicators for visibility protection.
- Fully integrate visibility as an objective in Air Plans.
- Raise awareness in the public, educational, industry and political sectors.
- Develop and recommend monitoring methods.
- Define national goals for visibility, relevant for different types of region within New Zealand.
- Continue research on air shed modelling, with an emphasis on understanding key causes of visibility degradation.

While no guideline for visibility was recommended, a proposed visibility indicator was included. This was identified as preliminary, with the intention that it be refined in time with regard to user comment and use. A combination of visual range and colour are proposed for the visibility indicator (Table 2.1). As no definition of “off” colour is included, the colouration component is left to the viewers’ discretion.

Table 2.1: Proposed visibility indicators for New Zealand (MfE, 1999a).

Category	Visual range +/-or Appearance
Excellent	>70 km +/-or No ‘off’ colour
Good	>20-70 km +/-or No ‘off’ colour
Acceptable	>20-70 km +/-or Discernable ‘off’ colour
Poor	<20 km +/-or Discernable ‘off’ colour
Alert	<20 km +/-or Distinct ‘off’ colour
Action	<8 km +/-or Distinct ‘off’ colour

### 2.3.5 Summary

The relationship between perception, light extinction and visibility management is complex for many reasons. Firstly, the same amount of pollution can have dramatically different effects on visibility depending on existing conditions. This effect can be accounted for by expressing visibility in terms of the deciview index, which represents a change in scenic quality that would be noticed by most people regardless of the initial visibility conditions. Another complexity is the impact of cloud cover and sun angle on what is seen. These factors impact on perception, but not on light extinction. While perception of visibility is important in visibility management, the effectiveness of different management measures in improving visibility is likely to be based on data on light extinction.

## 2.4 Monitoring Methods

Previous Sections most commonly refer to visibility in terms of light extinction or deciviews. Visibility can also be expressed in terms of visual range or less commonly as an index based on apparent contrast. Whatever the description used, some method of monitoring and quantifying visibility is required. This Section looks at different monitoring methods and the conversion of monitoring data into meaningful expressions of visibility. Particular attention is given to the measurement of light extinction, as subsequent Sections focus on this method of quantifying visibility degradation.

### 2.4.1 Visual Range

Visibility is often described in terms of visual range (VR), which is the greatest distance at which a small black object is visible along a horizontal path in the atmosphere in the daylight (Koschmieder, 1924) and is described by the formula:

$$\text{Visual Range} = \frac{3.91}{B_{\text{ext}}} \quad \text{Equation 2.7}$$

Visual range is most commonly reported based on measurements made at international airports, where specific targets are established and observations are made at regular intervals. Visual range data have often been collected for many years, allowing long-term analysis of relationships and trends (e.g., Stuart & Hoff, 1994) and even visibility model forecasting (Trier, 1994). Figure 2.8 shows the relationship between light extinction and visual range, illustrating the large effect that small increases in concentrations of particles and gases have in reducing visual range.

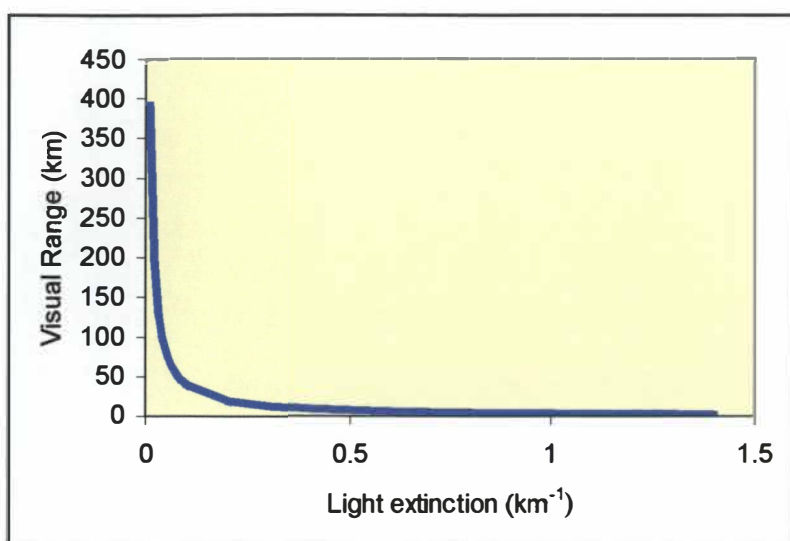


Figure 2.8: The relationship between visual range and light extinction as described by Koschmieder (1924).

## 2.4.2 Digital Camera

The method of monitoring that is likely to be most closely aligned to the perception of visibility is the digital camera. The digital camera is generally used in preference to photographic film or slides because variations in colour associated with the processing of film are avoided. Little information is available on the relationship between digital images and visibility perception. However, studies carried out on the colour perception of film photographs compared to the natural scene (Henry *et al.*, 1991) show that while there is a good correlation between the two assessments, the colour comparisons were greatly distorted. This discrepancy is largely attributable to the colour effects of the film, which tend to highly saturate yellows and reds, but may be due in part to the ability of the eye-brain system to subtract the effects of path luminance from the natural scene (Henry *et al.*, 1991). Differences in colour perception are reduced by the use of digital camera or video image (Henry, 1994).

While scene monitoring of visual images (e.g., using a photographic record) can provide a qualitative representation of the scenic appearance of visual air quality, there are difficulties in using these images quantitatively as an indicator of extinction. Difficulties arise because of the contrast changes that such factors as sun angle and cloud cover impart on the scene (USEPA, 1998a). Methods have been developed for converting scene-monitoring data to optical indices, such as quasi extinction coefficients which use a second camera directly aligned between the initial camera and the target (Richards, 1988). This works by comparing the difference in the luminous intensity between the near camera and the distant camera. However, in urban environments this is unlikely to be a practical option.



Visual range data collected using a digital camera can be quantified based on the contrast between two objects within the image. This technique is referred to as apparent contrast and is detailed in the following Section.

### 2.4.3 Apparent contrast

Apparent contrast provides a measure of visibility based on the difference in colour and/or tone between two objects in the distance. Horvath (1994) gives the contrast of an object ( $C$ ) against a background as the relative difference of the radiance of the object ( $L_o$ ) and the radiance of the background ( $L_b$ ) and expresses this as:

$$C = (L_o - L_b) / L_b \quad \text{Equation 2.8}$$

An alternative expression applied by Wilson (1999) to the Christchurch environment (see Section 2.6) measures contrast units ( $C$ ) based on the ratio of  $I$ , the luminous intensity of a light surface, to  $I'$ , the luminous intensity of a dark surface.

$$C = \frac{(I - I')}{I'} \quad \text{Equation 2.9}$$

Using this relationship targets become indistinguishable at  $C \leq 0.02$ .

A major limitation of this approach as a method of quantifying the effect of particles and gases is the impact of illumination effects on the observed contrast. Therefore, while it may provide a good measure of quantifying what is seen (i.e., visual perception), it is of limited use in assessing the effect of pollution on visibility. The most suitable method of quantifying the effect of pollution on visibility is the monitoring of optical properties of the atmosphere. These techniques are detailed in the following Section.

### 2.4.4 Optical measurements

#### Light extinction

Transmissometry is the primary method for measuring total light extinction. A long path transmissometer measures the light extinction in the atmosphere by emitting an incandescent light beam of constant intensity from a fixed point. The centre cone of this beam is captured by a photometer receiver, positioned in a direct line from the beam, which measures the light's intensity, and consequently, the quantity of light absorbed from or scattered out of the beam. Chopping of the light beam allows the computer at the receiving end to distinguish between the lamp signal and

background ambient lighting. While a transmissometer can measure total light extinction it is unable to distinguish the different components of the extinction budget. Because the measurement of individual components of the extinction budget (i.e.,  $B_{sp}$ ,  $B_{ap}$ ,  $B_{ag}$ ) is important in assessment of sources of visibility degradation, these must each be measured separately. Measurement techniques for each of these components are presented in turn.

### **Light scattering ( $B_{sp}$ )**

The primary method for measuring light scattering as a result of particles is a nephelometer. A nephelometer measures light scattering by drawing samples of air into a light proof housing unit and illuminating them with diffuse visible light. It is a point source method based on the principle that the total light scattered out of a path is the same as the reduction of light along the path, owing to scattering.

One of the main difficulties in measuring light scattering relates to the presence of moisture. As detailed in Chapter 2, light scattering caused by nitrates and sulphates is enhanced under high relative humidities. However, in many applications the measurement of light scattering by atmospheric moisture is not desirable. Consequently, many nephelometers were designed with heated inlets to evaporate moisture in the sample stream. This also has implications for water absorbing particles, such as nitrates and other volatiles in the air stream. At 90% relative humidity (RH), a 1 degree difference between ambient and the sampling chamber temperature will cause the sampling chamber relative humidity to reduce to about 84% RH, while a 4 degree temperature difference equates to a sample chamber RH of 70% (Malm, *et al.*, 1996). In many of the earlier visibility studies (e.g., Groblicki, 1981), the nephelometer sampling chamber was warmer than ambient temperature and therefore underestimated scattering due to absorbed water at high relative humidities.

The nephelometers of choice for visibility studies are the Optec NGN series (USEPA, 1998a). In addition to minimising the modification of ambient particles by sampling under ambient condition, the Optec systems have been designed to address problems with other nephelometers. These include deficiencies in inlet sizing, large truncation error<sup>6</sup>, poorly defined optical response and electronics problems (USEPA, 1998a).

---

<sup>6</sup> Truncation error occurs owing to the instrument detector being unable to measure the scattering over the whole 180° range. Typically nephelometers have measured from about 10° to 170°. The Optec system measures from about 5° to 175°.

The Optec NGN2, like other nephelometers, has a light source that illuminates the particulate at visible wavelengths. Light is scattered by particles and detected by a photomultiplier tube over the angles 5° to 175°. Only wavelengths in the 500-600 nm range are measured, as these correspond to the response of the human eye. The lower detection limit for the instrument is  $\sim 1 \text{ mm}^{-1}$  for a 10 minute average (USEPA, 1998a). Typical uncertainties for the OPTEC instrument are in the order of 5-10% (Malm, *et al.*, 1996). Although the cut point<sup>7</sup> of the NGN2 analyser has not been well characterised (Malm, *et al.*, 1996), Pryor, *et al.*, (1997) suggested that particulate light scattering ( $B_{sp}$ ) from the open chamber of the NGN2 nephelometer is approximately equal to total aerosol light scattering.

Light scattering by particles can also be estimated using particle size data by applying Mie theory using hygroscopic growth models. A number of models have been developed and good correlations with measured light scattering (nephelometry) are observed (e.g., Hoff *et al.*, 1996 for RH<90%; Eldering *et al.*, 1994).

### **Particle absorption ( $B_{ap}$ )**

In visibility studies, particle absorption is measured using integrating plate transmission measurements (Watson, 2002) or an aethalometer. The aethalometer measures the attenuation of a light beam that is passed through particles collected on a filter. The difference in attenuation between the exposed filter and a blank portion of the filter is proportional to the amount of light absorbing material on the filter tape. The attenuation signals are converted to black carbon mass concentrations (as this is what the instrument is often used to measure), based on the assumption that all light absorbing material is elemental carbon. The detection limit of the aethalometer is  $10 \text{ ngm}^{-3}$  elemental carbon for a 1-minute average (USEPA, 1998a).

### **Gaseous absorption ( $B_{ag}$ )**

Light absorption by gases can be calculated based on concentrations of nitrogen dioxide ( $\text{NO}_2$ ), as  $\text{NO}_2$  is the only gas typically present in ambient air that absorbs light. The most common analytical method for measuring nitrogen oxides is ozone chemiluminescence (ISO 7996:1985). A typical nitrogen oxide analyser operates such that the airflow is alternated between two processes. One passes the air through a catalytic converter, reducing nitrogen dioxide to nitric oxide. This nitric oxide is then additional to the nitric oxide already present in the sample. This allows for a measurement of  $\text{NO}_x$ . The other airflow bypasses the converter allowing for measurements of  $\text{NO}$  alone. Nitrogen dioxide is calculated based on the difference between measurements of total oxides

---

<sup>7</sup> The cut point of a particulate sampling system is the aerodynamic particle diameter at which 50% of the suspended particles are able to penetrate through the inlet to the filter (Chow, 1995).

of nitrogen (NO<sub>x</sub>) and nitric oxide measurements (CRC, 1999). The analyser records concentrations in parts per billion. Hodkinson (1966) derived the following formulae for the conversion of NO<sub>2</sub> concentrations to light absorption:

$$\text{Bag} = 175K(\text{NO}_2) \quad \text{Equation 2.10}$$

Where K is the absorption coefficient for NO<sub>2</sub>.

### 2.4.5 Visibility Surveys

Visibility assessment surveys have been used both as a tool for monitoring visibility and for determining appropriate standards for visibility degradation, based on public perception.

The use of human observation as a method of monitoring visibility, outside of the standard visual range airport type assessment, has been trialled in several locations in New Zealand (Person, 1996). Such surveys typically involve a number of observers who rate visibility on a daily basis from a predetermined location. The success of this approach in providing meaningful visibility information has been limited, however, in part owing to difficulties in quantifying or standardizing the observations.

A more useful application of a visibility survey is to assess public perception of visibility degradation. This typically involves the rating of visibility in a set of images and a rating of the acceptability of the visibility. From these ratings, and corresponding light extinction data, a level of visibility can be established that compares with a proportion of the population's acceptable criteria. An application of this method for establishing a visibility standard in Denver is discussed in Section 2.3.4.

### 2.4.6 Summary

A number of methods for monitoring visibility have been identified. Each method is aligned to a particular aspect of visibility. These include how a view is seen (digital camera), the impact of pollution (transmissometer/components of extinction), and the ability to detect an object in the distance (visual range), the clarity of an object in the distance (apparent contrast) and the perception of visibility (survey). The latter tool is best used in conjunction with a predetermined set of images, from a digital camera for example, as visibility perception depends on location and direction of view.

The use of any particular method of measuring visibility will depend on the outcome sought. For example, a digital camera may be appropriate for obtaining a long-term visual record, but would not

be the method of choice for quantifying the effect of pollution on visibility. From a management viewpoint, quantifying the effect of pollution is of prime importance. The most direct method for doing this is monitoring of optical characteristics of the atmosphere. The following Section describes the application of this type of monitoring, and how it can be used in conjunction with other monitoring to assess sources of visibility degradation.

## **2.5 Sources of visibility degradation**

### **2.5.1 Methods for assessing sources of reduced visibility**

Coincidental measurement of the extinction coefficient and the contaminants potentially contributing to visibility reduction is a technique typically used in the United States to assess causes of visibility degradation. This method, which is a statistical estimate of what proportion of haze is caused by each aerosol and gas type, is broadly known as extinction budget analysis (USEPA, 1998a). This method can help identify the type of sources that contribute to the haze. For example, if sulphate is shown to be responsible for 75% of the extinction coefficient, the major sources responsible for the haze must emit sulphur dioxide.

The extinction budget analysis method requires the measurement of light scattering due to particles, light absorption due to particles, light absorption due to gases, total light extinction, and speciation of particulate. Because the analysis requires considerable resources, several studies have attempted extinction budget analysis without measuring the full suite of parameters (e.g., White *et al.*, 1994). Such variations have included:

1. Calculating total extinction by summing measurements of light scattering and absorption.
2. Using elemental carbon concentrations to calculate absorption due to particles, that is, assuming all particle absorption is due to elemental carbon.

While the assumption that total extinction can be calculated using measurements of scattering and absorption appears to be reasonable, recent comparative work indicates that this assumption can significantly underestimate actual absorption by particles (Malm *et al.*, 1996).

An extension of the extinction budget analysis approach is the use of elemental analysis and receptor modelling. This method is based on the principle that relative quantities of different chemicals in ambient particulate can be used to indicate the sources of the emissions. The ratio of chemicals in a sample of particulate is compared to the ratios observed for individual sources that may contribute to ambient concentrations. Source ratios, commonly called profiles, will vary with different fuel composition and with changes in technology. This method of using ratios of



chemicals to determine sources is called receptor modelling. Receptor modelling requires elemental analysis of particulate for quantities of trace metals, as well as speciation into primary constituents such as elemental carbon and nitrate. Elemental analysis is typically carried out using X-Ray Fluorescence (XRF) or Proton Induced X-Ray Emission (PIXE).

A number of receptor modelling methods can be used to identify the source profiles. Common methods include chemical mass balance (CMB), principal components analysis (PCA) and positive matrix factorization (PMF).

### **2.5.2 Analysis of particle composition**

Specific methods for measuring optical components of the light extinction budget were discussed in Section 2.4. In addition to these measurements, extinction budget analysis requires identification of the components of the particulate before sources contributing to reduced visibility can be identified. This particle component analysis is referred to as speciation and is important because of the impact of particle composition on light absorption and scattering, as discussed in Section 2.2.2. The relative contribution of different chemical species to particle concentrations in any location will vary depending on sources and atmospheric reactions. As indicated in Section 2.2.2, the main components of particles are organic carbon, elemental carbon, nitrate, sulphate, chloride, ammonium, water and geological material.

Some speciation of particles was carried out in Christchurch during 1989 and 1990 (Brady *et al.*, 1999). Carbonaceous material was found to contribute 70% of the fine particulate matter. Over two thirds of the carbonaceous material (69%) was elemental carbon. Absolute concentrations of other species were not reported, although it was noted that sulphate was more abundant than nitrate in Christchurch. However, the analysis method for nitrate was similar to that used in Brook & Dann (1999), which did not include denuder systems and was found to underestimate nitrate for the reasons discussed in Section 2.2.2. Consequently, it is likely that the speciation work conducted in Christchurch in the late 1980's underestimated nitrate concentrations.

### **2.5.3 Extinction budget analysis case studies**

Visibility studies using an extinction budget type analysis have been carried out primarily in the United States and Canada. The greatest quantity of data is from the United States where light extinction has been monitored since 1992 largely as a result of the 1977 Clean Air Act amendments, which included regulations relating to visibility degradation. A cooperative visibility monitoring effort was established between the USEPA and several state and federal agencies and was named the Interagency Monitoring of PROtected Visual Environments (IMPROVE). The contribution of different species to light extinction and the extent of reduced visibility in the United

States varies from east to west. In the east, sulphate is the greatest contributor to degraded visibility, contributing 64% of aerosol extinction on clear days and up to 80% on the worst days. Organic carbon is the next greatest contributor, accounting for 12% on the best days and 9% on the worst days. Nitrate also contributes 12% on the best days and 5% on the worst days. In the west, sulphate accounts for 35-45%, organic carbon 19-22%, crustal material 16-20% and nitrates 12-15% (USEPA, 1998b).

Outside of the United States, extensive visibility studies are less common. In the Korean city of Seoul, light extinction was found to average  $0.791 \times 10^{-3}$  during smoggy periods compared to  $0.297 \times 10^{-3}$  on clear days (Baik *et al.*, 1996). Sulphates and nitrates were major components of the haze and the effect of relative humidity on size distribution was noted. A similar study in Hong Kong, suggested that around 39% of the light extinction was attributable to light scattering by particles, 19-29% light absorption by particles, 17% to gaseous absorption, 4.3% to Rayleigh scattering, with the 16% unaccounted for associated with instrumentation bias (Lai & Sequeira, 2001).

Major investigations into visibility reduction in the United States include the Denver Brown Haze study in the early 1980's, which was followed by the Northern Front Range Air Quality Study (NRFAQS), a more comprehensive study in the 1990's, and a study of visibility in the Grand Canyon area. The latter study, titled MOHAVE (Measurement of Haze and Visual Effects), was conducted in the late 1990's. In addition, a major visibility study, the Regional Visibility Experimental Assessment in the Lower Fraser Valley (REVEAL), was conducted in Canada in 1993. A summary of each of these studies is presented in the following boxes.

### REVEAL I & II



*“Poor” and “very good” visibility in Chilliwack, Lower Fraser Valley.*

**Name:** Regional Visibility Experimental Assessment in the Lower Fraser Valley

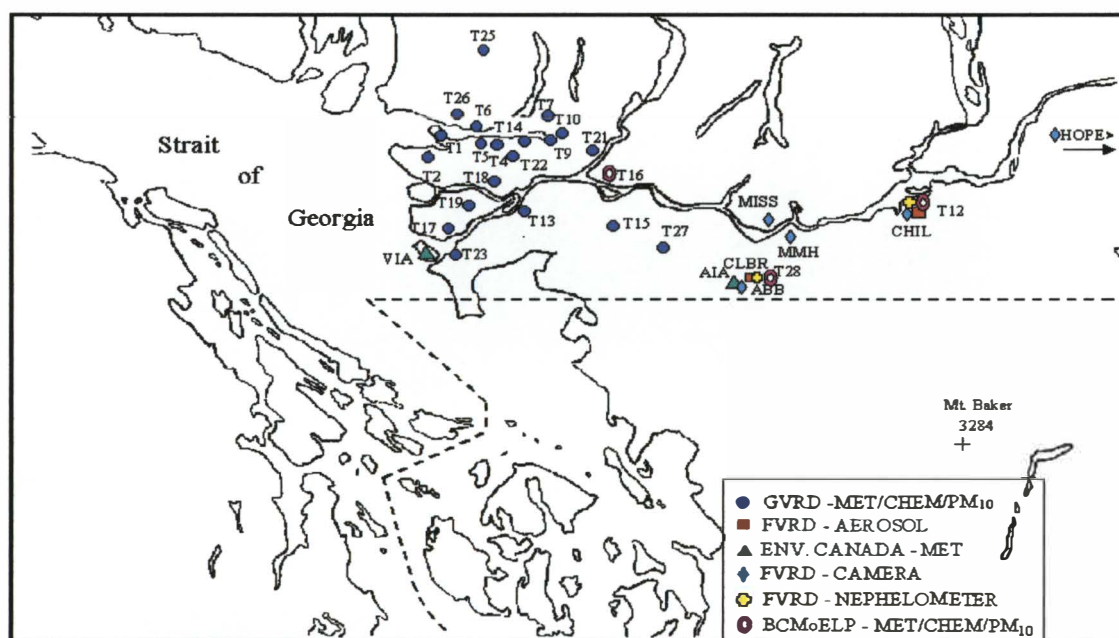
**Location:** Lower Fraser Valley, British Columbia

**Basis for study:** Visibility in the Lower Fraser Valley was believed to be declining (Pryor, *et al.*, 1997). A high value was placed on visibility by both residents and from a tourism perspective (McKendry, pers comm, 1999). The Ministry for Lands and Parks was considering regulatory approaches for protecting visibility in the Lower Fraser Valley.

**Purpose:** To characterise summertime visibility and ambient aerosol loadings in south-western British Columbia. In particular, to determine the spatial and temporal patterns of visibility aerosol concentrations, to determine estimates of the light extinction budget in Chilliwack, to apportion aerosols responsible for summertime visibility to general source types, and to develop estimates of the anthropogenic portion of ambient aerosols (Pryor, *et al.*, 1997).

**Monitoring period:** Intensive study during July and August 1993 (REVEAL I) and a less intensive monitoring programme from April 1994 to June 1995 (REVEAL II).

**Monitoring sites:** Intensive monitoring was conducted in Chilliwack, and in Clearbrook during REVEAL I. REVEAL II monitoring sites are shown below.



GVRD = Greater Vancouver Regional District, FVRD = Fraser Valley Regional District, BCMoELP = British Columbia Ministry of Environment, Land, and Parks

#### **Instrumentation/ Sampling:**

PM<sub>2.5</sub> collected for chemical analysis (inorganic ions, elements, and integrating plate method for absorption) – 24-hour average data collected on Mondays and Wednesdays using IMPROVE samplers<sup>8</sup>. An exception to this set up was a five-day enhancement period (of poor visibility)

<sup>8</sup> The IMPROVE sampler is a particulate speciation sampler that was designed specifically for the IMPROVE monitoring programme



when data were collected every six hours. Other instrumentation included an Optec NGN-2 nephelometer measuring light scattering, relative humidity and temperature and SCENE monitoring using automated camera systems. Hourly data were collected for meteorological parameters, PM<sub>10</sub> using a TEOM, SO<sub>2</sub>, NO<sub>2</sub>, O<sub>3</sub> and CO, and estimates of visual range from airport data.

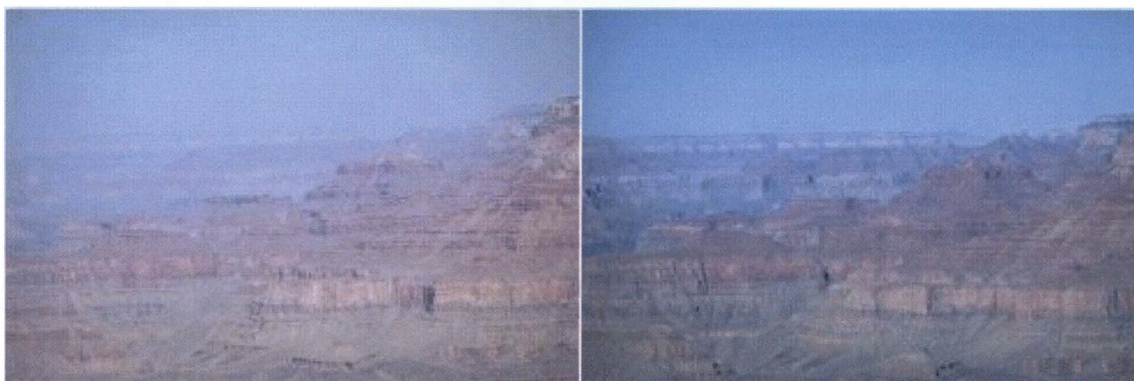
**Key observations:** Aerosol concentrations were found to be highly variable both spatially and temporally, with organic carbon being the primary contributor to fine particulate mass (35-46%). However, nitrates and sulphates dominated particle light scattering, accounting for 55-67% of the mean B<sub>sp</sub>. Hourly PM<sub>10</sub> concentrations exceeded 30 µgm<sup>-3</sup> on an average of one hour in every 10 and occasionally exceeded 50 µgm<sup>-3</sup>. Over half of the PM<sub>10</sub> existed in the fine PM<sub>2.5</sub> size fraction.

**Receptor Modelling:** Sources of fine mass assessed for the two monitoring sites using receptor modelling gave the following sources, listed in order of contribution:

Clearbrook – Mobile emissions, secondary aerosols, primary geological material, industrial emissions and a marine contribution

Chilliwack - Mobile emissions, secondary aerosols, primary diesel emissions, primary geological material, a marine contribution and a local component (dominated by iron).

## MOHAVE



*The Grand Canyon National Park, Arizona on “a hazy day” and “a clear day”*

**Name:** The Measurement Of Haze And Visual Effects study (MOHAVE)

**Location:** The study area included much of Southern California and Nevada, Arizona and Utah. However, the focus of the study and the most intensive monitoring was on the Grand Canyon National Park.

**Basis for study:** The Grand Canyon National Park is a class-one visibility area and is therefore subject to the United States (1977) Clean Air Act amendments (detailed in Section 2.3.4).

Visibility in the area is frequently degraded as a result of long-range transport of pollutants. The Grand Canyon is a major tourist attraction and consequently, poor visibility in the area is a significant concern.

**Purpose:** To determine sources of visibility reduction in the area, particularly the contribution of the Mohave Power Project, as well as from other point sources and regional emissions.

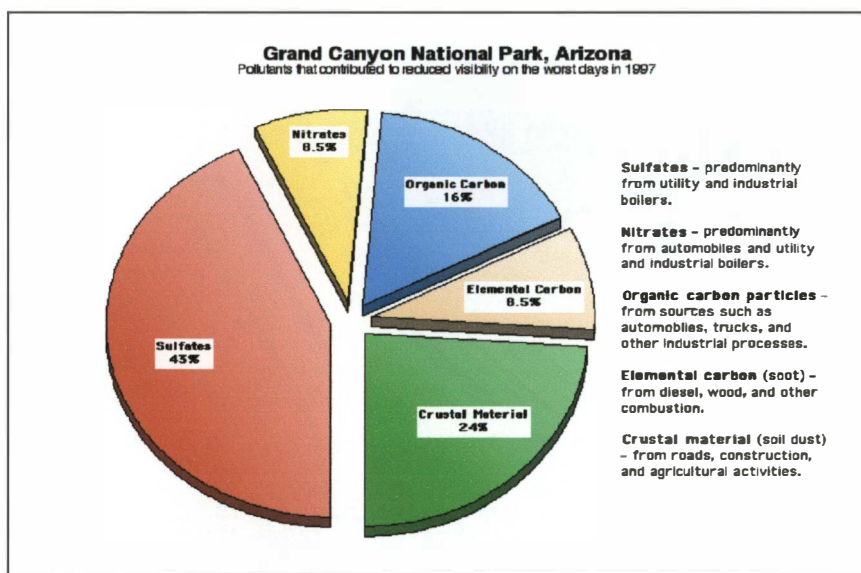
**Monitoring period:** The summer and the winter months of 1992.

**Monitoring sites:** IMPROVE monitoring sites scattered throughout the study area measured particle concentration and composition. A MOHAVE visibility site employing independent measurements of extinction, scattering and absorption using optical techniques was established in Meadview, Lake Mead National Recreational Area.

**Instrumentation/ sampling:**

Two transmissometers (Optec LPV-2), a nephelometer (Optec NGN-2) and IMPROVE samplers. Light absorption was measured using the integrating plate method based on particle samples collected using the IMPROVE samplers.

**Key observations:**



In the Grand Canyon area elemental carbon and soil were the main contributors to  $B_{ap}$ .

Significant transport of visibility reducing contaminants occurs, with contributions from sources in California and Las Vegas. Although the contribution of different contaminants to reduced visibility varies from site to site (Malm & Gebhart, 1997) and the sources of these contaminants differ (Henry, 1997), the majority of the haze is attributed to emissions from the south-west, which contains the populous and industrial areas of southern California (White *et al.*, 1994).

Difficulties in the apportionment of the extinction budget prompted further studies of the physio-chemical-optical properties of the particulate at the Grand Canyon. Malm & Day (1999) found



that the mass scattering efficiency of the coarse particles was at times near to  $1.0 \text{ m}^2 \text{ g}^{-1}$ , greater than the  $0.4$  to  $0.6 \text{ m}^2 \text{ g}^{-1}$  that had been assumed. Conversely, the fine particle absorption coefficients for organic carbon and sulphate were substantially less than the nominal values of  $4.1$  and  $3.0 \text{ m}^2 \text{ g}^{-1}$  typically used.

**Receptor modelling:** The dominant source of elemental carbon was transport, in particular diesel vehicles, although residential fuel combustion and fires were also identified as contributors to elemental carbon emissions (Malm & Gebhart, 1997).

**Contributions to visibility research:** A method of identifying sources of sulphur oxides contributing to visibility impairment at the Grand Canyon was developed by Eatough *et al.*, (1997). The basis of the method was characterising chemical profiles for sulphur oxides using concentrations of total fluoride (gas and aerosol), spherical alumino-silicate particles, particulate selenium, arsenic, lead, bromine and absorption by particles.

A comparison of the IMPROVE absorption data calculated using the integrating plate method and estimated absorption based on elemental carbon concentrations showed that the latter method was likely to underestimate absorption. Malm *et al.*, (1996) found that based on concentrations of elemental carbon, estimates of particle absorption accounted for 5% of light extinction, compared to direct measurements of light absorption, which indicated a 30% contribution to extinction.

## NFRAQS

**Name:** Northern Front Range Air Quality Study.

**Location:** Colorado's Northern Front Range includes the eastern part of the Rocky Mountains and extends from Palmer Divide to Cheyenne Ridge, and acts as a barrier to atmospheric transport of pollutants between eastern and western United States. The major population centres are located between Denver and Cheyenne. Denver is the largest of these and is of particular interest owing to the occurrence of brown haze.

**Basis for study:** Causes of brown haze in Denver have been a topic of research for over two decades. Despite this, the cloud remains a visible reminder that not all of Denver's air quality problems have been resolved.

**Purpose:** To determine sources of air pollution in the Denver urban region and to collect data upon which to base informed decisions regarding air quality management and attainment of federal standards.

**Monitoring period:** Winter 1996 (44 days), summer 1996 (45 days) and winter 1997 (60 days).

**Monitoring sites:** Welby, Brighton, Evans (satellite site), Longmont, Fort Collins.

**Instrumentation/sampling:** Optec NGN-2 nephelometers at all sites and Optec NGN-2 configured with size selective PM<sub>2.5</sub> inlets at Welby and Brighton. In addition to this, the Brighton site also had a TSI multi-wavelength nephelometer fitted with a PM<sub>2.5</sub> size selective inlet. Two transmittometers (Optec LPV-2) used during the study were located in Denver (not at a specific site) and at Fort Collins. Aethalometers (Magee Scientific AE-10M) were located at the Welby, Brighton and Evans sites.

**Key observations:** PM<sub>2.5</sub> concentrations measured during the monitoring periods ranged from 1-51 µg m<sup>-3</sup> (24-hour average). No particulate samples exceeded the guideline concentration of 65 µg m<sup>-3</sup> during any of the sampling periods. Approximately 45-50% of the PM<sub>10</sub> was PM<sub>2.5</sub>. Carbon, ammonium nitrate and ammonium sulphate made up 82% of the PM<sub>2.5</sub> mass during the winter months. Carbon constituted 43% of average PM<sub>2.5</sub> at Welby and 34% at Brighton during the 1997 winter.

Secondary ammonium nitrate and ammonium sulphate contributed more than 50% of the PM<sub>10</sub> at the northern non-urban sites. Ammonium nitrate contributions were twice those of ammonium sulphate in Denver. Sulphate is neutralised by ammonia and is present as ammonium sulphate. The Northern Front Range is ammonium rich, allowing complete neutralisation of nitric acid. Consequently, reducing or doubling sulphate will have negligible effect on nitrate. Diurnal variations in secondary nitrate were small at Welby and Brighton, with slightly higher values during the afternoon and overnight periods.

**Receptor modelling:** Vehicle exhaust was the largest PM<sub>2.5</sub> carbon contributor, comprising approximately 85% of PM<sub>2.5</sub> carbon in Denver and approximately 75% at the rural sites. The majority of this appeared to be from light duty gasoline vehicles (LDGV) in the urban Denver sites. In Brighton, Longmont and Fort Collins the diesel vehicle contribution was nearly equal that of the LDGV. Road dust contributed 4.2% and 3.6% of the PM<sub>2.5</sub> carbon at Welby and Brighton respectively. Meat cooking contributed on average, 6.3% of the PM<sub>2.5</sub> carbon at Welby and 2.1% at Brighton.

On average, wood combustion contributed 8% of carbon at Welby and 3.8% at Brighton, although on occasions such as Christmas and New Year holidays the contributions were as high as 50%. No burning restrictions were imposed during these periods and temperatures were some of the coldest of the 1997 winter. Overall, the wood burning contributions were much less than those measured during the winters of 1987 and 1988, prior to the introduction of wood burning controls, when the contribution from this source was comparable to that from vehicles.

## 2.5.4 Summary

Sources of visibility degradation can be assessed using a combination of an extinction budget analysis and particulate speciation measurements. The methodology is further enhanced by

elemental analysis of the particles and identification of sources based on elemental fingerprints. These methods have been used to assess factors contributing to impaired visibility in Denver, Vancouver, and the Grand Canyon. In these locations, secondary particles are found to be a significant contributor to visibility degradation.

## **2.6 Haze investigations in New Zealand**

A number of studies have been carried out in New Zealand on visibility related issues. A broad range of topics have been addressed including monitoring using digital cameras/video (MfE, 1998), public perception of visibility issues (NIWA, 1998), a literature review of overseas studies and their relevance to New Zealand (Person, 1996), and an attempt to identify major contributors to reduced visibility in Auckland and Christchurch (Thompson, 1996).

The digital camera/ video camera monitoring of visibility was a joint project carried out by the Manawatu-Wanganui Regional Council, Taranaki Regional Council, Environment Waikato, Hawkes Bay Regional Council and the National Institute of Water and Atmospheric Research (NIWA) (MfE, 1998). The purpose of the study was to determine a cost-effective technique for visibility monitoring in New Zealand. Methods examined included:

- Community surveys.
- Digital cameras/ video and image processing.
- Particle size distributions.
- PM<sub>10</sub> and elemental analysis.

The study concluded that, although subjective, visibility surveys appeared to be the easiest method for monitoring visibility. Digital cameras were thought to have promise, but further work on image processing was required (MfE, 1998).

A study of how the public perceives visibility was carried out by NIWA in the areas of Auckland, Hawke's Bay, Hamilton City, Dunedin and Christchurch (NIWA, 1998). The main findings were:

- In Auckland, the majority of the participants thought that visibility had deteriorated and that motor vehicles were the primary cause of reduced visibility.
- Most respondents rated visibility in Hawke's Bay as excellent, and there was little indication of perceived deterioration.
- In Hamilton, visibility degradation was mostly attributed to natural causes such as fog and rain.

- Dunedin residents considered the standard of visibility in the area as very high and predicted that weather had the main effect on visibility. Of the anthropogenic sources, domestic heating was thought to be the main contributor to reduced visibility.
- Although Christchurch was initially included in the survey, households in Christchurch were reluctant to respond to the questionnaire. Consequently, results were unable to be reported due to the small sample size (31).
- In all areas, visibility was identified as an issue of importance.

Person (1996) summarised the IMPROVE (Interagency Monitoring of PROtected Visual Environment) and SCENES (Subregional Cooperative Electric Utility, Department of Defense, NPS and EPS Study) programmes implemented by the USEPA. Person's (1996) assessment predicts that:

- Unlike the United States studies, sulphate concentrations will not significantly contribute to visibility degradation in New Zealand.
- NO<sub>x</sub> and diesel emissions from motor vehicles will be responsible for visibility degradation in Auckland.
- In Christchurch and Hamilton, reduced visibility will be strongly influenced by carbon emissions from combustion processes such as wood burning.

An investigation of the source apportionment method of assessing sources of particulate in New Zealand was carried out by NIWA in 1996 (Thompson, 1996). Elemental analysis of particles was carried out in Auckland, Hamilton and Christchurch. As source profiles are not defined for New Zealand conditions, samples were assessed relative to overseas profiles. Thompson (1996) concluded that the application of the overseas profiles was not sufficiently accurate and that further work to determine local source profiles was required before meaningful results could be obtained.

Chemical analysis was carried out on aerosol collected in Christchurch during 1989 and 1990 (Brady *et al.*, 1999). Samples were analysed for ammonium, nitrate, chloride, sulphate, elemental carbon and organic carbon. It was concluded that ammonium sulphate and chloride are more dominant than ammonium nitrate. However, measurement methods used for nitrate sampling did not include denuder systems and consequently, could significantly underestimate nitrate concentrations (as illustrated in Brook & Dann, 1999). Brady *et al.*, (1999) suggested that elemental carbon and sulphate compounds are major contributors to total light extinction in Christchurch. However, this conclusion is based on results of overseas studies (e.g., Groblicki *et al.*, 1981) that identify elemental carbon as a major contributor in other locations, rather than actual monitoring of optical parameters. Brady *et al.*, (1999) identified the need for further work relating to particulate speciation and visibility in Christchurch.

The most recent research into visibility degradation in Christchurch was described in Wilson (1999). This includes an assessment of digital images for apparent contrast, the relationship between degraded visibility and meteorological conditions, and an estimation of the contribution of different components of the extinction budget to reduced visibility. During the daytime, light scattering by particles was found to account for 46% of the extinction budget. Light absorption by particles contributed 37%, absorption by gases 17% and light scattering by gases 3%.

## 2.7 Summary

Particles and gases in the air degrade visibility by scattering and absorbing light. The amount of light scattered depends primarily on particle size, with particles in the size range 0.3 – 0.7  $\mu\text{m}$  scattering light most effectively. Light absorption by particles depends on composition, while absorption by gases in the air is effectively limited to  $\text{NO}_2$ . The perception of these effects on reduced visibility is the basis for visibility monitoring and management. However, the relationship between visibility perception and light extinction is non-linear and depends on a number of factors including illumination, range of particle sizes and direction of view.

Methods for monitoring visibility include digital camera/video, visual range, apparent contrast, surveys and the measurement of the optical characteristics of the atmosphere (i.e.,  $B_{\text{ap}}$ ,  $B_{\text{sp}}$ ,  $B_{\text{ag}}$ ). The latter measurements combined with particulate composition analysis form the basis for a technique for assessing sources of visibility degradation. The application of this type of technique as a part of this research will be a first for New Zealand and should answer previous unknowns regarding sources of visibility degradation in Christchurch.



## Chapter 3 Air Quality in Christchurch

### 3.1 Introduction

Air pollution and its impact on visibility, health and amenity has been a major issue in Christchurch for many years. Documentation of concern goes back to the 1930's, when the Sunlight League campaigned for the installation of smokeless heating appliances in all new houses. The issue has spanned over half a century as regulatory authorities have failed to successfully address air quality issues in the city. Leading into the new millennium, 87% of Christchurch residents believed that something should be done about Christchurch's air pollution problem (Lamb, 2001).

Poor visibility in Christchurch may be a result of natural or anthropogenic emissions or more likely, a combination of both. As little can be done about natural sources, such as sea salt or wind blown dusts, sources of anthropogenic emissions are of prime concern. Domestic heating is one source of emissions that impacts significantly on the air quality. The 316,622 residents of Christchurch live in approximately 123,000 households (Statistics New Zealand, 2002), of which approximately 45% burn solid fuel for domestic home heating during the winter months (Wilton, 2001). Motor vehicle use per capita is also high, with about 306,000 motor vehicles belonging to residents of the city. Emissions from these and other sources, such as industrial or natural emissions, are exacerbated by meteorological conditions in Christchurch, which are conducive to high pollution concentrations and reduced visibility. This Chapter gives an overview of the impact of local meteorological conditions on visibility, reviews trends in concentrations of contaminants that might influence visibility, and outlines a framework for the management of visibility.

### 3.2 Meteorology

Meteorology influences visibility in a number of ways. In particular, low wind speeds and stable air inhibit the dispersion of contaminants released into the air and influence the visual impacts of cloud and fog in the lower atmosphere, affecting what is seen and how it is perceived. This Section provides an overview of meteorology in Christchurch, the impact it has on concentrations of contaminants and visibility, as well as processes relating to fog formation and how these impact on what is seen.

The meteorology of Christchurch is complex, primarily because of its geographical location. The Port Hills, Southern Alps, coastline and the gentle slope of the Canterbury Plains all contribute to local wind patterns.

Drainage flows or katabatic winds represent downslope movement of cool air, which occurs under the influence of gravity. In Christchurch, these flows can take place as a result of both the Port Hills and the slope of the Canterbury Plains. These types of winds are ineffective at transporting air pollutants away from the city, because of low wind speeds and flow reversals (Sturman, 1985). The drainage flows transport pollutants from the areas around the Port Hills and the western suburbs towards the inner city (Gimson, 1998). The impact of drainage flows from the Port Hills in reducing contaminant concentrations on high pollution nights is observed at a number of monitoring sites across the city. In particular, the Beckenham monitoring site shows significant reductions in contaminant concentrations as the airflow from the nearby hills reaches that area (van den Assem, 1997). However, the convergence of airflow from katabatic flows on the Port Hills with airflows from the Canterbury Plains can lead to stagnated air nearer the inner city (Kossman & Sturman, 2002).

The north-easterly sea breeze is also common in Christchurch and provides localised air movement. The sea breeze develops on the Canterbury Plains when the synoptic weather conditions produce light winds and the Earth's surface heats the air in contact with it so that it becomes warmer than that over the sea. This wind is common under a variety of conditions, including the north-westerly flow when it is often associated with an enhancement of the lee trough north-easterly (McKendry *et al.*, 1988). The north-easterly sea breeze is also very apparent when large-scale winds are from the south-westerly direction. Larger scale winds are also influenced by the topography of the area. The Southern Alps, located approximately 70 km to the west of Christchurch, reach heights of 2000-3000 metres and create a blocking effect, whereby prevailing winds from the west must either pass over the mountains or be diverted through Cook Strait to approach Christchurch from the north-east (McKendry, 1988). Winds passing over the mountains may produce north-westerlies over the city, or may overlie the coastal north-easterly. The consequential wind direction and wind speed impacts on air quality and visibility in the city. The effects of these wind systems on air pollution patterns across the city have been investigated by Sturman (1985).

In addition to wind patterns, atmospheric stability also impacts on air pollution. The majority of emissions in Christchurch are released into the lower layers of the atmosphere. The dispersion of these emissions depends on the stability of the atmosphere, as a more turbulent atmosphere mixes and dilutes the pollutants, resulting in lower concentrations. Atmospheric stability is determined by the vertical temperature gradient. Neutral stability occurs when the temperature decreases by 1 °C for every 100 metres ascended. If it decreases by more than 1 °C it is considered unstable and this promotes vertical mixing and dispersion. The atmosphere is considered stable if the temperature decrease is less than 1 °C per 100 metres or the temperature increases with height. The increase of

temperature with height is described as a temperature inversion, or inversion layer. The ability of the atmosphere to mix vertically is controlled by its stability, with buoyant vertical motion being inhibited under stable conditions and enhanced under unstable conditions. A neutral atmosphere often results from the vertical mixing of the air due to mechanical processes, resulting in a 'well-mixed' neutral temperature profile. However, where the surface is relatively rough (e.g. in complex terrain and in some urban areas), mechanically-induced turbulence may cause vertical mixing, even if the atmosphere is stable.

In the lower troposphere, the primary cause of temperature variations (and consequently stability) is surplus of radiation by day that is dissipated mainly through turbulent sensible and latent heat, while at night the ground surface has a radiative deficit. Consequently, the temperature near the ground follows a sinusoidal diurnal temperature variation, as the ground absorbs heat during the daytime and cools after sunset, emitting radiation. Thus the stability of the atmosphere near the Earth's surface varies with time of day. During the daytime, the ground is heated by the sun, increasing the negative temperature gradient, giving an unstable atmosphere. The greater vertical mixing generated by the unstable air enhances dispersion of pollutants. Consequently, elevated pollution levels during the daytime are not common. During the evening, the air closer to the ground cools faster than the upper layers due to its contact with the Earth's surface, which loses heat through terrestrial radiation, creating a stable inversion layer. Only a small amount of mixing occurs and atmospheric conditions are conducive to elevated pollution levels.

When temperature inversion conditions restrict the vertical dispersion of pollution from ground level sources, reduced visibility is referred to as the surface layer haze. In surface layer haze, the top edge of the pollution layer is typically visible as a distinct line, and occurs as a result of the capping of a mixed layer by the temperature inversion. This contrasts with uniform haze, which occurs when pollutants are uniformly distributed both horizontally and vertically from the ground to a height well above the highest terrain, because the mixed layer depth is well above ground level (and the field of view of an observer). Similarly, an elevated haze layer, which occurs when the pollution distribution is not in contact with the ground, is indicative of a layered (essentially stable) atmospheric structure that is independent of the surface processes described above.

Meteorology also effects visibility through the impact of humidity and the formation of fogs. Radiation fogs occur when the low ground temperatures cool a layer of air near the earth's surface resulting in the condensation of moisture in the form of fog. These fogs typically occur on cold cloudless nights are common in Christchurch during the winter months.

The impact of meteorology on air pollution and visibility in Christchurch has been well characterised. Detailed studies of the impact of meteorology on air pollution have spanned a number of decades (Owen and Tapper, 1977; Sturman, 1985; van den Assem, 1997; Gimson, 1998 and Wilson, 1999). While the majority of these studies considered relationships between contaminant concentrations and meteorology, Wilson (1999) focused on the impacts of meteorology on visibility. Results showed that higher light extinction values in Christchurch occurred under south-west non-specific and foehn circulation conditions. Wilson (1999) concluded that these were consistent with the major categories conducive to elevated pollution levels identified by Owens and Tapper (1977). Of the three synoptic classifications, anticyclone, cyclone and non-specific, the strongest correlation was found between anticyclonic conditions and elevated light extinction values (Wilson, 1999).

In a comparison of meteorological conditions on hazy and clear days in Christchurch, Wilson (1999) found significant impacts of:

- Wind speed with hazy days occurring when wind speeds were low.
- Temperature at 7.5 metres, with warmer temperatures on clear days particularly during the morning 09:00 to 11:00 period.
- A temperature inversion between the hours 09:00 and 11:00.
- Relative humidity, with hazy days occurring under elevated relative humidity between the hours 0900 to 11:00.
- Vapour pressure at 09:00 to 11:00, with higher vapour pressure on clear days.

Wilson (1999) concluded that wind speeds and temperature had the most significant impact on visibility with poor visibility occurring under low wind speeds and temperature inversion conditions, and that the conditions conducive to poor visibility in Christchurch were similar to those identified as being conducive to poor air quality in previous studies (e.g., Gimson, 1998).

### **3.3 Air quality monitoring**

#### **3.3.1 Monitoring network**

Air quality has been monitored in Christchurch since the 1960's, when measurements of total suspended particulate (TSP) were taken primarily to determine trends in lead concentrations in the city. While TSP is still measured in Christchurch for that purpose, evidence in the 1980's suggested that suspended particulate (PM<sub>10</sub>), a smaller fraction of the TSP, was responsible for adverse health effects (MfE, 1994). Consequently, PM<sub>10</sub> has been measured in Christchurch since 1988. While it is an even finer portion than this that is of concern for visibility (i.e., particles less

than 2.5 microns in diameter), trends in the larger size fractions may be indicative of trends in the finer size fraction.

Other contaminants measured in the city since 1988 include sulphur dioxide (SO<sub>2</sub>), carbon monoxide (CO), nitrogen dioxide (NO<sub>2</sub>), nitrogen oxide (NO), and light scattering due to particles. Of these, measurements of nitrogen oxides (NO<sub>2</sub> and NO) and light scattering are of interest in assessing visibility. Light scattering ( $B_{sp}$ ) has been measured using a Belfort nephelometer and is usually a strong indicator of visibility. Two limitations in using the results from this instrument to assess the impact of light scattering on visibility in Christchurch are the reliability of its operation and the height of the sample inlet, which is three metres above ground. Meteorological variables such as wind speed, wind direction, relative humidity and air temperature at 1 metre and at 10 metres are also continuously recorded at the same site. These data are logged and archived as 10-minute averages.

### 3.3.2 Trends

Trends in visibility degradation in Christchurch may be reflected to some extent by changes in concentrations of contributing species. Assessing trends in Christchurch air pollution concentrations is complicated by a number of factors. Changes in monitoring sites since the 1960's have limited the data available for trend analysis. Missing data and different methods of measurement also complicate the analysis, and climatic variations make the assessment of trends in emissions difficult. Notwithstanding these factors, a downward trend in seven-day average TSP is evident from the long term monitoring data collected (Figure 3.1a). As indicated above, changes in TSP may reflect changes in smaller size fractions of interest from a visibility perspective, particularly if combustion is a major source of TSP. However, if TSP is dominated by the larger particles, these trends are unlikely to have significant implications for visibility. Figure 3.1b shows a significant decrease in lead concentrations in Christchurch. Although not relevant with regard to visibility effects, changes in lead concentrations in Christchurch are of particular interest in observing the effectiveness of management options introduced nationwide to reduce lead emissions (Figure 3.1b). While fewer data are available for other contaminants, some trend analysis is possible.



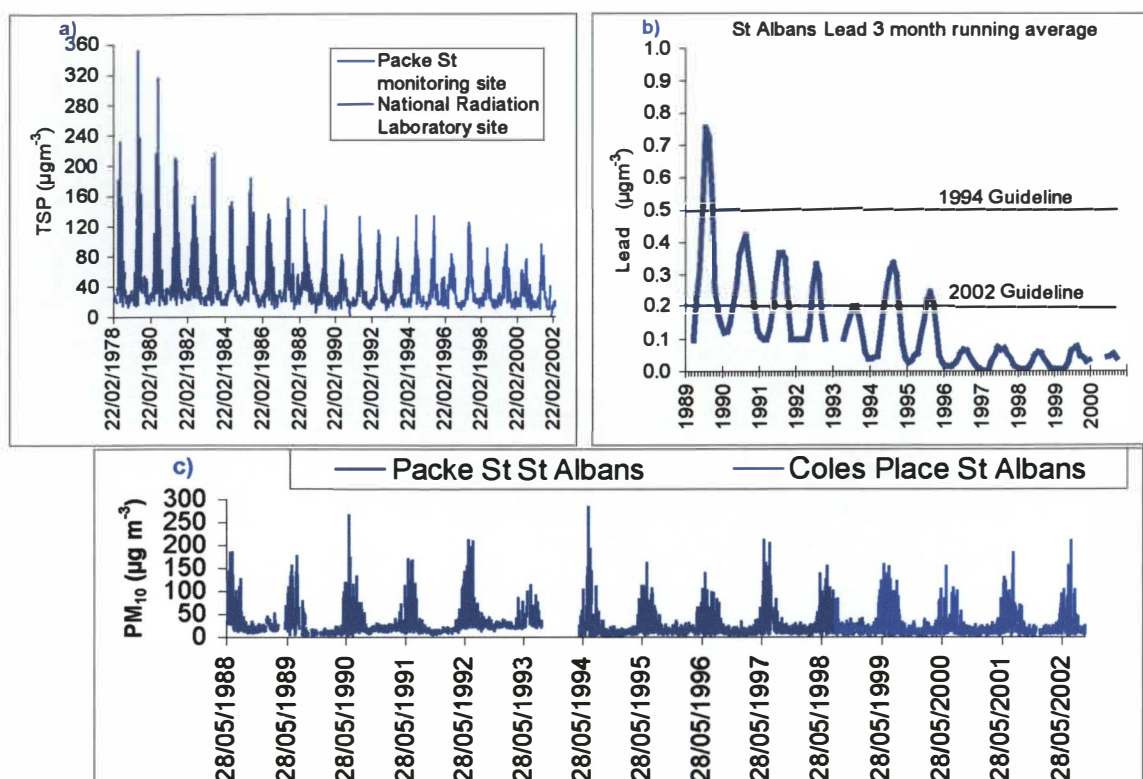


Figure 3.1: Seven-day average TSP (a), Lead (b) and daily  $\text{PM}_{10}$  (c) concentrations in Christchurch from 1978-1994, from 1989-2000, and from 1988 to 2002 respectively (data supplied by Environment Canterbury) – changes in colour in TSP and  $\text{PM}_{10}$  monitoring indicate results from different monitoring sites.

In addition to TSP measurements, concentrations of  $\text{PM}_{10}$  have been measured in Christchurch since 1989. Figure 3.1b shows variations in  $\text{PM}_{10}$  concentrations since 1988. No significant trends in these concentrations are evident, although seasonal variations in  $\text{PM}_{10}$  concentrations are apparent. Figure 3.2 shows the maximum  $\text{PM}_{10}$  concentrations measured in Christchurch each year, as well as the number of days the 24-hour average concentration exceeded the ambient air quality guideline of  $50 \mu\text{g m}^{-3}$ . Maximum  $\text{PM}_{10}$  concentrations range from around 100 to  $300 \mu\text{g m}^{-3}$  and guideline exceedences are measured on around 30 times per year on average. The distribution of the  $\text{PM}_{10}$  concentrations is illustrated in Figure 3.3, which compares measured  $\text{PM}_{10}$  concentrations to the Ministry for the Environment's indicator categories. This shows some consistency in the proportion of days when  $\text{PM}_{10}$  concentrations were in the "good" category from 1994. However it is likely that this is a result of changes in monitoring methods and data quality assurance since 1994. Some variability also occurs as a result of seasonal bias in the monitoring, for example a large proportion of the summer data for 1993 were missing. Ambient air quality monitoring of  $\text{PM}_{2.5}$  concentrations in Christchurch has been limited to monitoring carried out during 1997 (Figure 3.4). A large proportion of the  $\text{PM}_{2.5}$  concentrations measured were greater than the interim guideline proposed by MfE in 1999 of  $25 \mu\text{g m}^{-3}$ . Like  $\text{PM}_{10}$ , concentrations of  $\text{PM}_{2.5}$  are higher during the winter months.

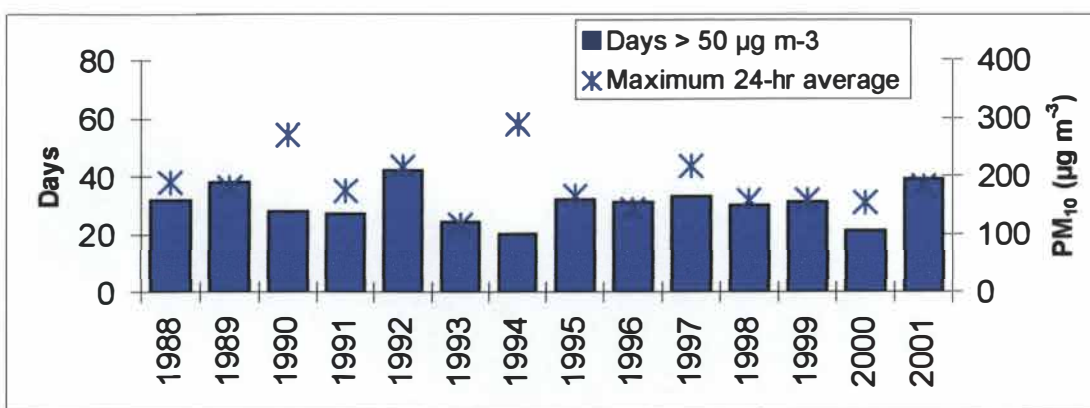


Figure 3.2: Guideline exceedences and maximum PM<sub>10</sub> concentrations at St Albans monitoring site from 1988 to 2001 (data supplied by Environment Canterbury).

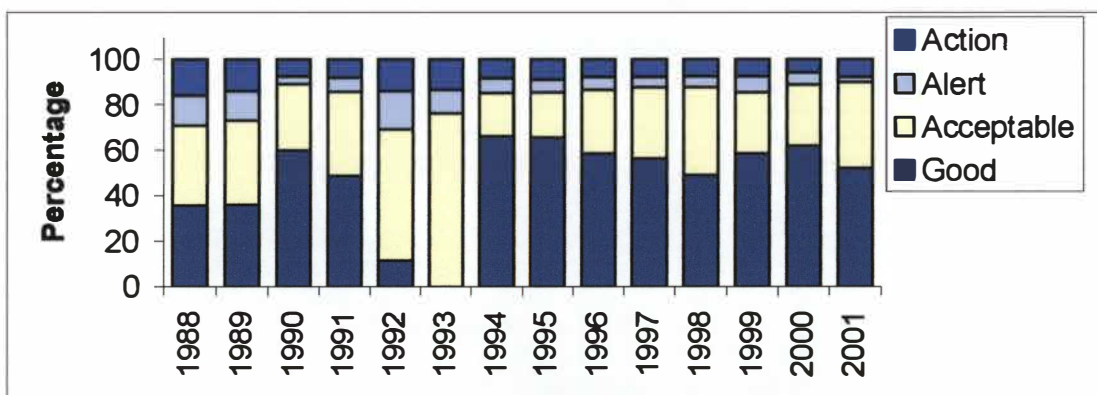


Figure 3.3: Comparison of PM<sub>10</sub> concentrations measured at St Albans to Ministry for the Environment indicator categories based on a PM<sub>10</sub> guideline of 50 µg m<sup>-3</sup> (data supplied by Environment Canterbury).

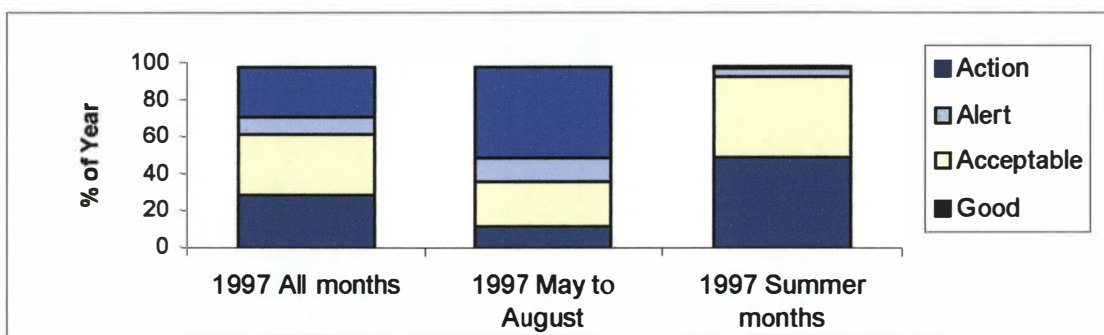


Figure 3.4: Comparison of PM<sub>2.5</sub> concentrations measured at St Albans in 1997 to Ministry for the Environment indicator categories based on an interim PM<sub>2.5</sub> guideline of 25 µg m<sup>-3</sup> (Ministry for the Environment, 1999) (data supplied by Environment Canterbury).

Other measurements of interest from a visibility viewpoint include NO<sub>2</sub> and Bscat (light scattering measured using a nephelometer). Figure 3.5a shows seasonal variations in NO<sub>2</sub> concentrations in Christchurch but no apparent long-term trends for the years 1994-2001. While nephelometer data has been collected since 1988, these data are unlikely to be reliable due to infrequent calibrations and equipment problems. Figure 3.5b shows the variations in light scattering data collected at temperature of 30 ° C at the St Albans monitoring site for 1998, the last year of Bscat monitoring at this site.

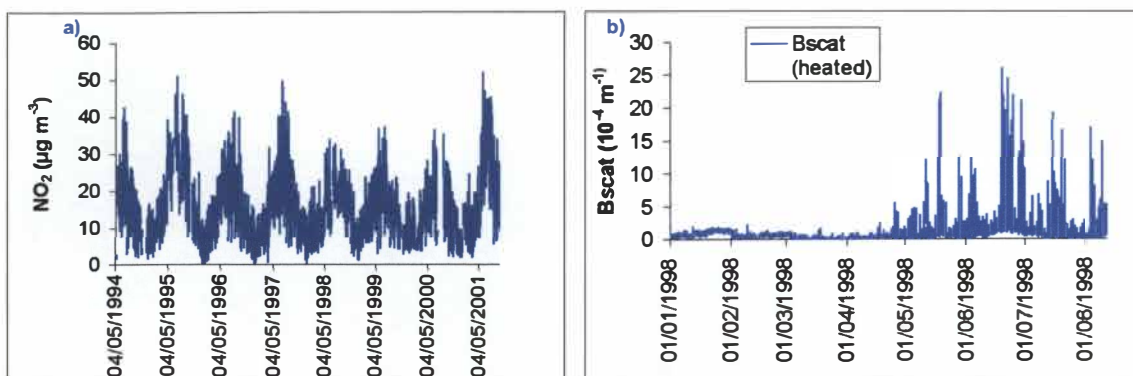


Figure 3.5: 24-hour average NO<sub>2</sub> concentrations from 1994 – 2001 (a) and Bscat measurements during 1998 heated to 30 °C at the St Albans monitoring site in Christchurch (b)(data supplied by Environment Canterbury).

### 3.3.3 Seasonal variations

Poor visibility, in particular brown haze in Christchurch, is a common occurrence during the winter months. However, as indicated in Chapter 1, haze episodes also occur during the summer time. In contrast, high concentrations of contaminants in Christchurch are primarily a wintertime phenomenon with guideline exceedences typically occurring during the months May to August (Figure 3.6). Concentrations of NO<sub>2</sub> and SO<sub>2</sub> are also slightly elevated during the winter months, although concentrations of these contaminants do not exceed guideline values. Given these seasonal variations in contaminant concentrations, it is possible that the factors contributing to summer and winter haze differ.

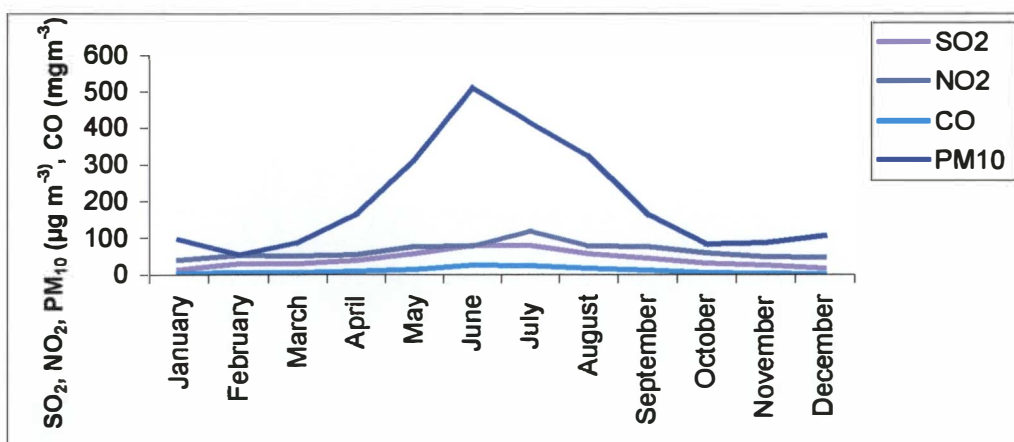


Figure 3.6 Maximum 24-hour average concentrations of PM<sub>10</sub>, NO<sub>2</sub>, SO<sub>2</sub>, and CO averaged monthly for the years 1993-1999 at the St Albans monitoring site (data supplied by Environment Canterbury).

### 3.3.4 Daily variations

Daily variations in air quality in Christchurch occur largely as a result of variations in meteorological conditions. As detailed in Section 3.2, low wind speeds coupled with temperature inversion conditions are most conducive to high concentrations of air contaminants. In Christchurch, these conditions typically occur in the evening, coinciding with the lighting of domestic fires and the evening traffic peak. Maximum concentrations of  $PM_{10}$  are typically observed around 22:00-23:00. Reduced visibility is most noticeable during the hours of daylight, in particular the morning period following a night of high pollution. Figure 3.7 shows that concentrations of contaminants do increase during the morning period, but that concentrations remain lower than for the previous evening.

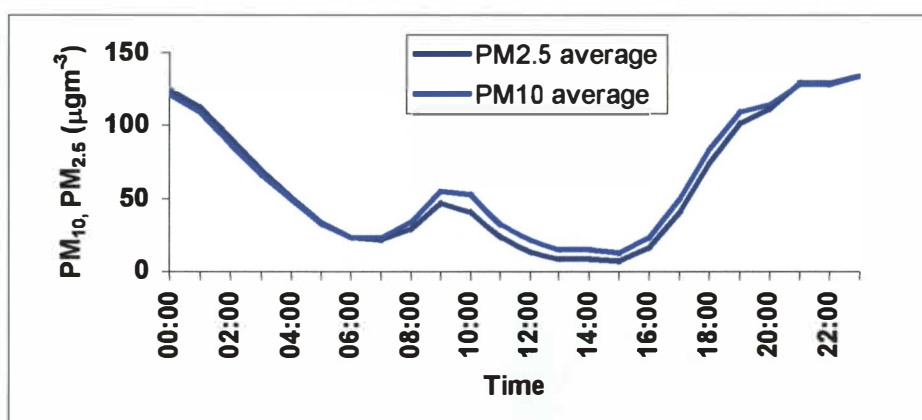


Figure 3.7: Typical average hourly concentrations of  $PM_{10}$  and  $PM_{2.5}$  on high pollution days during 1997 (data supplied by Environment Canterbury).

Daily variations are also observed in the portion of  $PM_{10}$  in Christchurch that is  $PM_{2.5}$ . On average, for high pollution days<sup>9</sup> during the winter the proportion of  $PM_{10}$  that is  $PM_{2.5}$  is about 90% (Foster, 1998). However, there are diurnal cycles in this proportion. During the evening and night time period almost all of the  $PM_{10}$  is  $PM_{2.5}$  (mean percent difference less than 20% on average), whereas during the daytime, when visibility issues are more noticeable, there is a larger proportion of the  $PM_{10}$  (around 50% on average) that is in the coarse size fraction. As it is the finer fraction ( $PM_{2.5}$ ) that generally plays a greater role in visibility reduction, it would seem from the relatively low concentrations that occur during the daytime, that these particles can have quite an impact on visibility even at low concentrations. Consequently, even if the sources of the problem were the same, measures proposed to improve 24-hour average  $PM_{10}$  concentrations to meet a health guideline of  $50 \mu\text{gm}^{-3}$  (see Section 3.5) may not be sufficient to significantly improve Christchurch's brown haze.

<sup>9</sup> Days when the 24-hour average  $PM_{10}$  concentration was greater than  $50 \mu\text{gm}^{-3}$



### 3.4 Legislative Background

Prior to the Resource Management Act (1991), air quality in Christchurch City was managed under the Clean Air Act (1972) by the Christchurch City Council and the former Department of Health. Clean Air Zone orders (1974 & 1984) established under this Act focused on domestic heating, as this was considered a significant source of air pollution. These orders prohibited the installation of open fires and restricted the installation of wood burners to models meeting the specifications of the Council. In 1991, the Resource Management Act (RMA) gave the Canterbury Regional Council the responsibility for air quality management in Christchurch.

The purpose of the RMA as is stated in Section 5 of the Act and, as it relates to air, is as follows:

1. To promote the sustainable management of air;
2. “Sustainable management” means managing the use, development and protection of air in a way, or at a rate, which enables people and communities to provide for their social, economic and cultural well being and for their health and safety while:
  - a) “sustaining the potential of air to meet the reasonably foreseeable needs of the future generations; and
  - b) safeguarding the life-supporting capacity of air; and
  - c) avoiding, remedying, or mitigating any adverse effects of the discharge of contaminants to the air on the environment.”

The RMA requires regional councils to prepare a Regional Policy Statement (RPS). The purpose of the RPS is to achieve the purpose of the RMA by providing an overview of the resource management issues of the region, and policies and methods to achieve integrated management of the natural and physical resources of the whole of the region. Objective one of the Canterbury RPS is to “Maintain or improve ambient air quality so that it is not a danger to people’s health and safety, and reduce the nuisance effects of low ambient air quality”. Visual impact is given as an example of a nuisance and amenity effect, and methods identified to achieve the objective include regional plans and strategies, resource consents and co-ordination, promotion, education and advocacy.

Prior to implementing any of these methods to control visibility, an assessment of whether controls are required and what sources are contributing to degraded visibility are necessary. These measures are an important component of the management of any air quality issue. The management of other air quality issues in Christchurch is detailed in the following Section.



### 3.4 Sources of PM<sub>10</sub> in Christchurch

In 1996, Environment Canterbury commissioned National Institute of Water and Atmospheric Research (NIWA) to carry out an emissions inventory to assess the relative contribution of different sources to emissions of air contaminants. That report indicated that domestic heating contributed around 80% of the PM<sub>10</sub> emissions in Christchurch (CRC, 1997). At that stage, around 42,000 households in the urban areas of Christchurch were found to use solid fuel burning for domestic home heating.

In 1999, Environment Canterbury carried out a second emission inventory for Christchurch to assess trends in emissions since 1996. That study found a significant increase in the number of households in Christchurch choosing solid fuel burning for domestic home heating, with 52,000 households in the urban area reliant on solid fuel. Figures 3.8 and 3.9 show the relative contributions of different sources to total PM<sub>10</sub> emissions and to emissions from domestic heating in Christchurch at that time.

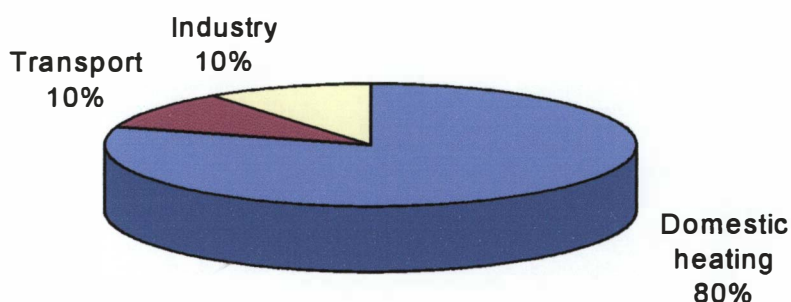


Figure 3.8: Relative contribution of sources to PM<sub>10</sub> emissions in urban Christchurch in 1999 (Wilton, 2001).

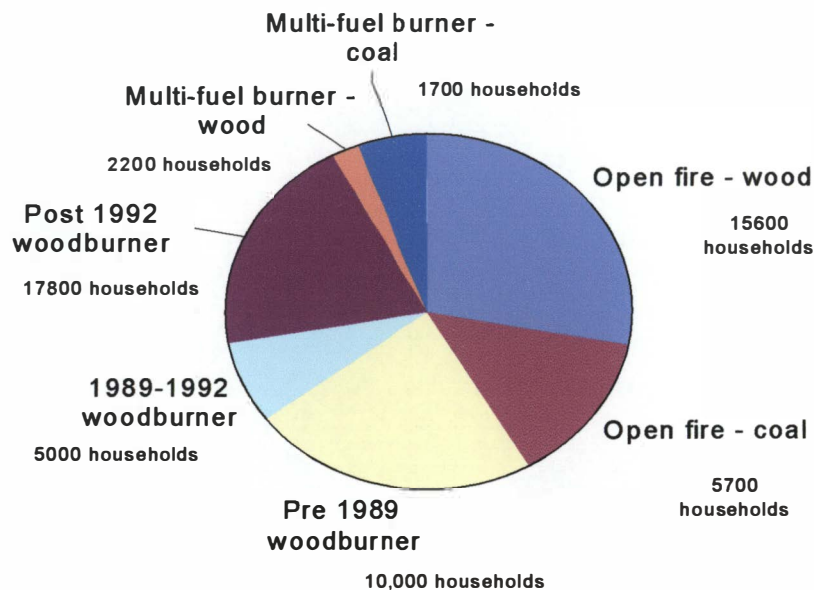


Figure 3.9: Relative contributions of different heating methods to PM<sub>10</sub> emissions from solid fuel burning in Christchurch in 1999 (Wilton, 2001c).

The emission inventories show differences in the time of day that emissions from different sources occur. Table 3.1 shows that the majority of domestic heating emissions occur during the evening (18:00-22:00) time period, whereas a large proportion of emissions from transport occur during the daytime (10:00-16:00) period. The timing of these emissions impacts on the contribution they make to 24-hour average PM<sub>10</sub> concentrations. This is because emissions that occur during the evening, when meteorological conditions are more conducive to pollution, will have a greater impact on concentrations than those that occur during the daytime when higher wind speeds result in greater dispersion.

Table 3.1: Daily PM<sub>10</sub> emissions (kg) by time of day (Wilton, 2001).

	PM <sub>10</sub> (kg) 06:00-10:00	PM <sub>10</sub> (kg) 10:00-16:00	PM <sub>10</sub> (kg) 16:00-22:00	PM <sub>10</sub> (kg) 22:00-06:00	Total PM <sub>10</sub> (kg)
<b>Domestic heating</b>	668	1479	5720	989	8856
<b>Motor vehicles</b>	328	541	428	65	1361
<b>Industry</b>	237	497	232	214	1180
<b>Total Christchurch</b>	<b>1233</b>	<b>2518</b>	<b>6380</b>	<b>1268</b>	<b>11397</b>

To account for the effect of the time of day when emissions occur and to establish the relationship between emissions and concentrations, a box model of this relationship was developed by NIWA (Gimson & Fisher, 1997). The outputs of the model were used to weight the emissions from different sources relative to their contribution to 24-hour average PM<sub>10</sub> concentrations. This model was based on a linear approach to the relationship between emissions and concentrations. Figure

3.10 shows the relative contribution to  $PM_{10}$  concentrations once this time of day factor is accounted for.

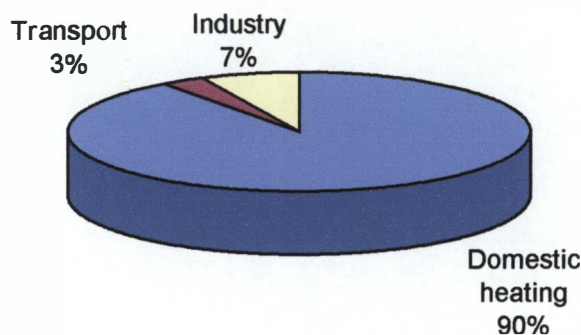


Figure 3.10: Relative contribution to  $PM_{10}$  concentrations in Christchurch in 1999 (Wilton, 2001b).

### 3.5 Air quality management in Christchurch

A consultative document preceding the Natural Resource Regional Plan for air (NRRP-air) identified  $PM_{10}$  as the primary air contaminant of concern in Christchurch because of the frequency and extent to which concentrations of  $PM_{10}$  exceed health guidelines (CRC, 1997). The Canterbury Regional Council prepared a draft plan in 1998 that proposed measures to reduce concentrations of  $PM_{10}$  so that the air in Christchurch was not a danger to people's health. These measures included a prohibition on the use of both coal and open fires, and a requirement that solid fuel burners be replaced 15 years after installation (CRC, 1998).

These measures were reviewed in 2000, when the results of the 1999 emission inventory became available. Because of the significant increase in the number of Christchurch households using solid fuel burning for domestic heating since 1996, the measures originally proposed in the 1998 draft air plan were no longer likely to achieve the then desired reduction of 74% in  $PM_{10}$  concentrations.

Alternative management options detailed in Wilton (2001) were considered for reducing  $PM_{10}$  concentrations in Christchurch. In 2002, an air plan containing the following components was notified:

- Prohibition on the use of open fires (from 2006).
- Prohibition on the use of any enclosed burner not meeting the low emission standard (beginning 2008 or 15 years after the appliance is installed).
- Prohibition on the installation of solid fuel burning appliances in new dwellings or buildings (from 2003).

- Prohibition on the installation of solid fuel burning appliances in dwellings or buildings that currently do not have solid fuel burning devices, including any extensions and alterations to those dwellings or buildings (from 2003).
- Setting of a low emission standard for new burners of 1.5 g/kg for replacement of existing solid fuel burning only (later changed by elected councillors to 1 g/kg).
- Provision of financial incentives.
- Extensive education and promotion.

Throughout the process of consultation on the air plan, visibility degradation was raised as an issue by members of the public. These included submissions on the draft NRRP-air and coal ban hearings which indicated that many people perceived the daytime brown haze to be a visual indicator of high particulate concentrations associated with adverse health effects. Consequently, it appears there is an expectation that measures to reduce the 24-hour average PM<sub>10</sub> concentration will significantly improve visibility in Christchurch. Investigations into the sources of reduced visibility in Christchurch should therefore assist in both understanding the relationship between the two issues (health effects of PM<sub>10</sub> and daytime visibility) and in the management of visibility.

### 3.6 Summary

Air quality in Christchurch is a major environmental issue spanning many decades. The greatest problem from a health perspective is suspended particulate concentrations, which result from a combination of cold wintertime temperatures, a reliance on solid fuel for domestic heating and meteorological conditions conducive to high pollution. Degraded visibility is the most noticed effect of air pollution and is also of concern because of its amenity effect. Concentrations of some contaminants, such as TSP and lead, appear to be decreasing. However, health guidelines for PM<sub>10</sub> are exceeded on about 30 days per year. Environment Canterbury, the regional council which has responsibility for air quality in Christchurch, has proposed measures to reduce 24-hour average PM<sub>10</sub> concentrations to meet an air quality target of 50 µgm<sup>-3</sup>. Contrary to public expectation, however, it can be argued that it is unlikely that these measures will result in significant improvements in daytime visibility, as peaks in PM<sub>10</sub> occur mostly at night time.

## Chapter 4 Site, Equipment and Methodology

### 4.1 Introduction

The context and theory for assessing factors contributing to visibility degradation in Christchurch are detailed in Chapters 2 and 3 respectively. This Chapter focuses on the research methodology, which has been designed to meet the objectives of the research, detailed in Chapter 1.

The research design includes detailed monitoring of contaminants and meteorology, as well as the optical characterisation of the atmosphere. The physical measurements and analysis methods undertaken are detailed in Section 4.2. This includes the method used to assess the relationship between light extinction and perception, integrating the use of digital images and surveys. The location of the monitoring site, the equipment used and some issues relating to monitoring methods are outlined in Sections 4.3 and 4.4.

### 4.2 Methodology

The research draws together both the physical and perceptual properties of visibility degradation.

Assessment of the physical properties included an intensive monitoring regime commencing in February 2000 and concluding in April 2002. This involved collection of data, such as:

- The optical properties of the atmosphere ( $B_{sp}$ ,  $B_{ap}$ ,  $B_{ag}$ ).
- Contaminant concentrations.
- Visual properties of the atmosphere (photographs).
- Meteorology.

A summary of the visibility monitoring programme, including periods of major instrument downtime is shown in Table 4.1. Air quality and meteorological data from other monitoring programmes was also available for the study. In particular, meteorological data from Environment Canterbury and the “Christchurch Air Pollution Study (CAPS)” sites, and  $PM_{10}$  data from the Environment Canterbury St Albans monitoring site were used in the analysis.

Table 4.1: Visibility monitoring programme.

	Sample collection regime	Monitoring period	Major downtime
Nephelometer – (Optec NGN3)	Continuous sampler 10 minute averages	February 2000 to April 2001	1-3, 7-10, 19-20 April 17-20 & 31 August



			1, 4-5, 30 September 1-2, 11-13 October 17-20, 25-27 November 3-4, 31 December 1-8, 13-15 January
Aethalometer (Magee Scientific)	Continuous sampler 10 minute averages	January 2000 to April 2001	24-26 June 12-13 July 28-30 October 27-30 April 2001
NO <sub>2</sub> analyser (API series 200)	Continuous sampler 10 minute averages	February 2000 to April 2001	10-17 March 21-22 September 12-17 October
Carbon analyser (Rupprecht and Patashnick series 5400)	Continuous sampler One hour averages	January 2000 to April 2001	26 January – 7 February 1-3 June 12-16 August 18-22 September 3-4, 18-20 October 20 November – 30 January
TEOM (Rupprecht and Patashnick series 100b)	Continuous sampler 10 minute averages	February 2000 to April 2001	
SASS sampler (MetOne)	Daytime sample period 06:00-13:00 – weekdays 24-hour sample period from January 2001	February 2000 to April 2001	1-11 February 1-25 April 13-25 July 17 November – 22 January
Digital camera (Kodak DC 260)	Instantaneous reading One per hour on hour	January 2000 to April 2001	
Meteorological parameters	Continuous sampling 10 minute averages	January 2000 to April 2001	

The different data sources were collated and data files based on common averaging periods were established. These included hourly averages for all components of extinction, PM<sub>10</sub> (TEOM), elemental and organic carbon and meteorology and a daily result based on the five to six hour average for PM<sub>10</sub> mass (gravimetric), elemental analysis, nitrates, sulphates and chlorides. Extinction estimates were based on the summation of the measured components plus Rayleigh scattering as overseas studies (e.g., Pryor *et al.*, 1997) have shown a good correlation between measured and estimated mean Bext using this method.

The data analysis methods for the hourly data included correlation, assessment of temporal variations including daily and seasonal variations and case studies. Analysis methods for the daily filter data included examination of summary statistics (e.g., means, ranges, distribution), inter-element correlations and factor analysis, including principal components analysis (PCA). Multiple regression methods were used to relate the light extinction (hourly data) and the particulate source contributions, determined using the PCA, to give the contribution of different sources of PM<sub>10</sub> to different components of light extinction. Further details of the data analysis methods are provided in Section 4.5.

The perceptual aspects of visibility degradation in Christchurch were assessed during 2001 using a survey of respondent's perception to a series of digital photos representing a range of visibility conditions. Section 4.6 details the methodology used for the survey.

### **4.3 Monitoring site**

As indicated in the introduction, the monitoring site used to assess contaminant concentrations and optical properties of the atmosphere should be located where the sampling will be representative of the visibility being characterised. One aspect of this is ensuring that the sampling height occurs within the layer of degraded visibility. The monitoring site selected for measuring optical parameters and particulate data was therefore the top of a six-story building at the Christchurch Polytechnic. Equipment was housed in a laboratory on the sixth floor and the sample tubing ducted through external windows to the roof. In the case of two instruments, the TEOM and the carbon analyser, this was not possible as a direct line of sampling is required. Holes were therefore drilled through the roof and sealant used around the outside of the sample lines to prevent leakage. Two instruments, the nephelometer and the SASS sampling system, were situated entirely on the roof.

One limitation of having a single fixed-point sampling location is the extent to which point measurements can be expected to characterise atmospheric optical properties over distances of several kilometres. This is not of major concern in haze investigations where pollution sources are widespread and adequate mixing occurs. Long-path measurement techniques would provide a better indication of pollutant concentrations across a sight path, but are very resource intensive and are not available for all types of data. Following Sections of this Chapter describe the instrumentation used and how collected data are integrated with surveying and digital camera data to address the research objectives of this thesis.

Another reason for the choice of monitoring site was the location of the Christchurch Polytechnic between the Environment Canterbury building, from which the digital images were being taken,

and the Port Hills, the backdrop to these pictures. As illustrated in Figure 4.1 the Polytechnic is located slightly to the east of Environment Canterbury. While a location within the direct line of view would have been preferable, access to a suitable monitoring site was not possible.

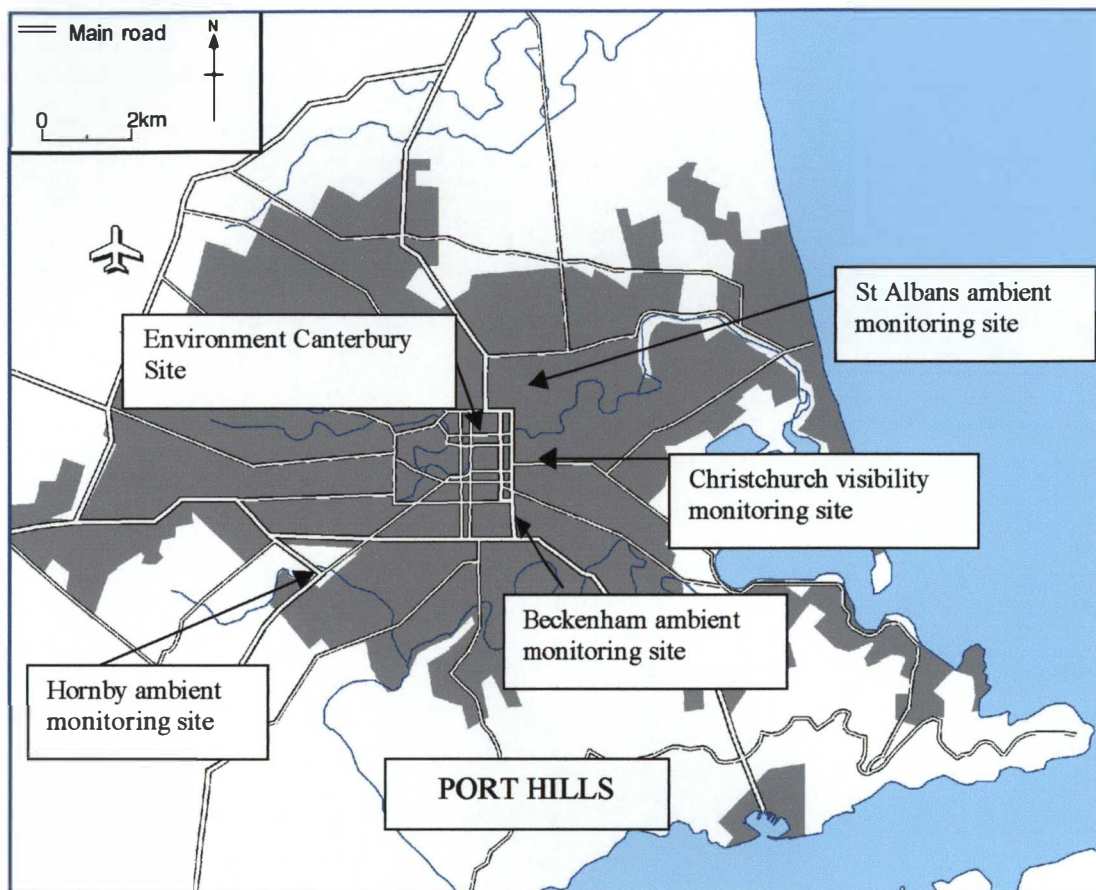


Figure 4.1: Location of the Christchurch Polytechnic, Environment Canterbury (photo site) and other air quality monitoring sites in Christchurch.

#### 4.4 Equipment

The contribution of different physical and chemical properties to reduced visibility in Christchurch was assessed using general principles of the extinction budget analysis technique described in Section 2.5. However, the combination of instrumentation used was unique to this application, as was the method of integrating results with perception (see Chapter 9). Simultaneous measurements of optical properties made within the visible pollution layer included:

- $B_{ap}$  using a Magee Scientific aethalometer.
- $B_{sp}$  using an Optec NGN2 nephelometer.
- $B_{ag}$  using an API chemiluminescence  $NO_2$  analyser.
- Light extinction would be estimated by summing the four contributing parameters  $B_{ap}$ ,  $B_{sp}$ ,  $B_{ag}$  and  $B_{sg}$  (Rayleigh scattering).

In addition to optical measurements, the following particulate measurements and speciation was carried out:

- $PM_{2.5}$  concentrations (Rupprecht & Patashnick, TEOM series 100b).
- Elemental carbon (Rupprecht & Patashnick series 5400 carbon analyser).
- Organic carbon (Rupprecht & Patashnick series 5400 carbon analyser).
- Nitrate (collected using MgO denuders and the SASS sampler, analysed using ion chromatography).
- Sulphate (collected using the SASS sampler, analysed using ion chromatography).
- Chloride (collected using the SASS sampler, analysed using ion chromatography).
- Elements (collected using the SASS sampler, analysed by Geological & Nuclear Sciences (GNS) using PIXE).

Nitrates, sulphates, chlorides and total fine particulate mass were sampled from 06:00-13:00, a period coinciding directly with daytime haze episodes in Christchurch. The sampling method used was a SASS particulate speciation sampler (Figure 4.2). The SASS unit comprises five separate



Figure 4.2: SASS sampler

sample lines each fitted with a  $PM_{2.5}$  size selective inlet and the capacity for the inclusion of an MgO denuder and up to two 47 mm filters in each sample cassette. The sample flow rate through each cassette was  $6.7 \pm 0.3$  l/min giving a total volume of around  $2.6 \text{ m}^3$  over a 7-hour period. The sampling head was located on top of a tripod at a height of about 2 metres. The vacuum pump is mounted in a separate environmental enclosure situated at the foot of the tripod. The processing unit was located at around 1 metre for easy access.

A major difference in the extinction budget analysis technique used was the inclusion of hourly concentrations of elemental and organic carbon, which were made using a Rupprecht & Patashnick series 5400 carbon analyser. In addition to these data, a TEOM<sup>®</sup> (Tapered Elemental Oscillating Microbalance) with a sample temperature of 40 °C, measuring 10-minute  $PM_{2.5}$  concentrations provided additional data on temporal characteristics of the haze episode. The analyser was located with the aethalometer, nitrogen dioxide analyser and carbon analyser in the science laboratory on the six floor of the Christchurch Polytechnic building (Figure 4.3). The nephelometer and SASS sampling system are both designed for an external operating environment and were therefore located on the rooftop.



A Kodak DC 260 digital camera, situated at the Environment Canterbury offices in Kilmore Street, was used to collect images of the haze at hourly intervals during the daytime. Features of the camera include automatic shutter speed and aperture adjustment, a 1536 by 1024 pixel charged couple device chip and optical zoom equivalent to 117mm focal length. In addition, the camera was fitted with a 2 x teleconverter to enhance the focal length to about 234mm. Script files were used to automate the collection of images. Figure 4.3 illustrates the images taken from the digital camera on the 20 July 2002.

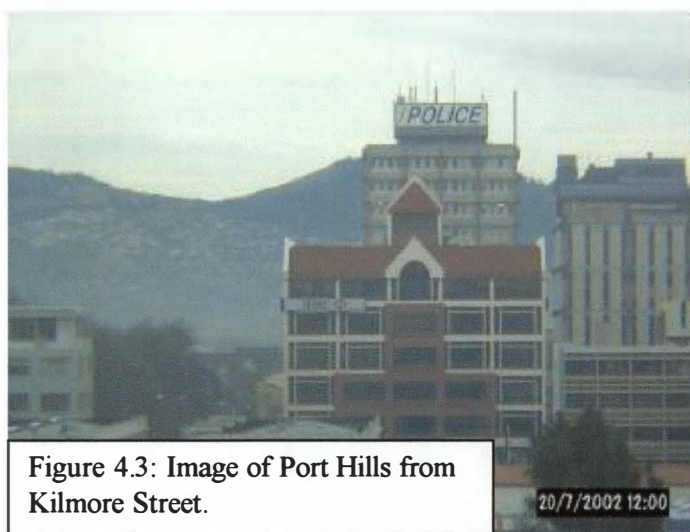


Figure 4.3: Image of Port Hills from Kilmore Street.

A number of issues can arise as a result of the methods used to measure different contaminant concentrations and atmospheric optics. In particular, issues relating to sample temperature can significantly influence concentrations of particulate and its constituents such as elemental and organic carbon. Variations in PM<sub>10</sub> concentrations measured using TEOMs operated at different sample

temperatures in Christchurch, detailed in Foster (1998), indicate that significant volatisation of particulate occurs during the winter months.

Similarly, the proportion of carbon that is elemental versus organic will depend on the methodology used. In the past, elemental and organic carbon concentrations have typically been determined using the thermal optical reflectance (TOR) method on samples collected on a quartz filter. This involves heating a sample through a series of temperature increases, converting the carbon evolved at each step to CO<sub>2</sub>, reducing the CO<sub>2</sub> to methane, and measuring the methane using a flame ionisation detector. At some temperature between 130 °C and 550 °C the sample chars, owing to pyrolysis of organic particles. The point at which charring occurs is detected by a decrease in the reflectance from the sample surface. All carbon measured up to this point is interpreted as organic carbon and all carbon evolved after this point is recorded as elemental carbon (Malm, *et al.*, 1996).



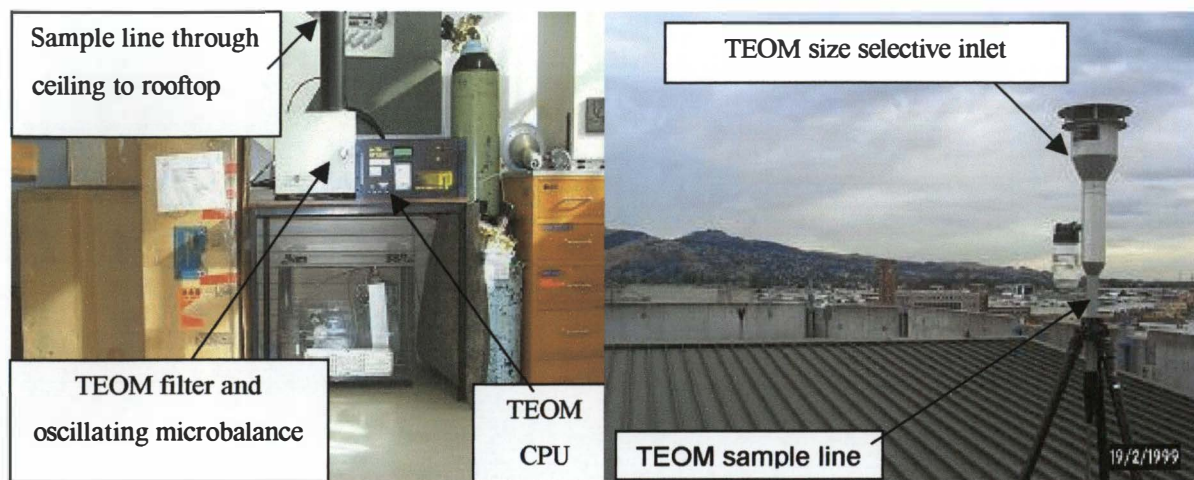


Figure 4.4: Illustration of TEOM sampler on the 6<sup>th</sup> floor and roof of the Christchurch Polytechnic.

The Rupprecht and Patashnick Co Inc Series 5400 carbon analyser (Figure 4.5), used in this study, has been designed for simultaneous hourly measurements of elemental and organic carbon. The analyser uses a similar technique to TOR described above, in that carbon is heated, oxidised to CO<sub>2</sub>, and then measured using a non-dispersive infrared CO<sub>2</sub> detector. The primary difference between the two methods is in the distinction between elemental and organic carbon. The Series 5400 uses a two-step temperature profile with a low temperature burn at 230 °C, representing organic carbon, and a high temperature burn at 750 °C, representing elemental carbon. Manufacturers of the instrument claim a high correlation with accepted manual filter based techniques.



Figure 4.5: Series 5400 carbon analyser on the 6<sup>th</sup> floor of the Christchurch Polytechnic.

#### 4.4.1 Conversions of instrument outputs

The calculation of light absorption by particles and gases is made using data from the aethalometer and NO<sub>2</sub> analyser respectively. Both data require conversions of concentrations ( $\mu\text{g m}^{-3}$ ) to optical

absorption ( $\text{Mm}^{-1}$ ). A brief description of the instrument outputs and the calculation applied to convert these data to light extinction follows.

Light absorption by particles was calculated based on measurements made using the aethalometer. Although this technique involves a direct measurement of optical attenuation at 880 nm and 325 nm, data outputs are in the form of black carbon (BC) concentrations. In this study, the output at the 325 nm wavelength was used. These gave slightly lower absorbance estimates than the 880 nm wavelength. The relationship between optical attenuation (ATN) and black carbon measurements is wavelength dependent and is described as:

$$\text{ATN} = \sigma(1/\lambda) \text{ BC} \quad \text{Equation 4.1}$$

where  $\sigma(1/\lambda)$  is the absorption cross section (sigma) that is wavelength dependent.

While the light absorption measurements are made at wavelengths in the ultraviolet (325 nm) and infrared (880 nm) regions, it is light absorption in the visible spectrum that impacts on visibility. The BC absorption coefficient in the visible spectrum is around  $10 \text{ m}^2 \text{ g}^{-1}$  (White, 1990) and is used in this study for conversion of BC measurements from the aethalometer.

Light absorption by gases was calculated based on the measurements made using the  $\text{NO}_2$  analyser. As detailed in Section 2.4, concentrations of  $\text{NO}_2$  can be converted to light absorption ( $B_{\text{ag}}$ ) based on the following formulae described in Equation 2.10 ( $B_{\text{ag}} = 175K(\text{NO}_2)$ ) where K is a dimensionless parameter that varies with wavelength and  $\text{NO}_2$  concentrations are in parts per million.

As concentrations of  $\text{NO}_2$  measured at the visibility monitoring site are presented in  $\mu\text{g m}^{-3}$  (based on the standard New Zealand conversion factor of 2.05 for  $0^\circ\text{C}$ ) Equation 4.2 is used to calculate light absorption. This is derived from Equation 2.10 for  $\text{NO}_2$  concentrations expressed in  $\mu\text{g m}^{-3}$  and is based on wavelengths in the blue part of the visibility spectrum (<http://www.aqd.nps.gov/ardnew/psd/flag/app2a.html>).

$$B_{\text{ag}} = 0.17 \text{ NO}_2 \quad \text{Equation 4.2}$$

This integrates a value for K of 0.0019, which is lower than the 0.00303 used by Wilson (1999), as the latter was selected for a wavelength of 530 nm. This represents the extinction efficiency and is determined based on the Beer-Lambert Law for absorbance by  $\text{NO}_2$  gas.

## 4.5 Data analysis

### 4.5.1 Factor analysis – PCA

Principal components analysis (PCA) is multivariate statistical method of data analysis that has been commonly used for analysis of atmospheric data since the 1980s. This includes meteorological data reduction, grouping of synoptic and chemical variables, forecasting atmospheric parameters, determining variability in atmospheric fields (Richman, 1986), and more recently for assessing sources of particulate pollution (Hopke, *et al.*, 1982; Ames, *et al.*, 2000). As a source apportionment tool for determining sources of particulate matter, PCA considers the covariance between concentrations of different species present in airborne particles.

In this study, PCA was used to determine a number of factors, referred to as profiles or fingerprints, which represent the similarity of relative concentrations of elements contained within particulate collected daily on filters. These profiles represent the ratios between different elements characteristic of different sources of particulate.

The particulate mass filters used in the PCA analysis were collected using the SASS sampling system described in Section 4.4. A total of 250 filters were analysed for total mass of elements using Proton-Induced X-ray Emission (PIXE) by Geological & Nuclear Sciences (GNS). The PIXE ion beam analysis method determines concentrations from the element specific X-ray emissions associated with the electron de-excitation process that occurs following bombardment of the filter with a proton beam. The x-ray scattering occurs across an angle of around 135 degrees and typically measures concentrations to accuracy of 1-10% (Trompetter & Markwitz, 2001). Elements measured using PIXE included sodium (11), bromine (35) iodine (53), lead (82) and mercury (80). Carbon (6) on the filters was also measured by GNS using a light absorbance method (Trompetter & Markwitz, 2001), based on the assumption that carbon was responsible for all absorbance. A Teflon filter media was used for the first 75 filters, which were collected from 9 February to 21 June 2000. Analysis of these filters found concentrations of many elements on the filters to be frequently below the detection limits. In an attempt to reduce this data loss, GNS recommended the use of polycarbonate filters. From 22 June 2000 until the completion of the study (filters 75 to 250) the filter medium used for the speciation sampling was polycarbonate.

The detection limits by element, compound and filter type are detailed in Table 4.2. Concentrations of elements below detection limits were included in the results for the PIXE analysis to prevent bias in PCA correlations. The dates, filter numbers and sampling duration for each of the filters is shown in Appendix B.

A separate set of 250 filters, collected using the same SASS sampling system and sampling regime, were analysed for nitrate nitrogen, sulphate, chloride and ammonium nitrogen. These were collected on a nylon filter medium and denuder system used to minimise loss of nitrogen. The nylon filters were stored in P35 vials filled with 20 mls of deionised water and analysed using a Dionex DX500 ion chromatography system. The mass of inorganic ions on the filters was measured using ion chromatography (IC).

Table 4.2: Limits of detection (LOD) for PIXE and IC analyses.

	Limits of detection (LOD) ng cm <sup>2</sup>													
	Na	Mg	Al	Si	P	S	Cl	K	Ca	Sc	Ti	V	Cr	Mn
Teflon	98	38	31	29	62	37	33	42	38	35	41	53	51	88
Polycarbonate	115	43	29	22	43	25	20	17	15	18	15	13	7	7
% above LOD	44	86	88	92	1	96	93	47	50	3	0	0	26	3
	Limits of detection (LOD) ng cm <sup>2</sup>													
	Fe	Co	Ni	Cu	Zn	Ga	Ge	As	Se	Br	I	Hg	Pb	El C
Teflon	80	88	96	126	157	188	238	292	361	443	94	652	784	350
Polycarbonate	6	8	5	5	6	5	7	9	10	15	115	17	23	350
% above LOD	73	9	30	10	20	2	0	3	1	11	22	1	1	90
	Limits of detection (LOD) µg/filter													
	Ammonia N		Chloride		Nitrate N		Sulphate S							
Nylon	0.1 µg		0.1 µg		0.1 µg		0.1 µg							
% above LOD	46		73		38		68							

The PIXE (mass per unit area) and ion chromatography results (total mass per filter) were converted to concentrations based on:

- The volume of airflow through the filter sample lines throughout the period of measurement (collected at the SASS control unit).
- A conversion of mass per unit area to mass per filter based on the exposure area of the 47mm filter being 11.94 cm<sup>2</sup>.

The mass concentration of PM<sub>2.5</sub> was measured gravimetrically from the Teflon and polycarbonate filters prior to PIXE analysis. Results of all analyses were collated in an Excel spreadsheet.

Concentrations of elements and ions were copied to a statistical analysis package SYSTAT version 9. Factor analysis using PCA was then performed on the data using an eigenvector analysis of the correlation matrix. A transformation of the data using a varimax rotation was then applied to produce factors closer to actual source profiles.



Of the 32 species measured, only 18 were included in the PCA analysis. Elements were initially excluded from the analysis if more than 30% of the data were below the limit of detection (Table 4.2). Exceptions were then made in the case of Zn, Sc and Mn because of their potential significance for local sources of particles. Source profiles and contributions to PM<sub>2.5</sub> mass determined from this analysis are detailed in Chapter 6.

As a test of the sensitivity of the data to the different filter media, a PCA analysis was carried out separately for the Teflon and Polycarbonate filters. Data were separated into two SYSTAT data files representing filters collected using each media and PCA analysis with varimax rotation applied to each. Results of this test are also discussed in Chapter 6.

#### **4.5.2 Multiple regression analysis**

Multiple regression analysis was used to determine the contribution of different sources of particles, identified using the PCA analysis, to light scattering. The multiple regression analysis was carried out using a backwards-stepwise regression. The stepwise analysis was set up to remove any sources from the equation if their alpha ('p') factor was greater than or equal to 0.15, that is if there was a 15% or greater probability that the relationship was due to chance.

The dependent variable in the analysis was the B<sub>sp</sub> (dry) outputs from the nephelometer, averaged for the period (e.g., 06:00 to 13:00 hours) to coincide with the time of filter sampling. The independent variables were the factor scores for the six factors identified in the PCA analysis.

#### **4.6 Visibility survey**

The perceptual aspects of visibility, in particular the relationship between visibility perception and light extinction were assessed using a survey of perceptual responses to a series of photographs depicting a range of light extinction conditions. The images used were collected at hourly intervals using a digital camera, operated from the Environment Canterbury building on Kilmore Street, directed at the Port Hills.

A selection of these images were used in a survey that required respondents to rate visibility in the image on a scale of 1-7 and to rate how acceptable the degraded visibility was. The following Sections describe the methodology used for the visibility survey. A copy of the survey questionnaire is shown in Appendix A.



#### **4.6.1 Selection of images**

Two sets of 16 images were selected to be included in the visibility survey. These were labelled list one and list two and each list represented images with a similar range of visibility degradation. Images were selected by sorting hourly light extinction data, collected from the visibility monitoring site during the period April to July 2000. Images corresponding with the highest and second highest extinction values were selected for lists one and two respectively and subsequent images chosen by selecting the 62<sup>nd</sup> and 63<sup>rd</sup> consecutive images. Because the data had been sorted in descending order of magnitude this resulted in a selection of images representing a range of light extinction values. In some instances images were not available or were unable to be used for example, for reasons of darkness or focus. In this instance the image was replaced with another image of similar light extinction, chosen by selecting the image corresponding to the next available light extinction value.

#### **4.6.2 Survey design**

An unbiased cross section of the Christchurch population was unable to be surveyed because the resources associated with obtaining a random unbiased survey were beyond the scope of this project. Thus results cannot be considered to be representative of the Christchurch population. The survey participants were primarily staff of Environment Canterbury, geography students, and friends and relatives. Results from each group were collected separately to allow for separate analysis should responses differ significantly across groups.

Participants were given a copy of the survey questionnaire or directed to a website, which contained images from either list one or list two. Respondents were asked to rate each image on a scale of 1-7, where 1 represented very polluted air and 7 very clear air. If respondents believed the reduced visibility to be related to weather conditions, rather than air pollution, they were asked to rate the picture as 0. Respondents were then asked to rate each image based on whether they believed it represented acceptable visibility or not.

#### **4.7 Summary**

The proposed methodology required the establishment of an air quality monitoring site at a height within the haze layer and a comprehensive air quality monitoring campaign. The Christchurch Polytechnic was selected as a suitable location and a monitoring site established on top of the sixth story of the science and nursing block. Measurements of the optical properties of the atmosphere, particulate concentrations and speciation, and meteorology were carried out during the period January 2000 to April 2002. A digital camera was also operated from the Environment Canterbury building in Kilmore Street and images collected at hourly intervals during the daytime for the

duration of the monitoring period. Data analysis methods selected included principal components analysis and multivariate techniques. The methodology also included a comparison between monitoring data and a survey of the perception of visibility degradation.

## Chapter 5 Measurements of visibility and air quality

Analysis of light extinction and air quality data measured at the Christchurch Polytechnic visibility site provides a comprehensive picture of visibility degradation in Christchurch. This Chapter presents these data as the first stage in meeting the objectives of the research and testing the research hypothesis that *“the physical and chemical factors contributing to reduced daytime visibility in Christchurch are complex, vary with season and have significant impact on perceived air quality.”* In particular, the research attempts to assess how different factors contribute to reduced visibility in Christchurch, to examine temporal variations in visibility degradation, and to assess the relationship between visibility perception and light extinction.

In this Chapter, the contribution of different components of light extinction is examined, as well as seasonal and temporal variations in visibility degradation. Details of data from the monitoring site for each month, as well as summary information on concentrations of contaminants measured at the monitoring site, are outlined in Section 5.1. A further breakdown of average values for each hour of the day is presented by month in Section 5.2. Section 5.3 examines the impact of meteorology on light extinction and Section 5.4 considers the relationship between different measurements made at the monitoring site.

Results from this Chapter feed into subsequent analyses, in particular Chapters 6,7 and 8, which consider in detail the contribution of different sources to visibility degradation.

### 5.1 Light extinction and air quality data

Figure 5.1 shows the maximum hourly light extinction values for each month of the year for all data (Figure 5.1a) and for the daytime period from 06:00 to 13:00. (Figure 5.1b). As the highest light extinction values (most degraded visibility) during the monitoring period occurred during evening periods of the winter months, maximum values in Figure 5.1a are significantly higher than those shown for the daytime in Figure 5.1b.

Seasonal variations are apparent in both data sets with higher light extinction values during the winter months. During the winter, maximum hourly average light extinction values were around  $3000 \text{ Mm}^{-1}$  and  $1000 \text{ Mm}^{-1}$  for evening and daytime values respectively. Average values were much lower at less than  $200 \text{ Mm}^{-1}$  for both time periods. During the summer months, daytime values were higher than evening values, with maximum hourly values of around  $300 \text{ Mm}^{-1}$ .

A breakdown of the daytime light extinction values (Figure 5.2) shows that light scattering by particles is responsible for the degraded visibility on these occasions; that it is a major contributor to light extinction values. This source is dominant during both summer and winter contributing up to  $800 \text{ Mm}^{-1}$ . The contribution of  $B_{ap}$  is typically less than  $100 \text{ Mm}^{-1}$  during the summer but increases to over  $200 \text{ Mm}^{-1}$  during the winter months. Daytime concentrations of  $\text{NO}_2$ ,  $\text{PM}_{2.5}$  and carbon are also highest during the winter months with maximum hourly values of around  $170 \mu\text{gm}^{-3}$ ,  $150 \mu\text{gm}^{-3}$  and  $80 \mu\text{gm}^{-3}$  respectively.

The dominance of light scattering for different ranges of light extinction values is also illustrated in Figure 5.3. This shows an increase in the proportion of light absorption by particles from 15% for all data to 26% for the highest 1% of light extinction values. Light scattering by particles also increases from 64% for all data to 75% for the top 10% of light extinction values, but reduces down to 70% for the top 1% of light extinction values.

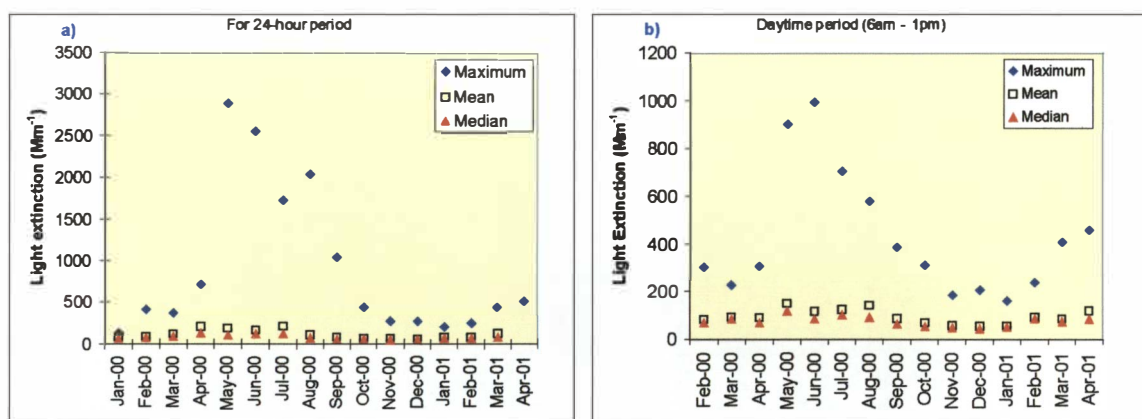


Figure 5.1: Monthly maximum, mean and median hourly light extinction values for all data (a) and for the period from 06:00-13:00 (b) from February 2000 to April 2001.

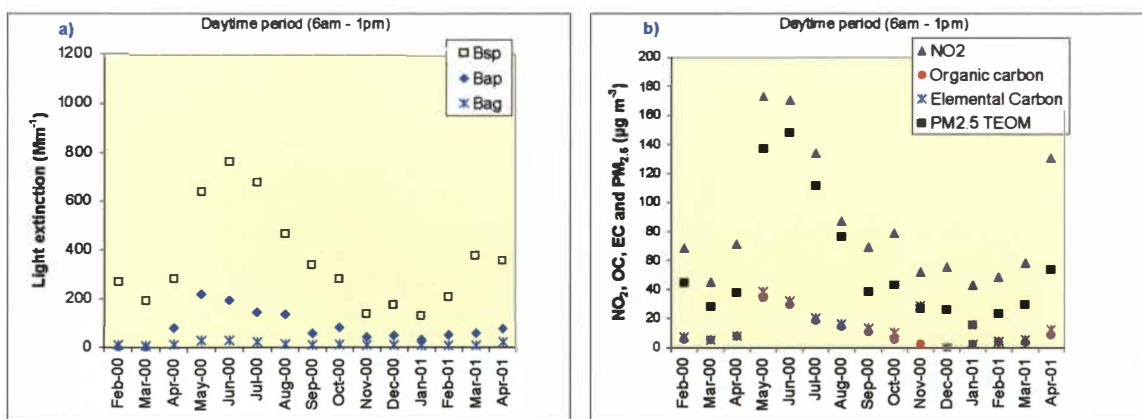


Figure 5.2: Maximum 1-hour average measurements of  $B_{sp}$ ,  $B_{ap}$  and  $B_{ag}$  (a) and  $\text{NO}_2$ , OC, EC and  $\text{PM}_{2.5}$  (b) for each month over the period February 2000 to April 2001.

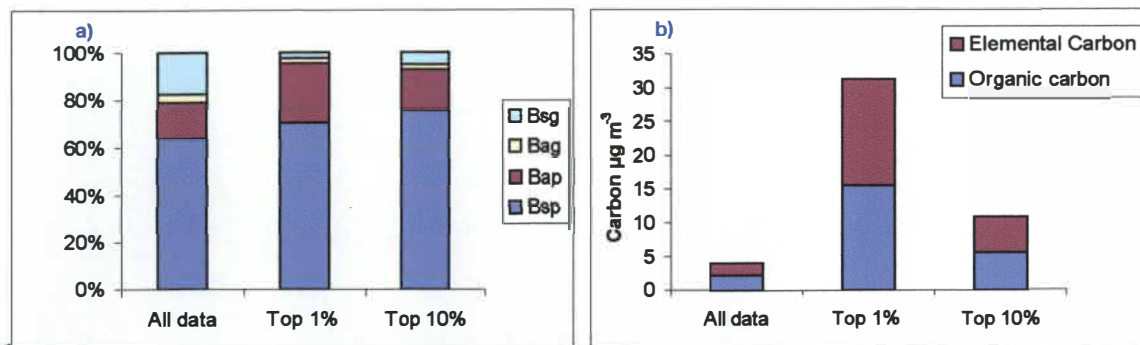


Figure 5.3: Relative contributions of B<sub>sp</sub>, B<sub>ap</sub>, B<sub>ag</sub> and B<sub>sg</sub> to light extinction (a) and carbon concentrations (b) for the period 06:00-13:00 for all data and the top 1% and 10% of light extinction values.

The higher light extinction values during the winter months is of interest as poor visibility in Christchurch during the summer time has been raised as a concern by Christchurch residents (see Figure 1.4). The distribution of degraded visibility in Christchurch for different months of the year is shown in Table 5.1. The assessment is based on the number of hours during the period 06:00-13:00 when the hourly light extinction values exceeded 160 Mm<sup>-1</sup> (see Chapter 9). The greatest frequency of poor daytime visibility occurred during the months of May and August 2000. The least number of hours of poor visibility, as a proportion of hours where data were available, occurred during the months November 2000 to January 2001.

Table 5.1: Seasonal variations in poor visibility.

Month	No. of hours between 06:00 and 13:00 with Bext >160 Mm <sup>-1</sup>	Hours >160 Mm <sup>-1</sup> as a percentage of available hours
February 2000	17	8%
March 2000	17	7%
April 2000	37	19%
May 2000	83	35%
June 2000	37	17%
July 2000	42	18%
August 2000	75	35%
September 2000	28	13%
October 2000	12	5%
November 2000	2	1%
December 2000	4	2%
January 2001	1	1%
February 2001	19	9%
March 2001	17	7%
April 2001	68	30%



Figure 5.4 shows daily variations in the components of light extinction and air quality on the day of the poorest daytime visibility during the monitoring period (20 June 2000), when the highest hourly light extinction value of just less than  $1000 \text{ Mm}^{-1}$  was recorded at 10:00. While higher light extinction values are apparent in the evening period, the impacts of light extinction are of greater concern during daylight hours. The main cause of visibility degradation in Christchurch on 20 June was light scattering by particles, with particle absorption being the second most significant variable. The relatively small contribution of light absorption by  $\text{NO}_2$  gas is of interest, as historically the brown colour of the wintertime haze has been attributed to  $\text{NO}_2$  concentrations (e.g., Ayrey, 2001). The small contribution of  $\text{NO}_2$  is consistent with overseas results. For example, Middleton and Laulainen report that in most cases the contribution of light absorption by  $\text{NO}_2$  gas is smaller than Rayleigh scattering ( $B_{\text{sg}}$ ). The dominance of  $B_{\text{sp}}$  is also consistent with overseas studies such as the MOHAVE study for the Grand Canyon and the Colorado Northern Front Range Air Quality Study described in Section 2.5.3.

The relationship between elemental and organic carbon concentrations on the 20 June is also of interest. Figures 5.2 and 5.5 to 5.8 indicate similar average concentrations of both elemental and organic carbon. However, the dominance of elemental carbon on the 20 June when light extinction was greatest is apparent from Figure 5.4. Figure 5.4 also shows elevated maximum daytime  $\text{PM}_{2.5}$  concentrations of around  $140 \mu\text{g m}^{-3}$  and hourly average  $\text{NO}_2$  concentrations around  $160 \mu\text{g m}^{-3}$ , approximately 80% of the health guideline value for  $\text{NO}_2$ .

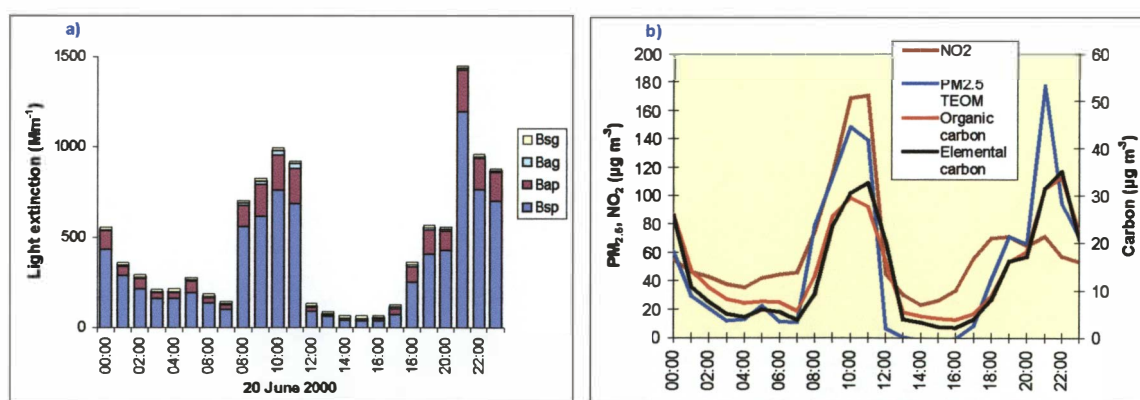


Figure 5.4: Hourly average  $B_{\text{sp}}$ ,  $B_{\text{ap}}$ ,  $B_{\text{ag}}$ ,  $B_{\text{sg}}$  data (a) and  $\text{NO}_2$ , OC, EC, and  $\text{PM}_{2.5}$  concentrations (b) for 20 June 2000.

## 5.2 Daily variations in light extinction and air quality

Daily variations in visibility monitoring data indicate an increase in average light extinction during the morning period, peaking at around 08:00 hours during the summer in February and March 2000 and 09:00 hours during the winter<sup>10</sup>.

Figure 5.5 shows daily variations in average light extinction and concentrations of NO<sub>2</sub>, PM<sub>2.5</sub> and carbon for the months February to May 2000. During February and March, all values were low with maximums occurring during the daytime around 08:00. Light extinction was dominated by B<sub>sp</sub>, which averaged less than around 80 Mm<sup>-1</sup> for each hour of the day. Concentrations of organic (OC) and elemental (EC) carbon were similar, with hourly average concentrations of each typically less than 5 µgm<sup>-3</sup>. Daily variations in light extinction changed for the month of April with an increase in light extinction and contaminant concentrations during the evening period. This coincides both in terms of season and time of day, with the onset of meteorological conditions conducive to elevated pollution levels (see Sections 3.2 and 5.3). Temporal variations are more exaggerated in May, with an increase in average concentrations for both the daytime and evening/night time periods. Although B<sub>sp</sub> remains dominant, the contribution of B<sub>ap</sub> increases during both the daytime and evening peaks. The corresponding EC concentrations responsible for the B<sub>ap</sub> average around 20 µgm<sup>-3</sup> for the morning peak and 35 µgm<sup>-3</sup> for the evening peak. Concentrations of NO<sub>2</sub> peak at around 17:00 hours, compared to around midnight for PM<sub>2.5</sub> during May. This is likely to reflect variations in sources with motor vehicles being the dominant contributor to NO<sub>2</sub> emissions in Christchurch (Wilton, 2001).

Figures 5.5 to 5.8 also show seasonal variations in NO<sub>2</sub> and PM<sub>2.5</sub> concentrations with time of day. Concentrations of NO<sub>2</sub> are highest during the morning period, around 9am, coinciding with the time of day when brown haze is most noticeable in Christchurch. This peak dominates 24-hour NO<sub>2</sub> concentrations during both the summer and winter months. An evening peak in NO<sub>2</sub> concentrations is also predominant during the winter months but is less significant during the summer months. This is likely to occur as a result of variations in meteorological conditions, rather than emission sources. A similar trend is observed with PM<sub>2.5</sub>, although for PM<sub>2.5</sub> concentrations are highest during the winter evening peak.

Light extinction variations and concentrations of NO<sub>2</sub>, PM<sub>2.5</sub> and carbon for the months June to September 2000 are shown in Figure 5.6. During June, temporal variations were similar to May,

---

<sup>10</sup> Seasonal differences in the peak concentrations relate to variations in emissions occurring as a result of households operating in relation to daylight savings time and the reporting of air quality data in New Zealand Standard Time.

although average light extinction values and concentrations were slightly lower. Evening peak values occurred earlier during June with minimal increases from around 19:00 hours, compared to steep increases until midnight during May. Figure 9.9 shows average wind speeds during these hours were similar for both May and June at around  $2\text{--}4\text{ m s}^{-1}$ . Concentrations of  $\text{PM}_{2.5}$  and carbon were slightly lower in June, accounting for the change in light extinction. In contrast,  $\text{NO}_2$  concentrations were higher on average during June, but had little impact on light extinction.

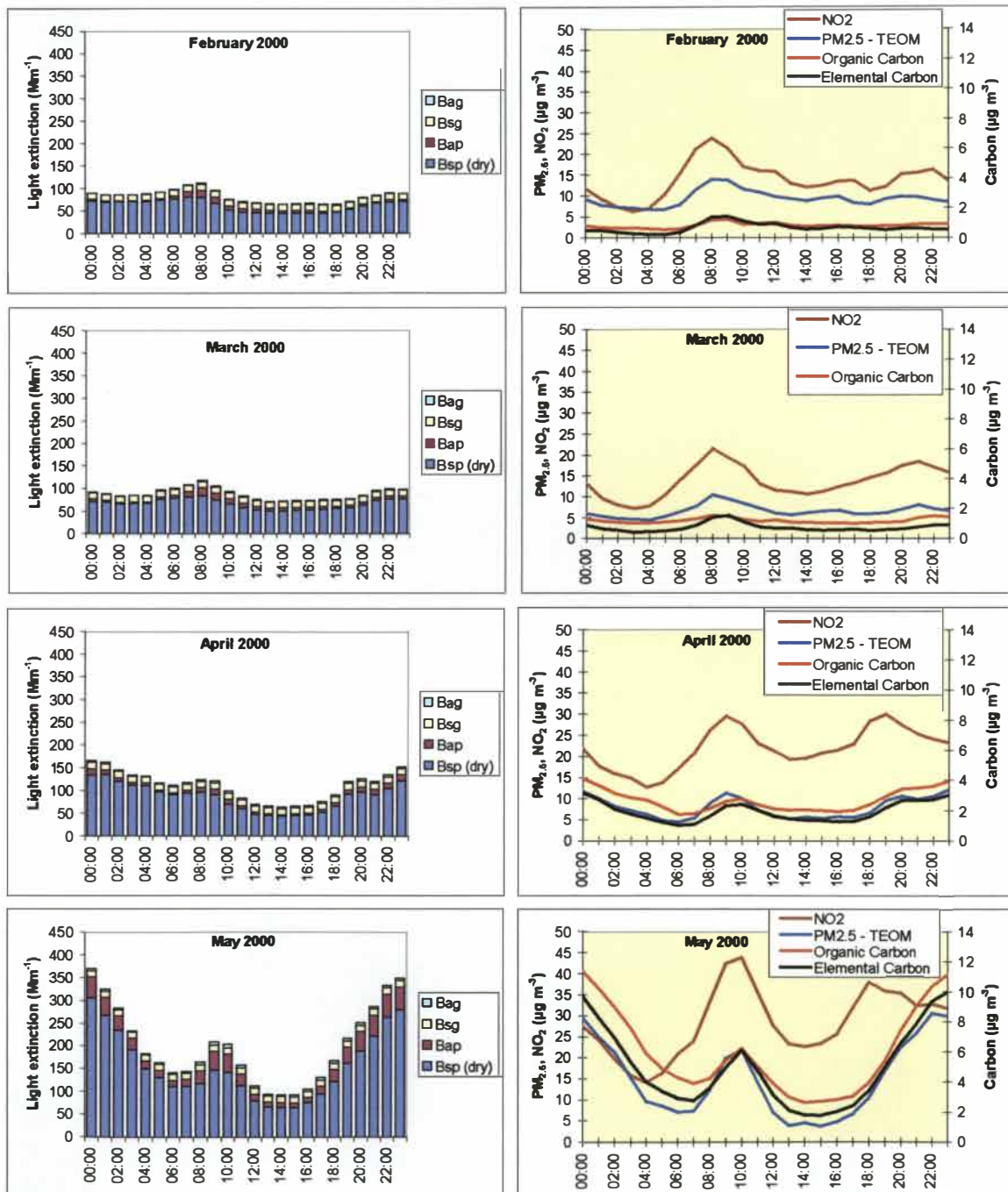


Figure 5.5: Daily variations in average light extinction values and concentrations of contaminants for the months February to May 2000.



In July,  $\text{NO}_2$  concentrations during the morning were similar to May and June but lower concentrations of other contaminants, particularly carbon, were recorded (Figure 5.6). As a consequence, the contribution of  $B_{\text{sp}}$  was reduced and light extinction values were lower. The reduction in concentrations of contaminants during July was atypical, as elevated concentrations are common during this month (Aberkane, 1999). July 2000, however, experienced unusual meteorological conditions that accounted for these lower values (see Section 5.3).

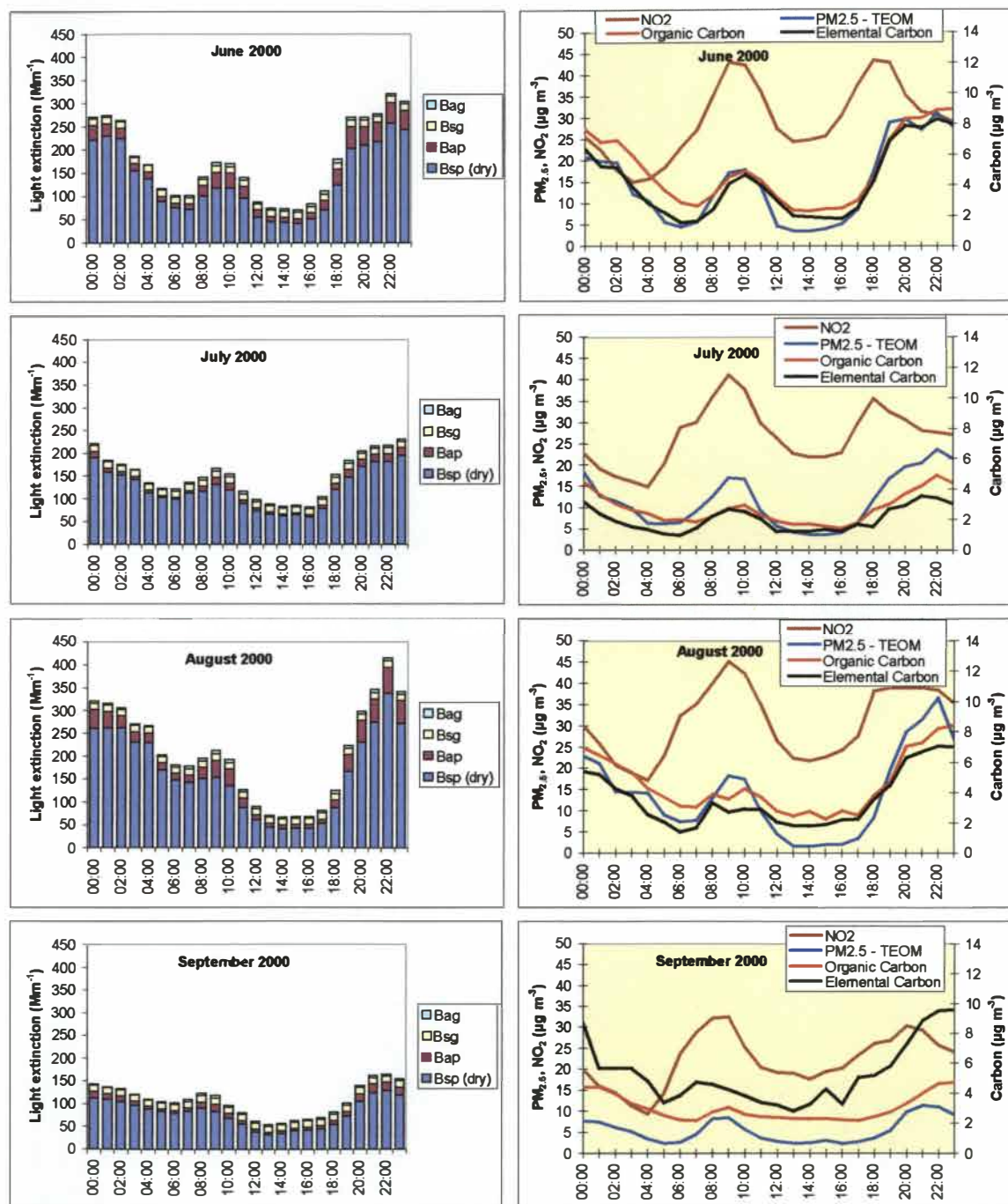


Figure 5.6: Daily variations in average light extinction values and concentrations of contaminants for the months June to September 2000.

Daytime light extinction values in August were similar in magnitude and composition to May with average values around  $200 \text{ Mm}^{-1}$  at 10:00. Concentrations of  $\text{PM}_{2.5}$  decreased significantly by September with a corresponding reduction in light extinction. Elevated EC concentrations in September appear to be an anomaly as total  $\text{PM}_{2.5}$  concentrations are lower and corresponding increases in  $B_{\text{ap}}$  are not observed.

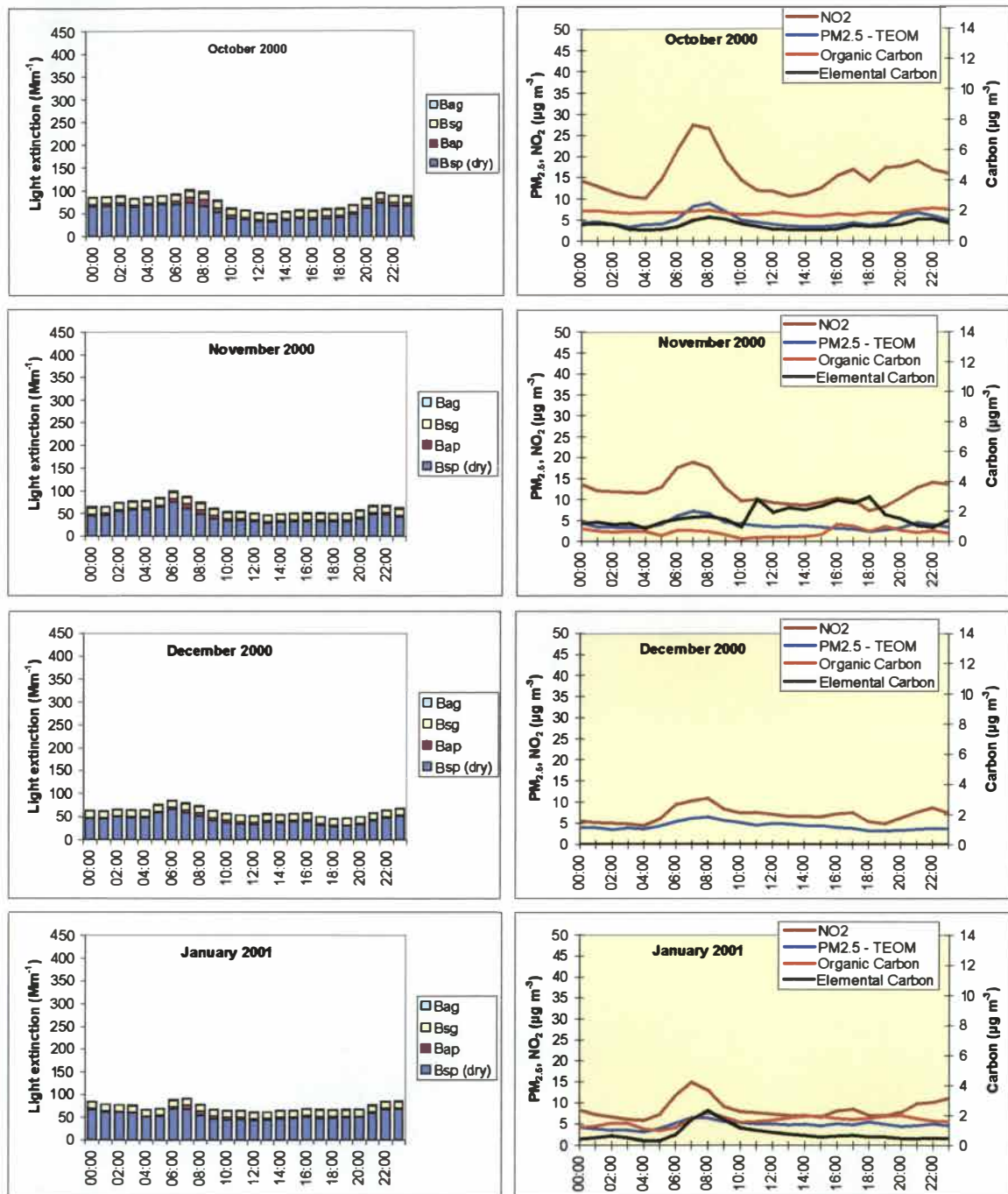


Figure 5.7: Daily variations in average light extinction values and concentrations of contaminants for the months October 2000 to January 2001.

Figure 5.7 shows daily variations in concentrations of  $\text{NO}_2$ ,  $\text{PM}_{2.5}$ , carbon and light extinction for the months of October 2000 to January 2001. These show low average light extinction values with



a slight increase during the morning. Average hourly  $\text{PM}_{2.5}$  concentrations are typically less than  $10 \mu\text{g m}^{-3}$  and  $\text{NO}_2$  concentrations are also lower than for other months. No carbon data were available during December because of an instrument malfunction.

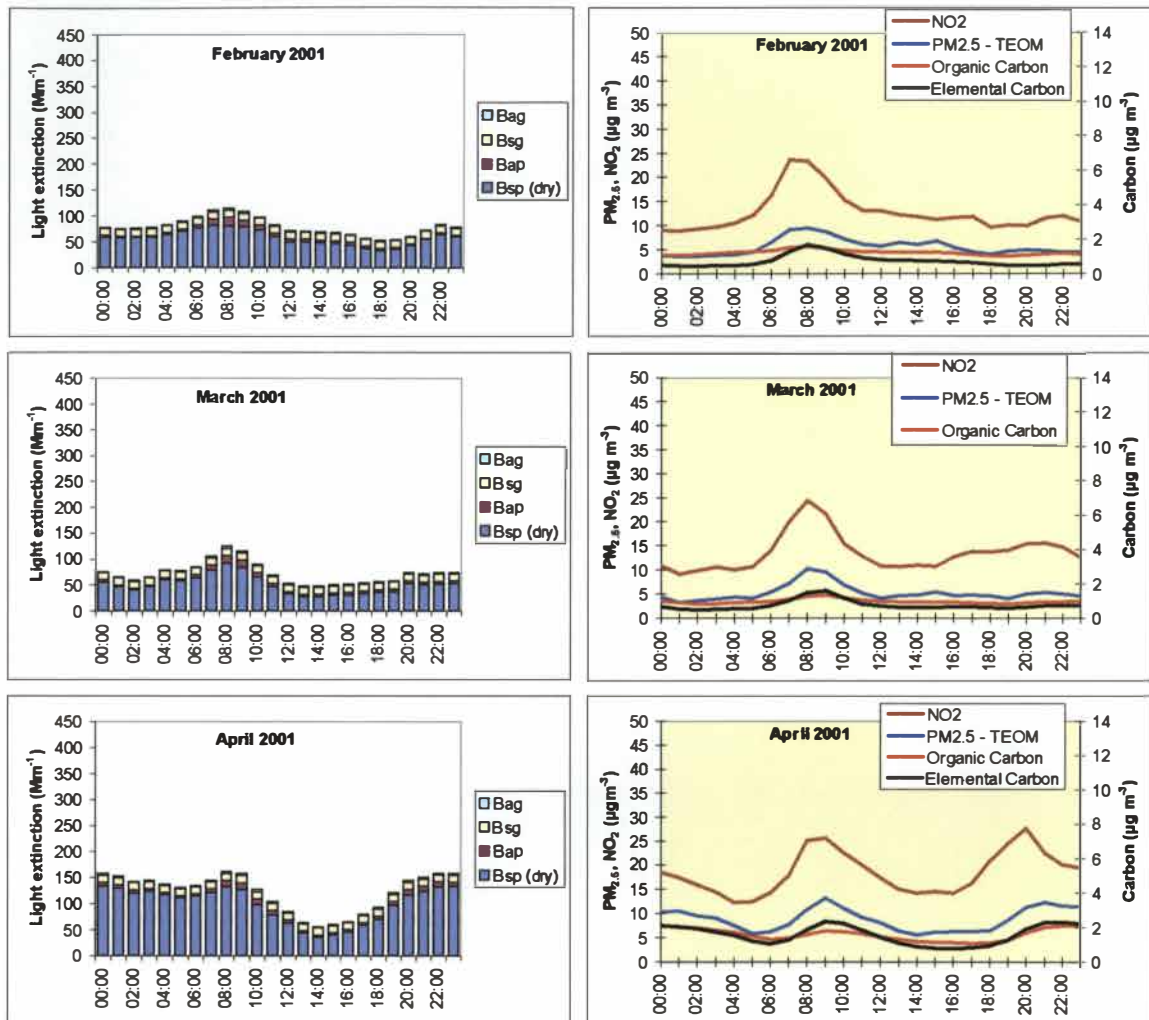


Figure 5.8: Daily variations in average light extinction values and concentrations of contaminants for the months February to April 2001.

Figure 5.8 shows average light extinction values for the months of February to April 2001 are similar to those for the same months during 2000 (Figure 5.5).

Overall, the main cause of visibility degradation during all months is light scattering by particles ( $B_{sp}$ ) and the contribution from this source increases at times when visibility is most degraded. Similarly, an increase in the amount of light that is absorbed by particles ( $B_{ap}$ ) occurs during episodes of poor daytime visibility.

Average hourly concentrations of  $\text{PM}_{2.5}$ , elemental carbon, organic carbon and nitrogen dioxide are highest during the winter months and peak both during the morning and evening during this season. In the summer, air quality data show similar trends to light extinction values with a slight peak

during the morning period. Organic carbon concentrations appear to be slightly higher on average than elemental carbon concentrations, particularly during the winter months.

### 5.3 Meteorology

The relationships between meteorology, air pollution and visibility in Christchurch are well documented (e.g., Owen and Tapper, 1977; Sturman, 1985; van den Assem, 1997; Gimson, 1998 and Wilson, 1999) and are summarised in Section 3.2. This Section provides a summary of the meteorological conditions, including seasonal variations throughout the visibility monitoring period, as well as some comparisons with light extinction data.

The meteorological parameters measured at the Polytechnic monitoring site included wind speed, wind direction, temperature and relative humidity data. The meteorological monitoring equipment was located on the roof of the building at a height of approximately 20 metres above sea level. The siting of the meteorological equipment was not ideal, as additional elevation above the roof of the building was limited. A comparison of wind direction data to that measured at a ground level monitoring site in Coles Place, St Albans (Appendix E) indicated that while some variations in wind direction were recorded, in general Polytechnic data were reasonably representative of wind directions over the city.

Figures 5.9a, 5.9b, 5.10a and 5.10b show seasonal variations in daily average relative humidity, wind speed, and rooftop temperature at the Christchurch Polytechnic site, and the difference between the temperature at 1 metre and the temperature at 10 metres measured at the St Albans air quality monitoring site. The latter parameter provides an indication of the strength of a temperature inversion within 10 metres of the ground, with a high negative value indicating a large increase in temperature with height.

For all months, relative humidity at the Polytechnic monitoring site was highest during the early morning until around 08:00 (Figure 5.9a). Relative humidity typically decreased between 08:00 and 14:00, returning to similar levels to the early morning during the evening. Although slight variations in relative humidity by month are apparent, no real seasonal trends are evident from these data. Relative humidity will typically be the inverse of air temperature, as the ability of the air to hold water is a function of its temperature.

Daily variations in average wind speed (Figure 5.9b) are opposite in pattern to variations in relative humidity, with lower wind speeds during the morning period, increasing during the afternoon and decreasing again in the early evening. Some seasonal variations are apparent with higher average wind speeds during the spring and summer months. During these months, the temperature

difference is typically between 1 and 10 metres. Variations in wind speed are closely related to the temperature gradient, as when the lower atmosphere is stable the air near the earth's surface becomes decoupled from that aloft. That is why it becomes calm at night. During daytime, surface heating reverses the temperature gradient and the prevailing wind aloft is re-connected to the surface.

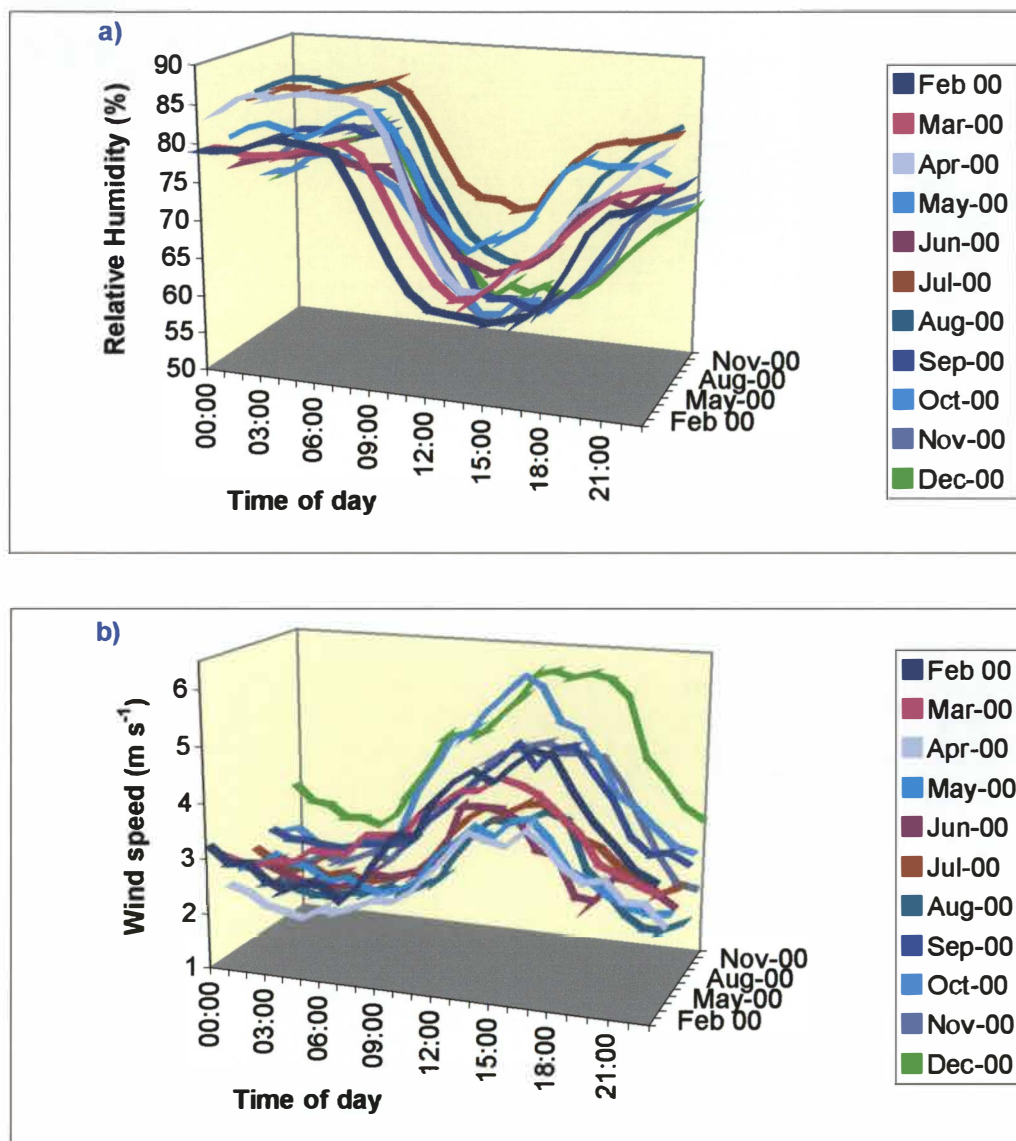


Figure 5.9: Daily variations in relative humidity (a) and wind speed (b) for the months February to December 2000.

Seasonal differences in rooftop temperature are also apparent with colder temperatures during the winter months (Figure 5.10a). Daily variations in temperature are minimal but appear to follow a similar profile to the wind speed data, with slight increases in temperature from around 08:00 decreasing again in the late afternoon. Seasonal differences in the indicator of an inversion close to the earth surface are difficult to determine because of missing data for most of the days during the months May and June 2000 (Figure 5.10b). Typically, the inversions are likely to be stronger during the winter months. However, the weather patterns during the winter of 2000 were unusual.

In particular, the prevalence of persistent periods of light north-easterly airflow over Christchurch in July resulted in minimal air pollution episodes and the warmest average temperatures for July on record (pers. com. Tony Trewinnard, Blue Skies Weather, 2000). This is apparent in the temperature difference profile for July, which indicates average temperature differences of greater than or equal to around zero for most of the time. In comparison, April 2000 shows the temperature difference between one and ten metres to be much less than zero for most of the time period from 17:00 to 11:00.

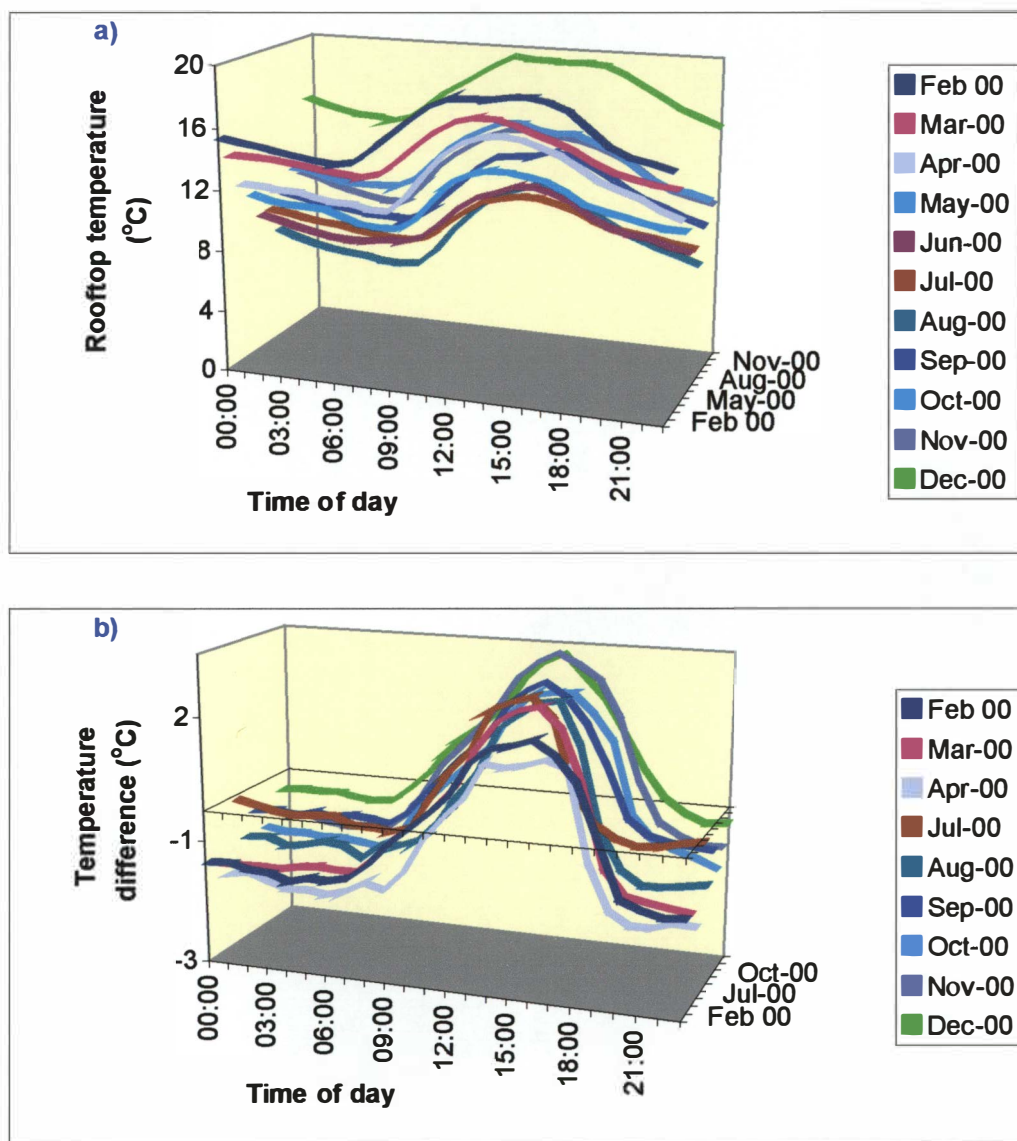


Figure 5.10: Daily variations in rooftop temperature (a) and temperature difference at the St Albans monitoring site (b) for the months February to December 2000.

### 5.3.1 Impact on light extinction

Sections 5.1 and 5.2 provided evidence that the most degraded visibility occurs during the winter months, particularly during the months April to September (Table 5.1). Light extinction values during these months were higher than during the summer months, with maximum values of around



1000  $\text{Mm}^{-1}$  recorded during the winter compared to around 450  $\text{Mm}^{-1}$  during the summer. Figure 5.11 shows that light extinction values greater than 400  $\text{Mm}^{-1}$  typically occurred with temperatures of less than 18 °C and wind speeds less than 2.5  $\text{m s}^{-1}$ .

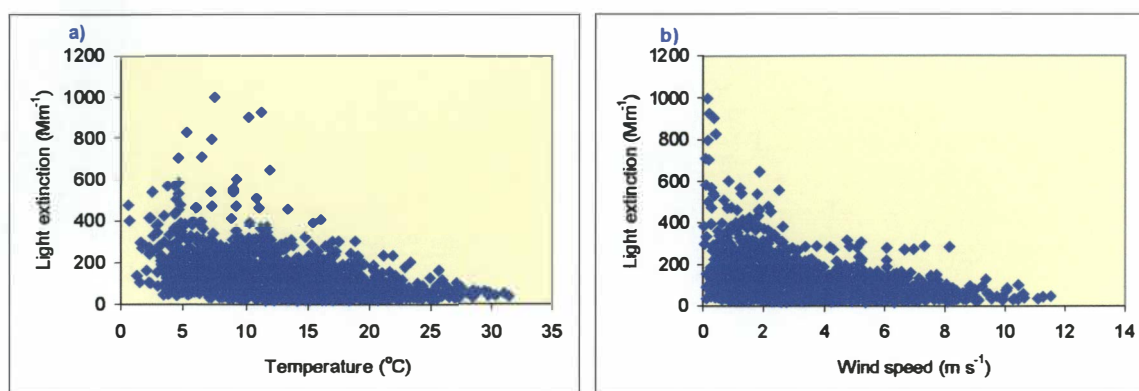


Figure 5.11: Hourly average light extinction by temperature (a) and wind speed (b) for daytime light extinction values from February 2000 to April 2001.

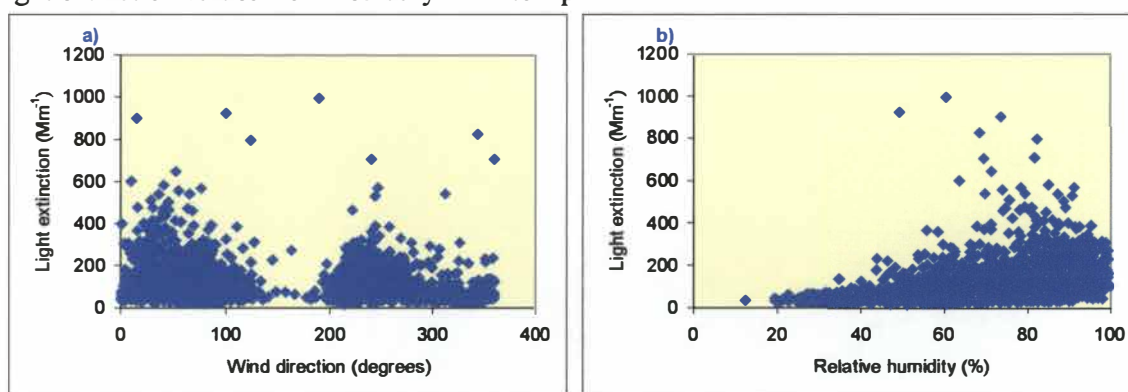


Figure 5.12: Hourly average light extinction by wind direction (a) and relative humidity (b) for daytime light extinction values from February 2000 to April 2001.

Figure 5.12 shows that the majority of the elevated hourly average light extinction values occurred when the wind was blowing from the easterly direction with some elevated levels also occurring with westerly winds. However, the majority (>60%) of the light extinction values greater than 500  $\text{Mm}^{-1}$  occurred when the wind speed was less than the 0.5  $\text{m s}^{-1}$  required to give an accurate wind direction output. Thus associations between elevated light extinction and wind direction for these data are inconclusive. The frequency of easterly winds is also greatest during the daytime.

Elevated light extinction values occurred across a range of relative humidity values from around 50% to 100%. This is consistent with overseas literature, which suggests that the impact of relative humidity on visibility degradation will depend on the composition of the particulate and will be most effective when particulate nitrates and sulphates are present.

Figures 5.13 and 5.14 show the relationship between hourly light extinction values and meteorological parameters for the months October to March and April to September respectively.



For ease of interpretation these are loosely referred to as summer and winter data. The most notable association during the summer months is between elevated light extinction values and low wind speeds, suggesting that wind based sources, such as sea spray and dusts are not a major source of elevated light extinction in Christchurch during these months.

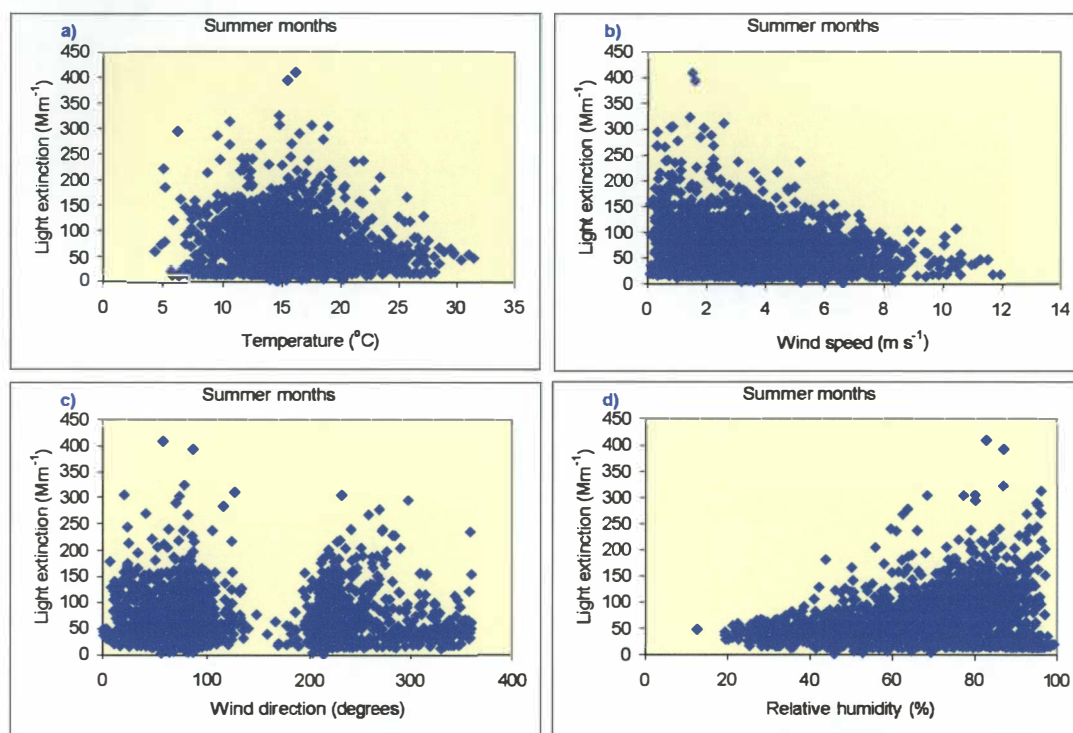


Figure 5.13: Hourly average light extinction and meteorological data during the months October to March.

During the winter months, the highest light extinction values occurred with wind speeds less than around  $0.5 \text{ m s}^{-1}$  and average hourly temperatures of between 4 and 12  $^{\circ}\text{C}$ . Light extinction values are typically less than  $300 \text{ Mm}^{-1}$  for wind speeds greater than around  $3 \text{ m s}^{-1}$  and for temperatures greater than 15  $^{\circ}\text{C}$ .

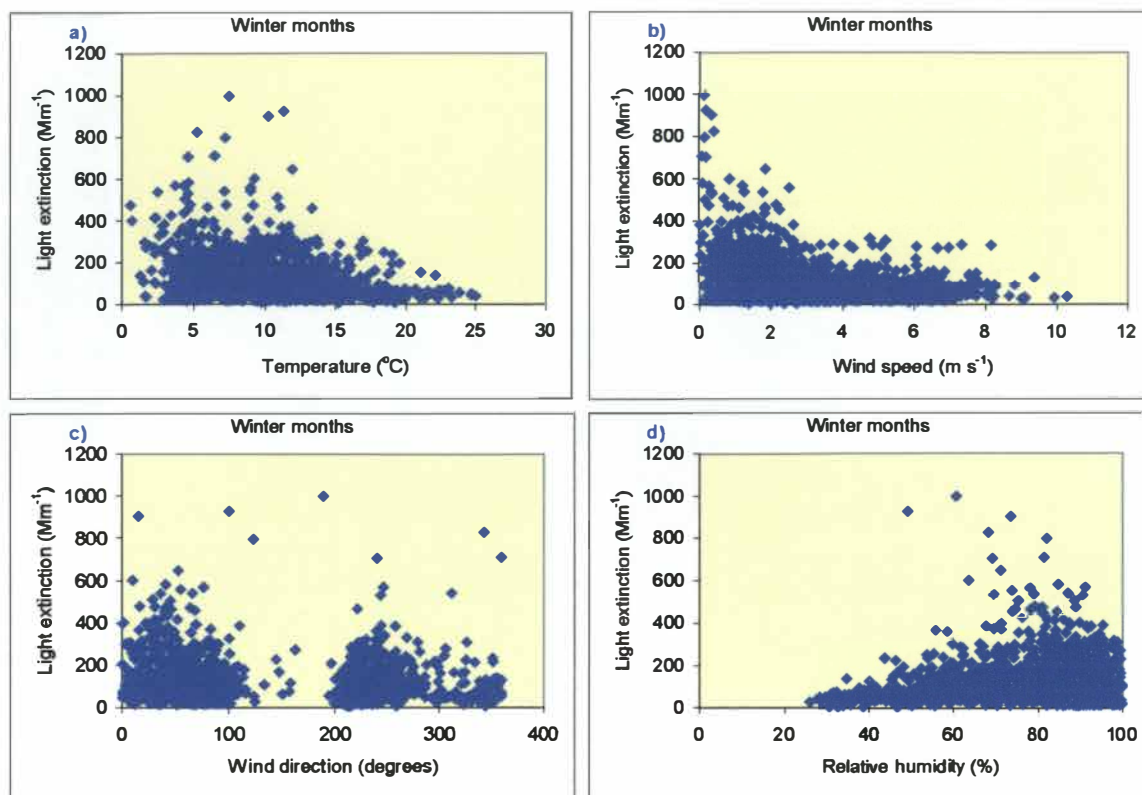


Figure 5.14: Hourly average light extinction and meteorological data during the months April to September inclusive.

Another meteorological parameter identified by Wilson (1999) as having a significant impact on visibility degradation in Christchurch is the temperature gradient. While a basic indicator of temperature inversion, namely the temperature difference between 1 and 10 metres, has been presented, further impacts such as the height of the stable layer can create a layering effect in the haze. This is illustrated later in Section 8.8.1, which shows the layering of haze on the 18 May 2000 and an increase in the height of the haze from 08:00 to 11:00.

Some data outlining the temperature profile for a selection of days during 2000 are available as part of the Christchurch Air Pollution Study (CAPS) that was carried out by a group of research organisations during July 2000. The timing of the study was unfortunate, as few occasions when meteorological conditions were conducive to elevated pollution occurred during July 2000. Figure 5.15 shows the temperature profile measured at Jade Stadium as a part of the CAPS study on the 24 July, the day of the highest light extinction values when some of the CAPS data were available.

At 06:00 and 07:00 a strong lower level inversion was present to around 20 metres, at which point it became weaker, with only a slight positive temperature gradient with height to around 40 metres. The strong inversion increased in height to around 30 metres at 08:00, with the temperature decreasing to 40 metres before increasing again to 60 metres (Figure 5.15). Although the temperature increased significantly between 08:00-09:00, the temperature inversion at 09:00 was

still persistent with the onset of solar heating. By 10:00 hours, surface heating by the sun has begun to erode the nocturnal inversion, which now remains only above 20 m. Further erosion of the inversion continues until noon when a lapse temperature profile is established.

The impact of meteorology on visible pollution and on contaminant concentrations and light extinction data from the visibility monitoring site on the 24 July is illustrated in Figures 5.16 and 5.17. A layered pollution haze evident in images taken at 08:00 and 09:00 is caused by the nocturnal inversion layer, which restricts the vertical dispersion of the pollution. The morning sun then heats the earth's surface and erodes the inversion creating a mixed layer between 09:00-10:00. This starts to grow allowing vertical mixing and the dispersion of pollution by 11:00. A comparison of these images and hourly average contaminant concentrations indicate a reduction in light extinction by 10:00, which is consistent with the changes in the temperature gradient at this time (Figure 5.15).

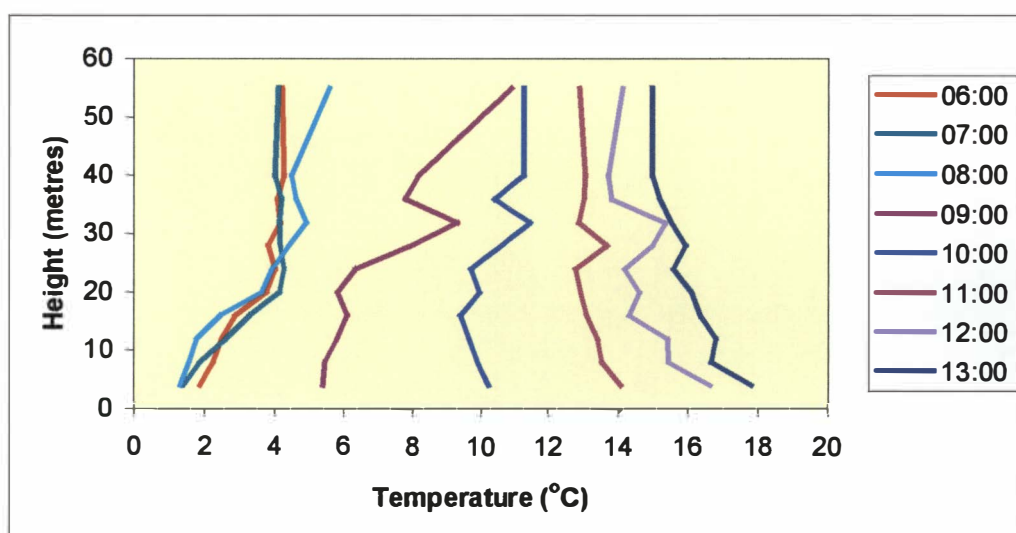


Figure 5.15: Temperature gradient from 0 to 60 metres measured at Jade Stadium on 24 July 2000.







Figure 5.16: Illustration of haze on 24 July 2000 from 0800 to 1100 hours.

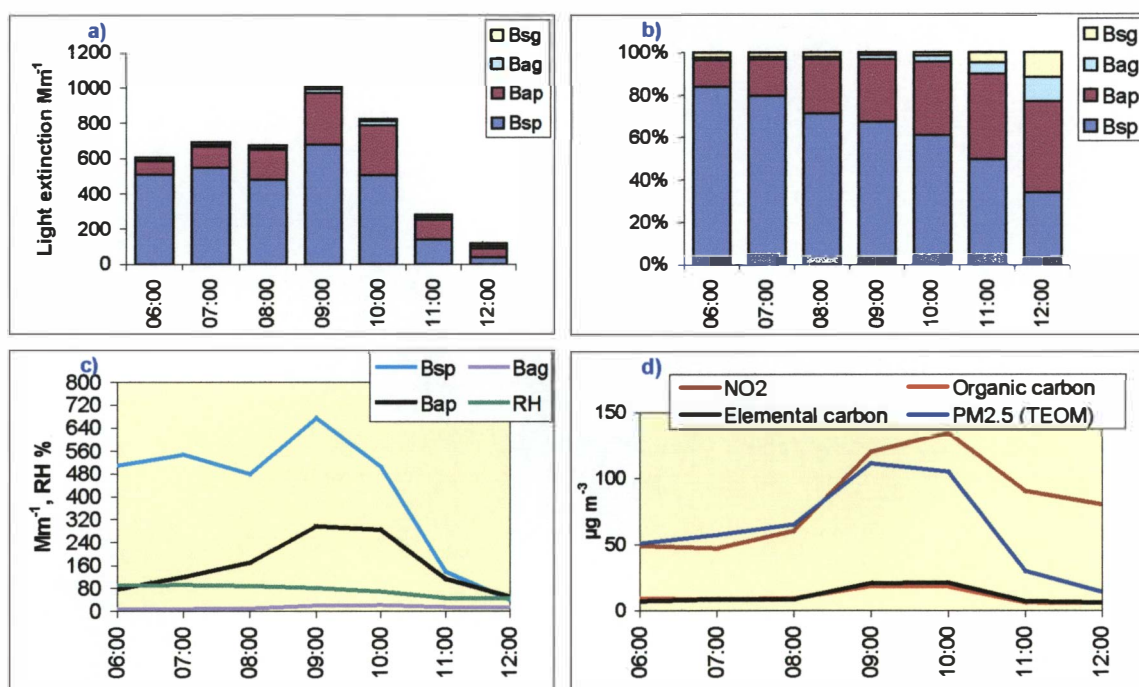


Figure 5.17: Daily variations in light extinction components (a and c) as percentage of total extinction (b) and concentrations of contaminants (d) on the 24 July 2000.

Figure 5.17 shows hourly variations in the components of light extinction on 24 July 2000 as well as changes in concentrations of NO<sub>2</sub>, PM<sub>2.5</sub> and carbon. An increase in EC concentrations occurs between 08:00 and 09:00, which increases the Bap contribution resulting in a total light extinction value of around 1000 Mm<sup>-1</sup> at 09:00. A significant reduction in light extinction is observed at 12:00 as concentrations of PM<sub>2.5</sub> and carbon decrease to less than 20 µg m<sup>-3</sup>.

## 5.4 Particulate measurements

A number of different measurement systems were used in the study with outputs relating to concentrations of particulate (PM<sub>2.5</sub>) and particulate carbon (elemental and organic). These include 10-minute average PM<sub>2.5</sub> concentrations measured using the TEOM, seven-hour average PM<sub>2.5</sub>

concentrations measured gravimetrically using the SASS sampler, hourly average elemental and organic carbon concentrations from the series 5400 carbon analyser, hourly average elemental carbon concentrations from the aethalometer, and seven-hour average elemental carbon concentrations measured on the SASS filters using light absorption.

Despite the number of seemingly similar measurements, variations in operating parameters and measurement methods (and assumptions) should result in significant differences in the monitoring outputs. This Section evaluates the relationships between carbon and PM<sub>2.5</sub> measurements in the context of these variations.

#### **5.4.1 PM<sub>2.5</sub> concentrations**

The main method of measurement of PM<sub>2.5</sub> concentrations at the monitoring site was the tapered elemental oscillating microbalance (TEOM) method. This method measures concentrations of particles based on the frequency of oscillation of a filter suspended on a tapered element. This is based on the principle of a direct relationship between particulate mass and the frequency of oscillation. The analyser was set to calculate 10-minute average PM<sub>2.5</sub> concentrations based on the average of measurements taken every six seconds. The method requires a constant sample temperature greater than the ambient air temperature. The standard sample temperature setting for the TEOM in New Zealand is 40 °C (MfE, 1999). Particulate concentrations in the 2.5 size fraction were obtained by use of a PM<sub>2.5</sub> size selective inlet.

Concentrations of PM<sub>2.5</sub> were also measured gravimetrically using the SASS sampler. This technique involved drawing air across a filter for a period of seven-hours during the daytime. As with the TEOM method, a size selective inlet was used to capture particles in the appropriate size fraction. For the period February 2000 to 21 June 2000, the standard Teflon filters were used in the sampler. From 22 June 2000, particles were collected on polycarbonate filters. While the purpose of collecting the particulate on these filters was for elemental analysis, they were also weighed for PM<sub>2.5</sub> mass prior to being sent to GNS for PIXE analysis. This involved preconditioning the filters prior to sampling, and reconditioning and post sampling weight measurement. The difference between the initial and final weights (µg per filter) was converted to a concentration (µg m<sup>-3</sup>) by dividing by the volume of air throughout the sample period (m<sup>3</sup>).

A number of problems arose as a result of the measurement of PM<sub>2.5</sub> mass on the SASS filters. In the first few months, a number of negative mass volumes were calculated. Eventually, problems with these measurements were overcome through the introduction of anti-static measures in the weighing procedures. However, little confidence can be placed in the initial PM<sub>2.5</sub> SASS mass measurements. Secondly, the replacement of Teflon filters with polycarbonate filters during June



2000 has implications for the mass measurements arising from the low collection efficiencies and the potential for flow resistance associated with the latter filters. While these filters are still suitable for elemental analysis, they are most likely to underestimate PM<sub>2.5</sub> mass because of the low collection efficiencies.

An additional difference in the mass of PM<sub>2.5</sub> collected using the two different methods will occur as a result of the elevated sample temperature of the TEOM. This method measures PM<sub>2.5</sub> mass at a temperature of 40 °C compared to the ambient temperatures of around 0-30 °C associated with the SASS sampling. Thus the latter method will capture more of the volatile component of the particulate and therefore should measure more mass than the TEOM.

Figure 5.18a illustrates the relationship between the seven-hour average TEOM concentrations and those measured gravimetrically using the SASS sampler. As anticipated, the relationship between the two measurements is poor with the coefficient of determination indicating that only 41% of the variance explained by the relationship.

In some locations, light scattering instruments have been used as a proxy for a particulate measurement system. Figure 5.18b shows the relationship between hourly PM<sub>2.5</sub> and light scattering by particles for the hours between 06:00 and 13:00 at the Christchurch visibility monitoring site. The large variations that are unexplained by the relationship ( $r^2=0.51$ ) highlight the obvious limitations of using light scattering as a measure of PM<sub>2.5</sub> mass, that is, that smaller particles scatter light more efficiently but will have less mass. Discrepancies in the relationship will also occur as a result of relative humidity as particle bound moisture will increase light scattering but subsequent increases in particle mass are unlikely as the TEOM operates with a sample line that is heated to 40 °C.

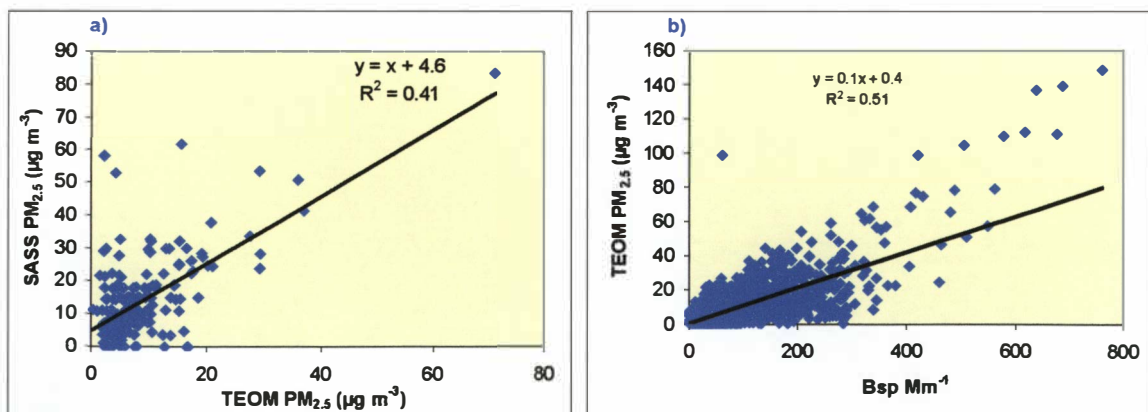


Figure 5.18: Comparison of seven-hour average PM<sub>2.5</sub> concentrations measured using the TEOM and SASS samplers (a) and hourly average PM<sub>2.5</sub> and B<sub>sp</sub> measurements during the hours 06:00 to 13:00 (b).

### 5.4.2 Elemental carbon measurements

The main method of measuring elemental carbon concentrations at the monitoring site was the Rupprecht & Patashnick series 5400 carbon analyser. This method measures both elemental and organic carbon concentrations based on differences in volatilisation temperatures with species volatilising at 230 °C being classified as organic. The organic carbon measurements obtained by this instrument include only the carbon component and not the mass associated with the corresponding hydrogen species. Other methods used to estimate elemental carbon concentrations include the aethalometer, which measures light absorption and outputs elemental carbon concentrations based on the assumption that all light absorbing material is carbon. A third elemental carbon concentration, provided with the PIXE results for the SASS filters, is based on the principle of light reflection. The results from the different techniques for estimating carbon concentrations were compared.

Figure 5.19 shows the average elemental carbon concentrations as measured by the aethalometer and the series 5400 carbon analyser. A reasonable correlation is observed with 68% of the variance explained by the relationship, although the aethalometer readings were about 20% less than those made using the series 5400. The reason for this variation is unclear but may be related to the volatilisation temperature for the series 5400 or assumptions regarding the light absorption efficiencies used to convert absorption into mass concentrations for the aethalometer. The latter explanation is quite plausible as studies (e.g., Liousse *et al.*, as reported in Pryor *et al.*, 1997) have shown variations in the absorption efficiency of elemental carbon varied from 5 to 20 m<sup>2</sup>g<sup>-1</sup>.

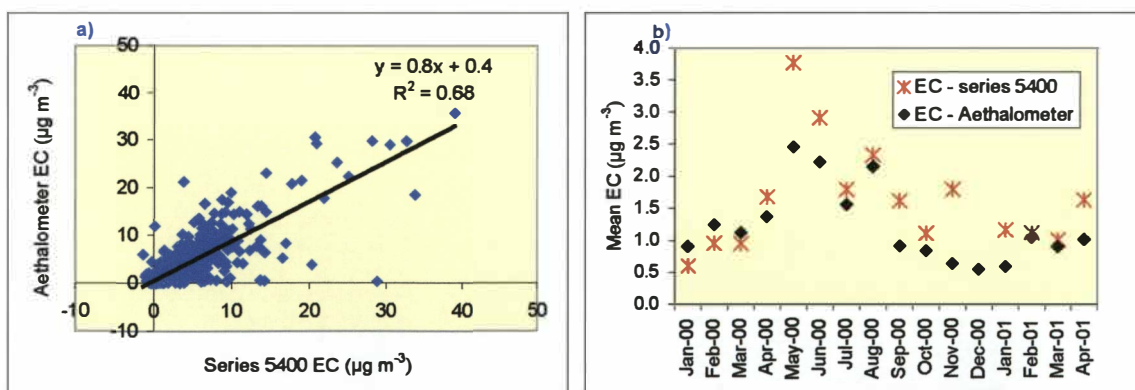


Figure 5.19: Comparison of hourly average elemental carbon concentrations for the hours 06:00 to 13:00 (a) and monthly average concentrations (b) from the series 5400 and aethalometer.

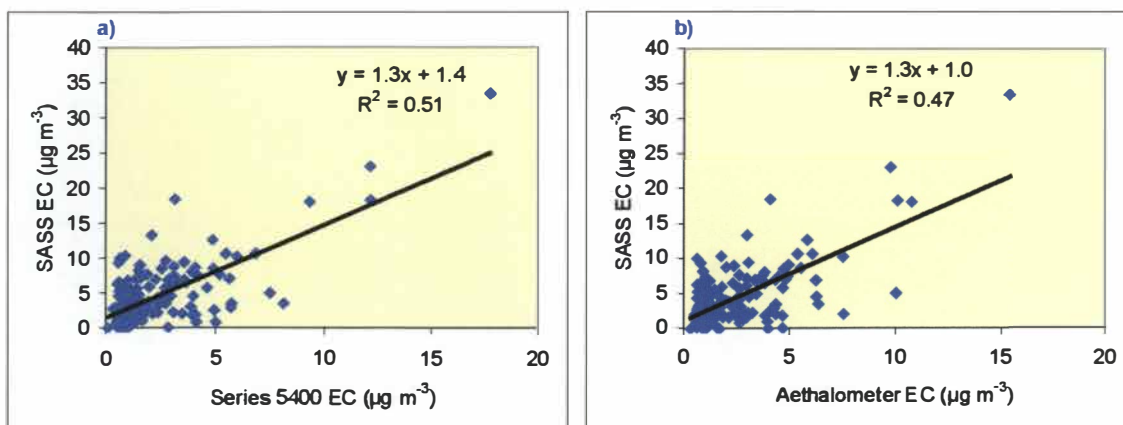


Figure 5.20: Comparison of seven hour average (06:00-13:00) aethalometer and series 5400 elemental carbon concentrations to (SASS) filter based measurements.

Of concern however, is the poor relationship between both these measurements and the seven-hour average (06:00-13:00) filter based elemental carbon measurements (Figure 5.20). This suggests some inaccuracies associated with the carbon measurements made at GNS, as the methodology in principle is similar to the aethalometer and results therefore should be consistent. Differences may be associated with the collection of particles on carbon based filter media as both the Teflon and polycarbonate filters contain carbon.

### 5.4.3 Elemental and organic carbon

The relationship between hourly average concentrations of elemental and organic carbon from the series 5400 carbon analyser during the period 06:00 to 13:00 is shown in Figure 5.21. Concentrations of organic carbon were slightly higher overall than elemental carbon. No real seasonal variations are apparent, although the proportion of total carbon that was elemental carbon was slightly higher during January and February 2000.

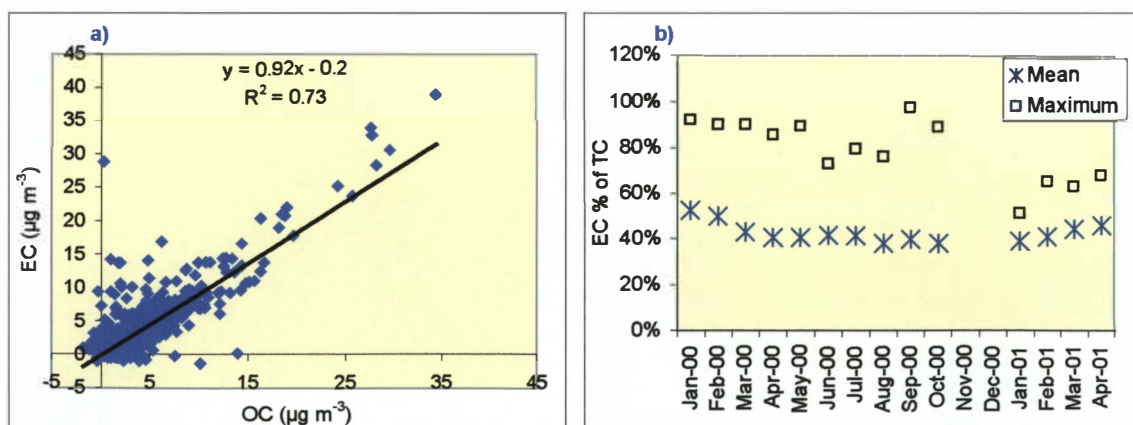


Figure 5.21: Hourly average elemental (EC) and organic carbon (OC) concentrations for the hours 06:00-13:00 (a) and the mean and maximum elemental carbon proportion of total carbon by month (b).

#### 5.4.4 Carbon proportion of PM<sub>2.5</sub>

The relationship between hourly total carbon measurements made using the series 5400 and concentrations of PM<sub>2.5</sub> measured using the TEOM for the daytime period is shown in Figure 5.22. Although the hydrogen and other chemicals associated with the organic component have not been accounted for, the relationship still suggests that at times a significant proportion of the PM<sub>2.5</sub> is not elemental or organic carbon. Similarly, measured concentrations of total carbon were often higher than the PM<sub>2.5</sub> measurements, particularly during the winter months (Figure 5.22). This is likely to illustrate the loss of some of the volatile organic component from the PM<sub>2.5</sub> measurements because of the heated sample line of the TEOM.

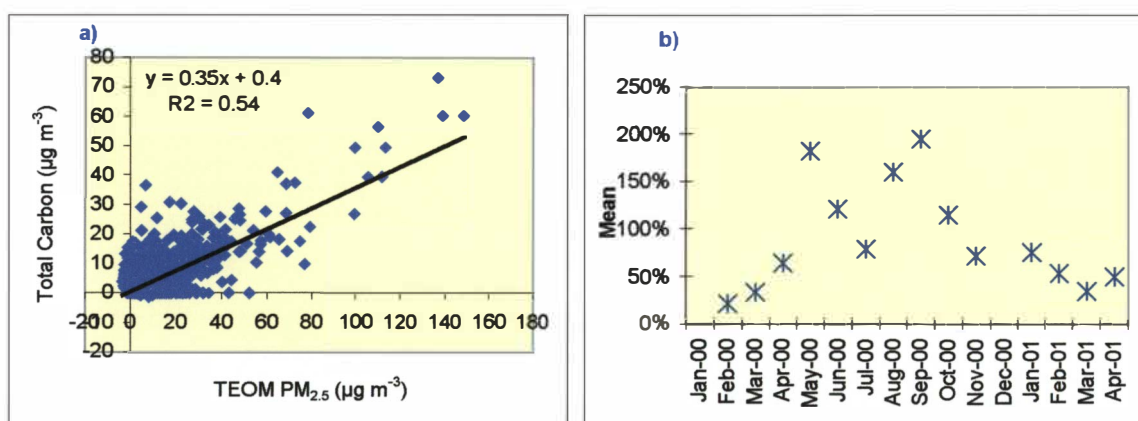


Figure 5.22: Comparison of hourly and monthly average PM<sub>2.5</sub> concentrations and total carbon concentrations for the daytime period from 06:00 to 13:00 (a) and total carbon concentrations as a proportion of TEOM PM<sub>2.5</sub> measurements (b).

#### 5.5 Summary

Light extinction data indicates that the poorest visibility in Christchurch occurs during the winter months. The highest light extinction values during these months occur during the evening periods, although degraded visibility is apparent during the daytime with hourly average light extinction values reaching levels of around 1000 Mm<sup>-1</sup>. During the summer a small increase in daytime light extinction data is apparent during most months.

The daytime haze episode is characterised by an increase in light extinction around 07:00-08:00, typically peaking around 10:00 and improving to give relatively clear visibility by midday. Light scattering by particles is the dominant source of the light extinction, although increases in light absorption by particles is also common during poor visibility episodes.

Poorest visibility was found to occur under low wind speeds, with light extinction values greater than 600 Mm<sup>-1</sup> occurring when wind speeds were less than 0.5 m s<sup>-1</sup> and values greater than 300 Mm<sup>-1</sup> under wind speeds of less than 3 m s<sup>-1</sup>. Similarly, highest values were recorded when the



temperature at the monitoring site was between 4 and 12 °C and when the relative humidity was between 50 and 100%. The relationships observed between meteorological conditions and visibility were generally consistent with previous, more detailed studies of the impact of meteorology on air pollution and visibility (e.g., Gimson, 1998; Wilson, 1999).

Comparisons of different monitoring methods for measuring similar parameters show some discrepancies. These are typically associated with the different operating parameters of the instruments, such as the different sampling temperatures or methods of defining elemental and organic components of particulate. The relative abundance of elemental and organic carbon during the daytime is similar for most pollution episodes, although elemental carbon concentrations were more than twice the organic component on the occasion of the worst visibility episode.

## Chapter 6 Sources of PM<sub>2.5</sub> mass

Chapter 5 provided a summary of the light extinction data and a comparison of particulate and carbon concentrations measured at the visibility monitoring site. Light scattering and absorption by particles were found to dominate light extinction on days of poor visibility. This Chapter focuses on the chemical analysis of these particles to assess possible sources that may contribute to the light extinction component attributable to particles. This is done using factor analysis, which has become a common method for assessing sources of ambient air particles over the last decade. Results of the factor analysis are combined with the light extinction data in Chapter 7 to determine the relative contribution of different factors to visibility degradation in Christchurch.

### 6.1 Concentrations of elements

Summary data for measured concentrations of elements are presented in Table 6.1. This includes the mean and median concentrations, maximums and minimums, as well as the number of observations (count) and the sum of all data. These show concentrations of elemental carbon are highest on average followed by sulphates, chloride, and nitrates. The maximum nitrate concentration of  $113.5 \mu\text{g m}^{-3}$  was the highest of any species followed by sulphate ( $73.8 \mu\text{g m}^{-3}$ ), chloride ( $42.7 \mu\text{g m}^{-3}$ ) and elemental carbon ( $33.5 \mu\text{g m}^{-3}$ ). Excluding these four dominant species, concentrations of Na, Al, Si, S and Cl are highest on average (Figure 6.1).

The values obtained in this study compare to 24-hour average concentrations of 19, 22 and  $13 \mu\text{g m}^{-3}$  for elemental carbon in Brisbane, New South Wales (NSW) and Melbourne respectively, and 2.6 and  $4.6 \mu\text{g m}^{-3}$  for nitrate and 10.8 and  $2.5 \mu\text{g m}^{-3}$  for sulphate in Brisbane and Melbourne (Chan *et al.*, 1997), although these concentrations are not directly comparable because of differences in monitoring period (7-hour average compared to 24-hour average). Some differences in the relativities are apparent. In particular, the sulphate to elemental carbon ratio is greater for the Christchurch visibility study and the nitrate to elemental carbon ratio is higher in Christchurch (0.40:1) and Melbourne (0.35:1), than in Brisbane (0.13:1). All three nitrate ratios are considerably lower than in California (3:1) where nitrates comprise a significant proportion of the particulate mass. It is likely that the ratios of sulphate and nitrate to elemental carbon concentrations would be even lower in Christchurch for a 24-hour average sampling period, particularly during the winter months.

In Brisbane and Melbourne the average sulphur to elemental carbon ratios are about 0.22 compared to 0.11 in Christchurch, possibly reflecting a greater use of diesel vehicles in the Australian areas.

Surprisingly, the ratio of lead to elemental carbon is similar for Christchurch as for Brisbane and NSW, despite New Zealand petrol being lead free. The same ratio in Melbourne, however, was three times higher. Differences in factors contributing to elemental carbon concentrations in these areas may account for these differences.

Table 6.1: Summary statistics for particulate collected on daytime filters from 06:00 to 13:00 from February 2000 to April 2001.

	Na $\mu\text{g m}^{-3}$	Mg $\mu\text{g m}^{-3}$	Al $\mu\text{g m}^{-3}$	Si $\mu\text{g m}^{-3}$	P $\mu\text{g m}^{-3}$	S $\mu\text{g m}^{-3}$	Cl $\mu\text{g m}^{-3}$	K $\mu\text{g m}^{-3}$
Mean	0.5	0.4	0.3	0.4	0.0	0.5	0.8	0.1
Median	0.1	0.3	0.3	0.4	0.0	0.4	0.6	0.0
Maximum	1.9	0.9	0.7	0.8	0.2	2.5	3.1	0.4
Count	164	164	164	164	164	164	164	164
Total	79	58	47	58	2	83	124	9
	Ca $\mu\text{g m}^{-3}$	Sc $\mu\text{g m}^{-3}$	Ti $\mu\text{g m}^{-3}$	V $\mu\text{g m}^{-3}$	Cr $\mu\text{g m}^{-3}$	Mn $\mu\text{g m}^{-3}$	Fe $\mu\text{g m}^{-3}$	Co $\mu\text{g m}^{-3}$
Mean	0.1	0.0	0.0	0.0	0.0	0.0	0.1	0.0
Median	0.0	0.0	0.0	0.0	0.0	0.0	0.1	0.0
Maximum	0.9	0.2	0.2	0.1	0.3	0.2	0.7	0.5
Count	164	164	164	164	164	164	164	164
Total	15	4	3	1	7	2	21	6
	Ni $\mu\text{g m}^{-3}$	Cu $\mu\text{g m}^{-3}$	Zn $\mu\text{g m}^{-3}$	Ga $\mu\text{g m}^{-3}$	Ge $\mu\text{g m}^{-3}$	As $\mu\text{g m}^{-3}$	Se $\mu\text{g m}^{-3}$	Br $\mu\text{g m}^{-3}$
Mean	0.1	0.1	0.1	0.1	0.1	0.1	0.1	0.2
Median	0.0	0.0	0.0	0.0	0.0	0.0	0.0	0.0
Maximum	1.0	1.0	1.0	1.0	0.8	2.0	1.8	4.0
Count	164	164	164	164	164	164	164	164
Total	10	11	10	11	9	17	21	39
	I $\mu\text{g m}^{-3}$	Hg $\mu\text{g m}^{-3}$	Pb $\mu\text{g m}^{-3}$	El C $\mu\text{g m}^{-3}$	Ammonium Nitrogen $\mu\text{g m}^{-3}$	Chloride $\mu\text{g m}^{-3}$	Nitrate Nitrogen $\mu\text{g m}^{-3}$	Sulphate $\mu\text{g m}^{-3}$
Mean	0.2	0.2	0.2	4.5	0.1	2.0	1.8	3.5
Median	0.1	0.0	0.0	3.1	0.0	1.2	0.0	2.6
Maximum	1.1	2.8	3.0	33.5	2.5	42.7	113.5	73.8
Count	164	164	164	164	163	163	163	163
Total	36	25	37	746	17	328	287	575

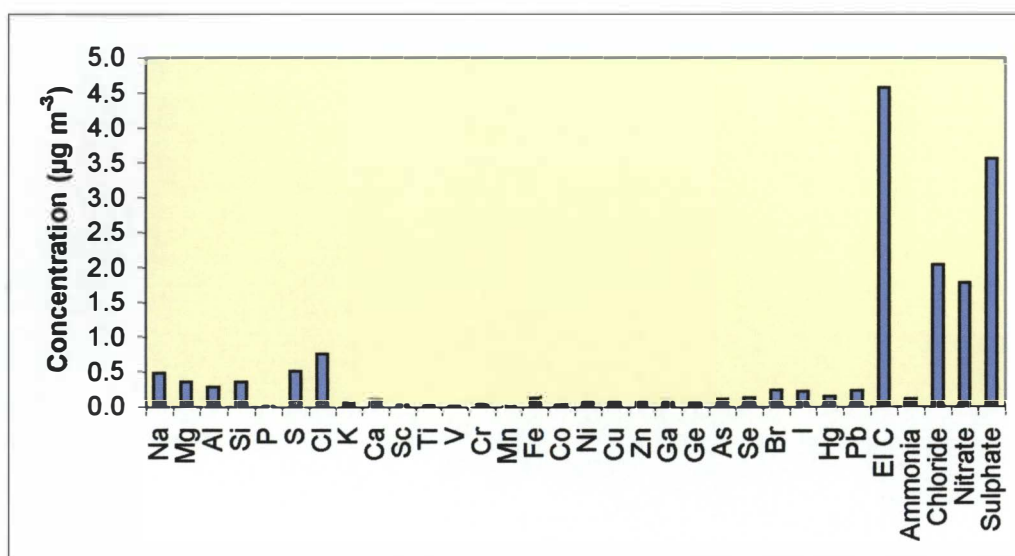


Figure 6.1: Average concentrations on filters for daytime particulate samples collected from 06:00 to 13:00 during the months February 2000 to April 2001.

### 6.1.1 Seasonal variations

Seasonal variations in the concentration of selected elements measured on the sample filters for the collection period from 06:00 to 13:00 are shown in Figure 6.2. More detailed summary statistics for these data are shown in Appendix C. Data for all months from February to November 2000 are included, although data for the months of February, April, November and July were limited to 10, 3, 13 and 12 samples compared to 19-23 samples in each of the other months. Data for the month of April, in particular, are unlikely to be representative of average concentrations for the month. Results for the period December 2000 to April 2001 are presented separately in Figure 6.3 as these data represent a 24-hour sampling period, as opposed to a seven-hour daytime period.



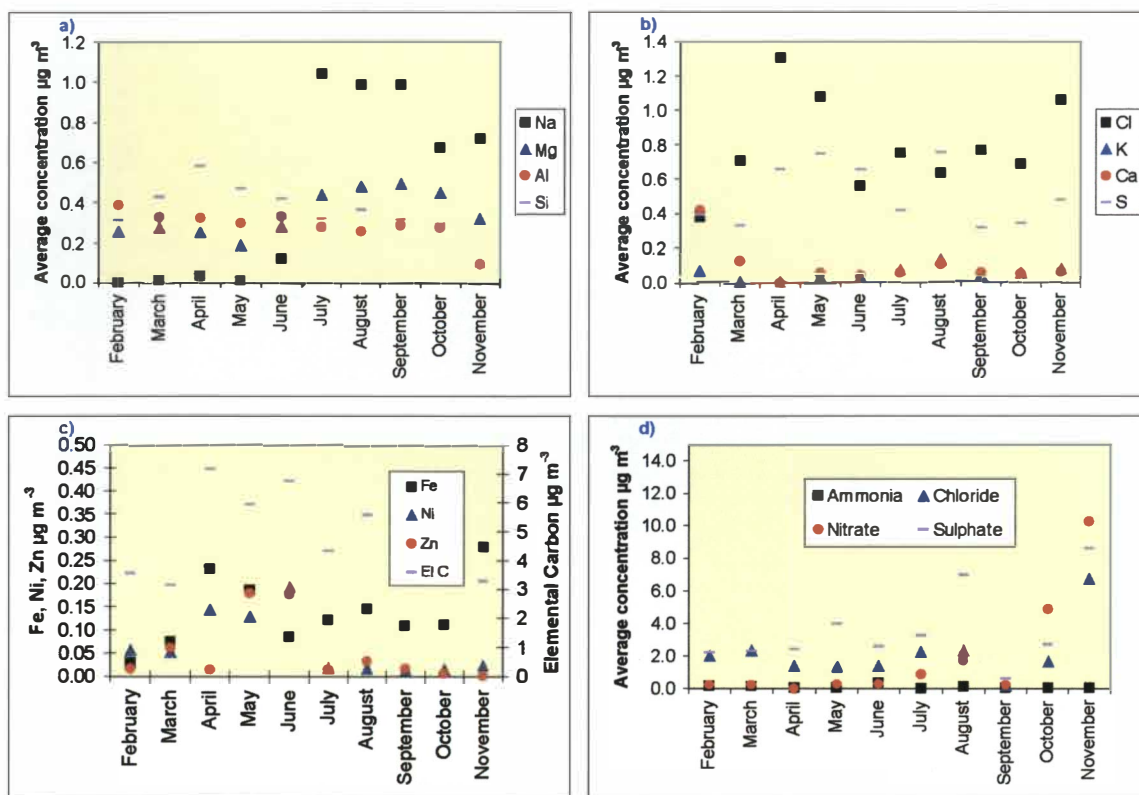


Figure 6.2: Average monthly concentrations of elements from February to November 2000 collected on filters during the hours 06:00 to 13:00 measured by PIXE.

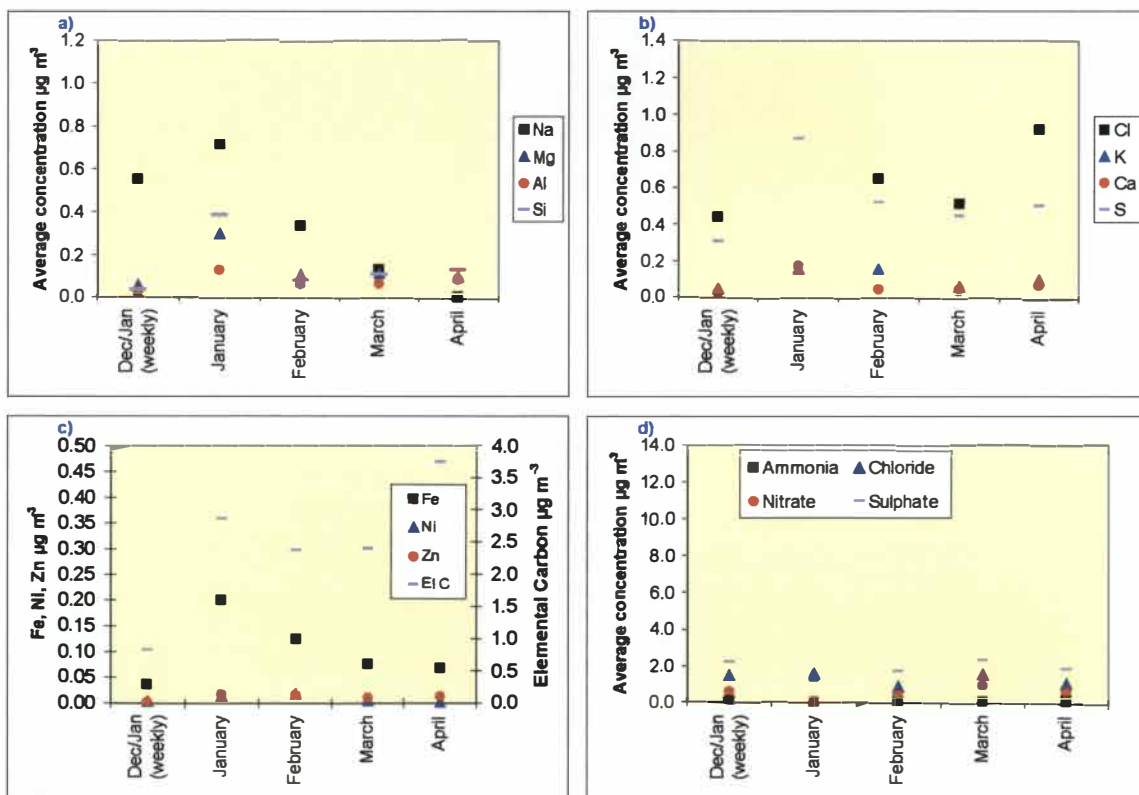


Figure 6.3: Average monthly concentrations of element from December 2000 to April 2001 collected on filters during the hours 06:00 to 13:00 measured by PIXE.

Concentrations of elemental carbon, the greatest contributor to PM<sub>2.5</sub> mass (Figure 6.1), and S are highest during the months April to August. Average Si concentrations may also be slightly higher during the months March to June and Ni during April to June. Average Zn, Fe and Cl concentrations are elevated during the months May/June for Zn and April/May for Fe and Cl, although the highest average Fe concentration was measured in November.

The average concentration for both Na and Mg appears to increase from July 2000 onwards. This may reflect an increase in concentrations of these elements in the air or could be related to the change in filter media from Teflon (Feb 00 – 21 June 00) to Polycarbonate (from 22 June 00). While the detection limits for the latter filter media were higher (115 compared to 98 ngm<sup>-3</sup> for Na and 43 compared to 38 for Mg), Na concentrations were detected on only 7% of the Teflon filters compared to 77% of the polycarbonate filters. Trompetter (pers comm. 2002) identifies some issues with the Na PIXE measurements, in particular that the low energy of the Na rays may prevent their complete detection, indicating that these data should be treated with caution.

Concentrations of nitrate, sulphate and chloride were highest during November, although high average concentrations were also recorded in August and October for sulphate and nitrate respectively. Average concentrations of NH<sub>4</sub><sup>+</sup> and Al showed no seasonal variations, and while average Ca concentrations were elevated in February, variations in data for the remainder of the year were minimal.

## 6.2 Correlations between elements

Data presented in Section 6.1 on the average monthly concentrations of different elements gives some indication of the way concentrations of different elements may relate to one another. For example, Mg and Na show similar seasonal variations to elemental carbon and sulphur. A Pearson correlation matrix (Table 6.2) provides a detailed analysis of the relationships between concentrations of elements on the filters. These relationships are also illustrated in a linkage diagram (Figure 6.4), which shows the interactions between different elements and the strength of the correlations for  $0.2 > r < 0.4$  (black line),  $0.4 > r < 0.6$  (purple line) and  $r > 0.6$  (blue line).

Table 6.2: Pearson correlation matrix for concentrations of elements on filters.

	EC	Na	Mg	Al	Si	S	Cl	K	Ca	Fe	Zn	NO <sub>3</sub> <sup>-</sup>	SO <sub>4</sub> <sup>-</sup>	Cl <sup>-</sup>	Sc	NH <sub>4</sub>	Mn	Ni
EC	1.000																	
Na	-0.093	1.000																
Mg	0.145	0.507	1.000															
Al	0.347	0.071	0.577	1.000														
Si	0.416	0.017	0.485	0.777	1.000													
S	0.657	-0.004	0.170	0.244	0.447	1.000												
Cl	-0.009	0.113	0.230	0.142	0.449	0.312	1.000											
K	0.273	0.121	0.103	0.073	0.126	0.461	0.342	1.000										
Ca	0.034	-0.037	0.136	0.217	0.160	0.162	0.257	0.254	1.000									
Fe	0.289	0.181	0.238	0.151	0.326	0.385	0.370	0.288	-0.048	1.000								
Zn	0.375	-0.177	-0.083	0.231	0.310	0.289	0.049	0.008	-0.017	-0.008	1.000							
NO <sub>3</sub> <sup>-</sup>	-0.073	0.034	0.066	-0.027	-0.024	-0.014	-0.004	-0.017	0.004	0.069	-0.030	1.000						
SO <sub>4</sub> <sup>-</sup>	0.056	0.074	0.115	0.052	0.080	0.133	-0.015	0.026	0.024	0.116	-0.006	0.850	1.000					
Cl <sup>-</sup>	-0.045	0.045	0.069	0.001	-0.002	0.020	0.045	-0.005	0.050	0.121	-0.027	0.858	0.792	1.000				
Sc	0.202	-0.207	-0.008	0.291	0.275	0.170	0.087	-0.042	0.128	-0.028	0.492	-0.018	-0.008	0.015	1.000			
NH <sub>4</sub>	0.233	-0.116	-0.081	0.115	0.077	0.196	-0.048	0.028	0.027	-0.114	0.260	-0.022	0.077	-0.013	0.166	1.000		
Mn	0.031	-0.052	0.071	0.107	0.130	0.059	0.013	-0.016	0.171	0.041	0.004	-0.014	0.017	0.036	0.206	0.001	1.000	
Ni	0.189	-0.180	-0.014	0.258	0.275	0.101	-0.031	-0.019	0.054	0.025	0.280	-0.024	-0.009	-0.025	0.238	0.077	0.315	1.000

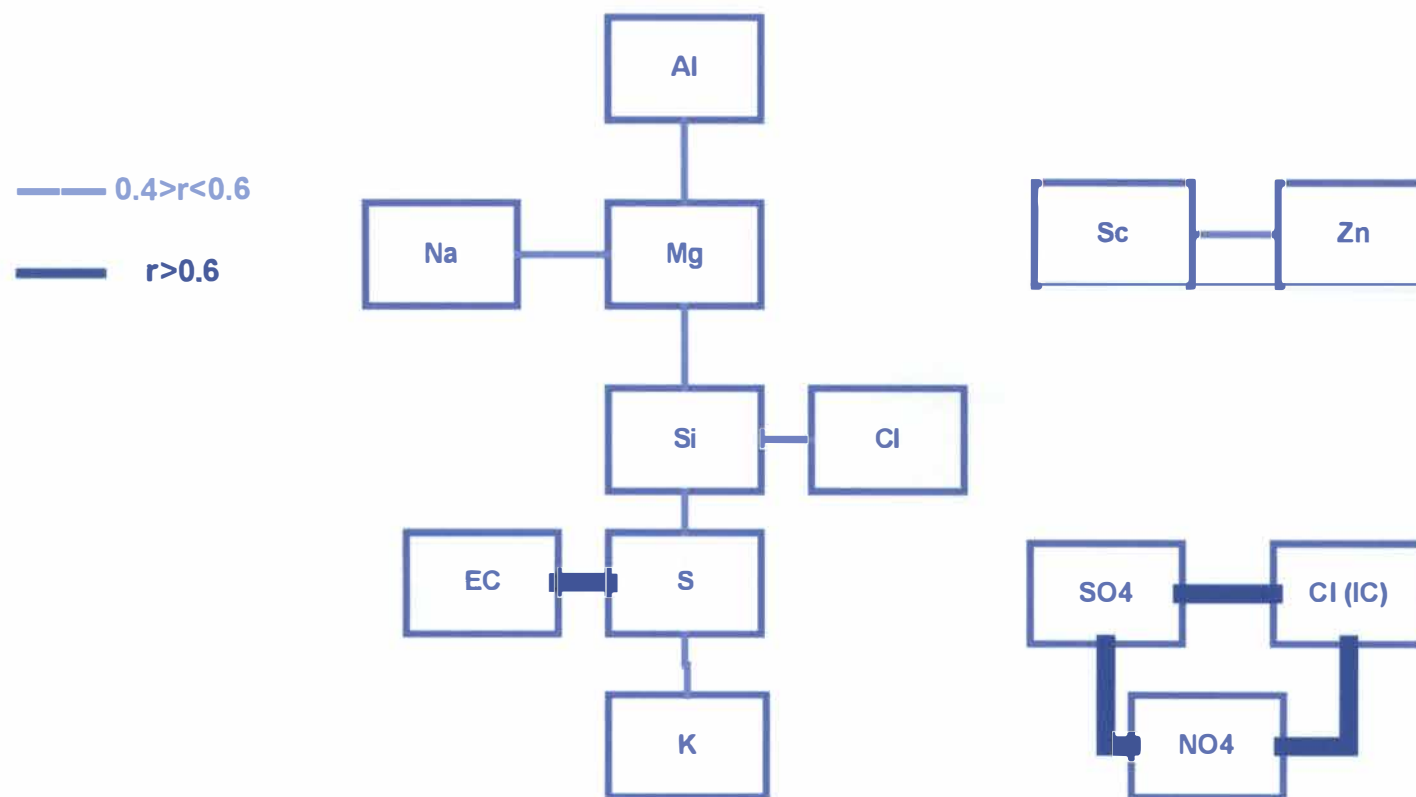


Figure 6.4: Linkage diagram showing correlations between concentrations of elements on the filters.



From Table 6.2, the main groupings of elements appear to be:

- EC, Si, S, Fe, Zn, K, Sc,  $\text{NH}_4^+$
- Na, Mg, Si, Fe, Cl
- Ca, K, Cl, Fe
- $\text{NO}_3^-$ ,  $\text{SO}_4^{2-}$ ,  $\text{Cl}^-$
- Mn, Ni

In addition to the correlation matrix for all filters, illustrated in Table 6.2, correlation matrices for the Teflon and polycarbonate filters were considered separately (Appendix D). These show some differences in the way the concentrations relate to one another. The main variations to the combined correlations are as follows:

Teflon Filters:

- Na and Fe both correlate with Cl
- Al correlates with  $\text{NO}_3^-$
- Cl and  $\text{Cl}^-$  are correlated.
- S and  $\text{SO}_4$  are loosely correlated

Polycarbonate Filters:

- No relationship between Na and Cl
- No correlation between soluble (IC) chloride and PIXE chloride.
- No relationship between S and  $\text{SO}_4$

The extent to which these represent differences associated with methodology (e.g., detection limits) or sources is uncertain. However, it appears that the filter media may play an important role in the analysis and may be the reason for the lack of correlation between Na and Cl and between S and  $\text{SO}_4$  in the combined analysis.

## 6.3 Factor analysis

A more detailed statistical analysis of the correlation between the concentrations of elements was carried out to assess the contribution of different sources of particulate. This involved analysis of the concentrations of elements and ions using principal components analysis to determine source profiles. Parameters were set to produce profiles for factors with eigenvalues greater than one. Data were rotated using varimax rotation.

### 6.3.1 Source profiles

The rotated loading matrix outputs for the factors identified using the PCA rotated loading matrix are shown in Table 6.3 with probable sources. The variance explained by these correlations is

about 70%, as shown in Figure 6.5. These data indicate factor relationships and do not provide an indication of the extent of contribution of different sources.

Factor one identifies sources consistent with soil particles. Factor two includes nitrates, sulphates and chlorides. Section 2.2 indicated that nitrates and sulphates formed as a result of atmospheric chemistry are referred to as secondary particles. However, ambient air mass concentrations can contain both primary and secondary nitrate and sulphate particles. Primary sources of sulphate include residential coal combustion and motor vehicles and wood combustion, although the proportion of total emissions is low at around 5%, 1% and 1% respectively (USEPA, 1998a). Both coal and wood combustion processes also emit primary nitrate, although the emission rates are even lower than for sulphates. The presence of chloride with these species may indicate an association with sea-spray emissions either as a direct sulphate emission, as sulphate comprises approximately 7.5% of saltwater, or as a result of chemical reactions between NaCl and nitric and sulphuric acid to give sulphates and nitrates.

A comparison of the concentrations of sulphate and nitrate relative to elemental carbon (e.g., Table 6.1) indicates that primary sources are unlikely to be dominant contributors to measured nitrate and sulphate concentrations. While primary sulphate emissions from sea-spray are possible, if this source were dominant within this profile other sea-spray prevalent elements such as Ca, Mg and K would be expected<sup>11</sup>. Thus it appears that the majority of the nitrates and sulphates represent secondary particles formed as a result of chemical reactions in the atmosphere. For the purposes of simplification, the sulphate and nitrate profile is generally referred to in subsequent Sections and graphs as secondary particulate.

Factors three and four contain elemental carbon and are therefore burning profiles. Factor five has been labelled sea salt because of the presence of Ca, Cl and K. The absence of Na from this profile is of concern, but may be due to the measurement problems already discussed. Factor six includes a few of the heavier metals Ni, Sc and Mn and may be related to an industrial source of particles.

The main limitations of the PCA factor designations are the lack of Na in the factor five profile and the lack of similar clustering for Cl<sup>-</sup>, measured using Ion Chromatography (IC) and Cl, measured using PIXE. The first issue may be explained by the higher level of uncertainty surrounding the accuracy of the Na measurements (see Section 6.1.1). In terms of the presence of chloride, the main differences in methodology between the two measurements are that the IC measures water

---

<sup>11</sup> It is assumed based on the uncertainties described previously and the unusual observed Na relationships that the PIXE analysis is not accurately detecting concentrations of this element

soluble chloride whereas the PIXE analysis will include both soluble and insoluble chloride. A field blank analysis of the nylon filter, however, indicated high blank concentrations of chloride, accounting for the majority of that measured. The ion chromatography chloride was subsequently removed from the analysis.

Table 6.3: Source profiles – PCA rotated loading matrix

	Factor 1	Factor 2	Factor 3	Factor 4	Factor 5	Factor 6
	Soil	Sulphates/ nitrates and chloride	Burning (Zn)	Burning (Fe)	Sea salt	Ni/ Industry?
<b>Mg</b>	<b>.88</b>					
<b>Al</b>	<b>.80</b>		<b>.34</b>			
<b>Si</b>	<b>.69</b>		<b>.30</b>	<b>.34</b>		
<b>Na</b>	<b>.52</b>					
<b>Nitrate</b>		<b>.96</b>				
<b>Chloride</b>		<b>.94</b>				
<b>Sulphate</b>		<b>.93</b>				
<b>Zn</b>			<b>.71</b>			
<b>Ammonium</b>			<b>.66</b>			
<b>Sc</b>			<b>.56</b>			<b>.40</b>
<b>EC</b>			<b>.52</b>	<b>.61</b>		
<b>S</b>			<b>.36</b>	<b>.77</b>		
<b>Fe</b>				<b>.74</b>		
<b>K</b>				<b>.65</b>	<b>.44</b>	
<b>Ca</b>					<b>.85</b>	
<b>Cl</b>				<b>.44</b>	<b>.53</b>	
<b>Mn</b>						<b>.74</b>
<b>Ni</b>						<b>.72</b>

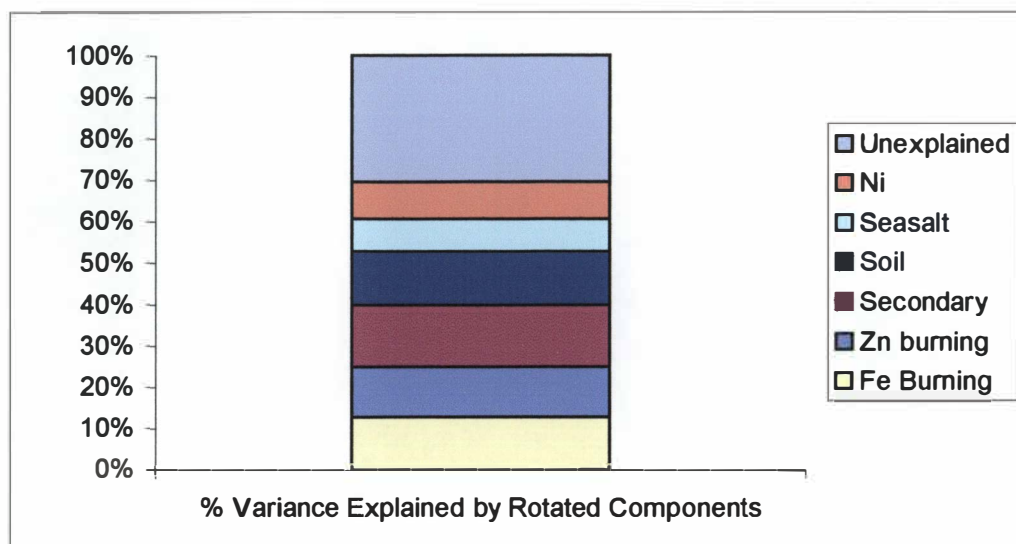


Figure 6.5: Percentage of variance explained by rotated components of PCA analysis.

The contributions of the different elements to the profiles identified in Table 6.3, with the exception of the chloride from the IC analysis, are shown in Table 6.4. These were determined by examining the relative contributions of each element to the total mass of material collected on the filters with the highest factor scores for each profile. Filters containing high factor scores for more than one profile were excluded, except in cases where there was no overlap in elements between profiles.

Table 6.4: Element contributions to source profiles.

	Soil	Sulphates/ nitrates	Burning (Zn)	Burning (Fe)	Sea salt	Ni
<b>Mg</b>	<b>23%</b>					
<b>Al</b>	<b>12%</b>		<b>6%</b>			
<b>Si</b>	<b>14%</b>		<b>7%</b>	<b>6%</b>		
<b>Na</b>	<b>51%</b>					
<b>Nitrate</b>		<b>13%</b>				
<b>Sulphate</b>		<b>87%</b>				
<b>Zn</b>			<b>6%</b>			
<b>Ammonium</b>			<b>&lt;1%</b>			
<b>Sc</b>			<b>3%</b>			<b>6%</b>
<b>EC</b>			<b>68%</b>	<b>62%</b>		
<b>S</b>			<b>9%</b>	<b>9%</b>		
<b>Fe</b>				<b>2%</b>		
<b>K</b>				<b>&lt;1%</b>	<b>8%</b>	
<b>Ca</b>					<b>6%</b>	
<b>Cl</b>				<b>20%</b>	<b>86%</b>	
<b>Mn</b>						<b>13%</b>
<b>Ni</b>						<b>81%</b>



The main contributors to the soil profile are shown in Table 6.4 to be Na (51%) and Mg (23%), with smaller but still significant amounts of Al and Si. The latter two elements appear to be more dominant in soil profiles in other countries. For example, Malm, *et al.*, (1996) indicated a dominance of Al, Si and Fe with smaller quantities of Ca and Ti in the Grand Canyon area.

The contribution of nitrate and sulphate particulate to particle mass has been calculated based on actual concentrations of nitrate and sulphate rather than the profiles and contributions identified in Table 6.4. This is because these compounds constitute secondary particulate by definition and therefore reconstruction to estimate contribution is unnecessary. In most urban atmospheres, concentrations of nitrate and sulphate are in the form  $(\text{NH}_4)_2\text{SO}_4$  and  $\text{NH}_4\text{NO}_3$  (Chan *et al.*, 1997). However, no correlations between ammonium and nitrate or sulphate are observed in the data. It is possible that the dominant atmospheric reaction resulting in elevated nitrate and sulphate concentrations in Christchurch is the neutralisation of NaCl emissions by sulphuric and nitric acid. In this instance, the nitrate and sulphate would be in the form of  $\text{NaNO}_3$  and  $(\text{Na})_2\text{SO}_4$ . However, no chloride depletion was observed. While no associations were found between the secondary particles and the Na concentrations, the uncertainties associated with the PIXE measurement of Na make conclusions regarding sources difficult. It is also possible that sulphates are in the form of sulphuric acid aerosol as the particulate form of  $\text{H}_2\text{SO}_4$  can occur under low temperatures and high relative humidity. Further studies are required to determine the form of secondary particles.

Two burning profiles are identified in the PCA analysis. While elemental carbon is the main contributor to both profiles, some variance in other elements is apparent. The first burning profile includes Al, Zn and Sc at 6%, 6% and 3% respectively. The second profile includes Cl and Fe at 20% and 2% respectively. Both profiles include around 9% S and around 6-7% Si.

The main combustion sources of particles in Christchurch are likely to be domestic heating (predominantly wood burning), and motor vehicles. To determine the likely elements associated with a wood burning profile, a number of filters from the burning of wood on a solid fuel burner were examined for this study using PIXE. These samples were taken during the testing of these burners for compliance with NZ standard 4013. Emissions from the burners were drawn through a dilution tunnel and collected on a filter in a laboratory situation. No other testing of the elemental composition of samples of wood appears to have been carried out in New Zealand. Table 6.5 shows the relative contribution of the different elements across the three filters. While the small sample size is a limitation, the results are reasonably consistent across the three different filters, with elemental carbon contributing around 52% of the PIXE mass. The next most dominant contributors are Si, Ca and Zn at 21%, 6% and 5% respectively. Other elements found in the fingerprint include S, Al, Na, Sc (3%), I (2%), and K and Fe (1%).

A similar assessment carried out in the United States (Fine *et al.*, 2002) found concentrations of organic and elemental carbon, Si, S, Cl, K, Zn and Ca were prevalent in wood smoke from open fires burning softwoods such as Loblolly Pine. In addition, that study measured ionic species in the samples and found concentrations of chloride, nitrate, sulphate and ammonium. These species were not measured in the New Zealand wood burning assessment. The most notable difference relative to the testing carried out in New Zealand is the absence of Cl in the latter analysis.

The low levels of K in the New Zealand wood burning samples (Table 6.5) are also of interest as this element is typically used as a biomass burning tracer (Keywood *et al.*, 2000). However, this appears to be explained by the choice of fuel, as Fine *et al.*, (2002) showed lower concentrations of K with the burning of pine, relative to other fuels. Mistra *et al.*, (1993) also showed a greater retention of K in the ash content of pine, than for other wood species, including aspen, poplar, red oak, white oak, white oak bark and Douglas fir bark.

Table 6.5: Burning profiles for wood burning from this study.

	Filter 1	Filter 2	Filter 3	Average
	%	%	%	%
<b>Na</b>	2	3	5	3
<b>Al</b>	3	3	3	3
<b>Si</b>	22	21	20	21
<b>S</b>	3	3	3	3
<b>K</b>	0	0	2	1
<b>Ca</b>	7	7	5	6
<b>Sc</b>	3	2	3	3
<b>Fe</b>	1	1	1	1
<b>Zn</b>	5	5	5	5
<b>I</b>	3	2	1	2
<b>EC</b>	51	53	51	52

A study of the New Zealand motor vehicle fingerprint was carried out by Markwitz *et al.*, (2001). That study collected filter samples using a GENT sampler in the Victoria Tunnel in Wellington during peak traffic periods. A total of 32 filters for PM<sub>2.5</sub> and for PM<sub>10-2.5</sub> were collected and analysed by GNS using PIXE. Four factors were identified (Table 6.6). However, factor one contributed over 95% of the particulate in the Mt Victoria tunnel.

Table 6.6: Composition of Mt Victoria tunnel “motor vehicle” fingerprints (from Markwitz *et al.*, 2001).

	Factor 1	Factor 2	Factor 3	Factor 4
	%	%	%	%
Fe	3.0			
EC	91.0			
S	4.8			
K	0.2			
Br		57.4		
Ca		35.2		
Si	1.1	7.4	39.8	
Cl				26.4
Al			25.5	
Mg			34.7	
I				23.8
Contribution	95.8%	0.6%	2%	1.6%

A comparison of Tables 6.5 and 6.6 with the composition of the burning profiles from the PCA analysis suggests that the factor three (burning Zn) profile is likely to relate to domestic heating and the factor four (burning Fe) profile is likely to be associated with motor vehicles. The presence of Zn, Sc, Al, S, Si and EC, in both the factor three fingerprint and the wood burning filters (Table 6.5) supports this conclusion. Although included in the PIXE analysis, Zn concentrations were not found to be a significant component of the motor vehicle fingerprints identified in Table 6.6, although subsequent factor analysis in Wellington have shown some zinc presence from motor vehicles (Davy, 2002). A similar consistency is observed between the motor vehicle fingerprint and the factor one source profile identified by Markwitz *et al.*, (2001) and shown in Table 6.6. The main inconsistency is the contribution of Cl, which accounts for less than 1.6% of the PM<sub>2.5</sub> mass in Markwitz *et al.*, (2001) but accounts for 20% of the burning Fe profile in this study (Table 6.4).

One limitation in the analysis is that both the Markwitz *et al.*, (2001) fingerprint study for motor vehicles and Table 6.5 fingerprint study for wood burning include traces of Fe. Although these showed a greater contribution for motor vehicles (3%), than for domestic heating (1%), Fe was not identified as a contributor to the Zn burning fingerprint. It is of concern no Fe was apparent in the factor analysis profile for wood burning in this study and consequently Fe was used as a unique identifier for motor vehicle emissions.

It has been proposed that the presence of Zn in the wood burning profile (Table 6.5) may occur as a result of the impact of a galvanized chimney because concentrations of Zn are not typically associated with wood burning (Phillip Hopke, pers comm. 2002). Although wood burners would typically use a galvanised chimney, open fires in Christchurch generally exhaust smoke through brick or non-galvanised chimneys. If the hypothesis of the galvanised chimney being the source of Zn were correct, then this profile may not include emissions from open fires. It is therefore possible that reliance on the Zn burning profile as an indicator of particulate from solid fuel burning may underestimate the contribution from this source. An emission inventory conducted for Christchurch in 1999 indicates that around 40-45% of the PM<sub>10</sub> from domestic home heating occurs as a result of open fires burning wood and coal (Wilton, 2001), suggesting that if this is the reason why zinc is included in the burning profile, then the contribution may be underestimated by 40-45%.

This explanation regarding the source of Zn in burning, however, is not supported by other studies, which show Zn emissions from wood burning in the absence of galvanised chimneys. For example, Fine *et al.*, (2002) showed that Zn contributes to wood smoke emissions from open fires and Risse & Harris (2002) showed that Zn is one of the main microelements retained in wood ash.

### 6.3.2 Source contributions to PM<sub>2.5</sub> mass

The relative contribution of the six different PM<sub>2.5</sub> sources to the mass of particulate on the filters was estimated by identifying an element unique to each source. The amount of particulate from that source on the filter was then estimated by multiplying the concentration of the unique element by the inverse proportional contribution of that element to the source profile. For example, to determine the mass contribution of factor three (domestic burning) for a filter containing 0.16 µg m<sup>-3</sup> Zn,  $0.16 \mu\text{g m}^{-3} \times 1/6\% = 2.67 \mu\text{g m}^{-3}$ .

The estimated mass from each source was then combined to give a total reconstructed PM<sub>2.5</sub> mass. Figure 6.6 shows the relationship between the reconstructed PM<sub>2.5</sub> mass and the measured PM<sub>2.5</sub> for each filter sample and gives an  $r^2$  value of 0.87 with  $y = 0.85x + 3$ . This indicates that the reconstructed PM<sub>2.5</sub> mass are typically just slightly lower than the PM<sub>2.5</sub> measurements calculated by summing the PIXE concentrations for each element and the EC filter measurements. This difference is not unexpected as the relationship between the concentrations of elements described using the PCA analysis only accounts for 70% of the variance in concentrations of elements.

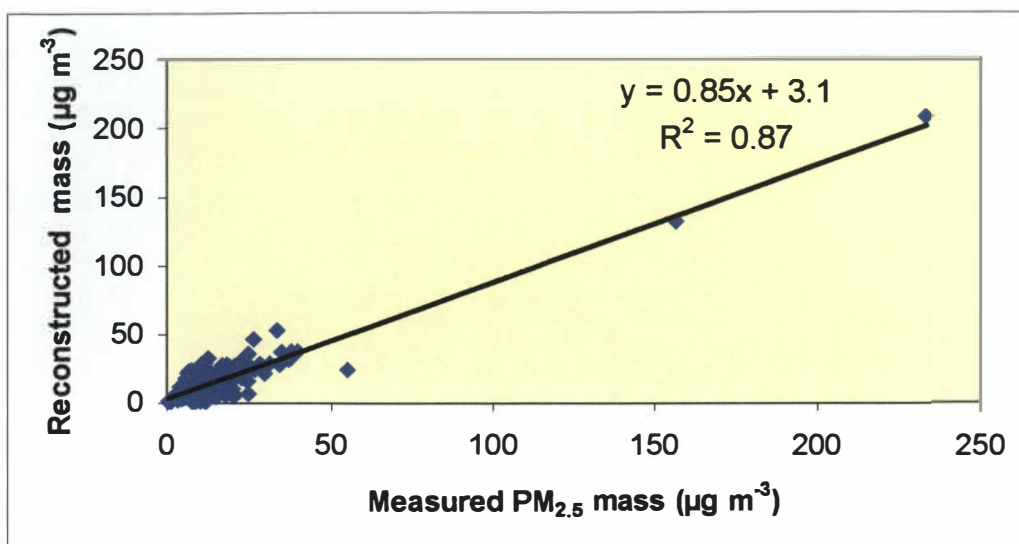


Figure 6.6: Reconstructed versus measured PM<sub>2.5</sub> mass (PIXE and filter based EC).

In addition to the amount of particulate measured using the PIXE and filter EC measurements, concentrations of organic carbon will also contribute to actual PM<sub>2.5</sub> mass and therefore light scattering by particles. An estimate of the organic carbon (OC) contribution to each of the two burning profiles was made based on OC concentrations measured using the series 5400 carbon analyser. These concentrations were multiplied by a factor of 1.4 based on the assumption that the carbon fraction of organic carbon aerosol is 0.71 (Pryor *et al.*, 1997). The hourly OC concentrations were averaged for the period 06:00 to 13:00 to coincide with the filter exposure period. These concentrations were not included in the original PCA analysis because there were too many occasions when OC concentrations were not available. The OC contribution to each profile was estimated using the average OC concentrations for the filters used to determine the source profiles (i.e., those with the high factor scores for each source). Thus the amount of OC in each of the two burning profiles was determined from the relationship between the OC and the PIXE plus EC mass. The OC mass equated to 47% of the PIXE/EC mass for the Zn burning profile and 41% for the Fe burning profile.

The relative contribution of each source to the estimated PM<sub>2.5</sub> mass was assessed for each month of the year (Figure 6.7). This shows an increased presence of the factor three burning profile during the months of May and June, which is consistent with this burning source relating to wood burning for domestic heating. Typically, emissions from domestic heating and associated high pollution episodes could be expected throughout the colder winter months. However, record warm temperatures recorded during July 2000 reduced the frequency of pollution episodes and may have influenced heating behaviour.



Results indicate that the main contributors to the PM<sub>2.5</sub> mass measured at the visibility monitoring site during the daytime are factor four, which most probably represents motor vehicle emissions, and factor two which comprises of secondary particulates.

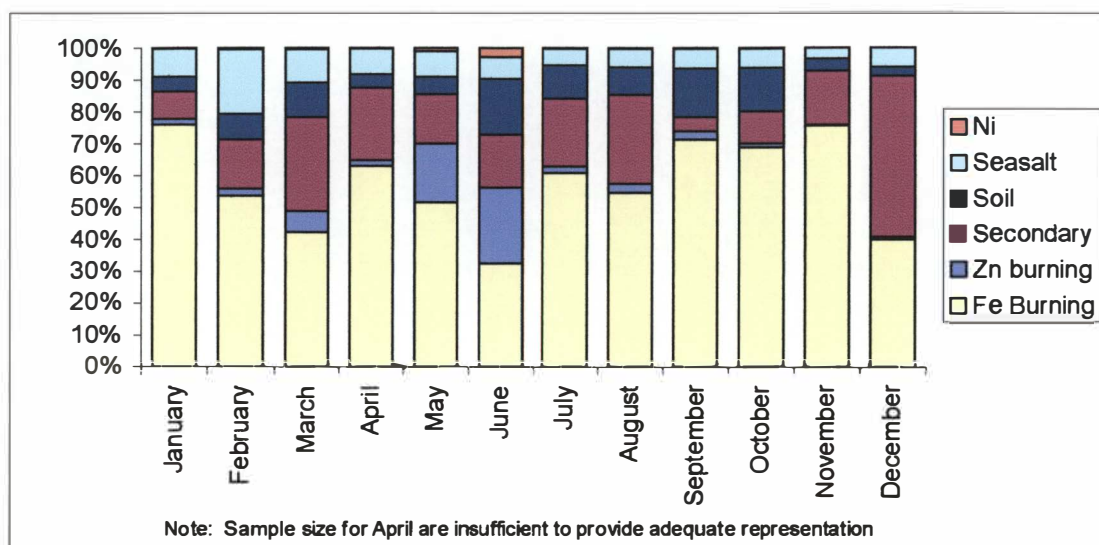


Figure 6.7: Average source contributions to PM<sub>2.5</sub> mass by month.

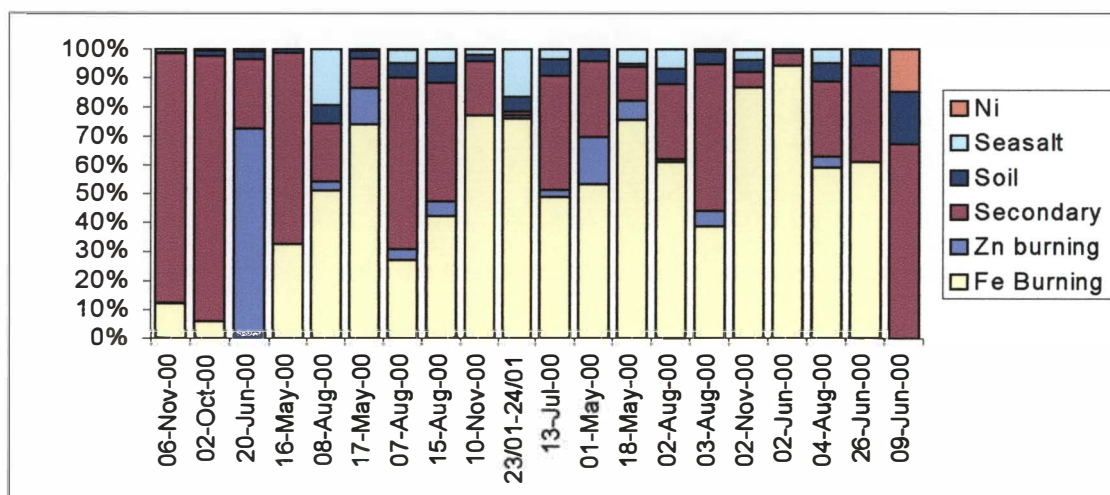


Figure 6.8: Source contributions to PM<sub>2.5</sub> mass for days of highest reconstructed mass – ordered from left to right based on highest reconstructed PM<sub>2.5</sub> emissions.

Source contributions to particulate mass on days when the sum of the elements and compounds measured were highest are shown in Figure 6.8. The main contributors on these days are secondary particles and the factor four (motor vehicle) burning profile. However, the 20 June 2000 filter is dominated by the factor three (domestic fires) burning profile. The two highest light extinction values occurred on 6 November 2000 and 2 October 2000 respectively. On both of these days nitrate and sulphate concentrations were much higher than on other days, with nitrate concentrations in excess of 100 µgm<sup>-3</sup> on the 6 November. While light extinction data were not

available on the 2 October, the maximum value for the 6 November was relatively low at 92  $\text{Mm}^{-1}$ . It is possible therefore that the measurement of nitrates on this day is in error as a higher light extinction value may be expected with elevated nitrate concentrations.

Figure 6.9 shows the measured concentrations of nitrates and sulphates for the same days of highest reconstructed mass. On both the 6 November and 2 October, nitrates are the dominant contributor, although the sulphate concentrations on the 6 November are also significant. This is unusual relative to most other days when reconstructed mass is high, as sulphate is the dominant contributor (Figure 6.10). The contribution of sulphate to the total secondary particulate concentrations ranged from 29% on the 2 October 2000 to 100%. The average daily contribution of sulphate to total secondary particulate was around 85%.

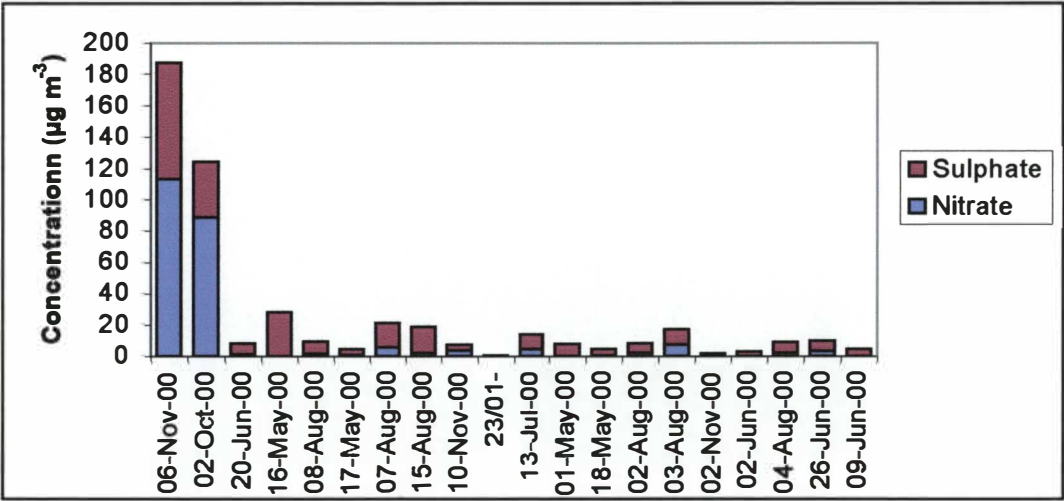


Figure 6.9: Contribution of nitrates and sulphates to secondary particulate mass for days of highest reconstructed mass – ordered from left to right based on highest reconstructed  $\text{PM}_{2.5}$  emissions.

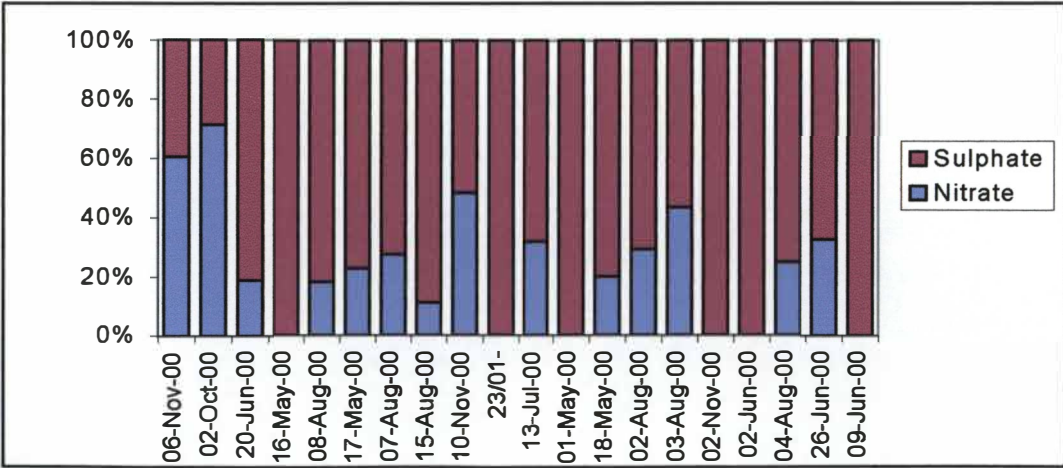


Figure 6.10: Relative contribution of nitrates and sulphate to total secondary particles for days of highest reconstructed mass – ordered from left to right based on highest reconstructed  $\text{PM}_{2.5}$  emissions.

Figure 6.8 shows an estimate of the relative contribution of different sources to PM<sub>2.5</sub> mass concentrations on different days throughout the sampling period. While results appear generally reasonable, they suggest some possible flaws in the methodology. In particular, the estimate of no motor vehicle contribution to PM<sub>2.5</sub> mass on the 20 June, when the highest light extinction values were recorded, is counter-intuitive given the high contribution on other similar days. Thus it is possible that there are some flaws in using concentrations of Fe and Zn in the distinction between motor vehicles and solid fuel burning emissions or measurement problems on some days. Similarly, no combustion sources are estimated on the 9 June because of the absence of both Fe and Zn concentrations on the filter. However, the elemental carbon concentrations measured on that day (Figure 6.11) make a significant contribution to the total PM<sub>2.5</sub> mass and therefore would result in a combustion source contribution to light extinction on the 9 June.

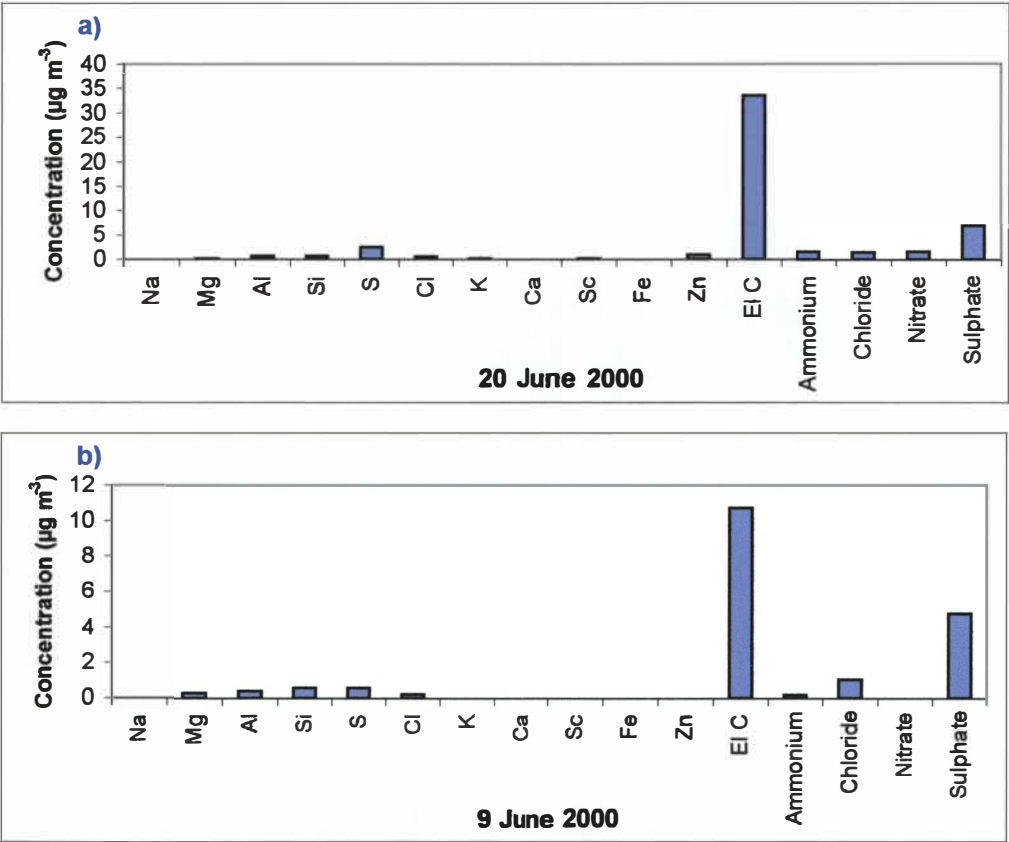


Figure 6.11: Concentrations of elements and ions on the 20 June (a) and 9 June 2000 (b).

### 6.4 Summary

The particulate speciation showed highest average concentrations of elemental carbon, sulphates and nitrates in that order. Organic carbon concentrations were similar to elemental carbon, although data were not available for the whole time. Statistical analysis of data suggested six sources contributing to measured PM<sub>2.5</sub> concentrations. Based on comparisons to source profiles

from New Zealand and overseas, these were thought to represent soil, sea-spray, secondary particles, domestic fires, motor vehicle emissions and an unidentified source of primarily nickel.

The contribution of each source to measured  $PM_{2.5}$  concentrations for each sample was estimated for each source. Motor vehicle emissions and secondary particles were found to be the key contributors to  $PM_{2.5}$  concentrations, although the domestic fire contribution was significant at times during the winter months. Of the secondary particles, sulphates were the dominant species contributing 85% of the daily concentrations of nitrates and sulphates, on average.

Some uncertainties associated with the analysis were identified. Issues associated with the presence of Zn in the domestic fires profile being associated with chemical reactions of the galvanized chimneys do not appear to be supported by the literature, which suggests that Zn is present in wood burning emissions from open fireplaces. The lack of Na in the sea salt profile was thought to be a result of the inaccuracies associated with the PIXE Na measurement on the polycarbonate filters.

Results of receptor modelling for  $PM_{2.5}$  apportionment are used in subsequent Sections to determine factors contributing to visibility degradation.

## Chapter 7 Source contributions to light extinction

Chapter 6 identified the contribution of a number of different sources to the mass concentrations of  $PM_{2.5}$  at the visibility monitoring site. The relationship between these sources and visibility degradation, however, depends on factors other than particulate mass. As detailed in Chapter 2, factors such as particle size and composition are more significant than mass in determining light extinction and visibility degradation. In this Chapter, the relationship between light extinction and the potential sources of particulate are examined.

### 7.1 Sources of particulate mass on high extinction days

Analysis of sources of particulate on the days with the highest average light extinction values suggests that secondary particles and motor vehicles are major contributors to  $PM_{2.5}$  mass on days when visibility degradation is worst (Figure 7.1). The light extinction values are based on the average light extinction for the period coinciding with the filter exposure period. Thus some are seven-hour averages (Figure 7.1a) and some 24-hour averages (Figure 7.1b) (see Appendix B for dates).

Although domestic home heating appears to be a significant contributor to  $PM_{2.5}$  mass on the 20 June, the contribution on other poor visibility days is small. The soil, Ni source and sea salt contributions are small on all days except the 1 August, when the sea salt makes up about 30% of the  $PM_{2.5}$  mass.

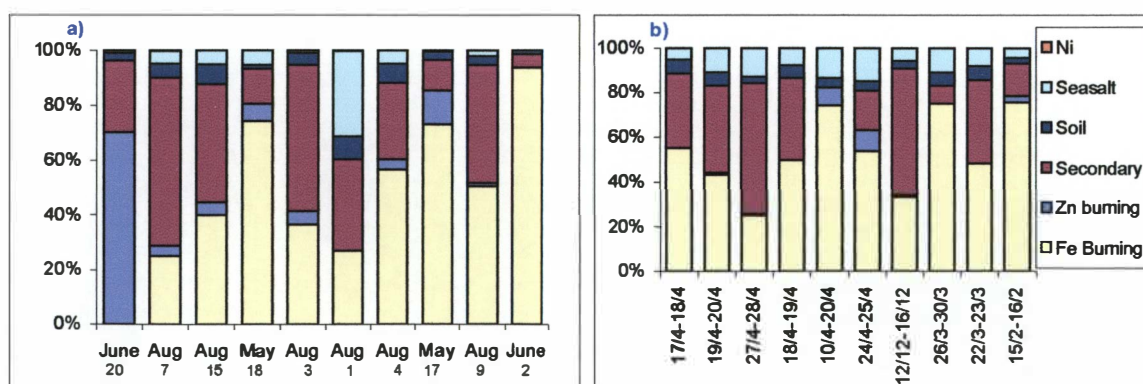


Figure 7.1: Relative contributions to  $PM_{2.5}$  mass on the ten highest light extinction values based on averages for daytime filters only (a) and for filters exposed for 24-hours (b).

Figure 7.2 shows the average contribution of each source across a range of light extinction values. These are broken down into two categories loosely labelled summer and winter, representing the



periods October to March and April to September respectively. With the exception of the domestic fire contribution during the winter months, the relative contributions for each grouping of data are similar for both seasons. The major contributor is usually Fe burning (about 50-60%), with secondary particles contributing around 30-45% when visibility is degraded. The main difference is that the light extinction values during the summer months are much lower, with the maximum filter average light extinction being  $151 \text{ Mm}^{-1}$  compared to  $546 \text{ Mm}^{-1}$  during the winter months.

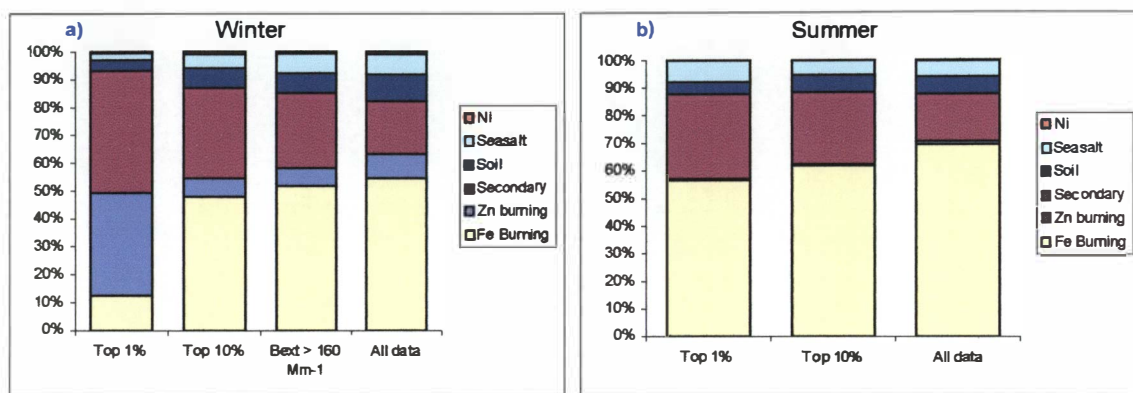


Figure 7.2: Relative contribution to PM<sub>2.5</sub> mass for a range of light extinction values during winter (a) and summer months (b).

## 7.2 Source strength and light extinction on all days

Figure 7.3 shows the relationship between elevated light extinction measurements (averaged for the filter measurement period) and source strengths (factor scores) for all sources identified in the PCA analysis. The strongest relationships are observed for factor two (secondary particles) and factor four (motor vehicles), although the latter relationship is very dependent on a single measurement and overall relationships are not generally strong. These results are generally consistent with comparisons of light extinction values and contributions to PM<sub>2.5</sub> mass illustrated in Section 7.1.

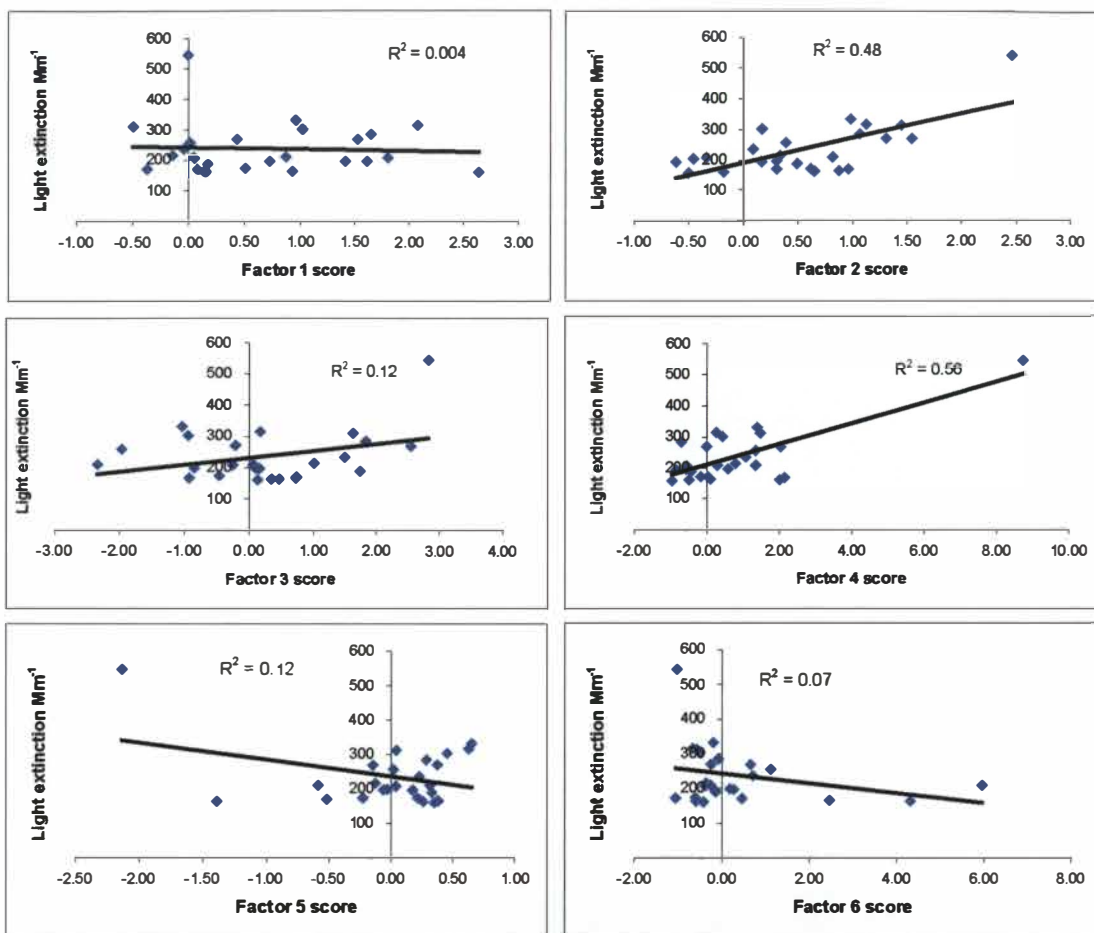


Figure 7.3: Relationship between PCA factor scores and light extinction

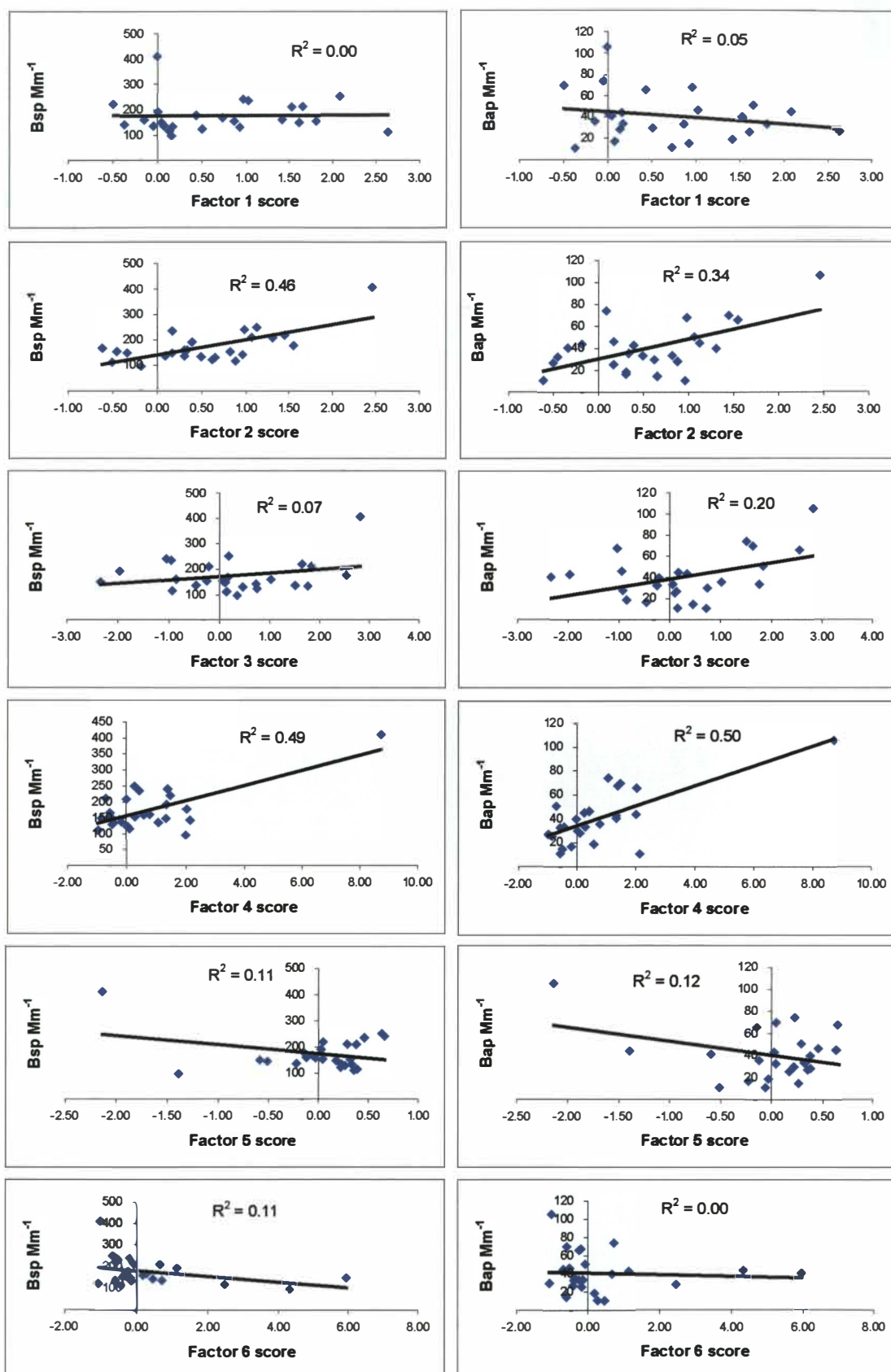


Figure 7.4: Relationship between PCA factor scores and light scattering and absorption.

A further exploration of the relationships between the PCA factor scores and light scattering and absorption components is shown in Figure 7.4. It should be noted that the light scattering and absorption components are not independent, as elemental carbon, the most effective element in absorbing light may also contribute to light scattering. Furthermore, meteorological conditions are likely to be conducive to the build up of both light absorption and light scattering contaminants at the same time. Thus, although factor two shows good correlations for light scattering and absorption, nitrates and sulphates are unlikely to contribute to light absorption.

### 7.3 Source contributions to light scattering

A multiple regression analysis was carried out using a stepwise linear regression to examine the relationship between the PCA factors and light scattering. The coefficients for the regression equation are detailed in Table 7.1. Both the individual regression analyses (Figure 7.4) and the significance levels of the coefficients of the multiple regression (Table 7.1) show that factors two and four have the greatest impact on light scattering by particles.

Table 7.1: Multiple regression coefficients and 'p' scores for light scattering by particles.

Effect	Coefficient*100	'p'
Constant	96	0.00
Factor one – soil	13	0.05
Factor two – secondary particles	53	0.00
Factor three – domestic fires	9	0.02
Factor four – motor vehicles	14	0.00
Factor six – Ni	6	0.04

The coefficients in the regression equation are estimated by the sample partial regression coefficients. The partial regression coefficient gives a rate of change (or slope) in the dependent variable (e.g.,  $B_{sp}$  or  $B_{ap}$ ) for each unit change in the independent variable when the other independent variables are held constant.

Factor five (sea-spray) was removed from the regression equation for  $B_{sp}$  because the 'p' statistic of 0.5 was greater than the predetermined cut off at 0.15, indicating a 50% probability that the relationship between light scattering and sea-spray was due to chance. The 'p' statistics for all other factors were less than 0.05 indicating less than 5% probability that the relationships were due to chance. The coefficient of determination ( $r^2$ ) of 0.75 suggests that 75% of the variance in light scattering values can be explained by the relationship described by the multiple regression analysis.

The regression coefficients were used to assess the relative contribution of each source to light scattering. The daily mass concentrations estimated for each source were weighted based on their relative contribution to light extinction. Figure 7.5 shows the relative contribution of each source to light scattering for the top 10 light extinction days for both daytime and 24-hour filters. These differ from previous graphs (Figures 7.1 and 7.2) in that they represent the contribution of sources to light scattering as opposed to PM<sub>2.5</sub> mass. During the winter and the summer months the greatest contributor to light scattering on high extinction days is the secondary particulate, although motor vehicle emissions (Fe burning) are also significant during the summer months (Figure 7.6).

The additional impact of the secondary particulate is consistent with overseas studies and is dependent on relative humidity. For example, a number of researchers (e.g., Middleton & Laulainen 2000 and Pryor, *et al.*, 1997) report equations for estimating light scattering coefficients for nitrates and sulphates of  $3 \cdot (0.7 / (1 - \%RH/100)) \text{ m}^2 \text{ g}^{-1}$ . The organic carbon component also has some humidity dependence and is estimated from  $4 \cdot (0.5 + 0.5 \cdot (0.7 / (1 - \%RH/100))) \text{ m}^2 \text{ g}^{-1}$ , based on the assumption that half of the organic carbon is hygroscopic. These compare to light scattering coefficients of 2.0 and 0.6  $\text{m}^2 \text{ g}^{-1}$  for other fine particles and coarse particles respectively (Middleton & Laulainen, 2000). Thus for an average humidity for Christchurch of around 70%, the estimated scattering efficiency for nitrates and sulphates of about 7  $\text{m}^2 \text{ g}^{-1}$  is much higher than for organic particles and coarse particles.

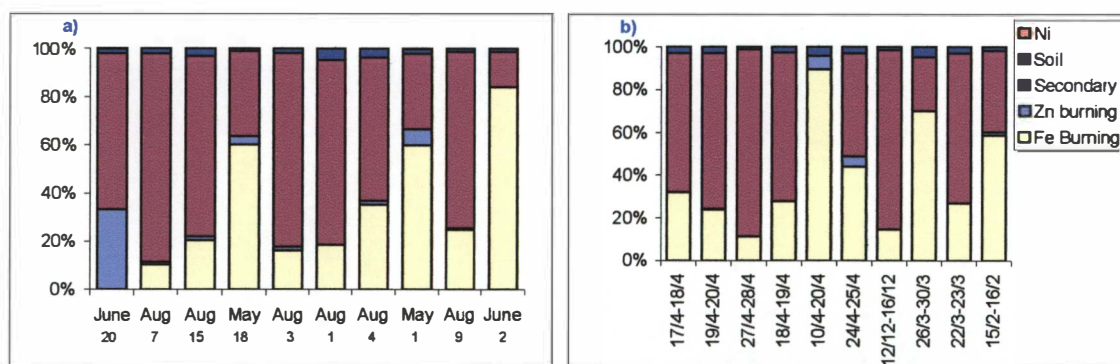


Figure 7.5: Relative contributions to light scattering on the ten days of highest light extinction values based on daytime filters only (a) and for filters exposed for 24-hours (b).



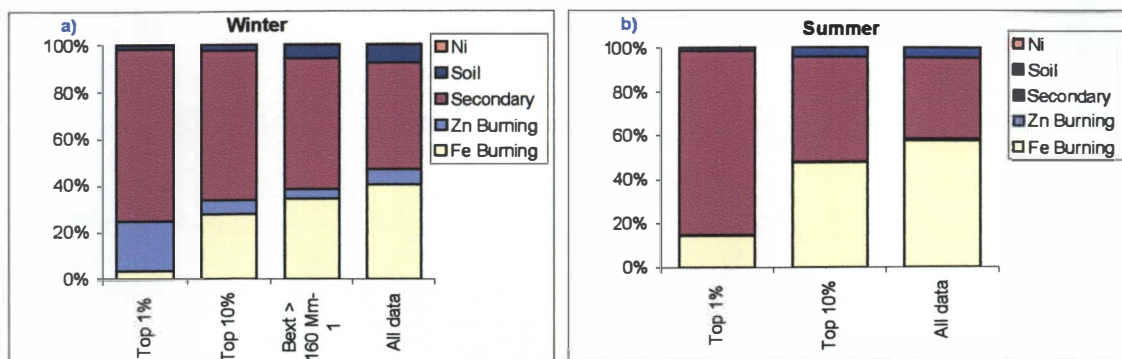


Figure 7.6: Relative contribution to light scattering for a range of light extinction values during winter (a) and summer months (b) – note no daily average Bext values during summer were greater than 160 Mm<sup>-1</sup>.

## 7.4 Source contributions to light absorption

The contribution of the different sources to light absorption was estimated based on the amount of elemental carbon from each source present on the filters. This requires the assumption that all absorption is due to elemental carbon. The literature indicates soil can be a significant contributor to light absorption (e.g., Malm, *et al.*, 1996), although this is only likely in areas where the soil is a major source of particulate and where elemental carbon concentrations are low. Because the soil contribution is relatively small, and because Figure 7.4 does not show a strong association between soil and light absorption, it is likely to be a reasonable assumption in this instance.

The elemental carbon component of both burning sources is similar at around 45% of the measured components. However, Figure 7.7 shows the relative contribution of motor vehicles (Fe burning) to be the main contributor to light absorption on days of high light extinction and for all days during both the summer and winter. This is because motor vehicle emissions are the more dominant contributor to PM<sub>2.5</sub> mass. Although Figure 7.7 shows the contribution of domestic fires to be significant for the top 1% of light extinction days, these data are based on results for two days only. Thus while it may seem that domestic heating is a major source of light absorption on the worst visibility days, the result is dominated by one specific instance, which is considered in detail in Chapter 8.

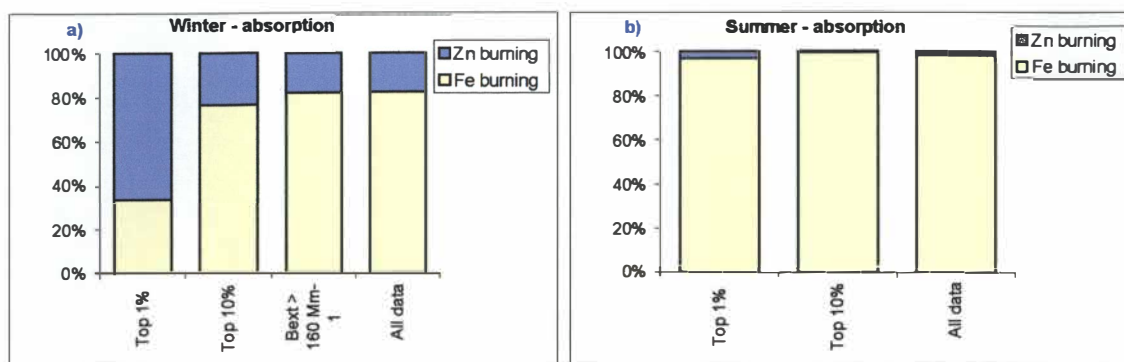


Figure 7.7: Relative contribution to light absorption for a range of light extinction values during winter (a) and summer (b) months.

## 7.5 Overall contributions to light extinction

As indicated in previous Chapters, total light extinction is estimated based on the measurements of  $B_{sp}$ ,  $B_{ap}$  and  $B_{ag}$  combined with a constant for  $B_{sg}$  of  $13.7 \text{ Mm}^{-1}$ . The light absorption by gas ( $B_{ag}$ ) component is assumed to be all  $\text{NO}_2$ , as this is the only atmospheric gas that absorbs light. The sources of particles and their contributions to  $B_{sp}$  and  $B_{ap}$  are detailed in Sections 7.3 and 7.4. This Section combines these results with data for  $B_{sg}$  (Rayleigh constant) and  $B_{ag}$  ( $\text{NO}_2$ ) to provide an overall assessment of the contribution of different sources to light extinction. Results are presented for high extinction days and by season. The relative contributions of the various influences on light extinction on a number of case study days are also examined in Chapter 8.

### 7.5.1 Contributions on high light extinction days

The main contributors to light extinction during the winter months, when the highest values occur, are secondary particles, contributing about 50% for the highest 10% of days, and the Fe burning source which is most likely to represent motor vehicles, contributing about 30% (Figure 7.8). On the top 1% of days, domestic fires (Zn burning) contribute about 20%. However, the top 1% represents only two filters, one of which is the 20 June, in which all the combustion particulate is estimated to be domestic fires (see Section 8.1.2). Motor vehicles (Fe burning) are generally the most dominant combustion source of particulate as indicated by the top 10% of values. The main sources of light extinction during the summer are also secondary particles and motor vehicles.

The extent of contribution from motor vehicles seems surprising given that light extinction is dominated by light scattering, of which the main contributor is secondary particulate (Section 7.3). However, Chapter 5 indicated that the contribution of light absorption to total extinction increased on the very high light extinction days. As motor vehicles contribute the majority of the light absorption and are significant in light scattering, their overall contribution of around 30% during

the winter and 40% during the top 10% of summer light extinction days is reasonable. In addition, it is possible that motor vehicles contribute towards the secondary particulate profile.

These summary data are likely to provide a good indication of the overall contributions. While daily data show the potential for significant variations in the contributions from day to day (Figure 7.9), some of these variations are a result of the source apportionment methodology, as discussed in Section 6.3.2. A breakdown of the secondary particulate component on days of high light extinction is shown in Figure 7.10. This shows that sulphate is the main contributor to concentrations of secondary particles on days of elevated light extinction.

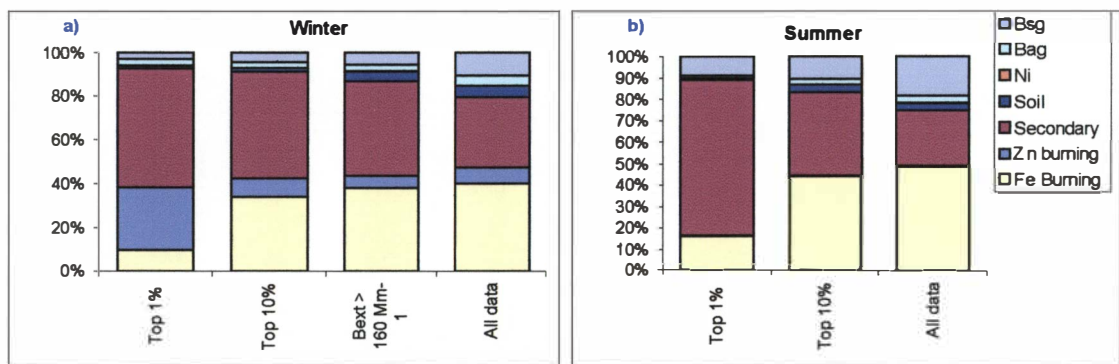


Figure 7.8: Relative contribution to light extinction during winter (a) and summer (b) months.

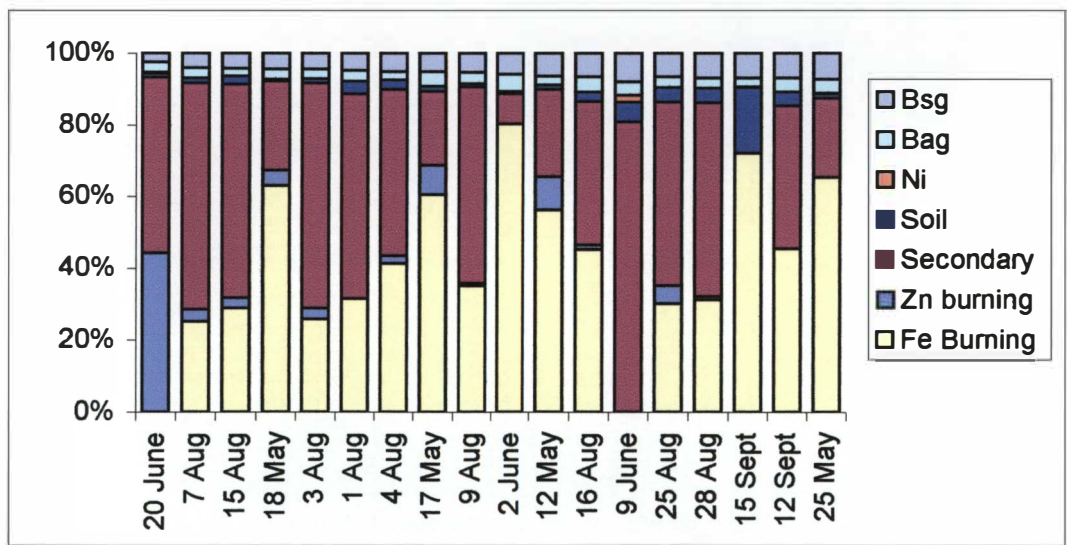


Figure 7.9: Relative source contributions to light extinction on days of elevated light extinction – ordered from left to right based on higher to lower light extinction values.

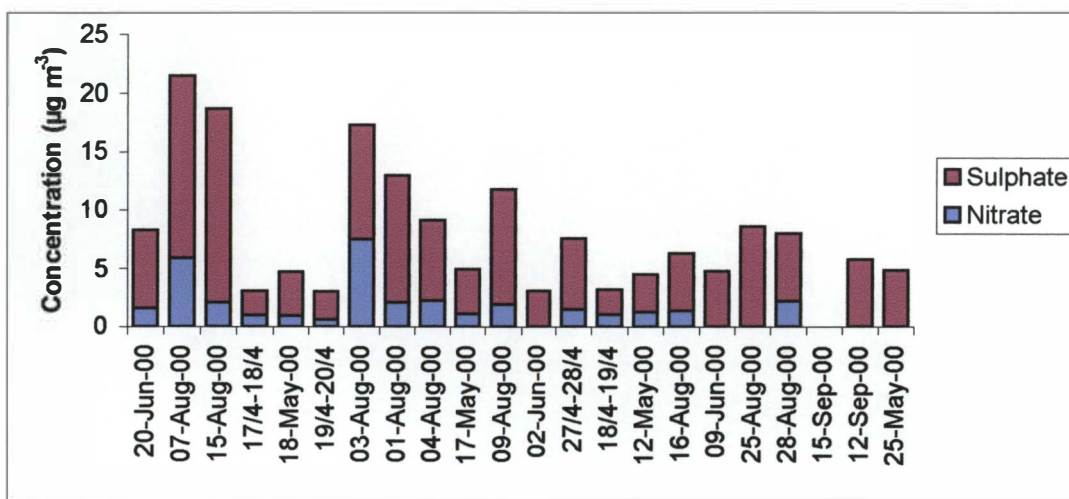


Figure 7.10: Concentrations of nitrate versus sulphate on days of elevated light extinction – ordered from left to right based on higher to lower light extinction values.

The dominance of nitrates and sulphates in contributing to light extinction is not unique to Christchurch. In the Fraser Valley, British Colombia, organics dominate aerosol mass (35-46%) but nitrates and sulphates are the main contributors to light scattering accounting for 55-67% of mean  $B_{sp}$  (Pryor, *et al.*, 1997). Similar relationships are observed in the United States, with sulphate being the greatest contributor to degraded visibility in the east, contributing 64% of aerosol extinction on clear days and up to 80% on the worst days. In the west, sulphate accounts for 35-45%, organic carbon 19-22%, crustal material 16-20% and nitrates 12-15% (USEPA, 1998b).

This study for Christchurch shows sulphate to be the dominant contributor to secondary particulate mass accounting for around 85% per day on average. Sources of sulphate in Christchurch could include emissions from sea-spray, coal combustion for industrial processes, domestic coal burning and diesel vehicles. The contribution from the latter in New Zealand may be high per vehicle relative to overseas locations owing to the elevated sulphur content of New Zealand diesel fuels, with up to 2,500 parts per million allowed, compared to a current maximum of 350 in Europe (Fisher *et al.*, 2002).

### 7.5.2 Seasonal variations in contributions to light extinction

Seasonal variations in the contribution of different components to average light extinction are shown in Figure 7.11. The main seasonal variations in sources of light extinction are an increase in the domestic fire contribution during May and June and a decrease in the secondary particulate contribution during September to November, when average light extinction values are lowest. While the December secondary particulate contribution appears significantly higher than September to October, this may be an anomaly as there are only a small number of samples during this period.



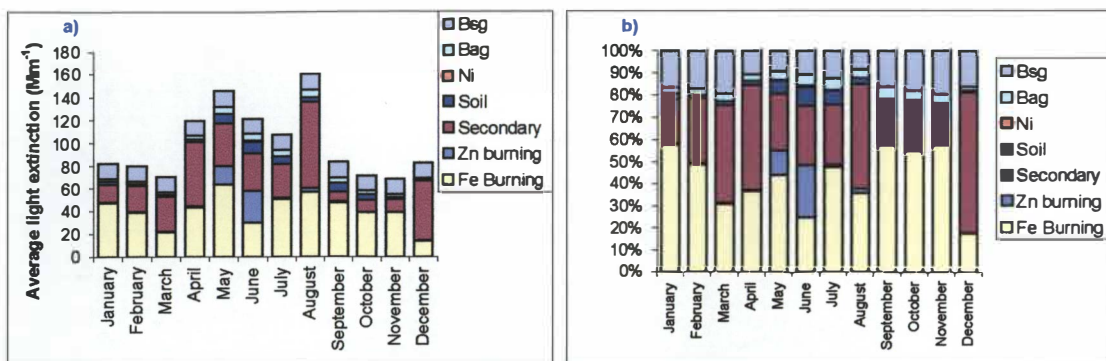


Figure 7.11: Seasonal variations in the contribution of different sources to average light extinction (a) and as a proportion of total light extinction (b).

## 7.6 Comparison to reconstructed light extinction

Figure 7.12 compares measured light extinction ( $B_{ap}$  and  $B_{sp}$  only) to reconstructed light scattering and absorption values based on light scattering and absorption efficiencies derived from laboratory studies. Estimates of reconstructed light extinction were made based on the top 10% of poor visibility days based on equations 7.1 and 7.2 for nitrates and sulphates and for organics, respectively (Middleton & Laulainen, 2000 and Pryor, *et al.*, 1997) and scattering efficiencies of  $2 \text{ m}^2 \text{ g}^{-1}$  for other fine particles (Malm *et al.*, 1996).

$$B_{sp} (\text{sulphates and nitrates}) = 3(0.7(1-\%RH/100))[\text{sulphate or nitrate}] \quad \text{Equation 7.1}$$

$$B_{sp} (\text{organic carbon}) = 4(0.5+0.5(0.7/(1-\%RH/100)))[\text{organic carbon}] \quad \text{Equation 7.2}$$

The coefficient of determination ( $r^2$ ) value of 0.4 for the relationship between measured and reconstructed light extinction (Figure 7.12) indicates a reasonable proportion of the variation between the two measures. Possible explanations for this variance include differences in the proportion of soluble organics in the Christchurch aerosol (Equation 7.2 is based on the assumption of 50% soluble), particulate mass sampling issues and differences between theoretical and actual light scattering or absorption values.

A comparison of the difference between the measured and reconstructed light extinction values ( $B_{ap}$  and  $B_{sp}$  only) and the estimated scattering or absorption by different components indicates a reasonable relationship for nitrate and sulphate scattering (Figure 7.13) with poorer relationships observed for other components ( $r^2 < 0.2$ ). Figure 7.13 suggests that Equation 7.1 overestimates light scattering when nitrate and sulphate concentrations are high and underestimates scattering at lower nitrate and sulphate concentrations. The intercept of the y-axis at  $B_{sp}$  (estimated) at around  $130 \text{ Mm}^{-1}$  shows the point at which Equation 7.1 appears to overestimate  $B_{sp}$ . This may relate to the



composition of the sulphate, for example a greater proportion of sulphate or nitrate may be in the more efficient light scattering  $(\text{NH}_4)_2\text{SO}_4$  and  $\text{NH}_4\text{NO}_3$  forms at lower concentrations. Other explanations include the chemistry of the particles. For example if the particles were internally mixed, resulting in more effective scattering, at lower concentrations but externally mixed with other species, resulting in less scattering at higher concentrations.

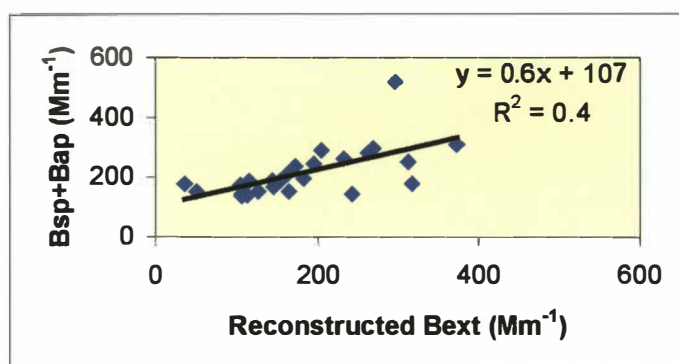


Figure 7.12: Relationship between reconstructed and measured light extinction ( $B_{ap}$  and  $B_{sp}$  only) averaged for the hours 06:00 to 13:00 for the top 10% of poor visibility days.

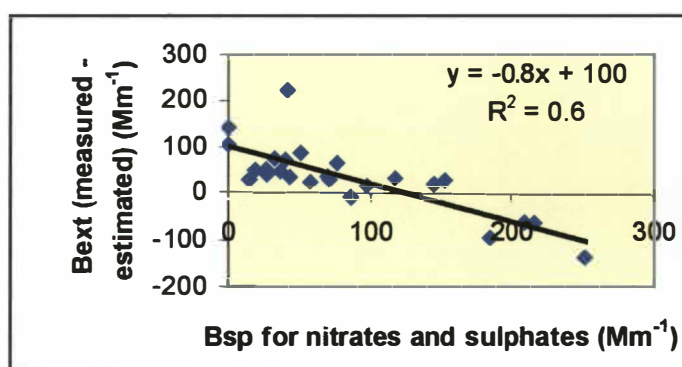


Figure 7.13: Relationship of the difference between measured and reconstructed light extinction and light scattering estimates for nitrates and sulphates.

## 7.7 Summary

The contribution of different sources of particulate to light extinction were assessed using a combination of techniques. Multiple regression analysis of the PCA factor scores was used to determine the relative significance of each particulate source to light scattering. Concentrations of secondary particles were found to be the most significant factor per unit mass, followed by motor vehicles. Light absorption was assessed based on the elemental carbon concentration associated with each burning source. While both sources had similar proportions of elemental carbon (~45%), motor vehicle enissions were most dominant in light absorption because of their greater abundance.

Overall, the main contributors to light extinction are secondary particles and motor vehicles. Seasonal variations in the relative contributions of different sources are minimal with an increase in the domestic fire contribution during the winter months. This is not unexpected, as emissions from this source can be expected to increase during the colder winter months.

These data provide an overview of the contribution of different sources to light extinction for days of poor visibility and by season. To provide a more detailed look at some specific haze episodes, Chapter 8 compares the contribution of different sources, light extinction data, meteorological data and scene images on a selection of poor visibility days.

## Chapter 8 Case Studies

Chapters 6 and 7 showed the contribution of different sources to days when the particulate mass and light extinction were greatest. While these Chapters provide a general understanding of the impact of factors contributing to these visibility events, the variability in sources and meteorological conditions surrounding these events prevent detailed understanding of the relationships between factors impacting on poor visibility in Christchurch. In this Chapter, the relationship between different factors contributing to poor visibility on a selection of these days is examined.

The days selected during the wintertime were the 18 May 2000 and the 20 June 2000 and in the summer the 22 and 28 February. The 18 May was selected because of the clear illustration of the erosion of the inversion layer and the subsequent mixing of visibility reducing pollutants in the images for this day. The 20 June was selected as a case study day because the studies maximum hourly light extinction value of around  $1000 \text{ Mm}^{-1}$  was measured at 10:00 on 20 June. Similarly, summer case study days were selected based on the daytime light extinction values.

### 8.1 Winter Haze

#### 8.1.1 18 May 2000

Elevated light extinction data for the 18 May and photographic images showing changes in the layering of haze make the 18 May an interesting haze episode to study. The temporal variations in light extinction and  $\text{PM}_{2.5}$  concentrations illustrated in Figure 8.1 are typical of a Christchurch winter haze episode with concentrations of particles increasing in the early morning, peaking around 10:00 and decreasing by midday. An illustration of the hourly images of the haze on the 18 May is shown in Figure 8.2.

These variations are governed by meteorological conditions, with wind speed and the nocturnal surface inversions being particularly dominant factors. The timing of the pollution peak and subsequent dispersion is consistent with the impact of solar heating, which causes an increase in sensible heat at the surface resulting in vertical mixing and the growth of the mixed layer (Spronken Smith, 2001). Figure 8.1c shows a decrease in wind speed from around  $2.3 \text{ m s}^{-1}$  at 08:00 to a low of  $0.7 \text{ m s}^{-1}$  at 10:00, coinciding with the highest daytime  $\text{PM}_{2.5}$  concentrations and poorest visibility (Figures 8.1a and 8.1d). Concentrations of  $\text{NO}_2$  however, were highest at 11:00 despite an increase in wind speed to  $1.3 \text{ m s}^{-1}$ . This may reflect chemistry as opposed to the physical

properties of the atmosphere as the formation of NO<sub>2</sub> from NO in the atmosphere may result in variances in maximum concentrations of the former.

A decrease in relative humidity was observed from around 89% at 07:00 to 75% at 10:00, although this primarily reflects an increase in temperature from 6.5 degrees on the roof of the Polytechnic at 07:00 to 11 degrees at 10:00 rather than any changes in vapour pressure. As indicated previously, the presence of moisture in the atmosphere influences visibility in a number of ways. Firstly, when the relative humidity is very high moisture in the air can create fogs and mists, which reduce visibility. Moisture in the air is also absorbed by particles such as nitrates, sulphates and some forms of organic carbon, increasing the particle mass to a size that most effectively scatters light. Water also plays a role in the formation of sulphates, as SO<sub>2</sub> readily dissolves in aerosol droplets and is oxidised more rapidly in solution to produce more aerosol sulphate (Sloane & White, 1986).

The concentration of sulphate measured on the 18 May (averaged for filter period of 06:00 to 13:00) was not especially elevated at around 3.8 µgm<sup>-3</sup>, compared to a maximum concentration of 73.8 µgm<sup>-3</sup> and average of 3.5 µgm<sup>-3</sup> across the whole study period. Nitrate concentrations were low at less than 1 µgm<sup>-3</sup>. Elemental and organic carbon comprised the majority of the particulate on the 18 May 2000 with about equal contributions of each. Because the secondary particle concentrations are low, the contribution of light absorption on the 18 May was higher than for other days of elevated light extinction. The light scattering component contributes only 60% of the light extinction and is likely to occur primarily as a result of light scattering by organic carbon and a small component of light scattering by sulphates under high humidity conditions.

Figure 8.1c shows the wind direction was north to north-east from midnight until 10:00, shifting to a south to south-west flow around 11:00. The wind direction during the daytime and evening of the 17 May 2000 were also easterly (seaward direction) indicating that concentrations measured during the daytime haze episode were most likely to have occurred as a result of local emissions occurring at the time of the event.

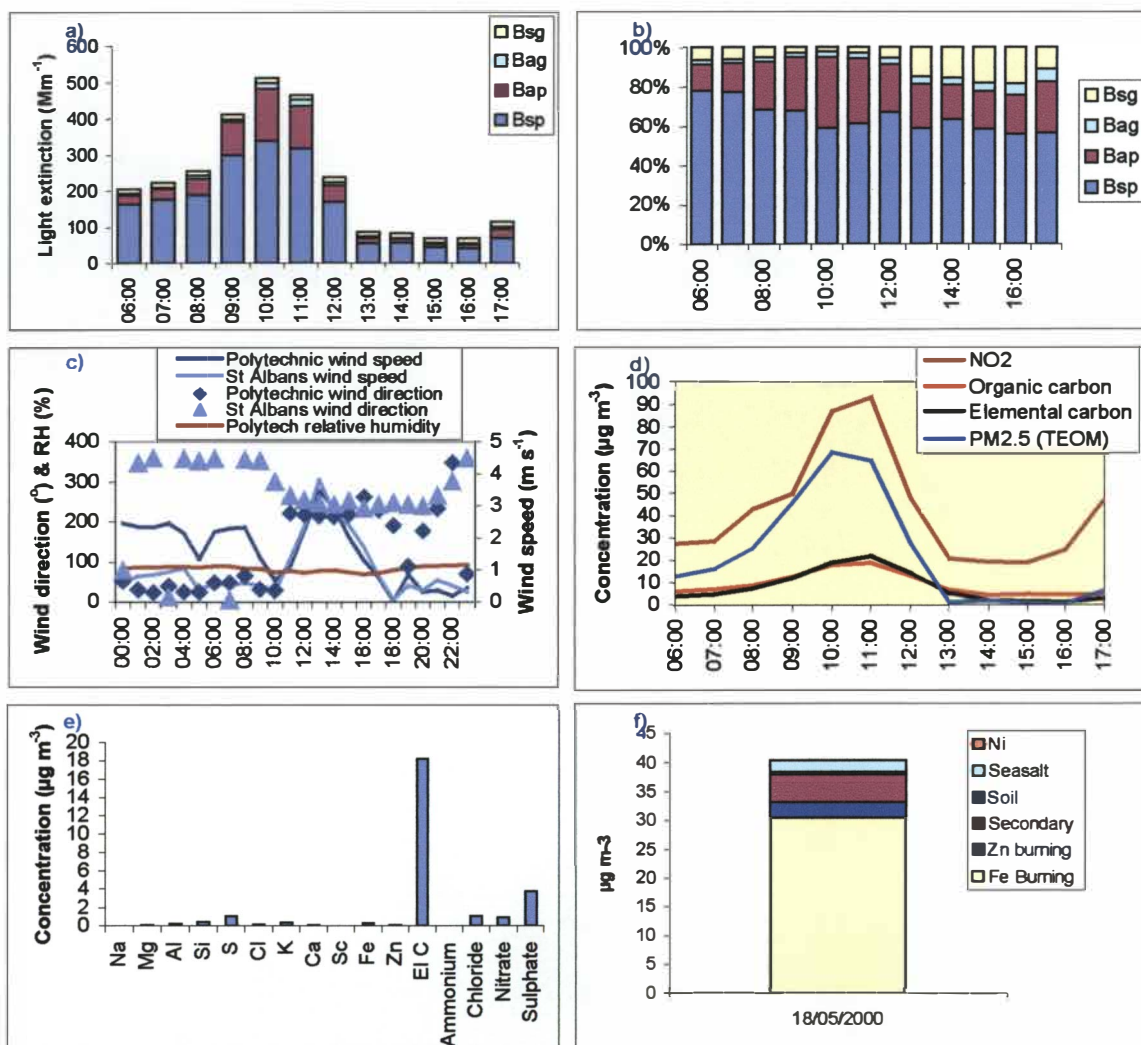


Figure 8.1: Temporal variations in light extinction (a, b and c), concentrations of contaminants (d) and elements (e) and filter compositions (f) for 18 May 2000.

Light scattering by particles is the greatest contributor to light extinction on the 18 May 2000 and is responsible for around 70% of the light extinction. Light absorption by particles is the second greatest contributor. Prior to the haze episode, light absorption accounted for around 10% of the extinction budget. However, this increased to around 33% at 10:00 when the visibility was most degraded. The dominant contribution of elemental carbon to particulate mass on the 18 May is illustrated in Figure 8.1f.





Figure 8.2: Images of Christchurch haze from 08:00 to 13:00 on the 18 May 2000.

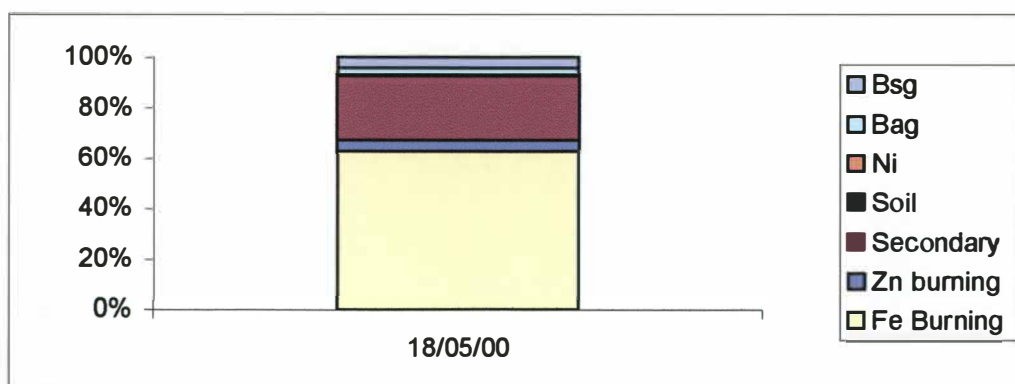


Figure 8.3: Contribution of different components to light extinction on the 18 May 2000.

Figure 8.3 shows the relative contribution of different factors, including sources of  $PM_{2.5}$  to light extinction on the 18 May. As expected, the contribution from secondary particles has increased compared to the mass contribution illustrated in Figure 8.1. This is because of the disproportionate effect of secondary particulate mass on light scattering as indicated by the multiple regression analysis detailed in Chapter 7.

An electron microscope image of the particles collected on the filter on the 18 May (Figure 8.4) shows the most dominant form of particulate is the odd shaped carbon chain type particle which is consistent with the mass dominance of the combustion source. The more rounded and oval shaped particles may reflect the secondary particulate contribution or some other source of spherical particles, such as pollens and spores. The dominant string-like patterns and clusters of lines are the teflon filter upon which the particles were collected.

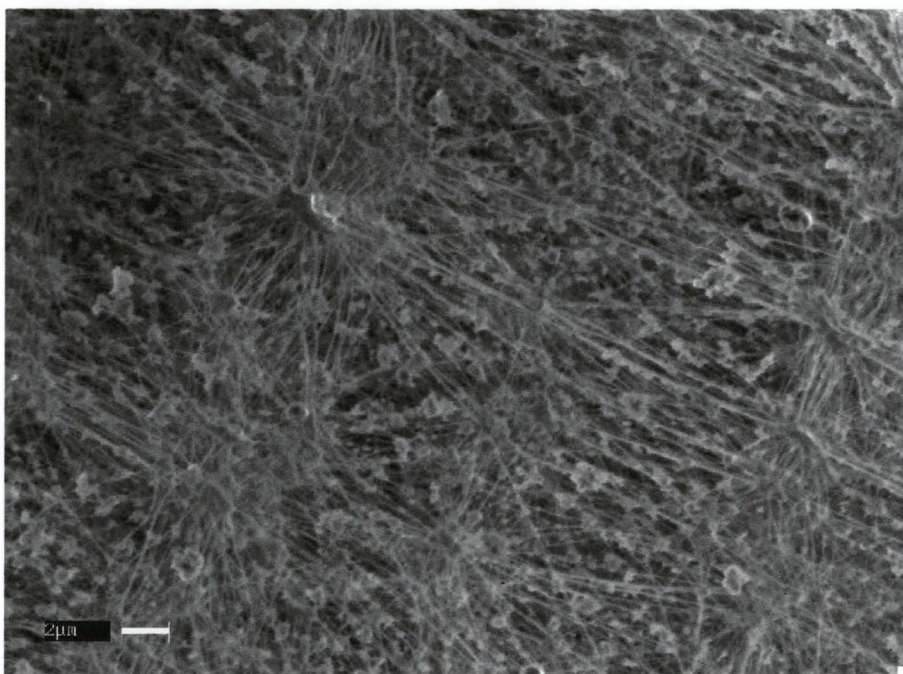


Figure 8.4: Electron microscope image of material collected on a filter on the 18 May 2000.



### 8.1.2 20 June 2000

Throughout the study period, the greatest reduction in light extinction (hourly average) was measured on the 20 June 2000 for the hour ending 10:00. The value of around 1000  $\text{Mm}^{-1}$  measured at this time was twice the highest value measured in the previous example for the 18 May 2000. Temporal variations in optical characteristics of the atmosphere and concentrations of contaminants at the monitoring site on 20 June 2000 are shown in Figure 8.5. An illustration of the images collected each hour during the pollution episode is shown in Figure 8.6.

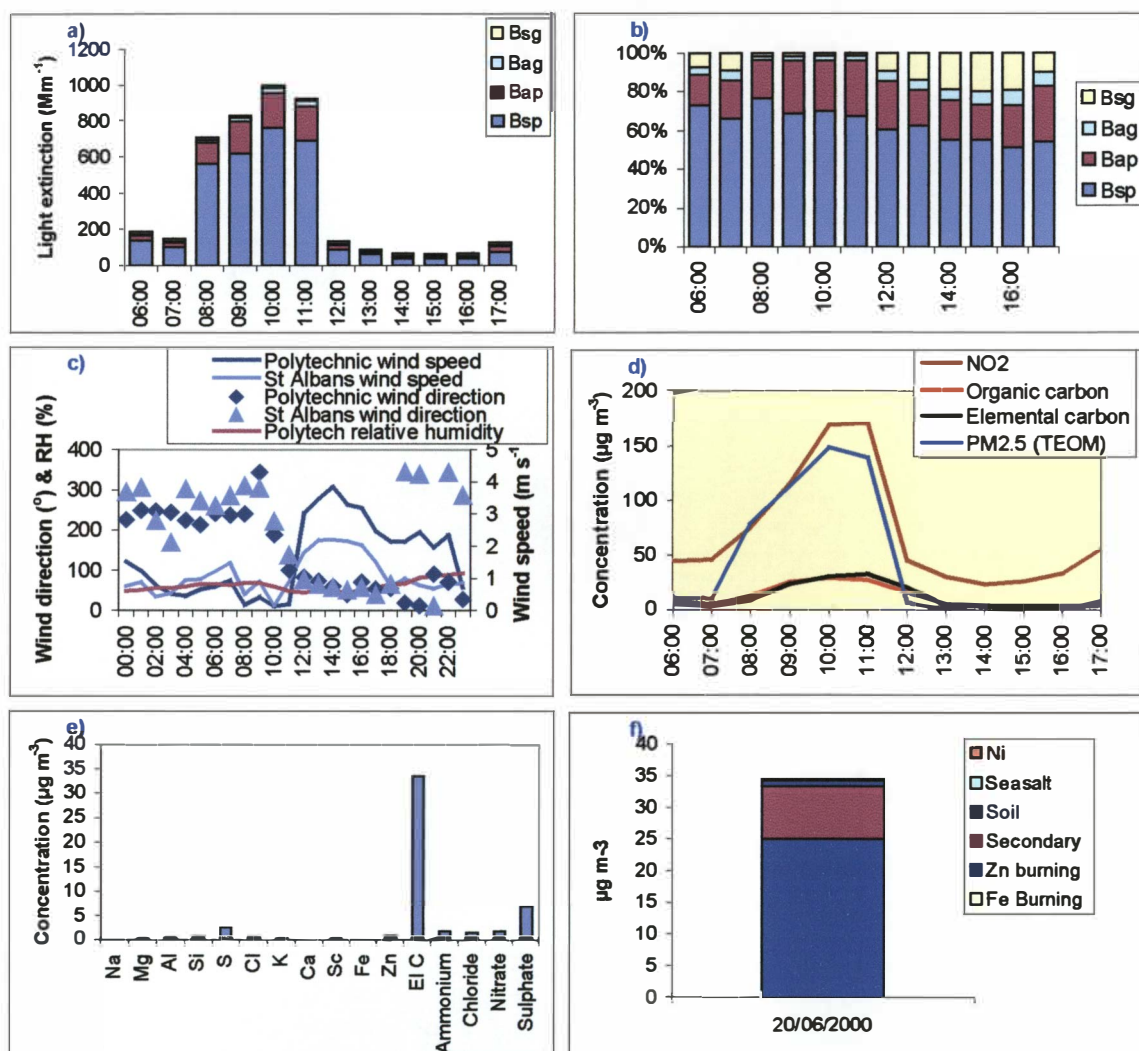


Figure 8.5: Temporal variations in light extinction (a, b and c), concentrations of contaminants (d) and elements (e) and filter compositions (f) for 20 June 2000.

Figure 8.5a shows a sharp increase in light extinction from less than 200  $\text{Mm}^{-1}$  at 07:00 to around 700  $\text{Mm}^{-1}$  at 8am. Concentrations of PM<sub>2.5</sub> (Figure 8.5d) show a similar pattern, although increases in NO<sub>2</sub> and organic and elemental carbon at this time are less prominent. The increase in light

extinction and  $\text{PM}_{2.5}$  concentrations coincides with a decrease in wind speed from around  $0.9 \text{ m s}^{-1}$  at 7am to  $0.2 \text{ m s}^{-1}$  at 08:00.

Unlike the 18 May 2000, the wind direction on the 20 June 2000 was predominantly westerly. The previous evening wind directions were also examined, as a re-circulation effect of evening emissions was one possible explanation for the elevated domestic heating contribution (Zn burning). However, the wind direction was consistently westerly from around 15:00 on the 19 June 2000. Another contrast to the 18 May 2000 was the low relative humidity, which reached a maximum of 69% at 08:00 and was around 60% when the maximum light extinction value was recorded at 10:00. The rooftop temperatures were also low at these times, around  $5^{\circ}\text{C}$  at 08:00 and  $7^{\circ}\text{C}$  at 10:00, indicating relatively low levels of moisture levels in the air.

Despite the lower relative humidity and vapour pressure, the concentration of sulphate on the 20 June 2000 was almost double ( $6.7 \mu\text{gm}^{-3}$ ) that measured on the 18 May 2000 ( $3.7 \mu\text{gm}^{-3}$  for relative humidity ranging from 75% to 89% and similar temperatures). Concentrations of  $\text{PM}_{2.5}$ , and elemental and organic carbon were also higher on the 20 June with a peak of around  $33 \mu\text{gm}^{-3}$  for elemental carbon compared to around  $22 \mu\text{gm}^{-3}$  on the 18 May 2000. The main reason for these differences is likely to be the consistently low wind speed on the 20 June 2000, which remained less than  $0.4 \text{ m s}^{-1}$  for the hours 08:00 to 11:00 inclusive. Differences in source contributions could also account for these variations.

Figure 8.5f suggests that domestic burning may account for the majority of the  $\text{PM}_{2.5}$  mass on the 20 June 2000. As no Fe was present on the filter, none of particulate has been apportioned to the motor vehicle (factor four) burning profile. In reality, it is likely that there is some motor vehicle contribution on this day and there may have been a measurement problem.

Light scattering by particles accounts for the majority of the light extinction throughout the pollution episode. An increase in the proportion of extinction from light absorption by particles is also observed, but is less than observed for the previous example of 18 May 2000. A greater contribution from secondary particulate to  $\text{PM}_{2.5}$  mass is observed relative to 18 May 2000. This may account for the greater contribution to light scattering, as in the presence of moisture, nitrates and sulphates increase to a size that is most effective in scattering light. However, the humidity range of 50-70% throughout the episode is likely to have had less impact on sulphate and nitrate scattering than in the previous example when the humidity was around 90%.

Figure 8.7 shows secondary particles are the most dominant source of light extinction on the 20 June, contributing over 50%, despite a much smaller contribution to particulate mass (Figure 8.5).

It is possible that this is an overestimate of the contribution as the regression analysis used to derive the contributions to light extinction do not account for day-to-day variations in relative humidity. The average humidity for the whole monitoring period was around 70%, which is slightly higher than the average humidity of 60% for the period 06:00 to 13:00 on the 20 June 2000.

A comparison of the 10:00 photographs for the 18 May and 20 June suggest a thicker, potentially browner, haze on the 20 June. Both light extinction data and concentrations of  $PM_{2.5}$  (measured by the TEOM) were twice as high on the latter occasion. The brown characteristic of the pollution on the 20 June is likely to reflect the additional particulate loading, as well as large variations in the size fractions of the particles. In addition, the sun angle may contribute to the appearance of this haze. The additional particulate loading is also apparent from the electron microscope image of the filter (Figure 8.8), which is dominated by carbon chain shaped particles rather than the background filter images of Figure 8.4.







Figure 8.6: Images of Christchurch haze from 08:00 to 13:00 on the 20 June 2000.

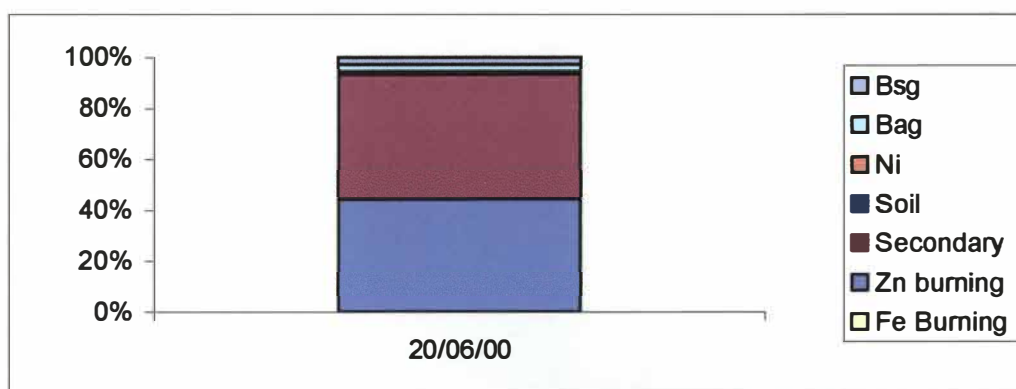


Figure 8.7: Relative contribution of sources to light extinction on the 20 June 2000.

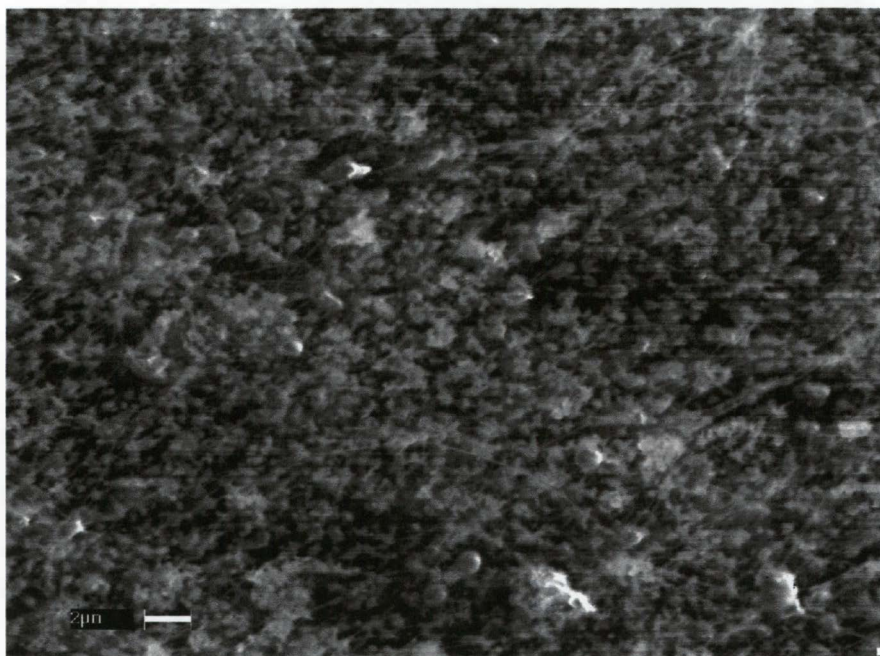


Figure 8.8: Electron microscope image of filter on the 20 June 2000.

## 8.2 Summer Haze

The main distinction between the summer and winter haze episodes is the degree of light extinction which reaches just less than  $1000 \text{ Mm}^{-1}$  during the winter (hourly average), but is typically less than  $300 \text{ Mm}^{-1}$  during the summer months. Notwithstanding this, episodes of summer haze are regularly reported by Christchurch residents, particularly looking from the Port Hills in the direction of the Southern Alps (Figure 1.3). This Section examines the monitoring data on two days when summer time haze was apparent from this vista.

### 8.2.1 22 February 2001

Poor visibility was apparent on the 22 February 2001 from the Port Hills looking in the direction of the Southern Alps and from the images looking from town towards the Port Hills from 08:00 to 10:00 (Figure 8.10). These compare favourably with the light extinction data illustrated in Figure 8.9, which shows elevated light extinction until around 11:00.

Daily variations in light extinction data measured on the 22 February are not as easily explained by variations in the meteorological data and contaminant concentrations as the case studies examined during the winter. In particular, light extinction only increases slightly between 06:00 and 08:00, despite a reduction in wind speed from  $4 \text{ m s}^{-1}$  to  $1 \text{ m s}^{-1}$ . Although the wind speed remains around  $1 \text{ m s}^{-1}$  until after midday, light extinction decreases significantly by 11:00. Similarly concentrations of  $\text{PM}_{2.5}$  show no significant reductions at 11:00 although the peak in concentrations around 15:00 is consistent with an increase in light scattering at that time. One reason for this variance could be that the particulates responsible for the elevated morning pollution episode are largely volatile and are therefore not measured by the TEOM  $\text{PM}_{2.5}$  continuous sampler, owing to the heated sample line ( $40^\circ\text{C}$  in accordance with New Zealand specifications).

Figure 8.9c shows wind direction from midnight to around 08:00 was north-to-north-east, and was followed by a westerly airflow with lower wind speeds. The relative humidity decreased from around 88% at 7am to 34% at midday, although corresponding temperature increases from  $17^\circ\text{C}$  to  $27^\circ\text{C}$  account for a large proportion of the reduction.

Figure 8.9a shows light extinction is dominated by light scattering. The reduction in light scattering around 11:00 corresponds with a decrease in relative humidity, but no other significant variations in concentrations of nitrogen dioxide or particulate. These data, combined with the high levels of sulphate and nitrate found on the filter, suggest that the poor visibility during the period 08:00 to

10:00 is associated with light scattering by sulphate and, to a lesser extent nitrate, which are both exacerbated by the elevated humidity. The decrease in RH at 11am occurs as a result of an increase in temperature. At 11am, light extinction drops to less than 50  $\text{Mm}^{-1}$  and light absorption becomes the main contributor to light extinction.

Figure 8.11 shows that while secondary particles do play a significant role in light extinction on the 22 February, the contribution from the Fe burning source is also important. No electron microscope images were taken for the summer months.

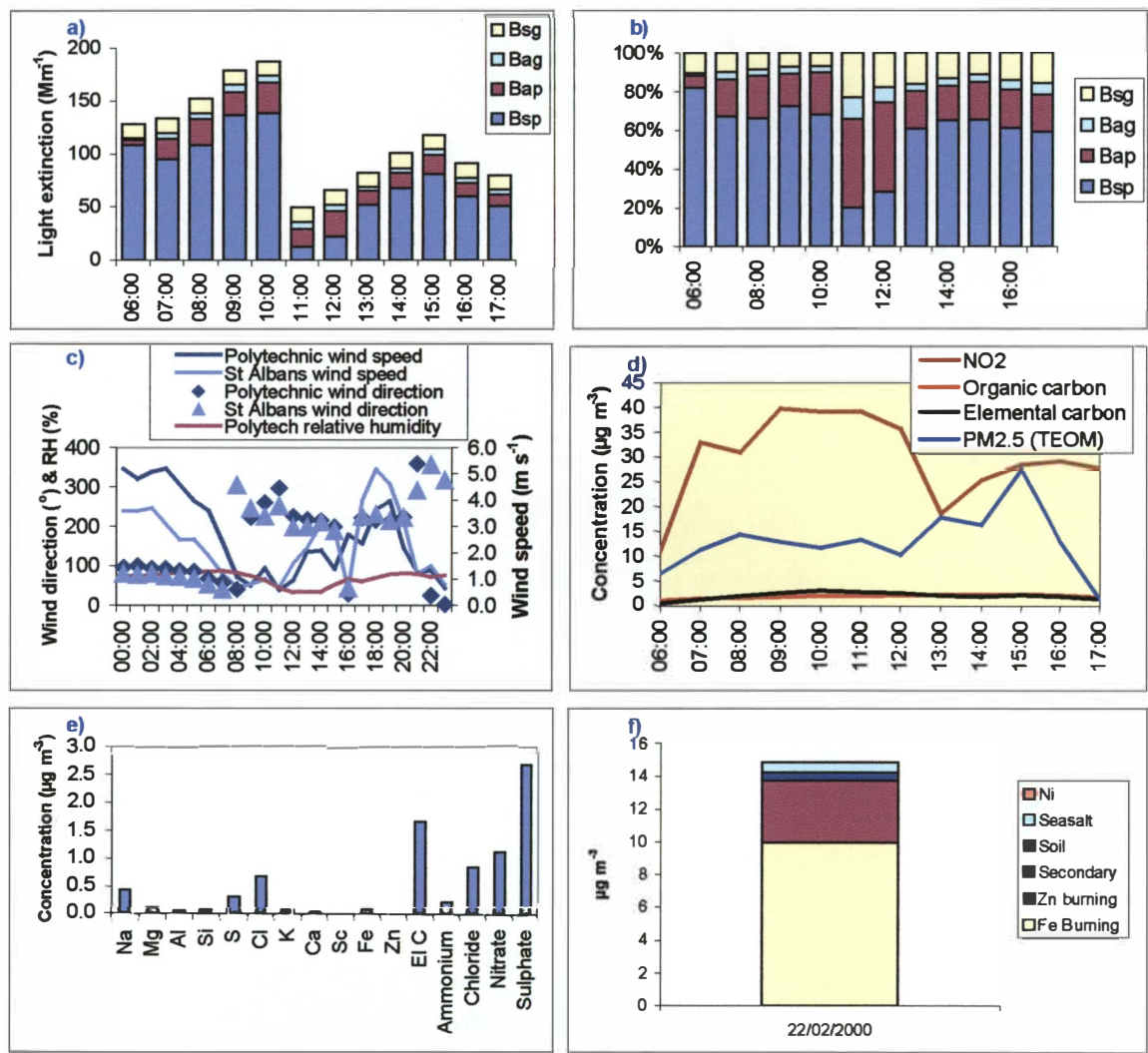


Figure 8.9: Temporal variations in light extinction (a, b and c), concentrations of contaminants (d) and elements (e) and filter compositions (f) for 22 February 2001.





Figure 8.10: Images of Christchurch haze from 8am to 1pm on the 22 February 2001.



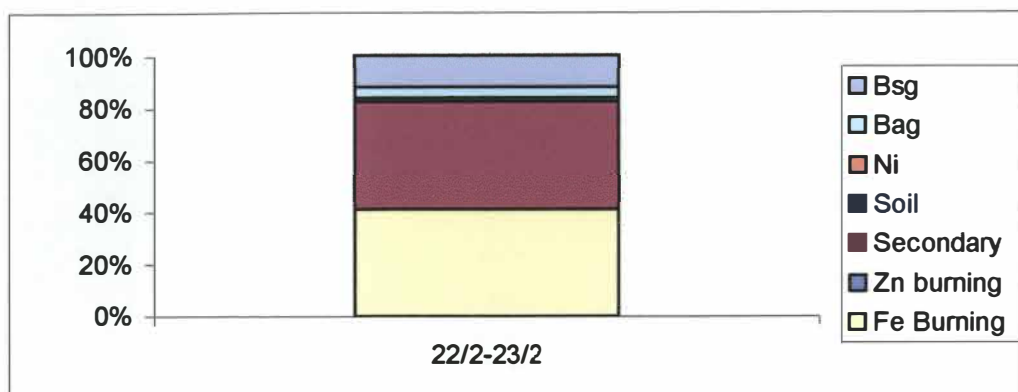


Figure 8.11: Contribution to light extinction on the 22 February 2001.

### 8.2.2 28 February 2001

The haze episode of the 28 February 2001 differs to the previous example on the 22 February in both the relationship between light extinction values and contaminant concentrations and the timing of the event. Figure 8.12 shows a peak in light extinction,  $\text{PM}_{2.5}$ , elemental carbon and organic carbon and  $\text{NO}_2$  concentrations at 08:00 with concentrations and light extinction decreasing significantly by 11:00.

This peak in concentrations occurs after a period of very low wind speeds (less than  $1 \text{ m s}^{-1}$ ) as emissions. The subsequent decrease in concentrations from 08:00 coincides with an increase in wind speed to  $2 \text{ m s}^{-1}$  by 10:00 and  $3 \text{ m s}^{-1}$  by 11:00. The wind direction during the period of low wind speed is variable at the St Albans site, most likely reflecting the inaccuracy of the sensor at wind speeds of less than  $0.5 \text{ m s}^{-1}$ , and north to north-easterly at the Polytechnic. The wind direction is clearly easterly following the increase in wind speed (Figure 8.12c).

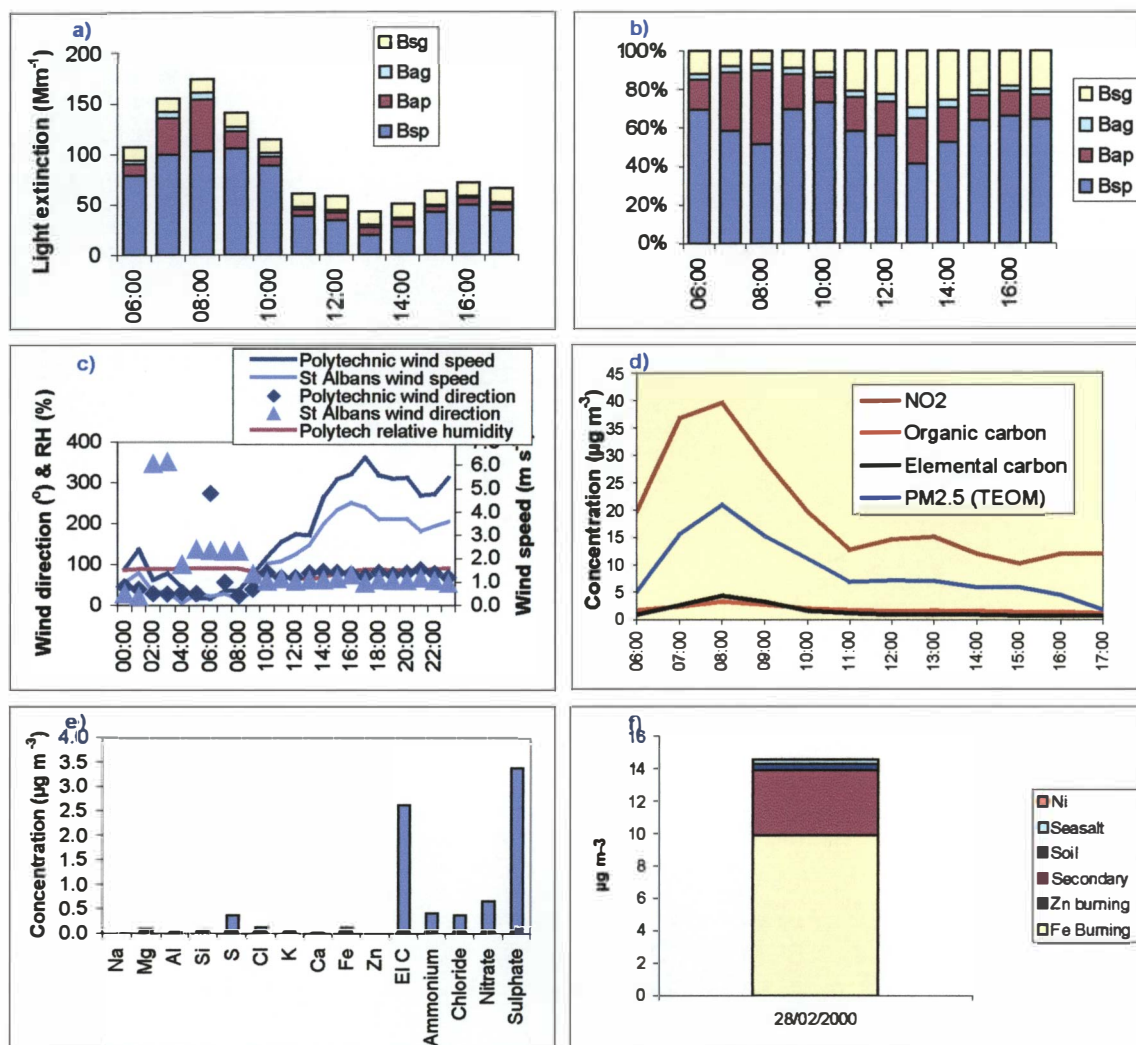


Figure 8.12: Temporal variations in light extinction (a, b and c), concentrations of contaminants (d) and elements (e) and filter compositions (f) for 28 February.

While the light extinction is dominated by light scattering, the peak level at 08:00 is a result of an increase in light absorption by particles, which contribute 44% of the total light extinction at 08:00. As light absorption is dominated by elemental carbon, the additional impact at 08:00 is likely to occur as a result of emissions from motor vehicles. Elevated concentrations of sulphate shown on the filters are also likely to be a significant contributor to the haze episode, particularly given the high relative humidity.



Figure 8.13: Images of Christchurch haze from 8am to 1pm on the 28 February 2001.

The images for the 28 February 2001 (Figure 8.13) show a visible haze at 08:00 which appears less dense but more uniformly distributed at 09:00. By 10:00, the haze appeared similar to a low cloud. Although the hourly average humidity had decreased by 10:00, the relative humidity may have been elevated at the time the photo was taken. By 11:00, the images show no indication of haze or cloud.



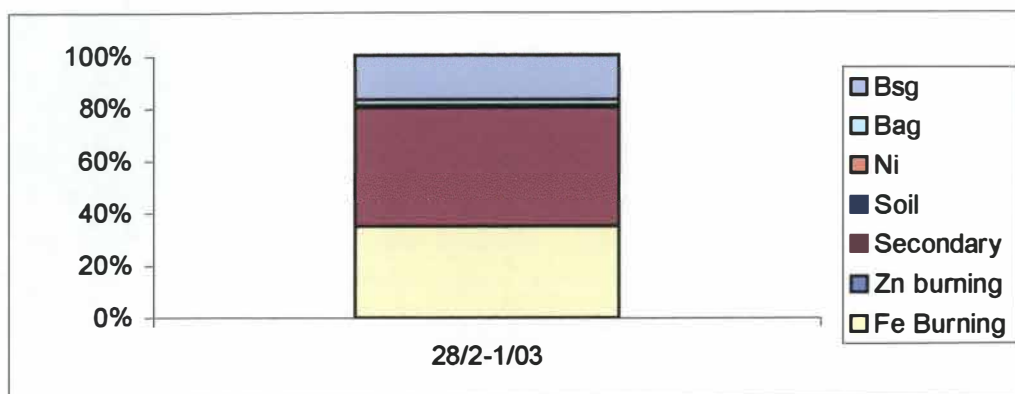


Figure 8.14: Contribution of different components to light extinction on the 28 February 2001.

Figure 8.14 shows the estimated contribution of different sources to total light extinction on the 28 February 2001. As suggested previously based on observations in Figure 8.10, the dominant sources are secondary particulates and the Fe burning source representing motor vehicle emissions. Although the impact of scattering by gases is a constant, this component is more significant during the two summer case studies because the overall extinction values are lower.

### 8.3 Comparison of case study days

The main difference between the summer and winter haze episodes was the degree of light extinction, which reached around  $1000 \text{ Mm}^{-1}$  (hourly average) during the winter months, but was generally less than  $300 \text{ Mm}^{-1}$  during the summer. Similar differences were observed in concentrations of contaminants, in particular total elemental carbon collected on the filter, which was less than  $5 \mu\text{gm}^{-3}$  on the two summer days and greater than  $20 \mu\text{gm}^{-3}$  on the two winter haze days examined. However, concentrations of sulphate varied less with season, with concentrations between  $2.5$  and  $5 \mu\text{gm}^{-3}$  on both the summer and winter days examined. This is consistent with Chapter 6 which indicated little seasonal variation in concentrations of sulphates and nitrates.

One of the interesting points highlighted by the case studies is the variation in causes of visibility degradation even within the same season. For example, light absorption by particles is negligible on the 22 February 2001, but is significant on the 28 February 2001. Similarly, the contribution of secondary particulates to light extinction is minimal on the 18 May 2000, but is the most dominant source on the 20 June 2000. The contribution of domestic burning relative to motor vehicles also varies on these two days, with the very high extinction day on the 20 June dominated by domestic burning and the 18 May dominated by motor vehicle emissions. The method, however, is subject to limitations and may not provide an accurate representation of these sources.

Comparison of the winter and summer haze images adds value to the assessment. They highlight a potential discrepancy in the relationship between visibility perception and light extinction, as the images on the 28 February 2001 portray a level of haze potentially worse than the  $175 \text{ Mm}^{-1}$  measured. The latter conclusion is personal opinion, which could be tested using a survey such as that described in Chapter 9. The survey of visibility perception and light extinction described in Chapter 9 does not include the images from 28 February 2001 as the photos selected for that study were from the period April to July 2000.

## 8.4 Summary

The complexities and variations in visibility degradation in Christchurch were assessed based on a selection of summer and winter haze episodes. On the two winter days, light extinction values varied between around  $500 \text{ Mm}^{-1}$  on the 18 May and  $1000 \text{ Mm}^{-1}$  on the 20 June 2000. Combustion sources were the dominant contributors to particulate mass, with motor vehicles dominating on the 18 May and domestic fires on the 20 June. On the latter occasion, however, secondary particles were the main cause of light extinction, accounting for around 50%.

The two summer case studies were characterised by lower light extinction values of around  $180 \text{ Mm}^{-1}$ . Light scattering by sulphates and nitrates was exacerbated by the presence of moisture in both instances and provided a significant source of visibility degradation. Motor vehicle emissions were also a likely source of visibility degradation on both days, accounting for around 30-40% of the total light extinction. On the 28 February 2001, a large component of the motor vehicle contribution was associated with light absorption, as a result of concentrations of elemental carbon.

In most cases temporal variations in light extinction were closely related to  $\text{PM}_{2.5}$  concentrations. The main exception was the 22 February, although this variation may be related to the  $\text{PM}_{2.5}$  sampling methodology. The influence of wind speed on light extinction was apparent, with pollution dissipating rapidly with increases in wind speed.

The case study data highlighted the complexities and potential variations in sources of visibility degradation in Christchurch, as well as providing some insight as to potential seasonal variations in extent and causes of haze. The impact of different factors is also examined in the following chapter, which focuses on visibility perception.

## Chapter 9 Visibility perception – fog, smog or haze

The perception of the impact of air pollution on visibility is the fundamental purpose for visibility management. Consequently it is important to be able to translate the scientific measurement of visibility degradation by light extinction to the perceptual aspects of poor visibility. Clearly there are some aspects of the latter that are not accounted for in the measurement of light extinction. In particular, the impacts of illumination, fogs and the acceptability of visibility degradation are not measured.

In Christchurch, the presence of fogs is likely to be a complicating factor in assessing and managing visibility. On many occasions, instances of low fogs have been mistaken for air pollution including the use of a photograph of fog in a local newspaper, supposedly depicting an air pollution episode (Ayrey, pers comm., 2001). In addition, the impact of fogs combined with air pollution can worsen both the actual and perceived visual impact of the latter.

Aspects of visibility perception are studied in this Chapter, through both a survey of responses to a selection of images covering a range of light extinction and humidity values, and by examining the relationships between light extinction and other data and visual images collected using a digital camera.

### 9.1 Visibility perception survey

A visibility perception survey, carried out during 2000, was designed to both provide information on the perceptual aspects of visibility degradation and to assess the applicability of the methodology for the determination of a standard for visibility in Christchurch. The latter assessment will be used in the design of a comprehensive survey, of a more representative sample of the Christchurch population, to be carried out by Environment Canterbury during 2004. The methodology used for this survey is detailed in Chapter 4.

#### 9.1.1 Survey results

The initial survey of a group of 40 respondents was divided evenly into two sub-groups. One sub-group was required to carry out the visibility survey based on photo list one and the other based on photo list two (see Section 4.2.2 for descriptions of photo lists one and two). A summary of the results for each group is presented in Tables 9.1 and 9.2 for lists one and two respectively, and in Figure 9.1.

In photo list one, the average visual air quality ratings (VAQ ratings) for the images representing good visibility were slightly lower and the ratings for poor visibility slightly higher than for list two. However, the differences between the VAQ for the two sets of photos were not statistically significant ( $p < 0.05$ ).

Another indicator of differences between the photo sets and their perception is the acceptability ratings. The acceptability ratings for list two show that the relationship between perceptions of visibility, based on the photos, and the measure of light extinction, are not necessarily related. In particular, list two photos one and six, with light extinction values of  $174 \text{ Mm}^{-1}$  and  $194 \text{ Mm}^{-1}$  respectively, scored 100% acceptability. Photo two in list two shows a contrasting result with a high unacceptability rating despite a relatively low light extinction value. Some disparity also occurs in list one, e.g., photo number four with the second highest extinction rating ( $293 \text{ Mm}^{-1}$ ) was scored as acceptable by 71% and photo number five, with a light extinction value of 125 had the lowest VAQ rating in the initial survey. These inconsistencies are examined in detail in Section 9.2, which considers factors that influence perception.

The “acceptability rating” band illustrated in Tables 9.1 to 9.3 indicates the level of light extinction at which more than 50% of respondents chose the “unacceptable” rating.

Table 9.1: Summary of initial visibility survey results for photo list one, organised in order of increasing light extinction.

List one	Date	Time	Extinction	RH %	Rooftop Temp°C	VAQ	% Acceptable	% Unacceptable
7	15-Apr	17:00	39	62	16.8	4.5	100%	0%
15	25-Apr	15:00	71	61.7	17.1	4.9	73%	27%
1	17-Jun	13:00	85	52.5	15.9	4.5	100%	0%
11	11-Jun	12:00	94	42.9	12.0	4.7	94%	6%
2	27-Apr	17:00	102	70.1	13.7	4.7	94%	6%
14	7-Jul	12:00	110	83.4	10.6	5.2	81%	19%
3	17-Apr	10:00	117	54.8	17.9	4.4	100%	0%
5	4-May	15:00	125	81.6	13.6	3.9	71%	29%
9	9-May	10:00	134	73.8	10.8	5.2	73%	27%
16	11-Jul	11:00	144	79.7	11.5	4.5	88%	12%
8	19-Jun	16:00	157	32.9	16.6	4.4	71%	29%
Acceptability Rating – based on 50% of respondents								
12	5-May	9:00	174	75.8	12.1	4.9	35%	65%
13	2-Jul	14:00	195	85.1	8.6	4.6	24%	76%



10	29-May	10:00	229	87.9	12.4	5.1	35%	65%
4	1-May	7:00	293	59.3	7.4	4.4	71%	29%
6	20-Jun	10:00	997	60.5	7.5	5.0	47%	53%

Table 9.2: Summary of initial visibility survey for photo list two organised in order of increasing light extinction.

List two	Date	Time	Extinction	RH %	Rooftop Temp°C	VAQ	% Acceptable	% Unacceptable
13	15-Apr	16:00	33	62	17.2	5.0	100	0
11	25-Apr	16:00	70	69.7	11.0	4.6	76	24
3	27-Apr	16:00	93	66.4	14.2	4.8	100	0
10	11-Jun	10:00	95	64.2	10.3	5.0	100	0
8	15-Apr	12:00	102	75.9	15.8	4.2	76	24
4	7-Jul	11:00	110	84	10.2	4.8	53	47
2	8-Jul	13:00	118	85.3	11.1	5.1	29	71
14	22-Jun	16:00	125	80.9	10.1	4.4	65	35
7	15-Apr	10:00	134	82.6	14.9	4.9	59	41
16	31-May	9:00	143	53.5	13.6	4.8	82	18
15	22-Jun	10:00	157	91.6	8.5	4.1	53	47
1	15-Jun	10:00	174	58.4	11.6	4.6	100	0
6	4-May	11:00	194	80.6	13.8	4.6	100	0
Acceptability Rating – based on 50% of respondents								
9	20-May	9:00	229	81	8.5	4.4	6	94
5	18-May	12:00	294	74.2	11.3	4.8	53	47
12	26-May	10:00	903	73.5	10.2	4.7	12	88

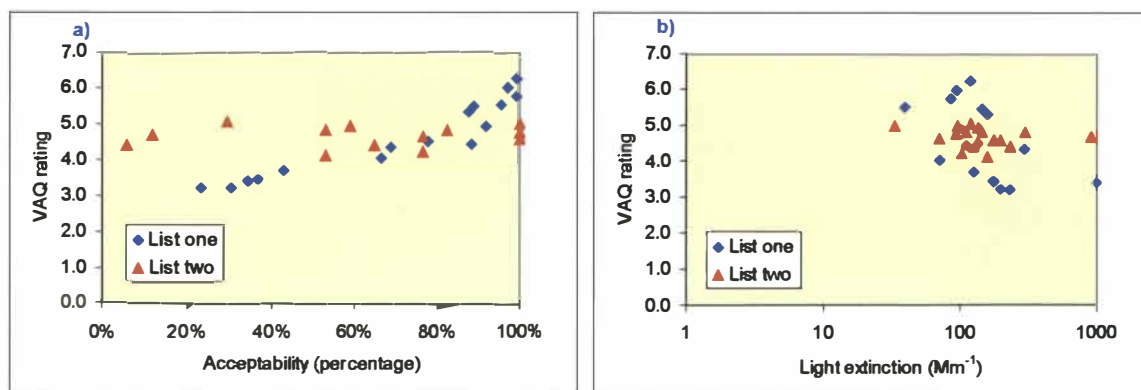


Figure 9.1: Comparison of the VAQ rating to the acceptability of haze (a) and to the corresponding light extinction values (b) for list one and two.

Additional survey work was carried out using the photo list one because of the greater consistency between the perception of images and the light extinction variables (see Figure 9.1). A further 120 respondents completed the survey, giving a total of 140 respondents for photo list one. Table 9.3 shows the results for all respondents. Note however, that these results are specific to the group sampled, which is dominated by staff of an environmental resource management agency and are not representative of the Christchurch public.

Table 9.3: Summary of visibility survey (photo list one) – all respondents.

List one	Date	Time	Extinction	RH %	Rooftop Temp°C	VAQ	% Acceptable	% Unacceptable
7	15-Apr	17:00	39	62	16.8	5.5	95	5
15	25-Apr	15:00	71	61.7	17.1	4.1	66	34
1	17-Jun	13:00	85	52.5	15.9	5.8	99	1
11	11-Jun	12:00	94	42.9	12	6.0	97	3
2	27-Apr	17:00	102	70.1	13.7	4.9	92	8
14	7-Jul	12:00	110	83.4	10.6	4.4	88	12
3	17-Apr	10:00	117	54.8	17.9	6.3	99	1
5	4-May	15:00	125	81.6	13.6	3.7	43	57
9	9-May	10:00	134	73.8	10.8	4.5	78	22
16	11-Jul	11:00	144	79.7	11.5	5.5	89	11
8	19-Jun	16:00	157	32.9	16.6	5.3	88	13
Acceptability Rating – based on 50% of respondents								
12	5-May	9:00	174	75.8	12.1	3.5	37	63
13	2-Jul	14:00	195	85.1	8.6	3.2	23	77
10	29-May	10:00	229	87.9	12.4	3.2	30	70
4	1-May	7:00	293	59.3	7.4	4.4	69	31
6	20-Jun	10:00	997	60.5	7.5	3.4	34	66

### 9.1.2 Development of a visibility standard for Christchurch

Results from the visibility survey suggest that light extinction of greater than 160-170  $\text{Mm}^{-1}$  is unacceptable to the majority of the survey respondents based on the pictures depicted in the survey (photo list one). Analysis of the light extinction data collected for this study indicates that hourly values greater than 160  $\text{Mm}^{-1}$  occurred between the hours of 06:00 to 13:00 on about 133 of the days (27%) of the monitoring period. It is important to note however, that despite the consistency between the two groups surveyed, it cannot be inferred that the light extinction values derived

through this survey are representative of the Christchurch population. There is likely to be bias in both of the samples surveyed.

A similar survey used to determine visibility standards for Denver and Lower Fraser Valley (detailed in Section 2.3.4) indicated acceptable values of  $0.076 \text{ km}^{-1}$  ( $76 \text{ Mm}^{-1}$ ) for Denver and  $0.09 - 0.105 \text{ km}^{-1}$  ( $90-105 \text{ Mm}^{-1}$ ) for the Lower Fraser Valley. In that survey two sets of 25 slides were used and the results combined to give 50 slides. Approximately 100 people judged each slide. A non-random approach to soliciting respondents was employed because of resource constraints.

One of the differences between the outcome of this survey and that conducted in Denver is likely to be the view used in the image, as characteristics of the view are likely to influence the relationship between light extinction, which is measured at a single point, and the acceptability or otherwise of corresponding images. This is because of the influence of factors such as scene characteristics, illumination and distance on the perception of visibility. For example, in the Christchurch survey the distance between the observation point and the background is less than 5 kilometres, minimising the impact of light scattering and absorption compared to what could occur across a longer distance, such as the view from the Port Hills of Christchurch to the Southern Alps.

### **9.1.3 Implications for further studies**

The results of this study suggest that a guideline or standard for visibility in Christchurch could be derived by means of a survey of visibility perception. However, it would appear that the value or standard obtained would be specific to a particular viewing point. For example, the city centre view towards the Port Hills, may not adequately represent longer views such as the Southern Alps from the Port Hills.

The relationship between the perception of visibility degradation from the photograph and the measured light extinction values is influenced by a number of factors. In particular, the presence of moisture in the atmosphere can impact on the rating of air pollution. In a similar study carried out in the United States, high humidity days were excluded from the survey. While this helps reduce inconsistencies in responses, it limits the assessment of visibility perception to exclude episodes where fog and cloud contribute to visibility degradation. In Christchurch, where the presence of sea fogs may often be mistaken for air pollution, information on such responses is desirable and hence high humidity days were included in this study. However, if the scope of further studies was limited to the establishment of a visibility standard, as opposed to the more broad objectives of this thesis, it may be useful to limit the photographs to days where the relative humidity is less than around 75%.

Two sets of photos were included in the initial survey to determine whether differences in the selection of images used would influence the value for visibility that was unacceptable to 50% of the respondents. In photo list two the two images around the 170-200  $\text{Mm}^{-1}$  light extinction levels were both rated acceptable by 100% of the respondents, whereas the 157  $\text{Mm}^{-1}$  photo was rated unacceptable by 53%. In comparison, photo list one generated responses that were more consistent with the corresponding light extinction values and provided a more clear cut point at which visibility was rated “unacceptable”. This observation highlights the benefits of conducting a pilot survey and evaluating responses to different images prior to selecting a final set or sets of images.

An additional variation to the methodology that should be considered is the inclusion of a greater number of images at the higher light extinction range. As detailed in Section 4.2.2, images were selected to evenly cover a range of light extinction values. While this approach may be suitable if the light extinction values were normally distributed, these data are right skewed giving a large difference between the highest and second highest values. Inclusion of a greater range of poor visibility images may allow better identification of “acceptable” visibility.

## **9.2 Factors influencing perception**

Results of the visibility perception study provide additional data on the factors that may influence perception of visibility. In particular, the survey identified a number of occasions when records of visibility perception did not relate well with measurements of light extinction. The extent to which these inconsistencies are caused by issues of visibility perception or are a function of the methodology is examined, as is the impact of other factors such as moisture and illumination in the Christchurch context.

### **9.2.1 Inconsistencies in the visibility study**

Section 9.1 identifies photos one, two and six in list two and photos four and five in list one as having poor relationships between the acceptability and VAQ ratings and the light extinction values. Survey results for these images are summarised in Table 9.4. Inconsistencies in these images are considered in turn and potential explanations explored.



Table 9.4: Survey and light extinction data for images with anomalous survey results.

List one	Date	Time	Extinction	Relative Humidity %	Rooftop temp °C	Average VAQ	% Acceptable	% Unacceptable
4	1-May	7:00	293	59.3		4.4	69	31
5	4-May	15:00	125	81.6		3.7	43	57
List two								
1	15-Jun	10:00	174	58.4		4.6	100	0
6	4-May	11:00	194	80.6		4.6	100	0
2	8-Jul	13:00	118	85.3		5.1	29	71

### List one photos

Photo four is an anomaly because it has a relatively high extinction value (second highest in list one), yet both the VAQ and acceptability rating suggest that visibility is not perceived to be very degraded. Figure 9.2 compares photo four to photo six, which represents the worst and second worst light extinction values in list one with comparable relative humidity values. There is a significant difference in the light extinction values for photos four and six ( $293 \text{ Mm}^{-1}$  and  $997 \text{ Mm}^{-1}$  respectively), which is likely to largely account for the differences in the perception of these images. However, the light extinction in photo four is greater than in photo five (Figure 9.3 - a) and other photos (e.g., photo 14 in Figure 9.3 - b), yet photo four is perceived to be less polluted. An assessment of the relationship between VAQ and relative humidity suggests that the latter impacts on visibility perception (Figure 9.4).

Photo five is an anomaly because it has a mid range extinction value, yet both the VAQ and the acceptability ratings suggest that air quality is perceived to be degraded by pollution. A potential explanation is that moisture in the air, as indicated by the high humidity value (82%), contributes to the perception of poor visibility at this time. However, a similar level of humidity in photo 14 does not have the same impact on visibility perception. Differences in illumination characteristics between these two images are evident with photo 14 showing sunlight penetrating through thick cloud cover. Thus it would appear that the impact of moisture in the atmosphere on perception of air pollution could depend on other factors, such as sun angle and cloud cover.

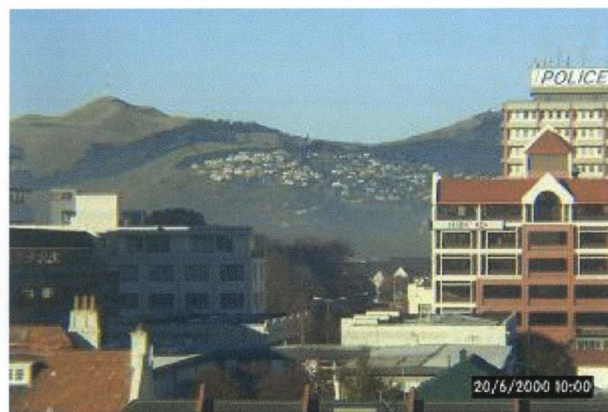


Figure 9.2: Comparison of photo four (left) with light extinction of  $263 \text{ Mm}^{-1}$  to photo six (right) with light extinction of  $1000 \text{ Mm}^{-1}$ .



Figure 9.3: Light extinction in photo 5 (left) is perceived to be greater than in photo 4 (Figure 9.2) and photo 14 (right).

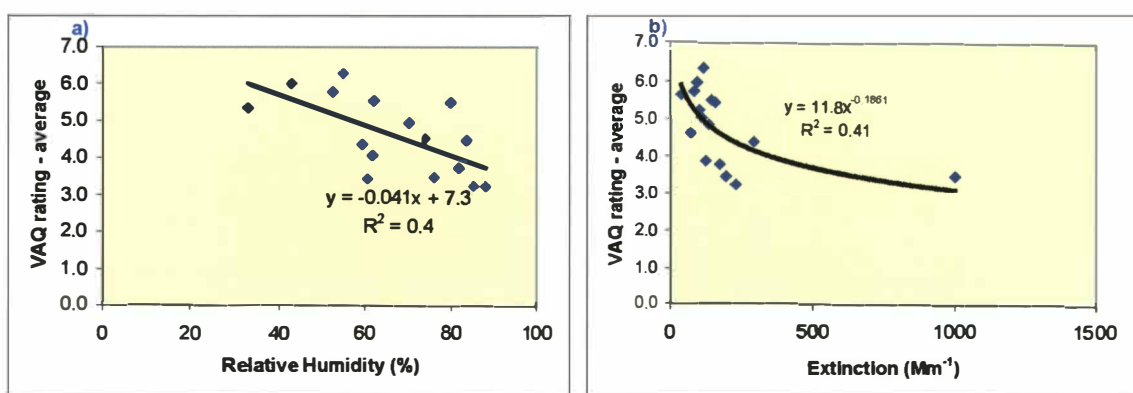


Figure 9.4: Comparison of VAQ rating with relative humidity and light extinction.

### List two photos

Photos one and six are anomalies because they both have mid range light extinction values yet were rated as acceptable by 100% of respondents. Both scored high VAQ ratings indicating that visibility was not perceived to be degraded by air pollution. Figure 9.5 shows that these images



appear relatively clear despite the elevated extinction levels. Relative humidity was high (80%) during the photo six episode, but was low (60%) during the photo one episode.

One possible explanation is the timing of the photographs relative to the collection of light extinction data. The light extinction data are based on an hourly average for the hour prior to the time the photo is taken. The photographs for one hour earlier are shown in Figure 9.5 (bottom row). In both instances, visibility degradation appears greater in the preceding photo. Thus the hourly average light extinction data may be biased by conditions in the early part of the hour and therefore the light extinction values used may not be representative of the conditions at the time the photo was taken. Methodological variations that could minimise this bias could include using a different averaging period, e.g., 10-minute average, or taking the photo during the midpoint of the averaging time.

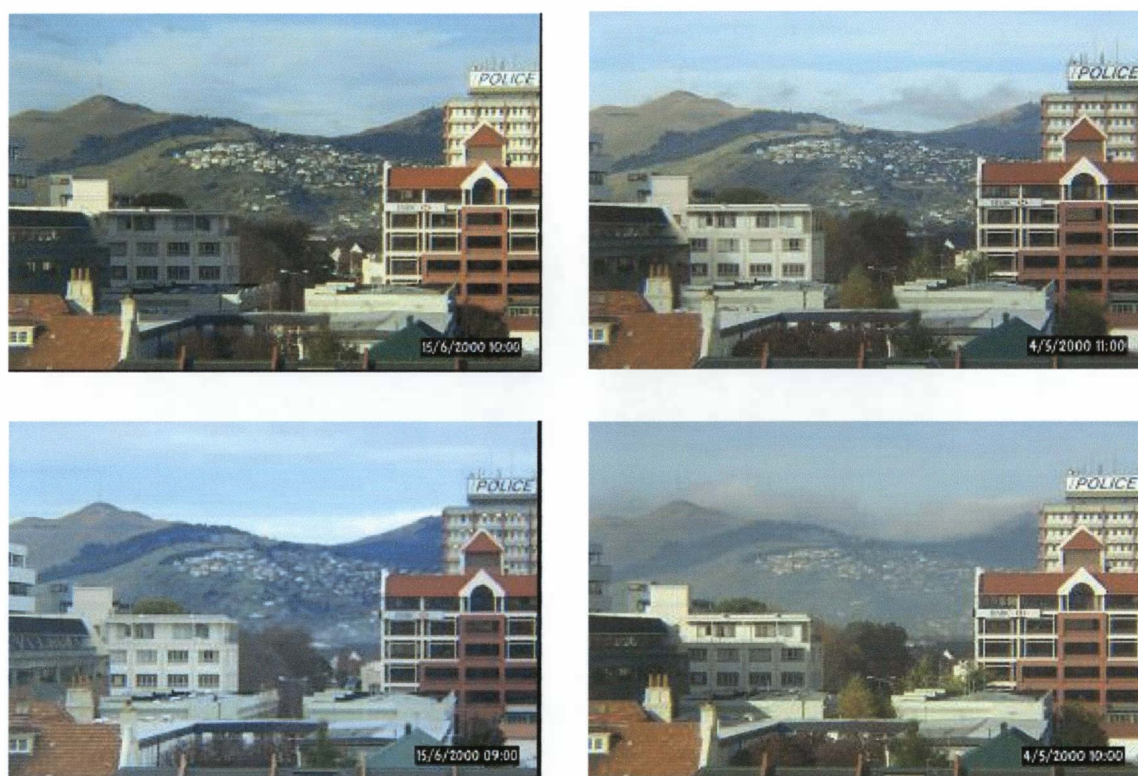


Figure 9.5: Comparison of photos one (top row left) and six (top row right) to the photo taken the preceding hour.

The other photo that appeared anomalous in list two was photo two. In contrast to photos one and six, photo two has a low light extinction rating but was rated as unacceptable by 71% of respondents. Interestingly, however, the VAQ rating for this photo is 5.1, indicating that the visibility was not perceived to be degraded by pollution. One possible explanation is that the respondents are correctly recognising that the reduced visibility depicted in the photo results from humidity (85%), but that they still indicate that the degree of reduced visibility is unacceptable.

Figure 9.6 illustrates the visibility degradation in photo two relative to photo twelve, which depicts the worst pollution episode of the list two photos.



Figure 9.6: Comparison of photo two (left) with a low light extinction value to photo 12 (right) with the worst light extinction.

### 9.2.2 Moisture

The impact of moisture on the perception of air quality is demonstrated in Section 9.2.1 by the high VAQ rating for photo five (list one). That photograph had a low light extinction value but a high relative humidity rating. In another photo (list two, photo two) the impact of moisture on reduced visibility may have been recognised by respondents but was still classed as “unacceptable”. The impact of moisture on perception was examined by comparing photographic records of events with light extinction and relative humidity data.



Figure 9.7: Impact of combination of moisture and air pollution on visibility on 4 May 2000.

Figure 9.7 shows poor visibility on the 4 May 2000 at both 09:00 and 10:00, with the 9:00 value representing the lowest light extinction value for which over 50% of respondents responded as “unacceptable”. Corresponding light extinction and relative humidity data presented in Table 9.5



indicates a higher light extinction value at 10:00 (10-minute average) than at 09:00, despite visibility at 9am appearing more degraded (Figure 9.7). Differences in obscuration may be associated with a change in relative humidity, which decreases from 89% at 09:00 to 82% at 10:00. This example shows the impact of the combination of both air pollution and vapour pressure on visibility. The significance of relative humidity is illustrated by improvements in visibility from 09:00 to 10:00, despite increases in concentrations of contaminants that might degrade visibility.

Table 9.5: Comparison of visibility data at 09:00 and 10:00 on the 4 May 2000.

Date	Time	Relative Humidity	Rooftop temp	PM <sub>2.5</sub>	Extinction	% B <sub>sp</sub>	% B <sub>sg</sub>	% B <sub>ap</sub>	% B <sub>ag</sub>
4-May	09:00	89	9.0	32	345	67%	4%	22%	8%
4-May	10:00	82	10.8	39	389	63%	4%	26%	8%

The colour of haze is one factor that is likely to influence the perception and acceptability of visibility degradation. In particular, a brown haze is less likely to be perceived as a fog and is more likely to be considered “unacceptable”. In the previous example, reduced visibility was a combination of air pollution impacts and fog. The appearance of the haze was a greyish white. In contrast, the high pollution images used in the visibility survey both had a brownish appearance, and comparatively low relative humidity values. Variations in the occurrence of brown haze as a function of light extinction values, relative humidity and sources (where available) was examined by comparing these data to the corresponding photographs.

Table 9.6 provides the light extinction, relative humidity and PM<sub>2.5</sub> data for the photographs illustrated in Figure 9.8, which were selected based on highest values for light extinction. The two highest light extinction values were measured at 10:00 on the 20 June and the 26 May. A comparison of images for these days (Figure 9.8) shows a brown haze in both instances, as well as a layering effect trapping the haze near to the earth’s surface on the 20 June. The PCA receptor modelling and light extinction analysis suggests that the main contributors to light extinction on the 20 June were secondary particles and wood burning. No data were available to determine the relative contributions of different sources on the 26 May.

A comparison of images from 09:00 on the 24 July and 10:00 on the 17 May shows the presence of brown haze on both occasions. Despite a slightly higher light extinction value on the 24 July, houses on the Port Hills are harder to distinguish on the 17 May. This appears to occur as result of a greater illumination of hills on the 24 July. The main contributors to light extinction on the 17

May appear to be motor vehicles (59%) and secondary particles (22%). No data were available to determine the relative contributions of different sources on the 24 July.

Similar light extinction values were measured on 1 and 9 August, the next highest light extinction days. However, visibility on the 1 August appears significantly more degraded than on the 8 August. One factor that is likely to be contributing to this is the amount of moisture in the air on the 1 August as illustrated by a relative humidity of 85%. Differences in illumination are also apparent with distinct differences in the brightness of the white parts of the buildings in the foreground on the 1 August. The haze on the 1 August also appears much whiter than on the other high extinction days. This may be a combination of the impact of moisture as well as the differences in illumination. Although motor vehicles and secondary particles are the dominant contributors to light extinction on both days, the secondary particulate contribution is greater on the 1 August.

Table 9.6: Summary data for high light extinction days.

Date	Time	PM <sub>2.5</sub>	Extinction	Relative Humidity	Temp °C	B <sub>sp</sub>	B <sub>sg</sub>	B <sub>ap</sub>	B <sub>ag</sub>
20 June	10:00	148	997	60	7.5	67%	1%	24%	8%
26 May	10:00	137	903	73	10.2	59%	1%	31%	8%
24 July	9:00	112	710	82	6.5	67%	1%	29%	2%
17 May	10:00	99	601	64	9.2	60%	2%	29%	9%
1 August	9:00	77	583	85	4.7	64%	2%	32%	2%
9 August	10:00	75	558	74	9.0	72%	2%	24%	2%





Figure 9.8: Haze photographs on days when visibility was most degraded.

### 9.3 Summary

A visibility survey was carried out to assess both the factors influencing visibility perception and to develop a methodology for determining a standard for visibility in Christchurch. The methodology used for the survey was sufficient to identify a level of visibility that was deemed acceptable to a large proportion of the respondents. While variations in the correlation between responses and light extinction did occur, reasonably consistent results were obtained.

An assessment of factors contributing to visibility degradation found that the impact of moisture is potentially greater than the impact of air pollution and that it can be very difficult to differentiate between the impact of moisture and that of pollution. The brown aspect of haze was found to be present only when light extinction values were very high but that other factors such as illumination and particle phase moisture are also likely to have some impact.



## Chapter 10 Discussion and conclusion

### 10.1 Major research findings

The purpose of this study was to test the hypothesis that “the physical and chemical factors contributing to reduced daytime visibility in Christchurch are complex, vary with season and have significant impact on perceived air quality” and to answer the following key questions:

- What causes reduced visibility and brown haze in Christchurch? That is, to what extent do different contaminants and physical properties contribute to light extinction in Christchurch?
- What variations exist, if any, in the composition of summer versus winter haze in Christchurch?
- What are the implications of this knowledge to the management of reduced visibility in Christchurch?
- What is the relationship between perceived air quality and light extinction in Christchurch?

The study identifies a number of physical and chemical factors that contribute to visibility degradation in Christchurch. The main factors are meteorological conditions and light scattering and absorption by particles. The complexity of these factors and their contribution to visibility degradation are highlighted by a number of study outputs including:

- The variability of different sources of particulate in causing visibility degradation on different days.
- The composition dependent relationship between the mass of particles and light scattering.
- Possible seasonal variations in the relationship between light extinction and visibility perception.
- Variations in the relationship between particle sources, meteorology and the impact on visibility degradation.

Other aspects of the hypothesis that were to be tested included the seasonal variations and impact on perceived air quality. Seasonal variations in the chemical and physical properties contributing to visibility degradation were found to be minimal, with the most notable being the contribution of domestic heating during the winter months. Good correlations between visibility perception and light extinction were found suggesting that overall, the light extinction measurements provided a good indication of perceived visibility.



The research was successful in answering key questions on the causes of visibility degradation in Christchurch. The main causes of reduced visibility and brown haze in Christchurch were found to be secondary particles (primarily sulphates) and motor vehicle emissions. The predominant physical processes were light scattering by particles, which was dominated by secondary particles, and to a lesser extent, light absorption by particles.

These results were similar to a number of overseas studies, which have found sulphates and nitrates to be significant contributors to visibility degradation. For example, in the Fraser Valley, British Columbia, nitrates and sulphates are the main contributors to light scattering accounting for 55-67% of mean  $B_{sp}$  (Pryor, *et al.*, 1997). In the eastern United States, 60-70% of aerosol extinction is attributed to sulphates, although contributions are lower in the west at around 30% (Malm & Day, 1999).

The main variations in summer and winter haze were found to be the extent of the light extinction values, which were typically much lower during the summer months, as were overall concentrations of particles and gases. Secondary particles and motor vehicle emissions were the main contributors during both the winter and summer months. The main seasonal variation in sources of particles was a small contribution from domestic home heating during the winter months.

The purpose of examining the relationship between perceived air quality and light extinction in Christchurch was to assess the ability to differentiate between Christchurch fogs and low cloud and visibility degradation caused by air pollution. Results of the visibility survey suggest a good relationship in general between light extinction and perceived air pollution, although in some instances atmospheric moisture did impact on perception.

## 10.2 Limitations of the research

Overall, the research has been successful in providing insight into the causes and complexity of visibility degradation in Christchurch. However, a number of methodological improvements would have provided better, more reliable data. In particular:

- The switching from Teflon to polycarbonate filters to improve the PIXE detection limits was unnecessary and may have negatively impacted on the PCA analysis. The most appropriate filter media for these studies appears to be the Teflo brand Teflon filters (Hopke, pers comm., 2002).
- The measurement of Na concentrations on the nylon filters using ion chromatography may have provided a more reliable estimate of concentrations of that element.

- Reducing the equipment downtime associated with the series 5400 analyser would have allowed for the inclusion of the organic carbon measurements in the PCA analysis.
- Changing the sampling period from the initial 06:00 to 13:00 daytime period to include a 24-hour average sample to improve the collection volume and PIXE detections for the summer period was not helpful. Although the night time concentrations of particles during the summer were low, having data for two separate collection times added some limitations.
- Conducting a random survey of a representative proportion of the Christchurch population to determine the acceptability or other of the degraded visibility and to determine the relationship between perceived air pollution and light extinction.

There are a number of concerns regarding the project outcomes that may have been influenced by these factors. One concern is whether the segregation between motor vehicle and domestic burning combustion processes is a true reflection of the relative emissions from these sources. In particular it is possible, although not likely, that the zinc burning profile is an indicator of enclosed burner emissions only and that the motor vehicle emissions profile also includes combustion emissions from fireplaces without galvanized chimneys.

Another concern is the lack of Na in what otherwise appears to be a classic sea salt source profile. This appears to be related to uncertainties associated with the measurement of Na using the PIXE methodology, as well as the use of the polycarbonate filters. The presence of high concentrations of chloride on the nylon filter blanks meant that the ion chromatography measurements of this element were inaccurate. However, Cl concentrations were also measured using the PIXE sampler so that the impact of this was minor.

Despite these limitations, the overall conclusions regarding the physical and chemical properties contributing to visibility degradation in Christchurch appear sound. Because the open fire contribution to  $PM_{10}$  in Christchurch is less than half of that from total domestic burning, even if the open fire contribution were included in the motor vehicle profile, the contribution from the latter source would still be significant. Management measures to improve visibility degradation in Christchurch should therefore target motor vehicle emissions and sulphate and nitrate formation. Further information on the atmospheric chemistry resulting in high concentrations of sulphates and nitrates in Christchurch is required before management of these contaminants should be attempted.

### **10.3 Implications for visibility management**

The study has significant implications for the management of visibility degradation in Christchurch. Firstly, it is important to note that existing measures proposed by Environment Canterbury to

reduce 24-hour average  $PM_{10}$  concentrations are unlikely to result in significant improvement in visibility in Christchurch. Although  $PM_{10}$  and  $PM_{2.5}$  concentrations in the city are well correlated, and are the main cause of visibility degradation, management measures to reduce 24-hour average  $PM_{10}$  concentrations target domestic fires. This is because domestic fires are the main contributor to high concentrations of  $PM_{10}$ , which occur primarily during the evening period. During the daytime concentrations are much lower and sources are dominated by secondary particles and motor vehicle emissions.

It is likely, however, that current national initiatives to improve vehicle engine technology and fuel specifications for New Zealand will result in some improvements in visibility in Christchurch. These measures include the requirement that all vehicles meet the emission controls mandatory in the countries of origin, the introduction of a 10-second rule for visible emissions from motor vehicles and a revision of the New Zealand fuel specifications to reduce the benzene and sulphur contents of the fuel. The basis for these measures is documented in the 1998 Ministry of Transport publication "The Vehicle Fleet Emission Control Strategy" (VF ECS), which indicates that these measures should result in significant reductions in emissions of  $PM_{10}$ , carbon monoxide and nitrogen dioxide, with time.

Sulphate particulate is influenced mainly by the concentrations of  $SO_x$  in the air. However, the impact of reductions in the sulphur content of diesels on concentrations of sulphate in Christchurch is uncertain. An emission inventory for Christchurch conducted in 1999 indicates that the main sources of  $SO_x$  emissions are industry, around 80%, and motor vehicles, around 15% (Wilton, 2001). With such a significant industrial contribution, it is likely that additional measures would be required to achieve significant results. The inventory did not include natural sources such as sea-spray.

The formation of nitrate is more complex, depending on concentrations of nitric acid (formed mainly from nitrogen oxides), relative humidity, temperature and the concentrations of sulphate and ammonium in the aerosol (Middleton & Laulainen, 2000). The main source of anthropogenic nitrogen oxides in Christchurch is motor vehicles, which contribute around 85% (Wilton, 2001).

In determining strategies for reducing concentrations of secondary particles, it is also important to consider the implications of atmospheric chemistry and the relationships between concentrations of different cations (e.g.,  $NH_4^+$ ) and anions (e.g.,  $NO_3^-$ ). For example, if management strategies reduced concentrations of sulphate without also reducing ammonia or nitrogen oxides, it is possible that the reduction in sulphate would be offset by an increase in nitrate, as more ammonia is available to retain nitrate in particulate form. In most locations ammonium is the dominant anion in

secondary particulate composition and thus is particularly important in these interactions. In this study, concentrations of ammonium were low (maximum  $2.5 \mu\text{gm}^{-3}$ ) and were poorly correlated with both nitrate and sulphate indicating that nitrates and sulphates may be present in an alternative form or that the sampling methods or analysis did not adequately measure concentrations of ammonium.

## 10.4 Future research

This study suggests that further research into the composition and sources of secondary particulate in Christchurch are necessary before additional management strategies for improving visibility in Christchurch can be developed. Moreover, the development of management strategies requires the integration of atmospheric chemistry including relationships between concentrations of different species, rather than the more straightforward approach of focusing solely on reductions in primary emissions.

A model for assessing the impact of emission management scenarios on visibility degradation in the United States was developed by Middleton & Laulainen (2000). The Visibility Assessment Screening Technique (VAST) considers the impact of changes in emissions of  $\text{SO}_x$ ,  $\text{NO}_x$  and VOCs on visibility, based on existing secondary particulate speciation data. It is likely that a similar approach would be required for Christchurch if strategies to improve visibility were necessary. Prior to exploring these options, however, additional information on the form of the nitrate and sulphate is necessary and should form a priority for further research.

From a policy perspective, however, additional surveys of the Christchurch community would be first required to determine whether or not visibility management measures are warranted. Subsequent research and the development of management measures could then occur as in accordance with the process described in Section 1.1.

In addition to future visibility research priorities, this study also identifies the need for the measurement of ground level concentrations of nitrate and sulphate to determine their contribution to 24-hour average  $\text{PM}_{10}$  concentrations in Christchurch. This should be a priority for air quality regulators in Christchurch as it may impact on the assessment of the effectiveness of management options to reduce  $\text{PM}_{10}$  concentrations in Christchurch (Wilton, 2001b) and have subsequent health implications.



## REFERENCES

- Aberkane, T. (1997), Annual air quality monitoring report 1997. Canterbury Regional Council report U98/43.
- Aberkane, T. (1999), Annual air quality monitoring report. Environment Canterbury Report, No. U00/78.
- Aberkane, T. (2001), Ozone monitoring in Christchurch. Canterbury Regional Council unpublished report.
- Ames, M. R., Gullu, G., Beal, J., Olmez, I. (2000), Receptor Modeling for Elemental Source Contributions to Fine Aerosols in New York State, *Journal of Air and Waste Management Association* **50**: 881-887.
- Ayrey, R. B. (1999), Air Quality Trends – suspended particulate. Canterbury Regional Council-unpublished report.
- Ayrey, R. B. (2001), Issues and Options for the Management of Adverse Effects from Motor Vehicle Emissions. Environment Canterbury Report U01/103.
- Baik, N., Kim, Y. P., Moon, K. C. (1996), Visibility study in Seoul. *Atmospheric Environment* **30** no 13, 2319-2328.
- Brady, T. J., Mikeal, L. A., Hay, J. E. (1999), Chemical Characterisation of Christchurch Aerosol. Unpublished report, School of Environmental and Marine Sciences, University of Auckland.
- Brimblecombe, P. (1986) Air Composition and Chemistry. Cambridge University Press, Cambridge.
- Brook, J. R., & Dann, T. F. (1999), Contribution of Nitrate and Carbonaceous Species to PM<sub>2.5</sub> observed in Canadian Cities. *Journal of Air and Waste Management Association*, **49**:193-199.
- Canadian Environmental Protection Act. (1998), National ambient air quality objectives for particulate matter. Canadian Environmental Protection Act.
- Canterbury Regional Council. (1996), Winter air quality report. Unpublished report Canterbury Regional Council.
- Canterbury Regional Council. (1997), Take a deep breath, A discussion document about Christchurch air quality. Canterbury Regional Council Report No R97/14.
- Canterbury Regional Council. (1998), Draft Natural Resources Regional Plan Part A: Air. Canterbury Regional Council Report No. R98/8.
- Canterbury Regional Council, 1999 – Online  
[Http://www.crc.govt.nz/crhome/gis&database/airpol/Airquality/0Contents/EMQAirFrontpages.htm](http://www.crc.govt.nz/crhome/gis&database/airpol/Airquality/0Contents/EMQAirFrontpages.htm).  
 14 December 2002.
- Carroll J. J. (1996), Air Pollution Meteorology, Course Reader. Atmospheric Science section, Department of Land, Air and Water Resources, University of California, Davis CA 95616, USA.

- Chan, Y. C., Simpson, R. W., McTainsh, G. H., Vowles, P. D., Choen, D. D., Bailery, G. M. (1997), Characterisation of chemical species in PM<sub>2.5</sub> and PM<sub>10</sub> aerosols in Brisbane, Australia. *Atmospheric Environment* Vol. 31 No 22, 3773-3785.
- Chow J. C., Watson, J. G. (1999), Draft Particulate Matter (PM<sub>2.5</sub>) Speciation Guidance Document. <http://www.epa.gov/ttn/>
- Chow, J. C. (1995), Measurement Methods to Determine Compliance with Ambient Air Quality Standards for Suspended Particles. *Journal of Air and Waste Management Association*. 45:320-382.
- Chow, J. C., Fairley, D., Watson, J.G., DeMandel, R., Fujita, E., Lowenthal, D.H., Lu, Z., Frazier, C.A., Long, G., Cordova, J. (1995), Source apportionment of wintertime PM<sub>10</sub> at San Jose, California, *Journal of Environmental Engineering*, May 378-387.
- Davy, P., Markwitz A., Trompetter, W. J. (2002), Elemental analysis and source apportionment of ambient particulate matter in the Wellington Region of New Zealand. Proceedings of the 16th International Clean Air and Environment Conference, Christchurch New Zealand.
- Eatough, D. J., Du, A., Joseph, M., Caka, F. M., Sun, B., Lewis, L., Mangelson, N. F., Eatough, M. (1997), Regional Source Profiles of Sources of Sox at the Grand Canyon During Project MOHAVE, *Journal of Air and Waste Management Association* 47:101-118.
- Eldering, A., Cass, G. R., Moon, K. C. (1994), An air monitoring network using continuous particle size distribution monitors: connecting pollutant properties to visibility via Mie Theory. *Journal of Atmospheric Environment* 28:16
- Ely, D. W., Leary, J. T., Stewart, T. R., Ross, D. M. (1991), The establishment of the Denver Visibility Standard. Paper presented at the Air & Waste Management Association 84<sup>th</sup> Annual Meeting & Exhibition, Vancouver, British Columbia June 16-21.
- Fine, P. M., Cass, G. R., Simoneit, B. R. T. (2002), Chemical Characterisation of Fine Particle Emissions from the Fireplace Combustion of Woods Grown in the Southern United States. *Environmental Science and Technology* 36, 1442-1451.
- Fisher, G., Rolfe, K., Kjellstrom, T., Woodward, A., Hales, S., Sturman, A., Kingham, S., Peterson, J., Shrestha, R., King, D. (2002), Health effects due to motor vehicle air pollution in New Zealand. Report to the Ministry of Transport.
- Foster, E. V. (1998), An investigation into measurement of PM<sub>10</sub> in Christchurch, Canterbury Regional Council, U98/69.
- Gebhart, K., Malm, W. C. (1997), Spatial and Temporal Patterns in Particle Data Measured During the MOHAVE Study, *Journal of Air and Waste Management Association*, 47: 119-135.
- Gimson, N., & Fisher, G. (1997), The relationship between emissions to air and measured ambient air concentrations of contaminants in Christchurch. Canterbury Regional Council Report U97(67).
- Gimson, N. R. (1998), Wintertime Meteorology and Air Pollution Dispersion in Christchurch. Canterbury Regional Council report U98/58.
- Groblicki, P. J., Wolff, G. T., Countess, R. J. (1981), Visibility-reducing species in the Denver "Brown cloud" – 1. Relationships between extinction and chemical composition. *Atmospheric Environment*, 15, No 12, 2473-2484.

- Henry, R. C. (1997), Receptor Model Applied to Patterns in Space (RMAPS) Part II – Apportionment of Airborne Particulate Sulfur from Project MOHAVE. *Journal of Air and Waste Management Association* 47: 220-225.
- Henry, R. C., Shibata, T., Chitwood, E. (1994), Construction and operation of a video based visual colorimeter for atmospheric research. *Atmospheric Environment* 28, No 5, 1065-1069.
- Henry, R. C., Shibata, T., Day, D. E. (1991), Comparison of Color Perception of Photographs and the Natural Scene. Proceedings of the 84th Annual Air and Waste Management Association Meeting and Exhibition, Vancouver, British Columbia.
- Hodkinson, J. R. (1966), Calculations of colour and visibility in urban atmospheres polluted by gaseous NO<sub>2</sub>. *International Journal of Air and Water Pollution*, 10: 137-144.
- Hoff, M. R., Guise Bagley, L., Staebler, R. M., Weibe, H. A., Brook, J., Georgi, B., Dusterdiek, T. (1996), Lidar, nephelometer, and in situ aerosol experiments in southern Ontario. *Journal of Geophysical Research* Vol 101, No D14, 19199-19209.
- Hopke, P.K., Roscoe, B. A., Dattner, S.L., Jenks, J. M. (1982), The Use of Principal Components Factor Analysis to Interpret Particulate Compositional Datasets, *Air Pollution Control Association Journal*, Vol 32, No 6. 637-642.
- Horvath, H. (1994), Remarks and suggestions on nomenclature and symbols in atmospheric optics, *Atmospheric Environment* vol 28 no 5: 757:759.
- Huo. X. X., Crisp P. T., Cohen D. D. (1998), Elemental Composition of Fine Aerosol Particles around Sydney during 1992 and 1993. *Clean Air and Environmental Quality Journal* Vol 32 28-38.
- Keywood, M. D., Ayres, G. P., Gras, J. L., Gillett, R. W., Cohen, D. D. (2000), Size distribution and sources of aerosol in Launceston, Australia during winter 1997, *Journal of Air and Waste Management Association* 50: 418-427.
- Koschmieder, H. (1924), Theorie der horixontalen sichtweite. *Beiter Phycisal freien Atmsophere*, 12, No 33.
- Kossman, M., & Sturman, A. P., (2002), Analysis of the surface wind field in Christchurch and coastal Canterbury during winter smog nights – results from CAPS2000. 16th International Clean Air and Environment Conference of the Clean Air Society of Australia & New Zealand, 19 - 22 August 2002.
- Lai, L. Y., Sequeira, R. (2001), Visibility degradation across Hong Kong: its components and their relative contributions. *Atmospheric Environment*. 35 (34) 5861-5872.
- Lamb, C., G. (2001), Christchurch household survey: A survey of Residents' opinions of Proposed Air Pollution Control Methods. Environment Canterbury Unpublished Report No U01/70.
- Laulainen, N., and Trexler, E. (1997), Assessing the relative contribution of biogenic and fossil processes to visibility-scattering aerosols found in remote areas: Near-term organic research program. *Journal of Air and Water Management* 47:212-215.
- Magee Scientific Company, (1992) Measurements of Aerosol Black Carbon. Magee Scientific Company.
- Malm, W. C., Day, D. E. (1999), Opticial properties of aerosols at Grand Canyon National Park. *Atmospheric Environment*, 34 (20) 3373-3391.

- Malm, W. C., & Gebhart, K. A., (1997), Source Apportionment of Sulphur and Light Extinction Using Receptor Modeling Techniques, *Journal of Air and Water Management* 47: 250-268
- Malm, W. C., Molenar, J. V., Eldred, R. A., Sisler, J. F. (1996), Examining the relationship among atmospheric aerosols and light scattering and extinction in the Grand Canyon area. *Journal of Geophysical Research* 101(14):19251-19265.
- Markwitz, A., Trompeter, W. J., and Davy, P. (2001), Elemental composition and source apportionment of fine particulate matter in the Wellington Region. IAEA/RCA Project RAS/8/082. IAEA conference, Daejeon, Korea, 29 October – 1 November, 2001
- McKendry, I. G., Sturman, A. P., Owens, I. F. (1988), Numerical simulation of local thermal effects on the windfield of the Canterbury Plains, New Zealand. *Journal of Geology and Geophysics (NZ)*, 31, 511-524.
- Middleton, P., & Laulainen, N. (2000), Examining impacts of visibility and PM strategies before Implementation. *Journal of Air and Waste Management Association*, 50: 875-880.
- Ministry for the Environment. (1994), Ambient air quality guidelines. Ministry for the Environment.
- Ministry for the Environment (MfE). (1997), Environmental Performance Indicators – proposal for fresh water and land. Ministry for the Environment.
- Ministry for the Environment. (1998), Visibility Monitoring as an environmental indicator. Ministry for the Environment.
- Ministry for the Environment (MfE). (1999a), Visibility in New Zealand: Guidance on measurement methods. Ministry for the Environment.
- Ministry for the Environment (MfE). (1999b), Visibility in New Zealand: Amenity value and Management. Ministry for the Environment.
- Ministry for the Environment (MfE). (1999c), Visibility in New Zealand: National Risk Assessment. Ministry for the Environment.
- Ministry for the Environment (MfE). (1999d), Good Practice Guide for air quality monitoring and data management. Ministry for the Environment.
- Mistra, M. K., Ragland, K. W., Baker, A. J. (1993), Wood ash composition as a function of furnace temperature. *Biomass and Bioenergy* Vol 4, No. 2, pp 103-116.
- Molenar J. V. (1997), Analysis of the Real World Performance of the Optec NGN-2 Ambient Nephelometer. Paper presented at Visual Air Quality: Aerosols and Global radiation Balance, Bartlett, New Hampshire.
- National Institute of Water and Atmospheric Research. (1998), Air visibility Telephone Survey Results. NIWA report AK97071.
- Owens, I. F., & Tapper, N. J. (1977), The influence of meteorological factors on air pollution occurrence in Christchurch. Proceedings of the 9th New Zealand Geography Conference, Dunedin, New Zealand, 33-35.
- Person, M. (1996), Visibility Program Evaluation: Relevance to NZ. National Institute of Water and Atmospheric Research report no AK96010.



- Pitchford, M. L., & Malm, W. C. (1994), Development and application of a standard visual index. *Atmospheric Environment* Vol 28, No 5:1049-1054.
- Pryor, S. C., Simpson, R., Guise-Bagley, L., Hoff, R., Sakiyama, S. (1997), Visibility and aerosol composition in the Fraser Valley during REVEAL. *Journal of the Air & Waste Management Association* 47: 147-156.
- Pryor, S. C. (1996), Assessing Public Perception of Visibility for Standard Setting Exercises. *Atmospheric Environment*, 30, 2705-2716.
- Pryor, S. C., & Sorenson, L.L., 2000, Nitric Acid-Sea Salt Reactions: Implications for Nitrogen Deposition to Water Surfaces, *American Meteorological Society* 39, 725-731.
- QUARG. (1996), Airbourne particulate matter in the United Kingdom. Third report of the Quality of Urban Air Review Group. Department of the Environment.
- Richards L. W., Stoelting, M., Hammarstrand, R. G. M. (1989), Photographic method for Visibility Monitoring. *Environmental Science and Technology* 23, 182-186.
- Richards, L. W. (1988), Sight path measurements for visibility monitoring and Research. *Journal of the Air Pollution Control Association*, 38, No. 6, 785-791.
- Richards, L. W. (1999), Use of the Deciview Haze Index as an Indicator for Regional Haze, *Journal of Air and Waste Management Association*, 49: 1230-1237.
- Richman, M. B., 1986, Review Article, Rotation of Principal Components. *Journal of Climatology*, 6: 293-335.
- Risse, M., & Harris, G. (2002), Best management practices for wood ash used as an agricultural soil amendment. Online - <http://hubcap.clemson.edu/~blpprt/bestwoodash.html#table1>, 18 November 2002.
- Schichtel, B. A., Husar, R. B., Falke, S. R., and Wilson, W. E. (2001), Haze trends over the United States, 1980-1995. *Atmospheric Environment*. 35 (30) 5205-5210.
- Sisler, J. F., & Malm, W. C. (1997), Characteristic of Winter and Summer Aerosol Mass and Light Extinction on the Colorado Plateau. *Journal of Air and Waste Management Association*. 47:317-330.
- Skoog, D. A. (1985), Principles of Instrumental Analysis, 3rd edition. Saunders College Publishing. Holt Reinhard and Winston, The Dryden Press.
- Slone, C. S., White, W. H., (1986), Visibility: An evolving issue. *Environmental Science and Technology*, 20 No 3: 760-766
- Spronken Smith, R. A. (2001), Comparison of summer and winter-time suburban energy fluxes in Christchurch, New Zealand. *International Journal of Climatology* 22:979-992.
- Statistics New Zealand. (2002), 2001 Census of Population and Dwellings. [Http://www/stats.govt.nz](http://www/stats.govt.nz).
- Stuart, R. A., Hoff, R. M. (1994), Airport Visibility in Canada-revised. *Atmospheric Environment*, Vol 28, No5, 1001-1007.
- Sturman & Zarwar Reza (2001), Application of back-trajectory techniques to the delimitation of a Clean Air Zone for the Christchurch airshed. Environment Canterbury Report U01/24.

- Sturman A. P. (1982), Statistical Analysis of Spatial Patterns of Smoke Concentrations in Christchurch. *New Zealand Geographer* 38, 1, 9-18.
- Sturman, A. P. (1985), An examination of the role of local wind systems in the concentration and dispersion of smoke pollution in Christchurch. *New Zealand Geographer*, 38, 67-76.
- Tang, I. N. (1996), Chemical and size effects of hygroscopic aerosols on light scattering coefficients. *Journal of Geophysical Research*, Vol 101, NO D14, 19245-19250.
- The National Park Service (1999), Online [Http://www2.nature.nps.gov/ard/vis/visprot.html](http://www2.nature.nps.gov/ard/vis/visprot.html). 10 October 1999.
- Thompson, A. (1996), Visibility degradation in New Zealand: Elemental Fingerprints of Particulates for Source Apportionment. National Institute of Water and Atmospheric Research report no AK96094.
- Trier, A. & Firinguetti, L. (1994), A time series investigation of visibility in an urban atmosphere-I. *Atmospheric Environment*, 28, 5, 991-996.
- Trompetter, W., & Markwitz, A. (2001), Ion Beam Analysis results of Air Particulate matter collected in Christchurch. New Zealand Geological and Nuclear Sciences report No. 2001/105.
- Twomey, S. (1977) Developments in Atmospheric Science 7, Atmospheric Aerosols. Elsevier Scientific Publishing, The Netherlands.
- USEPA. (1998a). Draft Visibility Monitoring Guidance Document. Research Triangle Park NC 27711.
- USEPA. (1998b). National Air Quality and Emissions Trends Report 1997. Online <http://www.epa.gov/oar/aqtrnd97/chapter6.pdf>. 7 July 1999.
- USEPA. (1996), Air quality criteria document for particulate matter. Research Triangle Park. North Carolina, United States.
- Van Den Assem, S. (1997), Dispersion of Air Pollution in the Christchurch Area. Unpublished PhD thesis, Geography Department, University of Canterbury.
- Watson, J. G. (2002), Visibility: Science and Regulation. Critical review, *Journal of Air and Waste Management Association* 52:628-713.
- White, W. H. (1990), The components of atmospheric light extinction: a survey of ground-level budgets. *Atmospheric Environment* Vol. 24, No. 10, pp 2673-2679.
- White, W. H., Macias, E.S., Nininger, R. C., Schorran, D. (1994), Size resolved measurements of light scattering by ambient particles in the southwestern U.S.A. *Atmospheric Environment* 28, No. 5, 909-921.
- Wilson R. & Spengler J. D. (1996), Particles in Our Air, Concentrations and Health Effects. Harvard University Press.
- Wilson, T. (1999), Meteorological and air pollution influences on wintertime visibility in Christchurch. Unpublished Masters thesis, Geography Department, University of Canterbury.
- Wilson, W. E., & Riest, P. C. (1994), A PC based Mie scattering programme for theoretical investigations of the optical properties of atmospheric aerosols as a function of relative humidity. *Atmospheric Environment* 28, 5:803-809.

Wilton E. (2001), Christchurch inventory of emissions – 1999. Environment Canterbury Report Number R01/28.

Wilton, E. (2001b), Estimates of the effectiveness of management options for reducing PM<sub>10</sub> concentrations in Christchurch - 2001. Environment Canterbury Report U01/97.

Wilton, E. (2001c), Variations to the air quality target for Christchurch and the associated impact on solid fuel burner numbers. Environment Canterbury Report U01/91.

## APPENDICES



## Appendix A: - Visibility Survey

The purpose of this survey is to assess the impact of air pollution on visibility and how this is perceived. You will find attached 16 pictures of the Port Hills of Christchurch taken from an office in the Central Business District. You are required to assess each picture in terms of visual clarity and the impact of air pollution.

For each picture you are asked to do 2 things, firstly you will be asked to rate the visibility in each picture on a scale of 1-7. The purpose of the survey is to determine your perception of the pollution for each picture. Following that you are asked to assess the acceptability or otherwise of the visibility depicted in each image.

### Rating

Rate the pollution in the pictures (1-16) on a scale of 1 2 3 4 5 6 7, where

1= extremely polluted, 2 = very polluted, 3 = moderately polluted, 4 = noticeably polluted, 5 = Slightly Polluted, 6 = clear, 7 = crystal clear.

If you consider that visibility in the picture is reduced as a result of weather (e.g., cloud) alone, use a rating of 0 instead of a rating from 1-7.

### Acceptability of pollution

This question is to determine whether, in your view, the visibility presented in the image is acceptable or unacceptable. Please select the appropriate response based on your view of the visibility in each picture.

## Appendix B: Filter sampling periods

Particulate speciation for elements, nitrates and sulphates was carried out for 250 samples collected from 9 February 2000 to 28 April 2001. The majority of samples were collected over the period 06:00 to 13:00. Table A1 details the sampling dates and times for each filter.

Table A1: Filter sample numbers, dates and times

Filter No.	Date	Start time	End time	Filter No.	Date	Start time	End time	Filter No.	Date	Start time	End time
1	9-Feb-00	10:00	02:00	85	05-Jul-00	06:00	01:00		Daily samples		
2	11-Feb-00	08:00	01:00	86	06-Jul-00	06:00	01:00	175	23/01-24/01	08:30	07:30
3	14-Feb-00	08:00	01:00	87	07-Jul-00	06:00	01:00	177	24/01-25/01	08:30	07:30
4	15-Feb-00	08:00	01:00	88	10-Jul-00	06:00	01:00	178	25/01-26/01	08:30	07:30
5	16-Feb-00	08:00	01:00	89	11-Jul-00	06:00	01:00	179	26/01-27/01	08:30	07:30
6	17-Feb-00	08:00	01:00	90	12-Jul-00	06:00	01:00	180	29/01-30/01	08:30	08:06
7	18-Feb-00	08:00	01:00	91	13-Jul-00	06:00	01:00	182	30/01-31/01	08:30	07:30
8	21-Feb-00	08:00	01:00	92	14-Jul-00	06:00	01:00	183	31/01-1/02	08:30	07:30
9	22-Feb-00	08:00	01:00	93	26-Jul-00	06:00	01:00	184	1/02-2/02	08:30	07:30
10	23-Feb-00	08:00	01:00	94	27-Jul-00	06:00	01:00	185	2/02-3/02	08:30	07:30
11	24-Feb-00	08:00	01:00	95	28-Jul-00	06:00	01:00	186	7/02-8/02	08:30	07:30
12	25-Feb-00	07:00	02:00	96	31-Jul-00	06:00	01:00	187	8/02-9/02	08:30	07:30
13	28-Feb-00	07:00	02:00	97	01-Aug-00	06:00	01:00	188	9/02-10/02	08:30	07:30
14	29-Feb-00	07:00	02:00	98	02-Aug-00	06:00	01:00	189	12/02-13/02	08:30	07:30
16	02-Mar-00	07:00	02:00	99	03-Aug-00	06:00	01:00	191	13/2-14/2	08:30	07:30
17	03-Mar-00	07:00	02:00	100	04-Aug-00	06:00	01:00	192	14/2-15/2	08:30	07:30
18	04-Mar-00	07:00	02:00	101	07-Aug-00	06:00	01:00	193	15/2-16/2	08:30	07:30
19	07-Mar-00	07:00	02:00	102	08-Aug-00	06:00	01:00	194	16/2-17/2	08:30	07:30
20	08-Mar-00	07:00	02:00	103	09-Aug-00	06:00	01:00	195	19/2-20/2	08:30	07:30
21	09-Mar-00	07:00	02:00	104	10-Aug-00	06:00	01:00	197	20/02-21/2	08:30	07:30
22	10-Mar-00	07:00	02:00	105	11-Aug-00	06:00	01:00	198	21/2-22/2	08:30	07:30
23	13-Mar-00	07:00	02:00	106	14-Aug-00	06:00	01:00	199	22/2-23/2	08:30	07:30
24	14-Mar-00	07:00	02:00	107	15-Aug-00	06:00	01:00	200	23/2-24/2	08:30	07:30
24	14-Mar-00	07:00	02:00	108	16-Aug-00	06:00	01:00	201	26/2-27/2	08:30	07:30
25	15-Mar-00	07:00	02:00	109	17-Aug-00	06:00	01:00	203	27/2-28/2	08:30	07:30
26	16-Mar-00	07:00	02:00	110	18-Aug-00	06:00	01:00	204	28/2-1/03	08:30	07:30
27	17-Mar-00	07:00	02:00	111	21-Aug-00	06:00	01:00	205	1/03-2/03	08:30	07:30
28	20-Mar-00	06:00	01:00	112	22-Aug-00	06:00	01:00	206	2/3-3/3	08:30	07:30
29	21-Mar-00	06:00	01:00	113	23-Aug-00	06:00	01:00	207	5/6-6/3	08:30	07:30
30	22-Mar-00	06:00	01:00	114	24-Aug-00	06:00	01:00	209	6/3-7/3	08:30	07:30
31	23-Mar-00	06:00	01:00	115	25-Aug-00	06:00	01:00	210	7/3-8/3	08:30	07:30
32	24-Mar-00	06:00	01:00	116	28-Aug-00	06:00	01:00	211	8/3-9/3	08:30	07:30
33	27-Mar-00	06:00	01:00	117	30-Aug-00	06:00	01:00	212	9/3-10/3	08:30	07:30
34	28-Mar-00	06:00	01:00	118	31-Aug-00	06:00	01:00	213	12/3-13/3	08:30	07:30
35	29-Mar-00	06:00	01:00	119	01-Sep-00	06:00	01:00	215	13/3-14/3	08:30	07:30
36	30-Mar-00	06:00	01:00	120	04-Sep-00	06:00	01:00	216	14/3-15/3	08:30	07:30
37	31-Mar-00	06:00	01:00	121	06-Sep-00	06:00	01:00	217	15/3-16/3	08:30	07:30
38	26-Apr-00	06:00	01:00	122	07-Sep-00	06:00	01:00	218	16/3-17/3	08:30	07:30

39	27-Apr-00	06:00	01:00	123	08-Sep-00	06:00	01:00	15	1/03/2000	08:30	02:00
40	28-Apr-00	06:00	01:00	124	11-Sep-00	06:00	01:00	219	19/3-20/3	09:30	08:30
41	01-May-00	06:00	01:00	125	12-Sep-00	06:00	01:00	221	20/3-21/3	09:30	08:30
42	02-May-00	06:00	01:00	126	13-Sep-00	06:00	01:00	222	21/3-22/3	09:30	08:30
43	03-May-00	06:00	01:00	127	14-Sep-00	06:00	01:00	223	22/3-23/3	09:30	08:30
44	04-May-00	06:00	01:00	128	15-Sep-00	06:00	01:00	224	23/3-24/3	09:30	08:30
45	05-May-00	06:00	01:00	129	18-Sep-00	06:00	01:00	225	26/3-27/3	09:30	08:30
46	08-May-00	06:00	01:00	130	19-Sep-00	06:00	01:00	227	27/3-28/3	09:30	08:30
47	09-May-00	06:00	01:00	131	20-Sep-00	06:00	01:00	228	28/3-29/2	09:30	08:30
48	10-May-00	06:00	01:00	132	21-Sep-00	06:00	01:00	229	29/3-30/3	09:30	08:30
49	11-May-00	06:00	01:00	133	22-Sep-00	06:00	01:00	230	30/3-31/3	09:30	08:30
50	12-May-00	06:00	01:00	134	25-Sep-00	06:00	01:00	231	2/4-3/4	09:30	08:30
51	13-May-00	06:00	01:00	135	26-Sep-00	06:00	01:00	233	3/4-4/4	09:30	08:30
52	16-May-00	06:00	01:00	136	27-Sep-00	06:00	01:00	234	4/4-5/4	09:30	08:30
53	17-May-00	06:00	01:00	137	28-Sep-00	06:00	01:00	235	5/4-6/4	09:30	08:30
54	18-May-00	06:00	01:00	138	29-Sep-00	06:00	01:00	236	6/4-7/4	09:30	08:30
55	19-May-00	06:00	01:00	139	2-Oct-00	06:00	01:00	237	9/4-10/4	09:30	08:30
56	20-May-00	06:00	01:00	140	3-Oct-00	06:00	01:00	238	10/4-11/4	09:30	08:30
57	23-May-00	06:00	01:00	141	4-Oct-00	06:00	01:00	240	11/4-12/4	09:30	08:30
58	24-May-00	06:00	01:00	142	5-Oct-00	06:00	01:00	241	12/4-13/4	09:30	08:30
59	25-May-00	06:00	01:00	143	6-Oct-00	06:00	01:00	242	17/4-18/4	09:30	08:30
60	29-May-00	06:00	01:00	144	9-Oct-00	06:00	01:00	243	18/4-19/4	09:30	08:30
61	30-May-00	06:00	01:00	145	11-Oct-00	06:00	01:00	244	19/4-20/4	09:30	08:30
62	31-May-00	06:00	01:00	146	12-Oct-00	06:00	01:00	245	20/4-21/4	09:30	08:30
63	01-Jun-00	06:00	01:00	147	16-Oct-00	06:00	01:00	246	23/4-24/4	09:30	08:30
64	02-Jun-00	06:00	01:00	148	17-Oct-00	06:00	01:00	248	24/4-25/4	09:30	08:30
65	06-Jun-00	06:00	01:00	149	18-Oct-00	06:00	01:00	249	26/4-27/4	09:30	08:30
66	07-Jun-00	06:00	01:00	150	19-Oct-00	06:00	01:00	250	27/4-28/4	09:30	08:30
67	08-Jun-00	06:00	01:00	151	20-Oct-00	06:00	01:00		Weekly samples		
68	09-Jun-00	06:00	01:00	152	24-Oct-00	06:00	01:00	170	6/12-13/12		
69	12-Jun-00	06:00	01:00	153	25-Oct-00	06:00	01:00	171	12/12-16/12		
70	14-Jun-00	06:00	01:00	154	26-Oct-00	06:00	01:00	173	9/01-13/01		
71	15-Jun-00	06:00	01:00	155	27-Oct-00	06:00	01:00	172	19/12-22/12		
72	16-Jun-00	06:00	01:00	156	30-Oct-00	06:00	01:00	174	16/01-20/01		
73	19-Jun-00	06:00	01:00	157	31-Oct-00	06:00	01:00	239	10/4-20/4		
74	20-Jun-00	06:00	01:00	158	01-Nov-00	06:00	01:00	176	23/01-27/01		
75	21-Jun-00	06:00	01:00	159	02-Nov-00	06:00	01:00	181	29/01-2/01		
76	22-Jun-00	06:00	01:00	160	03-Nov-00	06:00	01:00	190	12/2-16/2		
77	23-Jun-00	06:00	01:00	161	06-Nov-00	06:00	01:00	196	19/2-23/2		
78	26-Jun-00	06:00	01:00	162	07-Nov-00	06:00	01:00	202	26/2-2/3		
79	27-Jun-00	06:00	01:00	163	08-Nov-00	06:00	01:00	208	5/3-9/3		
80	28-Jun-00	06:00	01:00	164	09-Nov-00	06:00	01:00	214	12/3-16/3		
81	29-Jun-00	06:00	01:00	165	10-Nov-00	06:00	01:00	220	19/3-23/3		
82	30-Jun-00	06:00	01:00	166	13-Nov-00	06:00	01:00	226	26/3-30/3		
83	03-Jul-00	06:00	01:00	167	14-Nov-00	06:00	01:00	232	2/4-7/4		
84	04-Jul-00	06:00	01:00	168	15-Nov-00	06:00	01:00	247	23/4-26/4		
				169	16-Nov-00	06:00	01:00				



## Appendix C: Monthly summary statistic for concentrations of elements

Table A2: Monthly summary statistics for concentrations of elements by month of year.

February	Na $\mu\text{g m}^{-3}$	Mg $\mu\text{g m}^{-3}$	Al $\mu\text{g m}^{-3}$	Si $\mu\text{g m}^{-3}$	S $\mu\text{g m}^{-3}$	Cl $\mu\text{g m}^{-3}$	K $\mu\text{g m}^{-3}$	Ca $\mu\text{g m}^{-3}$	Sc $\mu\text{g m}^{-3}$	Fe $\mu\text{g m}^{-3}$	Ni $\mu\text{g m}^{-3}$	Zn $\mu\text{g m}^{-3}$	El C $\mu\text{g m}^{-3}$	NH <sub>4</sub> N $\mu\text{g m}^{-3}$	Cl <sup>-</sup> $\mu\text{g m}^{-3}$	NO <sub>3</sub> $\mu\text{g m}^{-3}$	SO <sub>4</sub> $\mu\text{g m}^{-3}$
Mean	0.00	0.26	0.39	0.32	0.39	0.38	0.07	0.42	0.05	0.03	0.06	0.02	3.55	0.16	2.00	0.23	2.2
Median	0.00	0.26	0.40	0.30	0.31	0.16	0.04	0.50	0.04	0.00	0.06	0.00	2.68	0.11	1.92	0.00	2.8
Maximum	0.03	0.36	0.52	0.50	0.88	1.41	0.36	0.87	0.12	0.24	0.16	0.16	11.06	0.43	3.25	2.30	4.1
Minimum	0.00	0.19	0.27	0.14	0.00	0.00	0.00	0.00	0.00	0.00	0.00	0.00	0.13	0.00	1.20	0.00	0.0
Count	10	10	10	10	10	10	10	10	10	10	10	10	10	10	10	10	10
Sum	0.03	2.59	3.91	3.16	3.91	3.78	0.68	4.20	0.49	0.30	0.56	0.16	35.53	1.58	20.04	2.30	22

March	Na $\mu\text{g m}^{-3}$	Mg $\mu\text{g m}^{-3}$	Al $\mu\text{g m}^{-3}$	Si $\mu\text{g m}^{-3}$	S $\mu\text{g m}^{-3}$	Cl $\mu\text{g m}^{-3}$	K $\mu\text{g m}^{-3}$	Ca $\mu\text{g m}^{-3}$	Sc $\mu\text{g m}^{-3}$	Fe $\mu\text{g m}^{-3}$	Ni $\mu\text{g m}^{-3}$	Zn $\mu\text{g m}^{-3}$	El C $\mu\text{g m}^{-3}$	NH <sub>4</sub> N $\mu\text{g m}^{-3}$	Cl <sup>-</sup> $\mu\text{g m}^{-3}$	NO <sub>3</sub> $\mu\text{g m}^{-3}$	SO <sub>4</sub> $\mu\text{g m}^{-3}$
Mean	0.01	0.28	0.33	0.43	0.33	0.71	0.01	0.13	0.04	0.07	0.05	0.06	3.15	0.14	2.34	0.23	2.3
Median	0.00	0.27	0.32	0.41	0.29	0.50	0.00	0.00	0.03	0.00	0.03	0.00	3.00	0.10	1.98	0.00	2.7
Maximum	0.14	0.45	0.46	0.67	0.97	1.90	0.10	0.69	0.15	0.35	0.23	0.27	7.10	0.45	6.56	2.23	7.0
Minimum	0.00	0.02	0.09	0.27	0.02	0.14	0.00	0.00	0.00	0.00	0.00	0.00	0.60	0.00	0.82	0.00	0.0
Count	23	23	23	23	23	23	23	23	23	23	23	23	23	23	23	23	23
Sum	0.27	6.38	7.62	9.85	7.57	16.25	0.29	2.90	0.83	1.70	1.20	1.41	72.53	3.13	53.78	5.38	53

April	Na $\mu\text{g m}^{-3}$	Mg $\mu\text{g m}^{-3}$	Al $\mu\text{g m}^{-3}$	Si $\mu\text{g m}^{-3}$	S $\mu\text{g m}^{-3}$	Cl $\mu\text{g m}^{-3}$	K $\mu\text{g m}^{-3}$	Ca $\mu\text{g m}^{-3}$	Sc $\mu\text{g m}^{-3}$	Fe $\mu\text{g m}^{-3}$	Ni $\mu\text{g m}^{-3}$	Zn $\mu\text{g m}^{-3}$	El C $\mu\text{g m}^{-3}$	NH <sub>4</sub> N $\mu\text{g m}^{-3}$	Cl <sup>-</sup> $\mu\text{g m}^{-3}$	NO <sub>3</sub> $\mu\text{g m}^{-3}$	SO <sub>4</sub> $\mu\text{g m}^{-3}$
Mean	0.04	0.25	0.33	0.58	0.66	1.30	0.00	0.00	0.03	0.23	0.14	0.02	7.17	0.07	1.39	0.00	2.4
Median	0.00	0.26	0.32	0.56	0.70	0.87	0.00	0.00	0.03	0.24	0.11	0.00	6.92	0.05	0.91	0.00	3.1
Maximum	0.11	0.31	0.42	0.64	0.92	2.47	0.00	0.00	0.04	0.25	0.26	0.05	8.07	0.10	2.37	0.00	4.1
Minimum	0.00	0.19	0.24	0.55	0.34	0.57	0.00	0.00	0.02	0.20	0.05	0.00	6.53	0.05	0.90	0.00	0.0
Count	3	3	3	3	3	3	3	3	3	3	3	3	3	3	3	3	3
Sum	0.11	0.75	0.98	1.75	1.97	3.91	0.00	0.00	0.10	0.69	0.43	0.05	21.51	0.20	4.17	0.00	7



May	Na $\mu\text{g m}^{-3}$	Mg $\mu\text{g m}^{-3}$	Al $\mu\text{g m}^{-3}$	Si $\mu\text{g m}^{-3}$	S $\mu\text{g m}^{-3}$	Cl $\mu\text{g m}^{-3}$	K $\mu\text{g m}^{-3}$	Ca $\mu\text{g m}^{-3}$	Sc $\mu\text{g m}^{-3}$	Fe $\mu\text{g m}^{-3}$	Ni $\mu\text{g m}^{-3}$	Zn $\mu\text{g m}^{-3}$	El C $\mu\text{g m}^{-3}$	NH <sub>4</sub> N $\mu\text{g m}^{-3}$	Cl <sup>-</sup> $\mu\text{g m}^{-3}$	NO <sub>3</sub> $\mu\text{g m}^{-3}$	SO <sub>4</sub> $\mu\text{g m}^{-3}$
Mean	0.01	0.19	0.30	0.47	0.74	1.08	0.04	0.05	0.05	0.19	0.13	0.18	5.93	0.06	1.30	0.24	4.0
Median	0.00	0.19	0.28	0.46	0.55	0.66	0.00	0.00	0.03	0.17	0.00	0.16	3.83	0.00	1.04	0.00	2.9
Maximum	0.26	0.33	0.50	0.82	1.89	3.07	0.37	0.73	0.24	0.44	0.49	0.81	23.00	0.92	4.74	1.25	28.6
Minimum	0.00	0.08	0.10	0.09	0.14	0.02	0.00	0.00	0.00	0.00	0.00	0.00	-0.72	0.00	0.00	0.00	0.0
Count	22	22	22	22	22	22	22	22	22	22	22	22	22	22	22	22	22
Sum	0.26	4.10	6.60	10.29	16.37	23.70	0.81	1.18	1.20	4.08	2.83	3.94	130.43	1.26	28.53	5.38	87

June	Na $\mu\text{g m}^{-3}$	Mg $\mu\text{g m}^{-3}$	Al $\mu\text{g m}^{-3}$	Si $\mu\text{g m}^{-3}$	S $\mu\text{g m}^{-3}$	Cl $\mu\text{g m}^{-3}$	K $\mu\text{g m}^{-3}$	Ca $\mu\text{g m}^{-3}$	Sc $\mu\text{g m}^{-3}$	Fe $\mu\text{g m}^{-3}$	Ni $\mu\text{g m}^{-3}$	Zn $\mu\text{g m}^{-3}$	El C $\mu\text{g m}^{-3}$	NH <sub>4</sub> N $\mu\text{g m}^{-3}$	Cl <sup>-</sup> $\mu\text{g m}^{-3}$	NO <sub>3</sub> $\mu\text{g m}^{-3}$	SO <sub>4</sub> $\mu\text{g m}^{-3}$
Mean	0.12	0.28	0.33	0.42	0.65	0.56	0.03	0.04	0.05	0.09	0.19	0.18	6.74	0.36	1.37	0.29	2.6
Median	0.00	0.23	0.32	0.37	0.59	0.36	0.00	0.00	0.01	0.05	0.00	0.00	4.75	0.09	1.12	0.00	2.7
Maximum	1.33	0.54	0.59	0.72	2.45	2.33	0.17	0.29	0.22	0.69	0.99	0.95	33.46	2.50	5.15	3.30	6.9
Minimum	0.00	0.13	0.17	0.27	0.18	0.00	0.00	0.00	0.00	0.00	0.00	0.00	0.00	0.00	0.00	0.00	0.0
Count	20	20	20	20	20	20	20	20	20	20	20	20	20	20	20	20	20
Sum	2.40	5.59	6.64	8.33	13.05	11.18	0.67	0.75	1.04	1.73	3.86	3.55	134.88	7.28	27.32	5.81	52

July	Na $\mu\text{g m}^{-3}$	Mg $\mu\text{g m}^{-3}$	Al $\mu\text{g m}^{-3}$	Si $\mu\text{g m}^{-3}$	S $\mu\text{g m}^{-3}$	Cl $\mu\text{g m}^{-3}$	K $\mu\text{g m}^{-3}$	Ca $\mu\text{g m}^{-3}$	Sc $\mu\text{g m}^{-3}$	Fe $\mu\text{g m}^{-3}$	Ni $\mu\text{g m}^{-3}$	Zn $\mu\text{g m}^{-3}$	El C $\mu\text{g m}^{-3}$	NH <sub>4</sub> N $\mu\text{g m}^{-3}$	Cl <sup>-</sup> $\mu\text{g m}^{-3}$	NO <sub>3</sub> $\mu\text{g m}^{-3}$	SO <sub>4</sub> $\mu\text{g m}^{-3}$
Mean	1.04	0.43	0.28	0.32	0.41	0.75	0.07	0.06	0.01	0.12	0.02	0.02	4.34	0.00	2.24	0.89	3.2
Median	1.28	0.37	0.30	0.34	0.38	0.72	0.08	0.07	0.00	0.13	0.01	0.01	2.58	0.00	1.97	0.00	2.9
Maximum	1.93	0.85	0.50	0.40	1.24	1.52	0.23	0.12	0.05	0.20	0.06	0.07	9.62	0.05	6.30	4.49	9.7
Minimum	0.08	0.07	0.04	0.05	0.07	0.06	0.01	0.00	0.00	0.03	0.00	0.00	0.07	0.00	0.00	0.00	0.0
Count	13	13	13	13	13	13	13	13	13	13	13	13	13	13	13	13	13
Sum	13.51	5.64	3.61	4.18	5.38	9.77	0.96	0.77	0.11	1.57	0.24	0.20	56.44	0.05	29.06	11.61	42

August	Na $\mu\text{g m}^{-3}$	Mg $\mu\text{g m}^{-3}$	Al $\mu\text{g m}^{-3}$	Si $\mu\text{g m}^{-3}$	S $\mu\text{g m}^{-3}$	Cl $\mu\text{g m}^{-3}$	K $\mu\text{g m}^{-3}$	Ca $\mu\text{g m}^{-3}$	Sc $\mu\text{g m}^{-3}$	Fe $\mu\text{g m}^{-3}$	Ni $\mu\text{g m}^{-3}$	Zn $\mu\text{g m}^{-3}$	El C $\mu\text{g m}^{-3}$	NH <sub>4</sub> N $\mu\text{g m}^{-3}$	Cl <sup>-</sup> $\mu\text{g m}^{-3}$	NO <sub>3</sub> $\mu\text{g m}^{-3}$	SO <sub>4</sub> $\mu\text{g m}^{-3}$
Mean	0.98	0.48	0.26	0.36	0.75	0.64	0.13	0.10	0.01	0.14	0.02	0.03	5.58	0.11	2.34	1.73	7.0
Median	1.04	0.42	0.24	0.35	0.67	0.47	0.10	0.05	0.00	0.14	0.02	0.02	4.79	0.00	1.96	1.55	6.8

Maximum	1.78	0.74	0.44	0.69	1.74	2.28	0.42	0.69	0.04	0.25	0.05	0.09	18.42	0.77	5.45	7.45	16.6
Minimum	0.00	0.19	0.12	0.20	0.10	0.33	0.02	0.01	0.00	0.07	0.00	0.00	0.00	0.00	0.00	0.00	0.0
Count	22	22	22	22	22	22	22	22	22	22	22	22	22	21	21	21	21
Sum	81.33	41.16	22.89	29.84	70.85	125.95	12.86	9.41	1.03	17.56	1.73	2.02	484.82	9.97	251.30	299.11	447

September	Na $\mu\text{g m}^{-3}$	Mg $\mu\text{g m}^{-3}$	Al $\mu\text{g m}^{-3}$	Si $\mu\text{g m}^{-3}$	S $\mu\text{g m}^{-3}$	Cl $\mu\text{g m}^{-3}$	K $\mu\text{g m}^{-3}$	Ca $\mu\text{g m}^{-3}$	Sc $\mu\text{g m}^{-3}$	Fe $\mu\text{g m}^{-3}$	Ni $\mu\text{g m}^{-3}$	Zn $\mu\text{g m}^{-3}$	El C $\mu\text{g m}^{-3}$	NH <sub>4</sub> N $\mu\text{g m}^{-3}$	Cl <sup>-</sup> $\mu\text{g m}^{-3}$	NO <sub>3</sub> $\mu\text{g m}^{-3}$	SO <sub>4</sub> $\mu\text{g m}^{-3}$
Mean	0.98	0.49	0.29	0.31	0.32	0.77	0.04	0.05	0.01	0.11	0.01	0.02	3.39	0.02	0.18	0.21	0.6
Median	1.12	0.51	0.27	0.33	0.28	0.69	0.03	0.05	0.01	0.11	0.01	0.01	2.83	0.00	0.00	0.00	0.0
Maximum	1.89	0.74	0.68	0.44	0.90	1.59	0.11	0.16	0.04	0.20	0.02	0.12	9.38	0.15	1.18	4.19	5.7
Minimum	0.00	0.21	0.15	0.23	0.09	0.44	0.00	0.00	0.00	0.05	0.00	0.00	0.82	0.00	0.00	0.00	0.0
Count	20	20	20	20	20	20	20	20	20	20	20	20	20	20	20	20	20
Sum	19.61	9.77	5.72	6.30	6.30	15.40	0.84	1.05	0.27	2.21	0.23	0.32	67.75	0.50	3.51	4.19	13

October	Na $\mu\text{g m}^{-3}$	Mg $\mu\text{g m}^{-3}$	Al $\mu\text{g m}^{-3}$	Si $\mu\text{g m}^{-3}$	S $\mu\text{g m}^{-3}$	Cl $\mu\text{g m}^{-3}$	K $\mu\text{g m}^{-3}$	Ca $\mu\text{g m}^{-3}$	Sc $\mu\text{g m}^{-3}$	Fe $\mu\text{g m}^{-3}$	Ni $\mu\text{g m}^{-3}$	Zn $\mu\text{g m}^{-3}$	El C $\mu\text{g m}^{-3}$	NH <sub>4</sub> N $\mu\text{g m}^{-3}$	Cl <sup>-</sup> $\mu\text{g m}^{-3}$	NO <sub>3</sub> $\mu\text{g m}^{-3}$	SO <sub>4</sub> $\mu\text{g m}^{-3}$
Mean	0.67	0.45	0.28	0.29	0.34	0.69	0.05	0.05	0.01	0.11	0.01	0.01	3.41	0.03	1.66	4.89	2.7
Median	0.75	0.44	0.27	0.29	0.25	0.50	0.05	0.04	0.01	0.09	0.01	0.00	2.49	0.00	0.00	0.00	0.0
Maximum	1.69	0.82	0.43	0.45	0.89	2.80	0.12	0.25	0.02	0.27	0.03	0.03	8.25	0.30	28.88	88.70	35.6
Minimum	0.00	0.04	0.19	0.23	0.06	0.34	0.01	0.01	0.00	0.06	0.00	0.00	0.00	0.00	0.00	0.00	0.0
Count	19	19	19	19	19	19	19	19	19	19	19	19	19	19	19	19	19
Sum	12.78	8.53	5.24	5.59	6.46	13.08	1.04	0.96	0.18	2.13	0.28	0.11	64.75	0.60	31.57	92.84	51

April	Na $\mu\text{g m}^{-3}$	Mg $\mu\text{g m}^{-3}$	Al $\mu\text{g m}^{-3}$	Si $\mu\text{g m}^{-3}$	S $\mu\text{g m}^{-3}$	Cl $\mu\text{g m}^{-3}$	K $\mu\text{g m}^{-3}$	Ca $\mu\text{g m}^{-3}$	Sc $\mu\text{g m}^{-3}$	Fe $\mu\text{g m}^{-3}$	Ni $\mu\text{g m}^{-3}$	Zn $\mu\text{g m}^{-3}$	El C $\mu\text{g m}^{-3}$	NH <sub>4</sub> N $\mu\text{g m}^{-3}$	Cl <sup>-</sup> $\mu\text{g m}^{-3}$	NO <sub>3</sub> $\mu\text{g m}^{-3}$	SO <sub>4</sub> $\mu\text{g m}^{-3}$
Mean	0.72	0.32	0.09	0.08	0.48	1.06	0.08	0.07	0.01	0.28	0.02	0.00	3.28	0.03	6.75	10.27	8.6
Median	0.61	0.33	0.10	0.07	0.42	0.79	0.07	0.07	0.00	0.29	0.02	0.00	2.77	0.00	0.39	0.00	2.4
Maximum	1.69	0.50	0.21	0.18	0.76	2.30	0.26	0.13	0.04	0.35	0.04	0.02	8.81	0.20	42.70	113.50	73.8
Minimum	0.20	0.16	0.00	0.00	0.32	0.35	0.00	0.01	0.00	0.12	0.00	0.00	0.00	0.00	0.00	0.00	0.0
Count	12	12	12	12	12	12	12	12	12	12	12	12	12	12	12	12	12
Sum	8.59	3.84	1.11	0.96	5.73	12.77	0.98	0.81	0.11	3.35	0.27	0.02	39.41	0.30	81.06	123.24	103

## Appendix D: Pearsons correlation matrices for Teflon and polycarbonate filters

Table A3: Pearsons correlation matrix for concentrations of elements on Teflon filters.

	Na	Mg	Al	Si	S	Cl	K	Ca	Sc	Mn	Ni	Zn	EC	NH <sub>4</sub>	Cl <sup>-</sup>	SO <sub>4</sub> <sup>-</sup>	NO <sub>3</sub> <sup>-</sup>	Fe
Na	1.000																	
Mg	0.102	1.000																
Al	0.059	0.543	1.000															
Si	-0.030	0.146	0.430	1.000														
S	0.010	-0.114	0.203	0.465	1.000													
Cl	0.333	-0.217	-0.191	0.091	-0.006	1.000												
K	-0.103	-0.046	0.160	0.037	0.326	-0.113	1.000											
Ca	-0.132	-0.036	0.004	-0.521	-0.209	-0.124	0.326	1.000										
Sc	0.098	-0.082	-0.089	-0.068	0.207	0.270	0.053	-0.002	1.000									
Mn	0.030	0.053	-0.204	-0.145	-0.047	-0.019	-0.074	0.123	0.105	1.000								
Ni	0.071	0.043	0.076	0.146	0.070	-0.125	0.011	-0.060	0.029	0.254	1.000							
Zn	-0.034	-0.295	-0.069	0.127	0.342	0.148	0.103	-0.172	0.365	-0.122	0.123	1.000						
EC	-0.091	-0.070	0.253	0.434	0.748	-0.187	0.500	-0.187	0.111	-0.084	0.118	0.345	1.000					
NH <sub>4</sub>	0.208	-0.044	0.228	0.055	0.412	-0.067	0.206	0.026	0.210	-0.117	0.037	0.368	0.439	1.000				
Cl <sup>-</sup>	0.339	0.198	0.024	-0.241	-0.170	0.340	-0.058	0.101	0.051	0.154	-0.206	-0.160	-0.245	0.091	1.000			
SO <sub>4</sub> <sup>-</sup>	0.037	-0.043	0.145	0.148	0.284	-0.042	0.034	-0.109	-0.058	-0.012	-0.048	-0.053	0.209	0.089	0.149	1.000		
NO <sub>3</sub> <sup>-</sup>	-0.098	0.043	0.220	0.127	0.333	-0.134	0.189	-0.014	0.097	-0.093	-0.079	0.132	0.323	0.181	0.100	0.216	1.000	
Fe	0.138	-0.023	0.042	0.356	0.226	0.221	-0.015	-0.319	-0.079	-0.028	-0.001	-0.052	0.237	-0.158	-0.161	0.056	-0.012	1.000

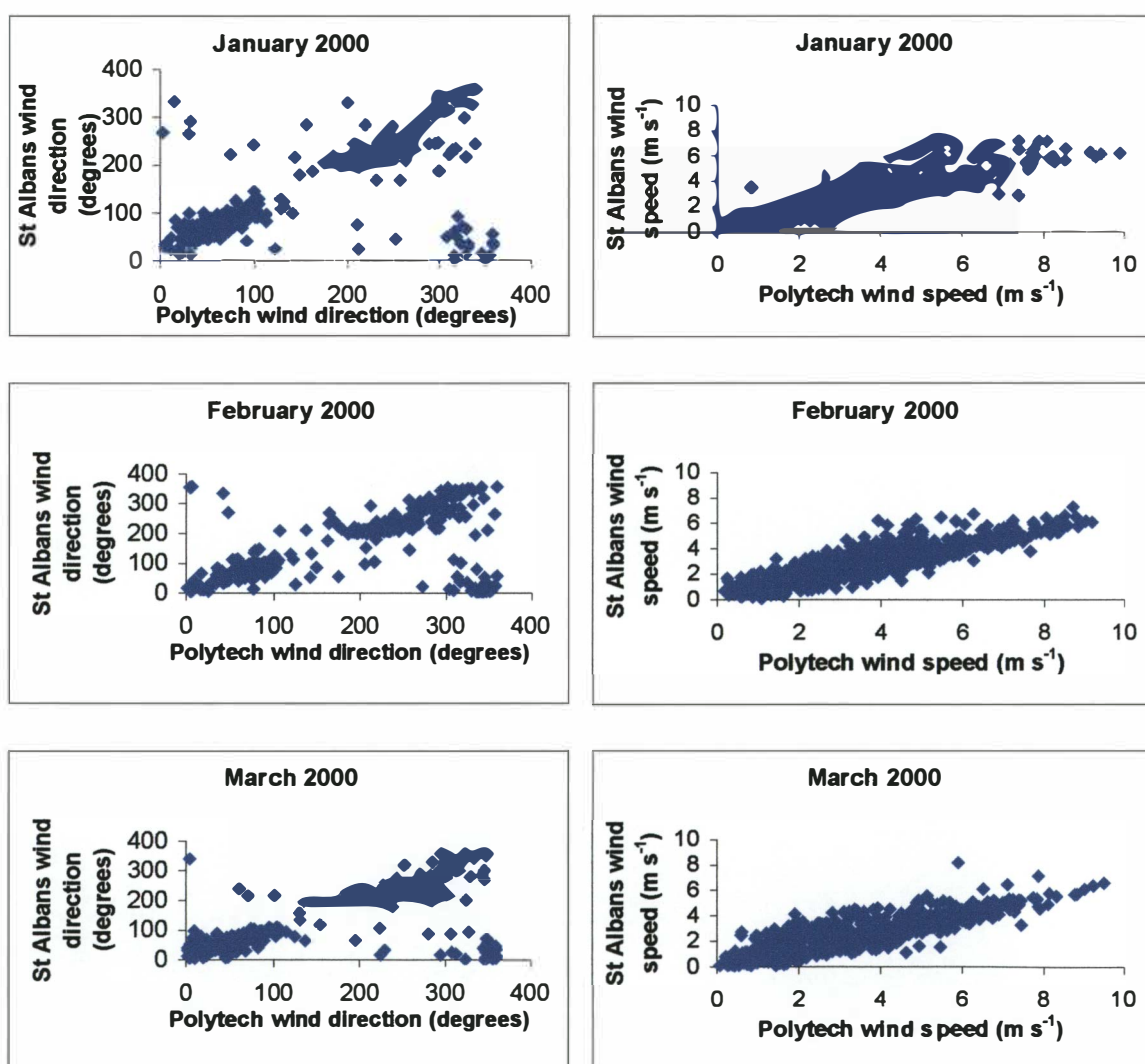
Table A4: Pearsons correlation matrix for concentrations of elements on polycarbonate filters.

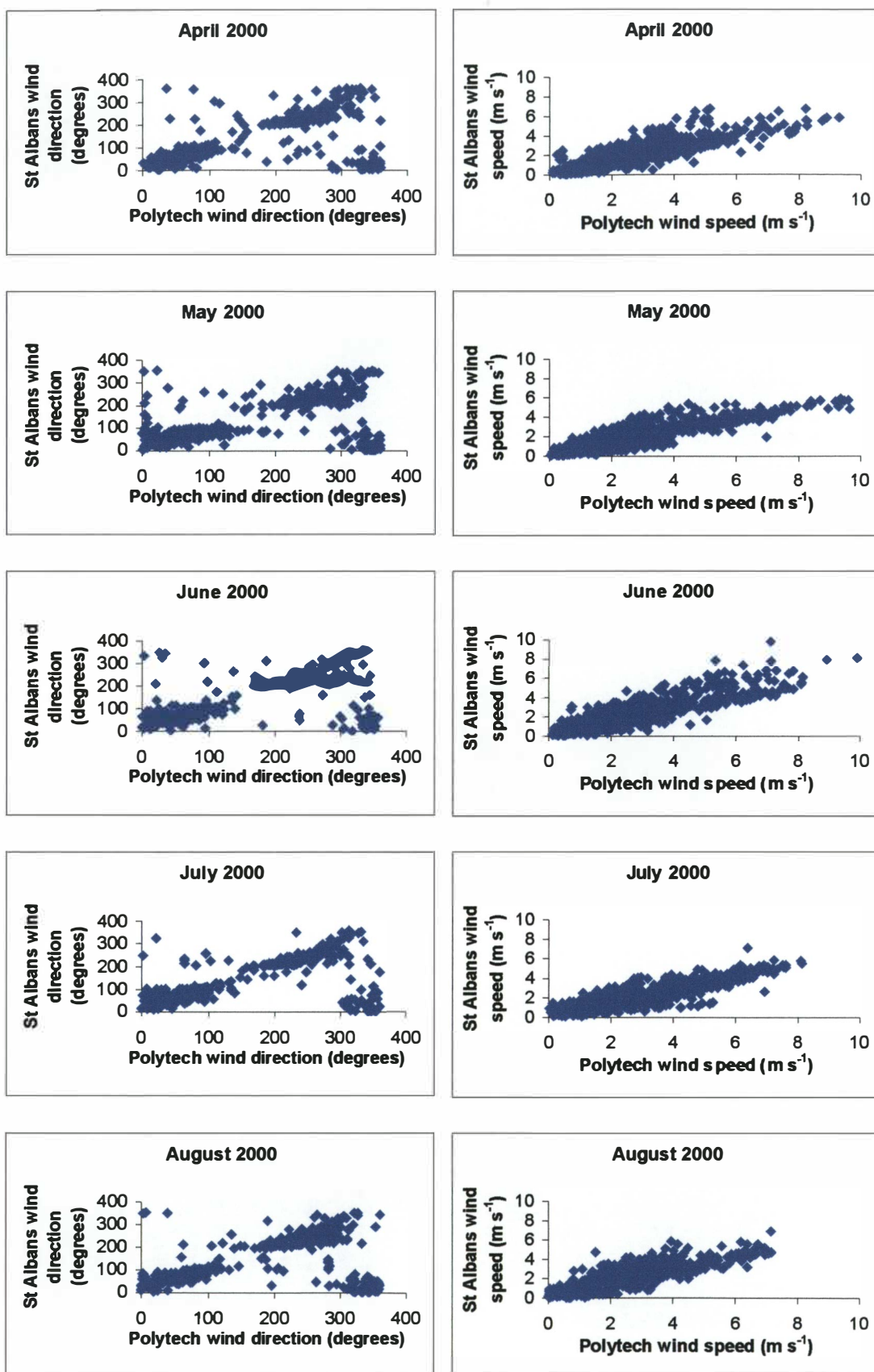
	Na	Mg	Al	Si	S	Cl	K	Ca	Sc	Fe	Mn	Ni	Zn	EC	NH <sub>4</sub>	Cl <sup>-</sup>	NO <sub>3</sub> <sup>-</sup>	SO <sub>4</sub> <sup>-</sup>
Na	1.000																	
Mg	0.535	1.000																
Al	0.459	0.781	1.000															
Si	0.390	0.717	0.751	1.000														
S	0.070	0.257	0.230	0.464	1.000													
Cl	0.117	0.272	0.237	0.616	0.412	1.000												
K	0.049	0.096	0.196	0.288	0.557	0.394	1.000											
Ca	0.153	0.353	0.279	0.551	0.590	0.630	0.440	1.000										
Sc	0.173	0.329	0.318	0.204	0.079	0.121	0.150	0.220	1.000									
Fe	0.297	0.384	0.285	0.462	0.543	0.508	0.472	0.482	0.197	1.000								
Mn	0.217	0.315	0.260	0.303	0.261	0.093	0.165	0.208	0.194	0.345	1.000							
Ni	0.184	0.264	0.315	0.198	0.236	0.182	0.527	0.293	0.366	0.476	0.312	1.000						
Zn	0.225	0.237	0.234	0.373	0.499	0.102	0.355	0.279	0.089	0.298	0.213	0.211	1.000					
EC	0.049	0.324	0.334	0.367	0.622	0.078	0.351	0.344	0.077	0.394	0.225	0.153	0.393	1.000				
NH <sub>4</sub> <sup>-</sup>	-0.075	-0.076	-0.010	-0.017	0.055	-0.042	0.020	-0.044	-0.089	-0.076	0.169	-0.051	-0.035	-0.016	1.000			
Cl <sup>-</sup>	0.041	0.062	0.011	0.027	0.048	0.027	-0.006	0.079	0.072	0.219	0.053	0.143	0.030	-0.015	-0.027	1.000		
NO <sub>3</sub> <sup>-</sup>	-0.005	0.059	0.014	0.020	-0.014	-0.005	-0.035	0.041	0.088	0.104	0.024	0.110	0.004	-0.103	-0.019	0.873	1.000	
SO <sub>4</sub> <sup>-</sup>	0.076	0.129	0.063	0.100	0.105	-0.012	0.021	0.127	0.094	0.164	0.096	0.153	0.127	0.012	0.085	0.846	0.903	1.000

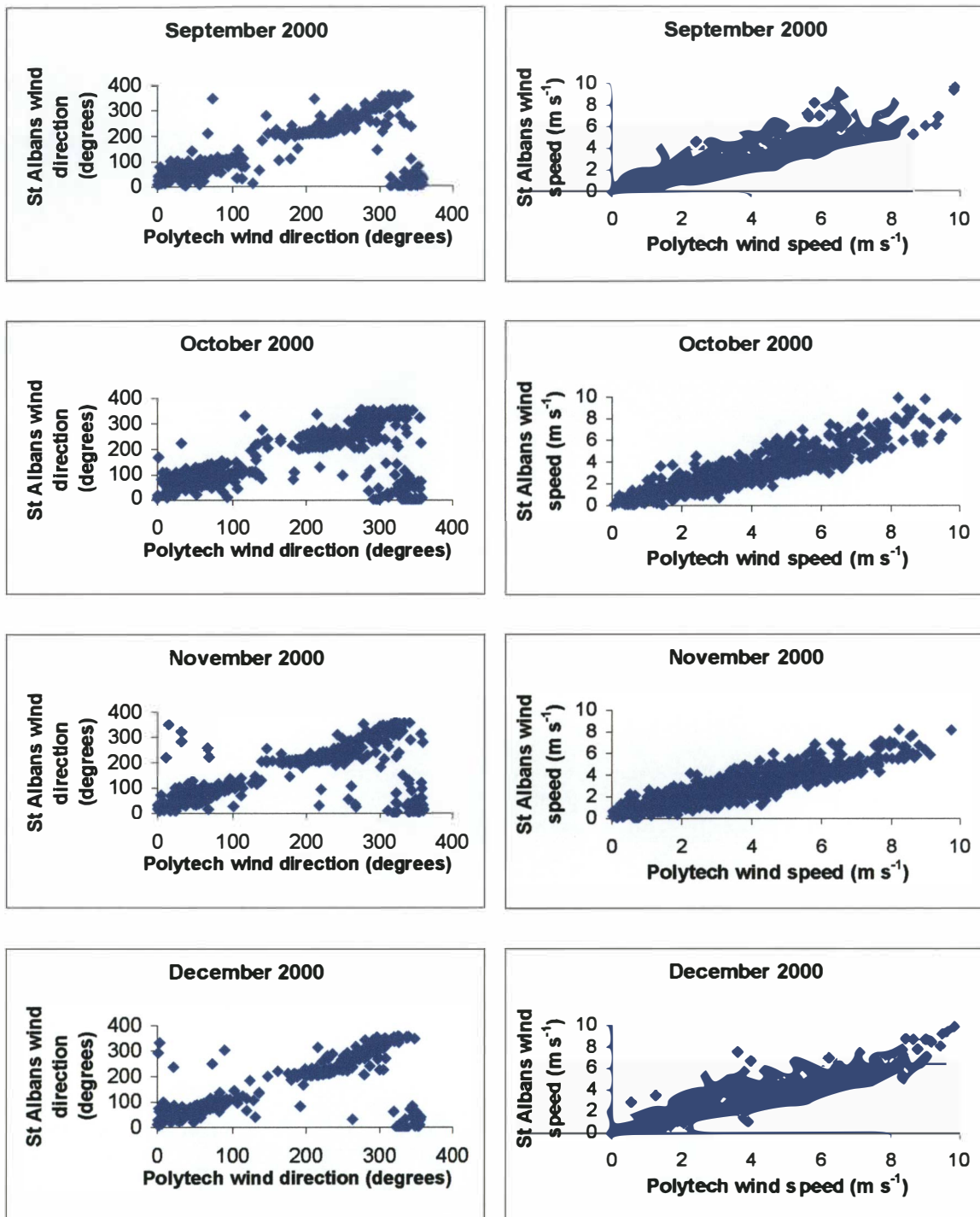


## Appendix E: Comparison of St Albans and Polytechnic wind data

The following graphs illustrate the relationship between hourly average wind direction and wind speed data measured at the Christchurch Polytechnic to corresponding measurements made at the St Albans ground level air quality monitoring site. Data are presented for each month of the year. Results indicate some differences in wind direction measurements on occasion, although generally wind direction data are comparable. In comparison, the wind speed was typically higher at the elevated Polytechnic visibility monitoring site.







## GLOSSARY OF TERMS

(adapted from USEPA, 1998a)

**Absorption:** Capture of incident light by particles or gases in the atmosphere.

**Absorption coefficient:** Proportion of incident light absorbed per unit distance. Typical units are inverse megameters ( $\text{Mm}^{-1}$ ).

**Accumulation mode:** A size range of particles, from about 0.1 to 3 micrometers, formed largely by accumulation of gases and particles upon smaller particles. They are very effective in scattering light.

**Aerosol:** A suspension of microscopic solid or liquid particles in air. Atmospheric aerosols govern variations in light extinction and, therefore, visibility reduction.

**Aethalometer:** An aerosol monitoring instrument that continuously measures particle light absorption (aerosol black carbon) on a quartz fiber filter.

**Agglomeration** The process of collisions of particles that stick together to become larger particles.

**Air light:** Light scattered by air (molecules or particles) toward an observer, reducing the contrast of observed images.

**Air pollutant:** An unwanted chemical or other material found in the air.

**Air pollution:** Degradation of air quality resulting from unwanted chemicals or other materials occurring in the air.

**Ambient air:** Air that is accessible to the public.

**Anion:** A negative ion, such as sulfate, nitrate, or chloride.

**Anthropogenic:** Caused by human activities (i.e., man-made).



**Apparent contrast:** Contrast at the observer of a target with respect to some background, usually an element of horizon sky directly above the target.

**Apportionment:** The act of assessing the degree to which specific components contribute to light extinction or aerosol mass.

**$b_{ap}$  Particle absorption coefficient:** A measure of light absorption in the atmosphere by particles. Standard reporting units are inverse megameters ( $Mm^{-1}$ ).

**$b_{ext}$  Extinction coefficient:** Measured directly by a transmissometer. Can be reconstructed from nephelometer and aerosol data. Represents the proportion of radiation reduced by scattering and absorption per unit distance. Standard reporting units are inverse megameters ( $Mm^{-1}$ ).

**$b_{sp}$  Particle scattering coefficient:** Measured directly by a nephelometer, the scattering coefficient includes scattering due to particles and atmospheric gases

**$b_{sg}$  Rayleigh scattering:** Standard reporting units are inverse megameters ( $Mm^{-1}$ )

**Bimodal distribution:** A distribution containing much of its elements in two distinct ranges of values. The size distributions of aerosols often show two peaks corresponding to about 1 and 10 micrometers in diameter.

**Brightness:** A measure of the light received from an object, adjusted for the wavelength response of the human eye, so as to correspond to the subjective sensation of brightness. For visually large objects, the brightness does not depend on the distance from the observer.

**Calibration:** The process of submitting samples of known value to an instrument, in order to establish the relationship of value to instrumental output.

**Coarse mode:** A size range of particles between 2.5 microns and 10 microns. Coarse particles are mostly composed of soils. The sum of the masses of coarse and fine particles (all particles smaller than 10 microns) is called  $PM_{10}$ .

**Color:** A qualitative sensation described by hue, brightness, and saturation.

**Color contrast or Contrast between two adjacent scene element colors:** Any difference in color difference hue, saturation, or brightness, between two perceived objects.

**Continuous:** An air analyzer that measures air quality components continuously.

**Contrast:** Relative difference in light coming from a target compared to the surrounding background, usually the horizon sky. Any difference in the optical quality of two adjacent images.

**Contrast change:** Minimum change in contrast perceptible to an observer.  
threshold.

**Contrast threshold:** Minimum apparent contrast at which a target is just perceptible.

**Contrast Ratio:** of apparent contrast to inherent contrast. The ability of an atmosphere transmittance to transmit an image without loss of contrast. It varies from 0% to 100% and depends on the length of the viewing path. When the object is darker than its background, it has a value between 0 and -1. For objects brighter than their background the value varies from 0 to infinity. When the contrast transmittance is equal to 0, the object cannot be seen.

**Datalogger:** An electronic device for measuring analog or digital signals and recording the results on a storage media. Many of them can record inputs on a number of separate locations, reporting them as separate "channels."

**Deciview (dv):** A haziness index designed to be linear with respect to human perception of visibility. A 1-2 dv change in haziness corresponds to a small, visibly perceptible change in scene appearance. Higher deciview values indicate more extinction and a corresponding decrease in visual range.

**Deliquescence:** The process that occurs when the vapor pressure of the saturated aqueous solution of a substance is less than the vapor pressure of water in the ambient air. Water vapor is collected until the substance is dissolved and is in equilibrium with its environment.

**Dew point:** The temperature at which humidity in the air will condense upon a solid surface.

**Edge sharpness:** Describes a characteristic of landscape features. Landscape features with sharp edges contain scenic features with abrupt changes in brightness.

**Elevated layer:** A pollution distribution that is not in contact with the ground.

**Externally mixed:** Particulate species that co-exist as separate particles without co-mingling or

combining.

**Extinction:** Process of reducing radiation transfer by scattering and absorption.

**Extinction budget:** Apportioning the extinction coefficient to atmospheric constituents to analyse/estimate the change in visibility caused by a change in constituent concentrations.

**Extinction coefficient:** Proportion of radiation reduced by scattering and absorption per unit coefficient distance. Standard units are inverse megameters (Mm). The atmospheric extinction coefficient, loosely referred to as "extinction," represents the ability of the atmosphere to absorb and scatter light. It equals the sum of the scattering and absorption coefficients.

**Fine particles:** Particulate matter with an aerodynamic diameter of 2.5 microns or less

**Haze (hazy):** A visual phenomenon resulting from scattering of light in a volume of aerosols. Condition of the atmosphere in which particles obscure a significant part of the vista.

**High volume:** A simple particle sampler consisting of a filter holder and a vacuum sampler (HI-VOL) cleaner blower, in a simple rain shelter. Some units have flow measuring or controlling features.

**Hue:** Attribute of color that determines whether it is red, yellow, green, blue, or other color. It is most strongly related to wavelength of light.

**Humidity:** Water in air, as a gas. Often measured as a percentage, compared to the maximum amount of water vapor the air can contain at that temperature.

**Hydrophobic:** Lacking affinity for water, or failing to adsorb or absorb water.

**Hygroscopic:** Characteristic of substances (e.g., particles in the atmosphere) having the property of absorbing water vapor from air. Also pertains to a substance (e.g., aerosols) that have an affinity for water and whose physical characteristics are appreciably altered by the effects of water.

**Illumination:** Application of visible radiation to an object.

**IMPROVE:** Interagency Monitoring of Protected Visual Environments, a collaborative monitoring

program established In the United States in the mid-1980's as a part of the Federal Implementation Plans. IMPROVE objectives are to provide data needed to assess the impacts of new emission sources, identify existing man-made visibility impairment, and assess progress toward the national visibility goals that define protection of 156 Class I areas.

**Inherent contrast:** Contrast of the target against the horizon sky background when viewed at the target. Same as intrinsic contrast. The contrast that would be seen between two adjacent scenic elements if there were no intervening atmosphere.

**Internally mixed:** Refers to the situation where individual particles contain one or more species. For example, water is internally mixed with its hygroscopic hosts.

**Ion:** A charged molecular group or atom.

**(IC) Ion chromatography:** A method of separating ions by their different speeds of passage through an ion-exchange resin. The ions are usually detected by their conductivity.

**Koschmeider:** The constant in the reciprocal relationship between standard visual range constant and the extinction coefficient (see standard visual range).

**Layered haze:** Haze that obscures a horizontal layer of a vista.

**Light extinction:** The absorption and scattering of light. The attenuation of light per unit distance due to absorption and scattering by the gases and particles in the atmosphere.

**LOD:** Limit of Detection

**Mie scattering:** Scattering by particles whose size is comparable to the wavelength of radiation. The attenuation of light in the atmosphere by scattering due to particles of a size comparable to the wavelength of the incident light. This is the phenomenon largely responsible for the reduction of atmospheric visibility. Visible solar radiation falls into the range from 0.4 to 0.8  $\mu\text{m}$ , roughly, with a maximum intensity around 0.52  $\mu\text{m}$ .

**Mixing layer:** An unstable layer of air that has turbulent mixing, usually due to solar heating of the ground. It is often capped by a stable layer of air.

**Mm<sup>-1</sup> Inverse megameter:** A unit of extinction related to SVR and dv. Higher extinction coefficients correspond to lower SVR values and higher deciview values.



**MOHAVE:** Measurement of Haze and Visual Effects

**Monitoring:** Measurement of air pollution and related atmospheric parameters.

**Nephelometer:** An optical instrument that measures the scattering coefficient ( $b_{sp}$ ) of ambient air by directly measuring the light scattered by aerosols and gases in a sampled air volume.

**Nuclei mode:** A size range of particles below about 0.1 micrometer in diameter. These particles are the nuclei around which larger particles grow.

**Optical depth:** The degree to which a cloud or haze prevents light from passing through it. It is a function of physical composition, size distribution, and particle concentration. Often used interchangeably with "turbidity."

**Optical monitoring:** Optical monitoring refers to directly measuring the behavior of light in the ambient atmosphere.

**PIXE:** Particle Induced X-ray Emission

**Particle scattering coefficient:** Proportion of incident light scattered by particles per unit distance ( $Mm^{-1}$ )

**Particulate matter:** Dust, soot, other tiny bits of solid materials that are released into and move around in the air.

**Path function:** Radiance per unit path length from a specified point along the path radiated towards the observer.

**Path radiance:** Radiance of path directed towards the observer. Or "airlight," is a radiometric property of the air resulting from light scattering processes along the sight line, or path, between a viewer and the object (target).

**Photochemical:** Any chemical reaction which is initiated by light. Such processes are important in the production of ozone and sulfates in smog.

**PM:** The acronym for airborne "particulate matter," an air quality parameter for which standards are maintained within NAAQS.

**PM<sub>2.5</sub>:** The acronym for that portion of PM that has an aerodynamic diameter of 2.5 microns or less.

**PM<sub>10</sub>:** The acronym for that portion of PM that has an aerodynamic diameter of 10 microns or less.

**Polarisation:** A property of light. Light can be linearly polarized in any direction perpendicular to the direction of travel, circularly polarized (clockwise or counterclockwise), unpolarized, or mixtures of the above.

**Precursor:** A substance or condition whose presence generally precedes the formation of another, more notable, condition or substance.

**Primary particles:** Suspended in the atmosphere as particles from the time of emission (e.g., dust and soot).

**Rayleigh scattering:** Scattering by gas molecules, whose size is small compared to the wavelength of radiation. Light scattering (principally blue light) by atmospheric gases. Perfectly clean air (100 percent Rayleigh scattering) would correspond to an SVR of 391 km at an elevation of 5,000 feet, which is the theoretical maximum for an SVR. Rayleigh scattering also corresponds to  $b_{ext} = 10 \text{ Mm}^{-1}$ , and is defined as 0 deciview.

**Reconstructed light extinction:** The relationship between atmospheric aerosols and the light extinction coefficient. Can usually be approximated as the sum of the products of the concentrations of individual species and their respective light extinction efficiencies.

**Reflectance:** Ratio of reflected to incident light.

**Regional haze:** A cloud of aerosols extending up to hundreds of miles across a region and promoting noticeably hazy conditions. Condition of the atmosphere in which uniformly distributed aerosol obscures the entire vista irrespective of direction or point of observation. Is not easily traced visually to a single source.

**RH:** Relative Humidity

**SASS:** Air sampling equipment for collecting concentrations of particles (PM<sub>2.5</sub>) on filters for subsequent analysis.

**Scattering:** Changing the direction of radiation at collisions with particles and gas molecules. The diversion of light from its original path. It can be caused by molecules or particles.

**Scattering coefficient:** Proportion of incident light scattered per unit distance. Standard units are coefficient inverse megameters ( $\text{Mm}^{-1}$ )

**Scattering efficiency:** The relative ability of aerosols and gases to scatter light. A higher scattering efficiency means more light scattering per unit mass or number of particles, this in turn means poorer visibility. In general, fine particles (diameter less than 2.5 microns) are efficient scatterers of visible light.

**Scene monitoring:** Scene monitoring is the monitoring of a specific vista or target. Optical and aerosol monitoring measure an abstract, but easily quantifiable parameter of the atmosphere. Scene monitoring captures the effects of all atmospheric parameters simultaneously, but in an inherently difficult manner to quantify. It is, for example, difficult to determine quantitatively which of two photographs represent "better" visibility conditions. Scene monitoring is generally done to help relate quantitative data in a "user-friendly" format.

**Secondary particles:** Formed in the atmosphere by a gas-to-particle conversion process.

**Sight path:** The straight line between the observation point and the target.

**Smog:** A mixture of air pollutants, principally ground-level ozone, produced by chemical reactions involving smog-forming chemicals. See also haze.

**Soot:** Black particles with high concentrations of carbon in graphitic and amorphous elemental forms. It is a product of incomplete combustion of organic compounds.

**Source:** Any place or object from which air pollutants are released. Sources that are fixed in space are stationary sources; sources that move are mobile sources.

**Standard visual range (SVR):** Visual range is the furthest distance that a human observer can resolve range a large dark target under the prevalent atmospheric conditions. Standard visual range is visual range standardized to Rayleigh scattering at an elevation of 5,000 feet ( $10 \text{ Mm}^{-1}$ ). The distance under daylight and uniform lighting conditions at which the apparent contrast between a specified target and its background becomes just equal to the threshold contrast of an observer, assumed to be 0.02.

**Surface layer haze:** A concentration of air pollution that extends from the ground to an elevation where the top edge of a pollution layer is visible.

**Temperature inversion:** Weather condition in which warm air sits atop cooler air, promoting stagnation and increased concentrations of air pollutants. A condition of a layer of atmosphere in which temperature increases with altitude. Such a layer is stable, and pollutants migrate through it very slowly. Also known as an inversion layer.

**TEOM (Tapered elemental oscillating microbalance):** A monitoring method for continuous measurement of mass of particles (PM<sub>10</sub> or PM<sub>2.5</sub>).

**Total suspended particulates (TSP):** Total particulate matter in a sample of ambient air.

**Transmission gauge:** A device for determining the amount of particles collected on a filter by the attenuation of light passing through the filter. Beta rays are sometimes used in place of visible light, and the resulting instrument is called a beta gauge.

**Transmissometer:** A device for assessing visibility conditions by measuring the amount of light received from a distant light source. Total light extinction is measured by integrating light scattering and absorption properties of the atmosphere.

**Transmittance:** The ratio of the light transmitted through a medium to the incident light. Light is attenuated by scattering and adsorption from gases and particles.

**Turbidity:** A condition that reduces atmospheric transparency to radiation, especially light. The degree of cloudiness, or haziness, caused by the presence of aerosols, gases, and dust.

**Uniform haze:** Pollutants that are uniformly distributed both horizontally and vertically from the ground to a height well above the highest terrain.  
particles from an air

**USEPA:** United States Environmental Protection Agency

**Visibility:** The ability to see an object or scene as affected by distance and atmospheric conditions; to perceive form, color and texture.

**Visibility indexes:** Aerosol indexes include the physical properties of the ambient atmospheric



particles (particle origin, size, shape, chemical composition, concentration, temporal and spatial distribution, and other physical properties). Optical indexes include coefficients for scattering, extinction, and absorption, plus an angular dependence of the scattering known as the normalized scattering phase function. Scenic indexes comprise visual range, contrast, color, texture, clarity, and other descriptive terms.

**Visibility degradation:** The impairment or degradation of atmospheric clarity. It becomes significant when the color and contrast values of a scene to the horizon are altered or distorted by airborne impurities.

**Visual air quality:** Air quality evaluated in terms of pollutant particles and gases that affect how well one can see through the atmosphere.

**Visual range (VR):** An expression of visibility; the maximum distance at which a large black object just disappears against the horizon.

## **GLOSSARY OF ELEMENTS (used in PIXE analysis)**

Na – Sodium

Ni – Nickel

Mg – Magnesium

Cu – Copper

Al – Aluminium

Zn – Zinc

Si – Silicon

Ga – Gallium

P – Phosphorous

Co – Cobolt

Ge – Germanium

S – Sulphur

As – Arsenic

Cl – Chlorine

Se – Selenium

K – Potassium

Br – Bromine

Ca – Calcium

I – Iodine

Sc – Scandium

Hg – Mercury

Ti – Titanium

Pb – Lead

V – Vanadium

E C – Elemental Carbon

Cr – Chromium

Mn – Manganese

Fe – Iron